# THE ACYLTRANSFERASE LYCAT CONTROLS SPECIFIC PHOSPHOINOSITIDES AND RELATED MEMBRANE TRAFFIC AND HORMONE RECEPTOR SIGNALING

by

Leslie N. Bone

B.Kin., McMaster University, 2009

A Dissertation

presented to Ryerson University

in partial fulfillment of the

requirements for the degree of

Doctor of Philosophy

in the program of

Molecular Science

Toronto, Ontario, Canada, 2017

AUTHOR'S DECLARATION FOR ELECTRONIC SUBMISSION OF A DISSERTATION

I hereby declare that I am the sole author of this dissertation. This is a true copy of the dissertation, including any required final revisions, as accepted by my examiners.

I authorize Ryerson University to lend this dissertation to other institutions or individuals for the purpose of scholarly research.

I further authorize Ryerson University to reproduce this dissertation by photocopying or by other means, in total or in part, at the request of other institutions or individuals for the purpose of scholarly research.

I understand that my dissertation may be made electronically available to the public.

THE ACYLTRANSFERASE LYCAT CONTROLS SPECIFIC PHOSPHOINOSITIDES AND RELATED MEMBRANE TRAFFIC AND HORMONE RECEPTOR SIGNALING

Leslie N. Bone

Doctor of Philosophy, 2017

Molecular Science, Ryerson University

## Abstract

Phosphoinositdes (PIPs) are a group of signaling phospholipids involved in regulating many cellular processes, including organelle dynamics, nutrient uptake, autophagy and apoptosis. Through the action of lipid kinases and phosphatases, phosphatidylinositol (PI) can be phosphorylated on three different positions of the inositol headgroup resulting in seven distinct PIP species. Substantial research has focused on elucidating the function and importance of headgroup phosphorylation while much less is known about the significance of the incorporation of specific acyl chains within PI. PI exhibits unique specificity of acyl chain composition, where majority contains 1-stearoyl-2-arachidonoyl acyl species. This unique acyl chain enrichment is, in part, controlled by the PI acyltransferase lysocardiolipin acyltransferase (LYCAT). How LYCAT and, in turn, incorporation of specific fatty acids, controls the function of PI and PIPs is poorly understood. Thus, I investigated the impact of LYCAT perturbation on PIP acyl profile and effects on PIP-dependent processes.

Perturbation of LYCAT by siRNA gene silencing resulted in a shift in the acyl profile of $PIP_2$ species to contain shorter species. Additionally, LYCAT silencing altered the cellular localization and levels of phosphatidylinositol-4,5-bisphosphate and phosphatidylinositol-3-

phosphate but was without effect on other PI species examined. Consistent with this, silencing of LYCAT perturbed the membrane traffic of transferrin receptor dependent on these specific PIPs. I also observed changes in PI-dependent receptor tyrosine kinase signaling pathways that control cell survival and proliferation, which are regulated by phosphatidylinositol-3,4,5-trisphosphate. LYCAT perturbation altered activation of Akt1, which impacted a number of Akt substrates.

Additionally, using fluorescence microscopy, I discovered that LYCAT is localized to peripheral ER vesicles that contain PI synthase enzyme, which is responsible for PI synthesis. These peripheral vesicles partially overlap with endoplasmic reticulum-plasma membrane contact sites marked by E-Syt2 but showed little overlap with the ER maker, KDEL.

Collectively, my results show that the PI acyltransferase LYCAT controls the function of specific species of PIPs, which in turn selectively impacts specific stages of endomembrane traffic and hormone receptor signaling. Hence, the regulation of acyl content of PI is an important new dimension for the control of PI and PIP function.

Acknowledgments

First and foremost, I would like to thank my supervisors Drs. Costin Antonescu and Roberto Botelho for this opportunity and for their constant mentorship and support throughout my graduate career. Thank you for your patience, advice and motivational speeches that you have given me.

I wish to thank my graduate committee, Drs. Warren Wakarchuk and Gregory Fairn. The feedback and support from my graduate committee has been of utmost value to me throughout the years. Additionally, I would like to thank Dr. Imogen Coe for taking part in my Ph.D. transfer exam and for being my cheerleader throughout my Ph.D.

Thank you to all the members of the Antonescu and Botelho labs, both past and present.

Finally, special thank you to my Mom, Dad, Step-Mom, Step-Dad, my siblings and my partner, Adam for their constant love, support and encouragement. I thank them for helping me whenever and however I needed during my Ph.D.

Table of Contents

List of Figures

List of Appendices

List of Abbreviations

| | |
|---|---|
| AGPAT | acylglycerolphosphate acyltransferase |
| CCP | clathrin-coated pit |
| CCV | clathrin-coated vesicle |
| CDP-DAG | cytidine diphosphate diacylglycerol |
| CDS | cytidine-diphosphate synthase |
| CME | clathrin-mediated endocytosis |
| DAG | diacylglycerol |
| DGK | diacylglycerol kinase |
| EEA1 | early endosome antigen 1 |
| EGF | epidermal growth factor |
| eGFP-CLCa | enhanced green fluorescent protein fusion of clathrin light chain a |
| EGFR | epidermal growth factor receptor |
| ER | endoplasmic reticulum |
| E-Syt | extended synaptotagmin |
| FYVE | Fab1, YotB, Vac1p and EEA1 |
| G3P | glycerol-3-phosphate |
| Gab1 | growth factor receptor protein 1 |
| GPAT | glycerol-3-phosphate acyltransferase |
| Grb2 | growth factor receptor-bound protein 2 |
| HPLC | high-performance liquid chromatography |
| $IP_3$ | inositol triphosphate |
| LC-ESI-MS/MS | liquid chromatography–electrospray ionization mass spectrometry |
| LCS | localization correlation score |
| LYCAT | lysocardiolipin acyltransferase |
| MCS | membrane contact site |
| mTORC | mammalian target of rapamycin complex |
| Nir | N-terminal domain-interacting receptor |
| NSLTP | non-specific lipid transfer protein |

| | |
|---|---|
| OCRL | Oculocerebrorenal Syndrome of Lowe |
| ORP | oxysterol-binding protein-related protein |
| OSBP | oxysterol-binding protein |
| PA | phosphatidic acid |
| PDK1 | phosphoinositide-dependent kinase-1 |
| PH | pleckstin homology |
| PI | phosphatidylinositol |
| PI(3)P | phosphatidylinositol-3-phosphate |
| $PI(3,4,5)P_3$ | phosphatidylinositol-3,4,5-trisphosphate |
| PI(4)P | phosphatidylinositol-4-phosphate |
| $PI(4,5)P_2$ | phosphatidylinositol-4,5-bisphosphate |
| PI3K | phosphatidylinositol-3 kinase |
| PIP | phosphoinositide |
| $PIP_1$ | monophosphorylated phosphoinositide |
| $PIP_2$ | diphosphorylated phosphoinositide |
| PIP5K | phosphatidylinositol 4-phosphate 5-kinase |
| PIPEROsome | phosphatidylinositol producing ER-derived organelle |
| PIS | phosphatidylinositol synthase |
| PITPNC1 | phosphatidylinositol transfer protein cytoplasmic 1 |
| PLA | phospholipase A |
| PLC | phospholipase C |
| PTEN | phosphatase and tensin homolog |
| ROS | reactive oxygen species |
| RPE | retinal pigment epithelial cells |
| Tfn | transferrin |
| TfR | transferrin receptor |
| TIRF-M | total internal reflection fluorescence microscopy |
| VAP | vesicle-associated membrane protein |
| VSVG | vesicular stomatitis virus G |

# Chapter 1
# Introduction

## 1.1. Membrane traffic

The cell surface acts as a platform for communication between external environmental cues and internal processes and activities. Membrane traffic is involved in nutrient uptake, receptor signaling, internalization of cargo and transport of newly synthesized molecules (Figure 1.1). These actions all involve the exchange of membrane from one organelle to the next and transport of various proteins and lipids (Antonescu et al., 2014). Tight regulation of these processes is required in order for the cell to maintain homeostasis. Membrane traffic is a dynamic process; for example, mammalian cells cycle 50-180% of the surface area of the plasma membrane in and out of the cell every hour as a result of endocytosis and exocytosis events (Steinman et al., 1983). In addition to constitutive membrane traffic, there is also regulated membrane traffic occurring in response to signals in the external environment (Roth, 2004). Membrane traffic is involved in many eukaryotic activities and helps establish higher order function in multi-cellular organisms.

There are many different mechanisms of membrane traffic that have distinct roles in the traffic of molecules like proteins and lipids. Endocytic traffic leads to the sorting of internalized material into multiple pathways including maturation, recycling and/or degradation. For example, receptors that modulate signal transduction such as epidermal growth factor receptor (EGFR) are often selected and sequestered into the degradative pathway where they traffic through early endosomes and late endosomes and are finally delivered to lysosomes (Tomas et al., 2014) effectively resulting in downregulation of growth factor signaling. Indeed, dysregulation of this pathway can cause uncontrolled cell growth leading to cancer (Díaz et al., 2012; Downes et al., 2007). Other receptors are internalized, sorted at early endosomes and then transported to recycling endosomes for delivery back to the plasma membrane (Mayle et al., 2012). A classic

example is transferrin receptor (TfR) that delivers the nutrient iron into the cell by binding iron—transferrin (Tfn) complexes. Recycling of this receptor allows for multiple rounds of iron uptake.

The biosynthetic pathway involves the transport of newly synthesized proteins from the endoplasmic reticulum (ER) to the Golgi apparatus and their subsequent delivery to various organelles (Urbé et al., 1997). The flow and transfer of membrane from one organelle to the next is a highly regulated process that involves many different factors including Rab GTPases, tethering effectors, soluble N-ethylmaleimide-sensitive factor attachment protein receptors (SNARES), and lipids such as phosphoinositides (PIPs).

Compromised membrane traffic caused by genetic mutations can have a significant impact on cellular homeostasis leading to human disease. For example, Oculocerebrorenal Syndrome of Lowe (OCRL) is a genetic disease, which causes defects in endosome to Golgi traffic and causes cataracts, mental retardation and renal failure (Howell et al., 2006; McCrea and De Camilli, 2009; Vicinanza et al., 2008). Dent's disease is another syndrome that is caused by inhibition of post-Golgi transport of the voltage gated chloride channel to the plasma membrane resulting in renal failure (Howell et al., 2006). Clearly, understanding the molecular mechanisms of membrane traffic is key to understanding cellular physiology and associated human diseases. Many regulators of membrane traffic have been uncovered and a key player is a group of signaling phospholipids called phosphoinositides.

## 1.2. History of PI signaling lipid

In the early 1950's, Hokin observed changes in the turnover of phospholipids upon stimulation of exocrine tissues in pigeon pancreas (Hokin, 1985). However, it was not until 1956, when

techniques to separate phospholipids improved that it was discovered that phosphatidylinositol (PI) was undergoing these major changes in turnover (Hokin, 1987). This process was termed the phosphatidylinositol effect. Seminal work by Hokin and Hokin throughout the 1950's found that the PI-effect occurred with many ligands and in a variety of tissues including guinea pig brain cortex, submaxillary and parotid glands, human sweat glands and toad and turtle bladder, to name a few (Hokin, 1985).

In 1963 it was determined that this PI-effect was due to the turnover of PI and its phosphorylated species, PIPs (Hokin, 1987, 1985). Using different radiographic techniques and differential centrifugation, it was determined that PI turnover occurred in the ER (Hokin, 1985). Further studies by the Hokins found that upon receptor mediated PIP hydrolysis, the levels of [$^{32}$P] metabolically-labelled PI increased, indicating that changes in PI phosphorylation were observed (Hokin, 1985). In particular, the importance of diphosphorylated PI first became apparent when this lipid was discovered to be the precursor to the important secondary messengers diacylglycerol (DAG) and inositol triphosphate ($IP_3$), which are generated upon stimulation of plasma membrane receptors (Hokin, 1985). Since then, the known roles and functions of PIPs have greatly expanded, as these lipids are involved in numerous signaling events, both as ligand binding molecules and as molecules that generate secondary signaling intermediates, and as such have been shown to be important in a wide variety of cellular processes, as discussed in more detail below.

## 1.3. Phosphatidylinositol

Phosphatidylinositol (PI) is a type of phospholipid that acts as a key regulator of membrane traffic, cell signaling, cytoskeletal remodeling and nuclear events (Vicinanza et al., 2008). Although PI only comprises 1-10% of total phospholipids in eukaryotic cells, PI is important for the temporal and spatial activation of molecular effectors required for maintenance of cell physiology (Cullen, 2011; Di Paolo and De Camilli, 2006; Lemmon, 2008). PI is a constituent of membranes of many archaea, some bacteria and all eukaryotes (Michell, 2008) but has only been studied and functionally characterized in a handful of organisms including a few archaea and bacteria and among the eukaryotic organisms, mammals, yeast and plants. Reports have suggested that the appearance of phospholipids containing an inositol headgroup may have evolved before the divergence of the archaeal and eukaryotic kingdoms (Michell, 2008).

PI is composed of a diacylglycerol (DAG) backbone containing two acyl chains in the *sn1* and *sn2* positions and an inositol headgroup connected to the glycerol backbone through a phosphodiester bond at the *sn3* position (Figure 1.2) (van Meer et al., 2008). The inositol headgroup can be phosphorylated on three different locations resulting in mono-, di- or tri-phosphorylated species. Through the action of lipid kinases and phosphatases, seven distinct PIP species can be generated (Hammond et al., 2014; Huotari and Helenius, 2011; Vicinanza et al., 2008).

### 1.3.1. Phosphoinositides – localization and membrane enrichment

The seven species of PIPs are unique to eukaryotes (Michell, 2008). They are important in the production of secondary messengers, providing membrane identity and acting as markers for the recruitment of soluble or membrane effector proteins involved in vesicle traffic and signaling (Di

Paolo and De Camilli, 2006; van Meer et al., 2008). PIPs represent 1-2% of total phospholipids in cells (Balla, 2013).

PIPs are synthesized locally on membranes by kinases and phosphatases, which allows for the tight control of PIP production resulting in membranes with unique and dynamic PIP signatures. These kinases and phosphatases contain membrane-targeting domains that recognize the individual PIPs. There are many different PI-binding domains, which allow proteins to bind specifically to individual PIP species, including Fab1, YotB, Vac1p and EEA1 (FYVE), pleckstin homology (PH), epsin N-terminal homology (ENTH) and phox homology (PX) domains. Studies have elucidated the intracellular localization of PIPs using PI-binding domain probes. As such, PIPs were determined to function as membrane ligands that anchor certain proteins to organelles or vesicles. Stabilization of membrane-protein complexes can be enhanced in multiple ways. For example, the presence of tandem lipid-binding domains increases avidity of binding between protein and lipid. Alternatively, proteins that possess multiple lipid/protein binding domains may require a specific combination of substrates to bind. Importantly, this mechanism known as "coincidence detection" also provides specificity within the ever-complex intracellular milieu.

The relative abundance of PIPs varies from one organelle membrane to another, with some membranes containing higher levels of specific PIPs than others (Vicinanza et al., 2008). Below is a brief overview of phosphatidylinositol-4,5-bisphosphate [$PI(4,5)P_2$], phosphatidylinositol-3-phosphate [PI(3)P], phosphatidylinositol-4-phosphate [PI(4)P], phosphatidylinositol-3,5-bisphosphate [$PI(3,5)P_2$] and phosphatidylinositol-3,4,5-trisphosphate [$PI(3,4,5)P_3$].

*Phosphatidylinositol-4,5-bisphosphate.* PI(4,5)$P_2$ represents 0.5-1% of total phospholipids and is mainly localized on the inner leaflet of the plasma membrane (Figure 1.3) (Dickson et al., 2014; Lemmon, 2008; McLaughlin et al., 2005). Although PI(4,5)$P_2$ is found in relatively low abundance in the cell, it is important for the production of PI(3,4,5)$P_3$ and the secondary messengers, DAG and $IP_3$. PI(4,5)$P_2$ plays essential roles in clathrin-mediated endocytosis (CME), actin cytoskeleton dynamics and overall gene expression (Antonescu et al., 2011; Logan and Mandato, 2006; Santagata et al., 2001). PI(4,5)$P_2$ has also been shown to be required for the activity of plasma membrane ion channels (Dickson et al., 2014).

*Phosphatidylinositol-3-phosphate.* PI(3)P comprises 0.02% of total phospholipids in cells (Cullen, 2011; Lemmon, 2008) and is most abundant on early endosomes, late endosomes and the intraluminal vesicles of multi-vesicular bodies (Bago et al., 2014; Gillooly et al., 2000; Liu et al., 2016). PI(3)P is required for the fusion of endosomes and is involved in sorting and traffic of cargo along the endocytic pathway.

*Phosphatidylinositol-4-phosphate*. PI(4)P comprises 0.05% of total phospholipids in cells (Cullen, 2011; Lemmon, 2008) and is concentrated on the Golgi, plasma membrane and late endosomes/lysosomes (Graham and Burd, 2011; Hammond et al., 2014). PI(4)P plays a role in intracellular traffic and including Golgi secretory pathway, contributes to the negative charge of the inner leaflet of the plasma membrane and contributes to PI(4,5)$P_2$ synthesis and maintenance of ion channels (Dickson et al., 2014; Hammond et al., 2012).

*Phosphatidylinositol-3,5-bisphosphate.* PI(3,5)$P_2$ comprises less than 0.04% of total phospholipids in cells (Cullen, 2011; Lemmon, 2008). PI(3,5)$P_2$ primarily localizes to late endosomes and lysosomes (Ho et al., 2012; McCartney et al., 2014). PI(3,5)$P_2$ is responsible for

endolysosomal morphology, traffic and acidification, autophagy, and signal mediation in response to stresses or hormonal cues (Ho et al., 2012).

*Phosphatidylinositol-3,4,5-trisphosphate.* PI(3,4,5)$P_3$, the only tri-phosphorylated species, is an important molecule in the phosphatidylinositol-3 kinase (PI3K)/Akt signaling pathway, and is mainly concentrated at the plasma membrane (Carlton and Cullen, 2005; Nakatsu et al., 2010). Some reports indicate that PI(3,4,5)$P_3$ can also be found on intracellular vesicles and endosomes, possibly derived from the plasma membrane (Gonzalez and McGraw, 2009). PI(3,4,5)$P_3$ levels are nearly undetectable in resting cells, however upon activation of receptor tyrosine kinases or G-protein coupled receptors, PI(3,4,5)$P_3$ levels increase (Asano et al., 2007; Toker and Cantley, 1997; Zhao and Vogt, 2008). PI(3,4,5)$P_3$ is implicated in a number of cellular processes that control cell survival, growth, proliferation and motility.

Mutations in genes encoding PIP metabolizing enzymes are responsible for human diseases including Lowe Syndrome, Charcot-Marie-Tooth disease, Alzheimer's disease and myopathy (McCrea and De Camilli, 2009).

### 1.3.2. Phosphoinositide kinases and phosphatases

PIP metabolizing enzymes include the phosphoinositide kinases and phosphatases that can be cytosolic or membrane bound and are responsible for the turnover of PIPs on intracellular membranes, resulting in distinctly concentrated PIP species (Figure 1.2). In mammals, 47 genes encode 19 kinases and 28 phosphatases (Sasaki et al., 2009). For example the synthesis and turnover of PI(3,4,5)$P_3$ is tightly regulated by the actions of multiple PIP metabolizing enzymes. First, the PI(4,5)$P_2$ precursor is generated by phosphorylation of PI(4)P by type I

phosphatidylinositol 4-phosphate 5-kinases (PIP5Ks). Then, the 3 position of $PI(4,5)P_2$ is further phosphorylated by class I PI3Ks to produce $PI(3,4,5)P_3$, an event that is antagonized by the phosphatase PTEN (phosphatase and tensin homolog) (Sasaki et al., 2009). The interconversion of PIPs is spatially and temporally organized, in part, due to the specific cellular localization and characteristics of PIP kinases and phosphatases. For example, the $PI(3,4,5)P_3$ phosphatase PTEN contains a C2 domain, which allows for membrane association and also contains a wide and deep catalytic pocket to accommodate the bulky headgroup of $PI(3,4,5)P_3$ (Hsu and Mao, 2015).

## 1.4. Phospholipids

In order to understand the importance and functions of PI and PIPs, we first need to gain insight into the general function of phospholipids in cells. PI and PIPs are among many major eukaryotic membrane phospholipids, which also include phosphatidylcholine, phosphatidylethanolamine, phosphatidylserine and cardiolipin (van Meer et al., 2008). The distribution of phospholipids among different organelle membranes is asymmetric, which contributes to the distinct functions and properties of each phospholipid. Collectively these phospholipids form structural biological membranes by assembling into the phospholipid bilayer.

*Phosphatidylcholine.* Phosphatidylcholine is cylindrical in shape, preferentially forming flat bilayer structures (Vance and Steenbergen, 2005). Phosphatidylcholine is the most abundant phospholipid in cells, representing 40-50% of total phospholipids (Vance and Steenbergen, 2005). Phosphatidylcholine can be utilized in cells for the production of precursor and signaling molecules including DAG, phosphatidic acid (PA) and arachidonic acid (Vance and Vance, 2004).

*Phosphatidylethanolamine.* Phosphatidylethanolamine, representing 15-25% of total cellular phospholipids, is most abundant in the mitochondria and lipid droplets (Bigay and Antonny, 2012; Vance and Steenbergen, 2005). Phosphatidylethanolamine is cone shaped due to its small headgroup, and, it plays a role in membrane fission and fusion (van Meer et al., 2008).

*Phosphatidylserine*. Phosphatidylserine is a negatively charged phospholipid comprising 2-10% of total cellular phospholipids, and is primarily found on the inner leaflet of the plasma membrane where it functions in maintenance of plasma membrane electrostatics (Bigay and Antonny, 2012; Vance and Steenbergen, 2005). Phosphatidylserine also localizes to endocytic compartments including early endosomes, late endosomes and lysosomes in macrophages (Yeung et al., 2008). Phosphatidylserine, together with PIPs, power the electrostatic field at the plasma membrane, endosomes and lysosomes, which is important in attracting cytosolic polycationic proteins (Platre and Jaillais, 2017; Yeung et al., 2008). Phosphatidylserine is involved in the recruitment and/or activation of proteins including protein kinase C and is a signal for phagocytosis and blood coagulation (Fairn et al., 2011; Yeung et al., 2006).

*Cardiolipin.* Cardiolipin is a mitochondrial phospholipid required for energy production and maintenance of the mitochondrial membrane proton gradient (Fagone and Jackowski, 2009; Vance and Vance, 2004). In the inner mitochondrial membrane, cardiolipin serves as a $Ca^{2+}$-binding site required for mitochondrial membrane permeabilization (Cao et al., 2004). Cardiolipin comprises 2-5% of total phospholipids in cells (Vance and Steenbergen, 2005) and is the only lipid that contains four fatty acid chains, which in the heart, contains largely linoleic acid (18:2), and two glycerol phosphate backbones (Sathappa and Alder, 2016). Diet has been shown to play a role in the acyl chain content of cardiolipin (Bradley et al., 2016). For example, mice fed a high-

fat diet (5% lard) increased 18:2 content by 20% (Aoun et al., 2012). Remodeling of the fatty acyl groups is important for cardiolipin function, and alterations have been shown to cause mitochondrial dysfunction and disease including cardiomyopathies and tumor progression (Bradley et al., 2016; Chicco and Sparagna, 2006).

Phospholipids not only exhibit specific enrichment in different organelles and membrane compartments, but also exhibit asymmetry in their distribution within lipid bilayers, suggesting that phospholipids have unique functions on specific leaflets of the lipid bilayer. Membrane asymmetry occurs due to multiple factors, including the biophysical properties of lipids, mechanisms that trap lipids to one leaflet, and lipid transporters (Fadeel and Xue, 2009; van Meer et al., 2008).

At least three different lipid transporter activities within membranes have been described and include flippases (ATP-driven inward movement of lipids), floppases (ATP-driven outward movement of lipids) and scramblases (spontaneous bi-directional movement) (Balla, 2013; Fadeel and Xue, 2009). For example, the floppase P4-ATPase is responsible for ensuring phosphatidylserine remains on the intracellular leaflet of the plasma membrane. However, during apoptosis or blood clotting, the scramblase TMEM16F is responsible for exposing phosphatidylserine on the extracellular leaflet of the plasma membrane (Hankins et al., 2015), which is an important signal for phagocytes to clear these dead cells from tissue. PIPs are highly concentrated on the cytosolic leaflet of the plasma membrane, which is in part due to the transport of these lipids from the ER following synthesis.

Disruption of phospholipid membrane asymmetry can cause diseases such as Tangier Disease, which is characterized by high atherosclerosis and is caused by a mutation in the ABCA1

transporter involved in transfer of cholesterol from the inner to the outer leaflet of membranes (Fadeel and Xue, 2009).

### 1.4.1. Phospholipid synthesis – Kennedy pathway

The ER is the main site of lipid synthesis where the basic molecule glycerol-3-phosphate (G3P) and acyl-CoAs are utilized in the *de novo* Kennedy pathway that ultimately produces phospholipids (Figure 1.4) (Coleman and Lee, 2004; Shindou and Shimizu, 2009; Takeuchi and Reue, 2009).

LysoPA is formed by the acylation of the *sn1* position of G3P by glycerol-3-phosphate acyltransferases (GPATs) (Coleman and Lee, 2004; Hermansson et al., 2011; Shindou et al., 2009; Takeuchi and Reue, 2009). Four different GPATs have been identified, which reside as integral ER-membrane proteins and outer mitochondrial membrane proteins (Hermansson et al., 2011; Takeuchi and Reue, 2009). Most cell types predominantly use GPAT3 and GPAT4, which are localized to the ER, whereas muscle and liver cells predominantly use GPAT1 and GPAT2 localized to the mitochondria (Yamashita et al., 2014). In most tissues, the mitochondrial GPATs are only responsible for 10% of GPAT activity, however GPAT1 in the liver accounts for up to 50% of GPAT activity playing a key role in triacylglycerol synthesis (Coleman and Lee, 2004). GPAT expression varies depending on the tissue. For example, GPAT1 mRNA levels are highest in adipose tissue and liver, whereas GPAT3 mRNA levels are highest in the kidney, heart, skeletal muscle, thyroid and testis (Takeuchi and Reue, 2009).

Acylglycerolphosphate acyltransferases (AGPATs, also known as lysoPA acyltransferases, LPAATs) are responsible for the addition of a fatty acid onto the *sn2* position of lysoPA, resulting

in PA (Hermansson et al., 2011; Shindou et al., 2009; Takeuchi and Reue, 2009; Yamashita et al., 2014). Mammals contain at least 16 members of the AGPAT family, which localize to the ER (Yamashita et al., 2014). However, some AGPATs are involved in both the *de novo* synthesis and in the acyl chain remodeling pathway and have acyltransferase activity toward other lysophospholipids including lysophosphatidylcholine, lysoPI and lysophosphatidylethanolomine. AGPAT1, AGPAT2 and AGPAT3 are broadly distributed in various tissues including the heart and liver (Yamashita et al., 2014). AGPAT1 and AGPAT2 have broad donor specificity for acyl-CoAs while AGPAT3 prefers arachidonoyl-CoA (20:4) and docosahexanoyl-CoA (22:6) (Yamashita et al., 2014). However, the majority of the members of the AGPAT family have not been characterized.

PA is an important precursor molecule used in the production of all phospholipids, but different biosynthetic pathways are used for synthesis of the various phospholipids. PA can be used to produce DAG, which is then used in the production of phosphatidylcholine, phosphatidylethanolamine, phosphatidylserine or triacylglycerol. Alternatively, PA can also be used to produce cytidine diphosphate diacylglycerol (CDP-DAG), which is then used in the production of PI, phosphatidylglycerol or cardiolipin (Shindou et al., 2009; Takeuchi and Reue, 2009; Vance and Vance, 2008).

### 1.4.2. PI synthesis

PI synthesis can occur through two pathways: the *de novo* pathway (Kennedy pathway, as described above) or through the PI cycle. D*e novo* synthesis occurs in the ER and generates PI with mainly saturated and monounsaturated acyl chains (Hicks et al., 2006). The PI cycle however is a cyclical pathway that involves the breakdown and regeneration of PI(4,5)$P_2$ and is thought to

occur at the ER and plasma membrane, possibly as a result of vesicular and/or non-vesicular lipid transfer (Balla, 2013) (Figure 1.5).

The PI cycle is important for the replenishment of $PI(4,5)P_2$ following phospholipase C (PLC) activation. Upon stimulation of G protein-coupled receptors, for example, which activates PLCβ, there is a depletion in plasma membrane $PI(4,5)P_2$ levels (Várnai and Balla, 1998). Following $PI(4,5)P_2$ hydrolysis, the first step of the PI cycle is the phosphorylation of DAG to PA by diacylglycerol kinases (DGKs) in either the ER or plasma membrane (Shulga et al., 2011a). The next step is the formation of CDP-DAG from PA and cytidine triphosphate (CTP), catalyzed by two cytidine-diphosphate synthase (CDS) enzymes, CDS1 and CDS2, both which reside as ER transmembrane proteins (Hermansson et al., 2011). PI synthase (PIS) converts *myo*-inositol and CDP-DAG into PI.

In mammalian cells, PIS was mainly thought to be localized to the tubular ER, however in 2011, PIS was also found to localize to ER-derived motile vesicles (Kim et al., 2011). These PIS vesicles tether to the growing ER, which are thought to remain a part of the ER. The cycling of the GTPase Sar1, which controls ER remodeling events, is required for PIS vesicle motility (Kim et al., 2011). PIS vesicles were termed PIPEROsomes, which stands for PI Producing Endoplasmic Reticulum-derived Organelle (Kim et al., 2011). Fluorescent probes showed that these vesicles do not contain CDS1 or CDS2 (Kim et al., 2011; Qi et al., 2016). Rab10, an important regulator of dynamic ER tubule formation, which localizes to the leading edge of newly formed ER tubules, colocalizes well with PIS (Amber R. English and Voeltz, 2013). It is likely that following the formation of CDP-DAG in the ER, PIS converts CDP-DAG to PI in PIPEROsomes which, through their motile network, may be able to transport PI to various membranes, including the plasma

membrane. Depletion of PI in the ER did not have a significant impact on plasma membrane levels of $PI(4,5)P_2$ suggesting that PI produced in the ER is not sent to the plasma membrane but rather, plasma membrane PI likely originates from PIPEROsomes (Kim et al., 2011).

The final stage of the PI cycle is the regeneration of $PI(4,5)P_2$ through conversion of PI into PI(4)P and finally into $PI(4,5)P_2$ by phosphatidylinositol 4-kinase and PIP5Ks, respectively. Important stages of the PI cycle are i) transport of PA from the plasma membrane to the ER and ii) transport of PI from the ER to the plasma membrane, which are partially mediated by membrane contact sites (MCSs) and transport proteins.

Thus, PI is synthesized in the *de novo* synthesis pathway and in the PI cycle, two distinct but important pathways that ensure cellular PI is available for conversion into PIPs. Following *de novo* synthesis of PI, PI undergoes fatty acid remodeling to ensure it is enriched with a unique fatty acid profile.

### 1.4.3. Fatty acid remodeling – diversifying phospholipid species

Fatty acid composition of phospholipids is an important factor in membrane properties and in the production of lipid mediators. The acyl chains of phospholipids are highly diverse, ranging in length and degree of saturation, resulting in a variety of distinct molecules. The profile of molecular acyl species found in native phospholipids in cells and tissues, however, is often remarkably different than the molecular species found in the precursor molecule PA. The incorporation of select acyl species can occur during *de novo* synthesis and in the remodelling pathway. The remodeling pathway, called the Lands' cycle, involves the replacement of existing fatty acyl chains with activated fatty acids in the form of fatty acyl-CoA, resulting in a chemically

diverse pool of phospholipids (Figure 1.4) (Lands, 1958). Shown in Figure 1.4 is a diagram of the Lands cycle specifically for PI remodeling, however, similar pathways with different enzymes function in the Lands cycle for production of other lipids.

During remodeling, fatty acyl groups from the glycerol backbone are replaced by other fatty acids to form mature molecules. This occurs through the concerted and coordinated action of phospholipases and lysophospholipid acyltransferases involved in deacylation and reacylation, respectively (Shindou et al., 2009; Zhao et al., 2009). Phospholipase $A_1$s ($PLA_1$s) and $PLA_2$s are postulated to be involved in the turnover of the fatty acids on the *sn1* and *sn2* positions, respectively (Yamashita et al., 2014).

Although not well understood, $PLA_1$ enzymes are believed to be involved in the remodeling of the *sn1* fatty acid. Compared with $PLA_2$s, only a few $PLA_1$s have been cloned or characterized. Mammals contain three intracellular $PLA_1$ proteins with similar sequence homology and include DDHD domain containing 1 (DDHD1, also known as PA-$PLA_1$), p125 and KIAA0725, which cleave the *sn1* fatty acid (Richmond and Smith, 2011). DDHD1 and KIAA0725 have been shown to cleave the *sn1* position of both PA and PI *in vitro* (Higgs and Glomset, 1996; Morikawa et al., 2007; Yamashita et al., 2010).

$PLA_2$ enzymes are a large family of over 30 enzymes that are well characterized in their localization, biochemical properties, and sequence homology (Yamashita et al., 2014). $Ca^{2+}$-independent $PLA_2\beta$ (i$PLA_2\beta$) has been proposed to play a key role in the Lands cycle for phosphatidylcholine remodeling (Yamashita et al., 2014). Inhibition of this enzyme results in reduced levels of lysophosphatidylcholine and additionally was shown to increase arachidonoyl incorporation into phosphatidylcholine in macrophages (Balsinde et al., 1997).

Lysophospholipid acyltransferases belong to two different families, AGPAT and membrane bound *O*-acyltransferase (Shindou et al., 2009; Zhao et al., 2009). Mammalian lysophospholipid acyltransferases have broad tissue distribution. Several are responsible for a single biochemical activity, and, the majority have broad substrate specificity (Zhao et al., 2009). For example, lysophosphatidylcholine acyltransferase 1 is expressed in alveolar cells in lungs and shows preference for lysophosphatidylcholine over other lysophospholipids with palmitoyl-CoA as the acyl donor (Bridges et al., 2010). Lysophosphatidylcholine acyltransferase 3 is localized to metabolically active tissues, including lungs and gastrointestinal tract, and can use lysophosphatidylcholine, lysophosphatidylethanolomine and lysophosphatidylserine, with preference for saturated acyl chains as substrates (Zhao et al., 2009). Mice with a mutation resulting in partial loss of lysophosphatidylcholine acyltransferase 1 function present with respiratory failure and decreased saturated phosphatidylcholine content (Bridges et al., 2010). Lysophosphatidylcholine acyltransferase 3 knockout mice exhibit decreased membrane fluidity in hepatocytes (Lee and Tontonoz, 2015). These studies illustrate that considerable regulation of the acyl chain profile of specific phospholipids occurs in cells through a network of PLAs and acyltransferases, which have emerging functions in controlling cell physiology. However, the mechanisms that regulate acyl chain composition of phospholipids and the impact of this regulation on cell physiology are not well understood.

### 1.5. Unique fatty acid enrichment of PI

PI and PIPs show a remarkably unique acyl chain composition compared to other phospholipids. Depending on the tissue and cell type, up to 70% of PI contains 1-stearoyl-2-arachidonoyl

(18:0/20:4) acyl chain content (Baker and Thompson, 1972; D'Souza and Epand, 2015; Hicks et al., 2006). The molecular composition of bi-phosphorylated ($PIP_2$) species found in whole cell extracts of various cell types including HeLa, THP-1 and A432, showed the predominant species was 18:0/20:4 (Ogiso et al., 2010). The enrichment of PI with specific fatty acids can conceivably occur during *de novo* synthesis, the PI cycle and the Lands cycle to produce 1-stearoyl-2-arachidonoyl-*sn*-glycero-3-phosphatidylinositol species (Shulga et al., 2011b). However, studies have shown that the acyl chain content of PI synthesized through the *de novo* pathway contain mainly saturated and mono-unsaturated acyl chains (Luthra and Sheltawy, 1976; MacDonald et al., 1975). The Lands cycle is distinct from the PI cycle in that the Lands cycle remodels the acyl chain content, while the PI cycles alters PI/PIP headgroup. Below, I examine possible mechanisms of establishing PI acyl chain specificity within the *de novo*, PI and Lands cycles.

### 1.5.1. Does acyl chain enrichment occur during de novo synthesis?

Biosynthesis of PI is part of a common pathway involved in the synthesis of other phospholipids. However, compared to PI, other phospholipids do not show similar acyl chain enrichment and thus seems likely that PI undergoes fatty acid remodeling. *In vitro* studies using macrophage microsomes under conditions described to measure *de novo* synthesis (endogenous CDP-DAG and PA with [$^{14}$C]G3P) found the acyl profiles of PA, CDP-DAG and PI contained a broad range of molecular species, where only 2-3% of *de novo* synthesized PI contained 1-stearoyl-2-arachidonoyl acyl species (Nakagawa et al., 1989). Other work showed that newly synthesized PI from rat liver microsomes incubated with dipalmitoyl CDP-DAG and [$^{3}$H]inositol results in dipalmitoyl [$^{3}$H]PI, which is hydrolyzed by $PLA_1$ and then reacylated with stearic acid in the

presence of an acyltransferase (Darnell et al., 1991a, 1991b). These data suggest that the fatty acid present on the *sn1* position of PI is determined by the action of $PLA_1$ and acyltransferases. Another study found significant differences in the acyl chain profile of PI and PA in mouse fibroblasts (Shulga et al., 2010). Additionally, PI in the ER and plasma membrane contain acyl species that are not present in PA, suggesting that PI is undergoing some sort of fatty acid remodeling following *de novo* synthesis (Shulga et al., 2010). Below I will outline some enzymes involved in PI metabolism, including PI synthesis and fatty acid remodeling that show preference for acyl chain profile of the substrate.

### 1.5.2. PI cycle enzymes show substrate specificity

Many enzymes of the PI cycle could contribute to 1-stearoyl-2-arachidoynoyl acyl chain enrichment in PI. One of the critical stages of the PI cycle is the phosphorylation of DAG by DGKs to produce PA. *In vitro* and *in vivo* studies have shown that one isoform of this enzyme, DGKε exhibits preference for its substrate DAG to contain 18:0/20:4 (Bunting et al., 1996; Lung et al., 2009; Shulga et al., 2011c; Topham and Epand, 2009; Walsh et al., 1994). DGKε$^{-/-}$ cells exhibit altered incorporation of stearic acid (Lung et al., 2009) and arachidonic acid (Milne et al., 2008) into PI. There are a number of DGK isoforms expressed ubiquitously in cells, and it is unclear how DGKε functions within the context of other DGKs, most of which do not exhibit substrate specificity for DAG based on acyl chain profile, in order to establish a "preferred" DAG intermediate with a specific acyl profile for PI generation.

Subsequent to DAG production, CDS enzymes produce CDP-DAG from PA. CDS2 appears to show substrate specificity in PA. *In vitro* studies showed that CDS2 prefers PA containing 1-

stearoyl-2-arachidonoyl acyl species (D'Souza et al., 2014). As mentioned above, CDS1 and CDS2 do not localize to PIPEROsomes, which are thought to make contact with a variety of membranes, but have been found to localize to the general ER (Kim et al., 2011).

The other isoforms of DGK and CDS1 however, do not show any acyl chain specificity. The last stage of PI synthesis involves PIS, an enzyme responsible for the production of PI from CDP-DAG and *myo*-inositol. Importantly, PIS does not exhibit acyl chain specificity towards its substrate (D'Souza and Epand, 2015). Hence, for the PI cycle to generate PI with unique acyl chain specificity, DGKε and CDS2 may work together in a form of substrate channelling, where only DAG with 18:0/20:4 is initially selected to produce PA and CDP-DAG for subsequent production of 18:0/20:4-enriched PI by PIS, despite the fact that this last step does not itself have substrate acyl chain preference.

### 1.5.3. PI phospholipases and acyltransferases that may function in the Lands cycle

In addition to the PI cycle, the Lands cycle also plays a role in enriching PI with 1-stearoyl-2-arachidonoyl acyl species. The Lands cycle involves phospholipases and acyltransferases, which function to enrich PI and PIPs with a particular acyl chain profile. Currently, there is no direct evidence that shows the involvement of $PLA_1$ enzymes in fatty acid remodeling in mammals. However, IPLA-1, the *Caenorhabditis elegans* homolog of DDHD1, is involved in the *sn1* fatty acid remodeling of PI (Imae et al., 2010), suggesting that DDHD1 may perform this function in mammalian cells. *Ipla-1* mutants replaced PI containing *sn1* stearic acid with vaccenic acid (18:1n11). Additionally, i*n vitro* studies found that IPLA-1 was able to hydrolyze the *sn1* fatty acid of PI (Imae et al., 2010).

Phospholipase $A_2$ ($PLA_2$) enzymes liberate the *sn2* fatty acid of PI and PIP species (Yamashita et al., 2014). In addition to acyl chain remodeling, some $PLA_2$ enzymes are responsible for producing free arachidonic acid under certain conditions. Arachidonic acid is an important signaling molecule used in the production of eicosanoids, a family of inflammatory compounds (Astudillo et al., 2011). Due to the importance of arachidonic acid in cell and systemic physiology, a substantial amount of research has focused on the enzymes responsible for the release and incorporation of arachidonoyl-CoA at the *sn2* position.

LysoPI acyltransferase 1 (LPIAT1, also known as membrane bound *O*-acyltransferase 7) and LPAAT3 have been shown to preferentially transfer arachidonoyl-CoA onto the *sn2* position of lysoPI and lysoPA, respectively (Gijón et al., 2008; Koeberle et al., 2010). LPIAT1 has been shown to be the major arachidonoyl-CoA acyltransferase in cells, as knockout mice showed significant decreases in 20:4-containing PI and $PI(4,5)P_2$ (Anderson et al., 2013; Lee et al., 2012). $LPIAT1^{-/-}$ mice were viable for 30 days but exhibited a smaller, atrophied cerebral cortex and hippocampus (Lee et al., 2012). Thus, LPIAT1 appears to be critical for neural development of mice and cortical lamination.

In contrast to the remodelling of the *sn2* position, the role of the Lands cycle involving $PLA_1$ enzymes and acyltransferases capable of selecting fatty acid groups and incorporation into lysoPLs is much less clearly understood. As mentioned above, DDHD1 and KIAA0725a show $PLA_1$ activity toward PI, which may generate lysoPI (*sn1*-lyso) within various membrane compartments. Importantly, lysocardiolipin acyltransferase (LYCAT) is suggested to be responsible for the selective incorporation of stearic acid onto the *sn1* position of PI (Imae et al., 2011).

### 1.5.4. PIP metabolizing enzymes with substrate specificity

In addition to selection of 1-stearoyl-2-arachidonoyl containing PI during *de novo* synthesis and the PI cycle, some enzymes involved in PIP conversion exhibit fatty acyl specificity or preference for their PI/PIP substrates. PIPs cycle between the seven different phospho-headgroup species through the action of kinases and phosphatases specific to each phospho-species. Some enzymes involved in PIP conversion exhibit substrate acyl chain profile preference. All three isoforms (α, β and γ) of PIP5K, which convert PI(4)P to PI(4,5)$P_2$, have been shown to prefer PI(4)P containing 18:0/20:4 and 18:0/18:1 over 16:0/16:1 (Shulga et al., 2012, 2011b). Kinetic analyses show that the isoforms exhibit highest activity for PI(4)P containing 1-stearoyl-2-arachidonoyl acyl species, with the difference in selectivity being largest for isoform γ (Shulga et al., 2012).

In addition, OCRL and synaptojanin-1, responsible for converting PI(4,5)$P_2$ to PI(4)P, also exhibit preference for PI(4,5)$P_2$ acyl chain content. Both OCRL and synaptojanin-1 show varying degrees of 18:0/20:4 substrate specificity with OCRL being much more selective (Schmid et al., 2004). Thus, enzymes from the PI cycle and the Lands cycle work together to ensure PI and PIP species are enriched with a 1-stearoyl-2-arachidonoyl acyl profile.

## 1.6. Transport of phospholipids in cells

An important aspect of organelle identity and function is the unique composition of lipids within the membrane of each organelle. In order for this to occur, cells transport lipids from the site of synthesis to target membranes. Due to the amphipathic nature of phospholipids, they need to be transported by specialized mechanisms from the ER to their target membranes. Cells have

various mechanisms of lipid transport, including lateral diffusion within a membrane (a spontaneous process), vesicular transport and non-vesicular transport mediated by MCSs and lipid transfer proteins (Lev, 2010; Loewen et al., 2003; van Meer et al., 2008). As the ER is the main organelle for lipid synthesis, it employs its vast network to make ER contacts with various other organelle membranes (Cullen, 2011; Lahiri et al., 2014; van Meer et al., 2008). At these ER-organelle contact sites, lipid transfer proteins facilitate non-vesicular exchange of lipids from the ER to target membranes (Giordano et al., 2013a; Toulmay and Prinz, 2011).

### 1.6.1. Membrane contact sites

The distance between MCSs can range from 10-30 nm in cytosolic gaps (Lahiri et al., 2015; Lev, 2010; Mesmin et al., 2013). MCS do not fuse with adjacent membranes but are stabilized by tethering proteins that maintain close proximity (Figure 1.6). Thus, non-vesicular lipid transport requires machinery that can tether two membranes to bridge the cytosolic gap, extract a lipid out of a membrane, protect it from the aqueous cytosolic environment and insert the lipid into the target membrane. Many lipid transfer proteins localize to MCSs (Lev, 2010). MCSs are highly dynamic structures that form in response to physiological conditions (Lev, 2010). Two integral ER-membrane proteins called vesicle-associated membrane proteins (VAPs), VAPA and VAPB, are key proteins involved in tethering of the ER to other membranes (Dong et al., 2016). The N-terminus of VAPs binds to many lipid transfer proteins containing FFAT (phenylalanines in an acid tract) motifs, which are typically enriched at MCSs for example, between the ER and plasma membrane (Dong et al., 2016; Lev, 2010).

MCSs exist between many different organelles including the ER-Golgi, ER-endosomes, ER-mitochondria and ER-plasma membrane. MCS have been observed between epidermal growth factor (EGF) receptor (EGFR)-containing late endosome/lysosomes and the ER (Eden et al., 2010). The ER protein tyrosine phosphatase, PTP1B, interacts with EGFR in multi-vesicular bodies where it plays a dual role in tethering the membranes as well as helping sequester the receptor for transport to the lysosome and causing dephosphorylation of EGFR (Eden et al., 2010). ER-endosome MCSs help regulate endosomal traffic (Phillips and Voeltz, 2016). Membrane contacts have also been observed between mature late endosome/lysosomes and the ER, which is mediated by the cholesterol sensor, oxysterol-binding protein (OSBP)-related protein 1L (ORP1L) which binds the late endosome/lysosomal small GTPase Rab7 and ER-localized VAPA (Rocha et al., 2009). This interaction is dependent on cholesterol levels (Rocha et al., 2009).

At ER-plasma membrane MCSs, the ER-resident proteins called extended synaptotagmin 1, 2 and 3 (E-Syt1, E-Syt2 and E-Syt3) tether the two membranes by binding $PI(4,5)P_2$ (Fernández-Busnadiego et al., 2015; Schauder et al., 2014). E-Syts contain an N-terminal anchor, which embeds in the ER, a synaptotagmin-like mitochondrial-lipid binding protein domain and C2 domains (Giordano et al., 2013a). The tethering function between the ER and plasma membrane is mediated by the C2 domain binding to $PI(4,5)P_2$ at the plasma membrane and by cytosolic $Ca^{2+}$. E-Syt2 and E-Syt3 bind to the plasma membrane at resting $Ca^{2+}$ levels while E-Syt1 binding is only triggered upon an increase in cytosolic $Ca^{2+}$ (Chang et al., 2013; Giordano et al., 2013a). These are just a select few MCSs that exist, which enable transport of lipids between membranes in order to maintain unique membrane composition.

### 1.6.2. Membrane contact sites involved in PI transport

More pertinent to PI and PIPs are MCSs that are responsible for the transport and control of PI and PIPs including ER-plasma membrane, ER-Golgi and ER-endosomes contact sites. The ER contains an integral membrane protein called Sac1, a 4-phosphatase, which, through MCSs, can regulate PI(4)P levels *in trans* on the plasma membrane and Golgi (Nemoto et al., 2000). The ER membrane proteins ORP5 and ORP8 tether the ER to the plasma membrane by binding PI(4)P via a PH domain. Simultaneously, ORP5 and ORP8 negatively regulate the levels of PI(4)P at the plasma membrane through exchange of phosphatidylserine to the plasma membrane and PI(4)P to the ER where Sac1 is localized (Chung et al., 2015) (Figure 1.6). As PI(4)P is transported to the ER and converted to PI, a gradient is established which drives phosphatidylserine transport to the plasma membrane (Chung et al., 2015).

MCS between the ER and Golgi are also involved in maintaining a PI(4)P gradient where OSBP acts as a sterol/PI(4)P exchanger (Levine and Munro, 1998; Mesmin et al., 2013). After cholesterol is transported from the ER to the t*rans*-Golgi, PI(4)P is then transported back to the ER for PI(4)P breakdown into PI (Mesmin et al., 2013). The PI(4)P gradient ensures directional sterol transport to the Golgi while simultaneously controlling PI(4)P levels.

These MCSs, where OSPB/ORP family cooperate with Sac1 on the ER, are important in negatively regulating PI(4)P levels (Chung et al., 2015; Mesmin et al., 2013; Moser von Filseck et al., 2015; Stefan et al., 2011). The pathways discussed above maintain sterol/phosphatidylserine transport dependent on the metabolic energy of PI(4)P. The hydrolysis of PI(4)P by Sac1 is responsible for maintaining this PI(4)P gradient where higher levels of PI(4)P occur on other

membranes, which in turn allows for the transport of sterol/phosphatidylserine from higher concentrations on the ER membrane to other membranes.

MCSs between the ER and endosomes involve sorting nexin 2 binding to VAP on the ER, thus sorting nexin 2 is a tether between ER and endosome MCSs. Sorting nexin 2 is a subunit of the retromer complex involved in retrograde traffic between the ER and Golgi. Working alongside sorting nexin 2 at ER-endosome MCS is OSBP, which mediates the transport of PI(4)P from endosomes to the ER for degradation (Dong et al., 2016). Unlike the membranes, which exchange PI(4)P for phosphatidylserine or sterol, this pathway of PI(4)P transport does not drive lipid transport of another lipid.

An additional MCS exists between the ER and late endosome. The ER transmembrane protein protruding binds to Rab7 and PI(3)P, localized on late endosomes, and is responsible for tethering the two membranes together (Raiborg et al., 2015). This interaction promotes plus-end directed traffic of late endosomes in neutrite outgrowths (Raiborg et al., 2015). PIPs are important in maintaining MCSs between various organelles, which help with the transport of sterol/cholesterol or help in ensuring proper cellular function.

### 1.6.3. Lipid transport proteins

Lipid transport at MCSs is greatly facilitated by lipid transfer proteins. Based on binding specificity and transfer capabilities, lipid transfer proteins can be grouped into three classes: phospholipid-, sterol- and sphingolipid-transfer proteins. In mammals, three classes of phospholipid transfer proteins exist, phosphatidylcholine-transfer protein, PI-transfer protein and the non-specific lipid transfer protein (NSLTP, also known as sterol carrier protein 2) (Gadella and Wirtz, 1994; Lev,

2010; Wirtz, 2006). OSBP and ORPs are considered sterol-transfer proteins. An example of sphingolipid-transfer protein is ceramide-transfer protein, which transport ceramide at ER-Golgi MCSs (Kawano et al., 2006).

Extensive *in vitro* studies have resolved the crystal structure and mechanism of lipid transfer proteins (Lahiri et al., 2015; Lev, 2010). The size of the hydrophobic pocket of lipid transfer proteins dictates lipid binding while the lid protects the lipid from the cytosolic aqueous environment (Lev, 2010; Wirtz, 2006). Lipid transfer proteins can exist in two different confirmations; closed confirmation when a lipid is enclosed in the pocket and open confirmation, when bound to a membrane (Lev, 2010). Lipid transfer proteins act to decrease the energy barrier between two membranes and facilitate the desorption of the lipid from the membrane (Lalanne and Ponsin, 2000).

Lipid transfer proteins are important in ensuring membranes transport the correct lipids in order to maintain membrane identity and function. There have been many studies that shows phosphatidylcholine-transfer protein binds exclusively to phosphatidylcholine (Kanno et al., 2007). One study monitored the transfer of radiolabelled phosphatidylcholine between membranes and determined that phosphatidylcholine-transfer protein specifically binds to the headgroup of phosphatidylcholine and found that binding is very sensitive to changes in headgroup (Kamp et al., 1977). *In vitro* studies using a fluorescence based approach to study the transfer of lipids from a donor to acceptor membrane showed NSLTP to be promiscuous in its binding capabilities ranging from diacetyl phospholipids, to cholesterol and glycolipids (Gadella and Wirtz, 1994). One function of the cytosolic NSLTP is cholesterol transport to the plasma membrane and to the peroxisome for β-oxidation of fatty acids (Wirtz, 2006). PI-transfer proteins

exhibit specificity for phosphatidylcholine and PI and transport these lipids based on the concentration of lipid present in the membrane (Kasper and Helmkamp, 1981). OSBP and the twelve mammalian ORPs have been proposed to be sterol-sensing and/or sterol-transfer proteins (Beh and Rine, 2004; Raychaudhuri et al., 2006). OSBP has a dual role of lipid transporter and ER-Golgi tether (Mesmin et al., 2013).

### 1.6.4. PI-transport proteins

More applicable to the transport of PI and PIPs are PI-transfer proteins. Mammals contain two different PI-transfer protein classes, class I and class II, which contain an N-terminal PI-transfer protein domain. PI-transfer proteins have been shown to be required for important signaling events including PLC-mediated hydrolysis of PI(4,5)$P_2$ at the plasma membrane (Y. J. Kim et al., 2013). PI-transfer proteins are important in controlling the lipid composition of membranes by ensuring membranes are enriched with particular PIPs that are required for these signaling events.

Class I is composed of PI-transfer protein α and PI-transfer protein β, which transfer PI and phosphatidylcholine between membranes *in vitro* (Phillips et al., 2006; Van Paridon et al., 1987). PI-transfer protein α is localized in the cytosol and nucleus, while PI-transfer protein β is localized in the cytosol and Golgi (de Vries et al., 1996). PI-transfer protein α is important in the nucleus to transport PIPs that bind to nuclear receptors; for example, PI(3,4,5)$P_3$ has been shown to stabilize steroidogenic factor-1 (Blind et al., 2014).

Class II PI-transfer proteins contains N-terminal domain-interacting receptor 2 and 3 (Nir2 and Nir3), and PI-transfer protein, cytoplasmic 1 (PITPNC1). Nir2 has been shown to be

responsible for the replenishment of PI(4,5)$P_2$ at the plasma membrane following receptor activation (Chang and Liou, 2015). Nir2 localizes to the cytosol and Golgi, but translocates to the plasma membrane following an increase in PA levels following growth factor stimulation or PLC activation (Chang and Liou, 2015; S. Kim et al., 2013; Kim et al., 2015). Nir2 contains a motif specific for VAPA and VAPB binding and a PH domain, which binds PI(4)P on the Golgi (Chang et al., 2013; Loewen et al., 2003). In resting cells, Nir2 plays a role in DAG levels in the Golgi, which is important for protein transport (Litvak et al., 2005). However, receptor stimulation resulting in low levels of PI(4,5)$P_2$ causes Nir2 to translocate to the plasma membrane where it assists in replenishing PI for PI(4,5)$P_2$ resynthesis (Chang et al., 2013; Chang and Liou, 2015; S. Kim et al., 2013). *In vitro* studies have shown that Nir2 is responsible for transporting PI from the ER to plasma membrane (Garner et al., 2012) (Figure 1.6). Using fluorescent probes in combination with pharmacological inhibitors, it was determined that Nir2 also binds to PA and plays an important role at ER-plasma membrane MCSs where it transports PA from the plasma membrane to the ER (Kim et al., 2015).

Additionally, E-Syt1 has been shown to be functionally linked to Nir2 to help mediate ER-plasma membrane contacts and assists in Nir2 recruitment during low PI(4,5)$P_2$ levels (Chang et al., 2013; Saheki et al., 2016). Thus, Nir2 acts as a PI-PA exchanger between the plasma membrane and ER. It could be possible that Nir2 plays a role in transporting PIPEROsome-mediated synthesis of PI to the plasma membrane during the PI cycle.

Nir3 functions have not been well characterized compared to its homologue, Nir2. Nir3 is responsible for maintaining basal levels of PI(4,5)$P_2$ by binding to PA at ER-plasma membrane MCSs (Chang and Liou, 2015). Using fluorescently labelled Nir3 and total internal reflection

fluorescence microscopy (TIRF-M), it was found that Nir3 is more sensitive to levels of PA than Nir2 and upon treatment with PA, Nir2 translocated from the cytosol to the ER-plasma membrane contacts. This was also confirmed with liposome sedimentation assays using recombinant Nir2 and Nir3 proteins (Chang and Liou, 2015).

Using purified PITPNC1 and liposomes, a fluorescent dequenching assay found that PITPNC1 preferentially binds PA produced from the phospholipase D pathway in addition to binding to PI (Garner et al., 2012). Analysis of PI or PA acyl species bound to isolated PITPNC1 showed that PITPNC1 preferred PI 18:0/20:4 and PA 16:0/16:1 and 16:1/18:1 (Garner et al., 2012). It has not yet been shown whether PITPNC1 is involved in PA transport from the plasma membrane to the ER, but it has been shown that PA produced from the phospholipase D pathway may not be used for PI resynthesis (Whatmore et al., 1999).

In addition to E-Syts playing a role in tethering of the ER-plasma membrane MCSs, studies have shown that they may also be involved in lipid transport. Mass spectrometry analysis of E-Syt2 expressed in mammalian cells showed that E-Syt2 co-purifies with several phospholipids including phosphatidylcholine, phosphatidylethanolamine and PI, showing no preference of lipid (Schauder et al., 2014). One model suggests that E-Syt2, in addition to tethering the ER-plasma membrane, can also function in concert with other lipid transfer proteins to transfer lipids between membranes (Schauder et al., 2014). Tethering proteins, MCSs and PI-transfer proteins are essential for the proper regulation and transport of PI and PIPs to various cellular membranes. Non-vesicular lipid transport is essential in regulating PIP levels on various membranes, which ensures organelles contain distinct profile of PIPs responsible for regulating organelle dynamics and functions.

## 1.7. PIPs are key regulators of cellular processes

After PI is synthesized and transported to the proper membranes, inositol kinases and phosphatases synthesize appropriate PIPs, which are then able to perform specialized functions. Three of the most well-studied PIPs, PI(4,5)$P_2$, PI(3)P and PI(3,4,5)$P_3$ are responsible for regulating key events that maintain homeostasis. The proper maintenance of these lipids on organelle membranes allows them to regulate cellular processes including endocytosis, endosomal maturation and signaling for cell growth. Here, I discuss these aspects of regulation and the individual functions of PI(4,5)$P_2$, PI(3)P and PI(3,4,5)$P_3$.

### 1.7.1. Phosphatidylinositol-4,5-bisphosphate

PI(4,5)$P_2$ is mainly localized to the plasma membrane where levels are subject to tight regulation through a variety of lipid metabolizing enzymes including PI kinases and inositol 4- and 5-phosphatases. Type I PIP5Ks are largely responsible for PI(4,5)$P_2$ synthesis in mammals (Antonescu et al., 2011; Nakatsu et al., 2010; Shulga et al., 2012). A dimerization motif in the N-terminus of PIP5Ks is required for plasma membrane localization and for PI(4,5)$P_2$ synthesis (Lacalle et al., 2015). The kinase activity of type I PIP5Ks were shown to be upregulated in the presence of PA (up to ten fold) (Jarquin-Pardo et al., 2007; Jenkins et al., 1994). Thus, enzymes responsible for PA production (phospholipase D and DGKs) could ultimately regulate PIP5K activity. Additionally, autophosphorylation and phosphorylation by protein kinase A within the catalytic domain suppresses PIP5K activity (Kwiatkowska, 2010). One study, using a protein-lipid overlay assay and PI(4,5)$P_2$ liposomes found that PIP5K binds to PI(4,5)$P_2$ and acts as an anchor

in the plasma membrane (Kwiatkowska, 2010; Szymańska et al., 2008). Another route of PI(4,5)$P_2$ synthesis, though minor, is from PI(5)P by PI4-kinases (Gericke et al., 2013) (Figure 1.2).

There are many 5-phosphatases responsible for the turnover of PI(4,5)$P_2$ including synaptojanin-1 and OCRL. Synaptojanins contain a phosphatase domain at the C terminus, which is responsible for hydrolyzing PI(4,5)$P_2$ to PI(4)P (Erneux et al., 1998).

*In vitro* studies have shown that plasma membrane levels of PI(4,5)$P_2$ are continuously and dynamically maintained by two pools of PI(4)P localized to the Golgi and plasma membrane, with the later contributing more (Dickson et al., 2014; Szentpetery et al., 2010). One model that has been proposed suggests that after PI is produced in the ER, it is delivered to the plasma membrane and Golgi via transport proteins (D'Souza and Epand, 2015; Dickson et al., 2014). Type IIIα PI4-kinases produce PI(4)P at the Golgi and plasma membrane (Dickson et al., 2014; Graham and Burd, 2011). Depletion of PI(4)P at the plasma membrane does not have significant effects on PI(4,5)$P_2$ cell surface levels (Hammond et al., 2012). Thus, it has been proposed that Golgi PI(4)P pools help supplement PI(4)P levels at the plasma membrane in addition to being converted into PI(4,5)$P_2$ upon transit from the Golgi to plasma membrane (Dickson et al., 2014).

PI(4,5)$P_2$ is a substrate for PLC signalling, which was one of the first functions identified for PI(4,5)$P_2$ (Berridge and Irvine, 1984). DAG produced from PI(4,5)$P_2$ plays a large role in PI resynthesis in the PI cycle, but also can remain at the cell surface where it activates protein kinase C, which in turn activates other cytosolic proteins through phosphorylation and effectors including plasma membrane ion channels (Mochly-Rosen et al., 2012). $IP_3$ enters the cytosol where it activates $IP_3$ receptors on the ER opening $Ca^{2+}$ channels and allowing $Ca^{2+}$ to enter the cytosol where it can then elicit $Ca^{2+}$-dependent signals. This includes stimulation of calcineurin,

which dephosphorylates the transcription factor, nuclear factor of activated T cells (NFAT), which then enters the nucleus to transcribes genes involved in cell proliferation (Feske, 2007). *In vitro* studies in HeLa cells showed PI(4,5)$P_2$ levels declined rapidly after PLC activation, resulting in redistribution of the PI(4,5)$P_2$ probe to the cytosol (Dong et al., 2016). Furthermore, prolonged receptor activation can lead to a compensatory burst of PI(4,5)$P_2$ resynthesis from PI(4)P, which was determined to be sourced from PI(4)P pools at the plasma membrane (Dong et al., 2016). Thus, PI(4,5)$P_2$ levels are highly dynamic and possess many mechanisms to control them.

### 1.7.2. PI(4,5)$P_2$ regulates clathrin mediated endocytosis

PI(4,5)$P_2$ is required for CME, a process that internalizes receptors and their ligands, transporters and other integral membrane proteins (collectively termed cargo) from the plasma membrane. CME is a highly controlled process, which is dependent on the recruitment of multiple factors including clathrin, cargo-binding adaptors such as adapter protein-2 (AP2) and endocytic accessory proteins to the plasma membrane (Antonescu et al., 2011; Garay et al., 2015; Porat-Shliom et al., 2013). PI(4,5)$P_2$ is a key regulator of this process as it is the main lipid binding partner of clathrin and many endocytic accessory proteins, including AP2, sorting nexin 9, epsin, CALM/AP180 and dynamin (Antonescu et al., 2011; Jost et al., 1998; Perera et al., 2006).

To initiate the process of CME, PI(4,5)$P_2$ recruits AP2 which recruits clathrin, which assemble into clathrin-coated pits (CCPs), structures that are formed by assembly of clathrin into lattices on the inner leaflet of the plasma membrane. These clathrin complexes act as scaffolds for the recruitment of cargo receptors and endocytic accessory proteins. Following membrane invagination and constriction of the neck of the CCP, the GTPase dynamin2 scissions the neck of

the pit forming a clathrin-coated vesicle (CCV) (Loerke et al., 2009). During the various stages of CCV formation, multiple 5-phosphatases (examples of endocytic accessory proteins) bind to clathrin, AP2 or other endocytic accessory proteins and localize to CCPs including OCRL, synaptojanin-1 and synaptojanin-2, all which regulate $PI(4,5)_2$ turnover (Antonescu et al., 2011; Perera et al., 2006). The spatial-temporal metabolism of $PI(4,5)P_2$ synthesis and turnover varies depending on the lifetime of the CCP (Antonescu et al., 2011; Perera et al., 2006).

Bulk $PI(4,5)P_2$ levels produced by PIP5K that localize diffusely within the plasma membrane regulate CCP assembly. In contrast, the localized turnover of $PI(4,5)P_2$ within CCPs by synaptojanin-1 and other 5-phosphatases controls multiple stages of CCV formation (Antonescu et al., 2011), including abortive turnover of some CCPs without producing an intracellular vesicle, vesicle scission and vesicle uncoating (Loerke et al., 2009). Synaptojanin-$1^{-/-}$ mice showed prolonged CCP formation, indicating that the hydrolysis of $PI(4,5)P_2$ by synaptojanin-1 is an important trigger for clathrin uncoating and is a key component of CME (Cremona and De Camilli, 2001; Hayashi et al., 2008).

One of the most commonly studied models of CME is transferrin (Tfn) receptor (TfR) endomembrane traffic (Maxfield and McGraw, 2004; Navaroli et al., 2012; Sheff et al., 2002). TfR is responsible for transporting the essential nutrient iron into the cell. Iron plays a vital role in oxygen uptake, electron transfer in the mitochondria, energy metabolism and muscle function. Iron is absorbed into circulation from nutrition by duodenal enterocytes and by macrophages, which release iron from internalized old red blood cells (Ludwig et al., 2015). Iron can also be stored in ferritin protein complexes, which are present in all cells. Iron levels in the blood are regulated by Tfn, a glycoprotein that has two high affinity binding sites for ferrous iron ($Fe^{3+}$).

TfR1 is a type II transmembrane glycoprotein that typically exists as a homodimer of 180 kDa (Daniels et al., 2006). Two disulfide bonds join two TfR monomers, each which contain a large C terminal domain responsible for binding to Tfn and a short N terminal domain. The intracellular N terminus contains a YTRF-motif that is required for internalization via binding to AP2 in the clathrin complex (Antonescu et al., 2014). TfR is regulated at the post-translational level dependent on intracellular iron levels through mRNA stability (Daniëls et al., 2014).

At the pH of the extracellular space, 7.4, iron-containing Tfn preferentially binds to TfR. This triggers the internalization of the TfR/Tfn/$Fe^{3+}$ complex via CME into CCVs. Once the complex is in the mildly acidic endosome, pH 5.5-6, $Fe^{3+}$ dissociates from the TfR/Tfn complex and is transported to the cytosol via the divalent metal transporter 1 (Yu et al., 2007). Tfn remains bound to TfR due to its high affinity to the receptor in acidic conditions. Following release of $Fe^{3+}$, the TfR/Tfn complex is recycled back to the plasma membrane. Following fusion of recycling endosomes with the plasma membrane and exposure to the neutral pH, Tfn is released due to it having 500 fold lower affinity for the receptor (Antonescu et al., 2014). TfR is constitutively internalized and recycled, with or without ligand binding. TfR recycles to the plasma membrane with a half-time of 10-15 min (van Dam et al., 2002).

Following internalization, TfR can undergo two distinct recycling pathways that differ in kinetics back to the plasma membrane (Figure 1.7). By following the movement of fluorescent Tfn through various endosomal pools, it was determined that 80-90% of Tfn recycles through the fast recycling pathway, which takes approximately 30 mins and transports Tfn from early endosomes to the plasma membrane, while the remaining TfR recycles through the slow recycling pathway through early endosomes to recycling endosomes to the plasma membrane

and takes 60-90 mins (Sönnichsen et al., 2000; van Dam et al., 2002). TfR traffic through the fast recycling pathway is regulated by Rab5 and Rab4 positive compartments, while the slow recycling pathway is regulated by Rab4 and Rab11 positive compartments (Kubo et al., 2015; Sönnichsen et al., 2000; Ullrich et al., 1996). Rab proteins cycle between active GTP-bound state and inactive GDP-bound state acting as an on and off switches. Rab proteins interact with many factors including sorting adaptors, tethering factors, kinases and phosphatases and motor proteins, all which are involved in the sorting of cargo, transport of vesicles and tethering of transport vesicles to target membranes (Ebine et al., 2011; Pasqualato et al., 2004). TfR endomembrane traffic has been extensively studied and represents a model that is commonly used to study CME and recycling.

### 1.7.3. Phosphatidylinositol-3-phosphate

PI(3)P is highly concentrated on endosomal membranes and plays a role in receptor signaling, endosomal tethering and fusion, and sorting of cargo. Proteins containing FYVE finger binding domains, such as early endosomal antigen 1 (EEA1), exclusively bind PI(3)P while the PX protein binding domains bind predominantly, but not exclusively, to PI(3)P (Bago et al., 2014; Gillooly et al., 2000; Lawe et al., 2000). PI(3)P is important for homo- and heterotypic fusion of EE via effector proteins involved in cargo sorting and transport to lysosomes, *trans*-Golgi network or plasma membrane. Endosomes containing cargo destined for degradation in the lysosome will mature along the pathway and require PI(3)P conversion to $PI(3,5)P_2$ by PIKfyve, a 5-kinase, which is required for degradation in the lysosome (Huotari and Helenius, 2011; Liu et al., 2016).

There are three classes of PI3Ks. Class I is the most studied, responsible for the production of PI(3,4,5)$P_3$. Type II is the least studied and type III, which contains the single isoform Vps34, is responsible for the production of PI(3)P from PI (Bago et al., 2014). Vps34 is unique among the other PI3Ks, as it only utilizes PI as a substrate. This is thought to be due to the relatively uncharged substrate recognition loop, compared to class I and II, which contain basic residues that can accommodate the negative charges of their substrates (Pirola et al., 2001). Though Vps34 is not the only source of PI(3)P, the use of an anti-Vps34 function blocking antibodies caused a 70% reduction of PI(3)P in endosomal fractions (Shin et al., 2005). Vps34 has been shown to play important roles in the Golgi-to-lysosome transport pathway (Brown et al., 1995), multi-vesicular body formation (Futter et al., 2001) and autophagy (Petiot et al., 2000).

Vps34 has been shown to be the major lipid kinase at the EE and is recruited via the GTPase Rab5. There are many mechanisms that regulate Vps34 activity including the kinase domain of p150 (Backer, 2008). Additionally, binding of Vps34 to the accessory protein Beclin-1 is required for autophagy (Backer, 2008). AMPK, a nutrient sensor, which functions to maintain energy homeostasis upon nutrient starvation in the cell (Hardie, 2007), has been shown to regulate different Vps34 complexes involved in pro- and non-autophagy pathways through phosphorylation of Beclin-1 or Vps34, respectively (J. Kim et al., 2013).

Another mechanism of PI(3)P production is through the conversion of PI(3,4,5)$P_3$ to PI(3,4)$P_2$ by the 5-phosphatase SHIP1 and then conversion to PI(3)P by the 4-phosphatase INPP4B (Bago et al., 2014), which has been shown to also be regulated by Rab5 (Shin et al., 2005). Myotubularin 1 (MTM1), a 3-phosphatase, is responsible for hydrolyzing PI(3)P to PI (Bago et al., 2014; Hsu and Mao, 2015).

### 1.7.4. PI(3)P and effector proteins regulate endosomal pools

The traffic and sorting of cargo through the endosomal pathway depends on the spatial and temporal regulation of PI synthesis and degradation and recruitment of effector proteins. As mentioned above, the presence of the GTPase Rab5 on early endosomes leads to the recruitment of Vps34 (Christoforidis et al., 1999; Jovic et al., 2010), which synthesizes PI(3)P. PI(3)P works together with Rab5 to coordinate the assembly of effector proteins involved in endosome function and maturation. There are multiple Rab proteins in the cell, but particularly Rab4, Rab5 and Rab11 are associated with early endosomes and recycling endosomes and Rab7 and Rab9 are associated with late endosomes (Liu et al., 2016; Mellman, 1996; Sheff et al., 2002) Rab proteins are often used to visualize various endosomal compartments in the cell. *In vivo* studies have shown that a loss of Rab5 disrupts the proper assembly of endocytic machinery resulting in reduced numbers of early endosomes, recycling endosomes and late endosomes, which significantly impacts endomembrane traffic (Zeigerer et al., 2012). Together, Rab5 and PI(3)P are important regulators in endosome maturation and fusion.

Within the context of this model of acquisition of early endosomal markers for vesicles derived from the plasma membrane, a large fraction of CCVs become PI(3)P positive endosomes containing EEA1, the latter which is involved in endosome tethering and fusion (Christoforidis et al., 1999). Recently it was determined that EEA1 undergoes conformational changes that allows for tethering and fusion events. As EEA1 tethers onto a vesicle, binding to Rab5 on the vesicle causes EEA1 to collapse and become flexible, which generates a force that pulls the vesicle toward the target membrane (Murray et al., 2016).

Not all endosomes, however, mature into EEA1 positive vesicles immediately following internalization. Depending on the cargo a fraction of endosomes will acquire APPL1 prior to maturing into EEA1-containing endosomes (Zoncu et al., 2009). Vesicles containing growth factor receptors such as EGFR have been shown to acquire APPL1 and acts as platforms for signaling complexes (Schenck et al., 2008). Zoncu *et al* found that in order for these endosomes to mature from APPL1 to EEA1 labelled compartments, a molecular PI switch involving PI(3)P synthesis from PI is required (Zoncu et al., 2009). Inhibition of PI3K with wortmannin or by using the inducible recruitment of the PI3-phosphatase, MTM1, to early endosomes resulted in EEA1 compartments disappearing and the appearance of more APPL1 compartments, particularly in the central regions of the cell where they were not normally found (Zoncu et al., 2009). Furthermore, they found that without this molecular switch there was enhanced growth factor signaling (Zoncu et al., 2009).

The conversion of PI(3)P to PI by MTM1 is another molecular switch, that is, in this case, required for proper endosome maturation required for exocytosis. Knockdown of MTM1 in HeLa cells reduced levels of TfR exocytosis but had no effect on TfR internalization (Ketel et al., 2016). This caused an accumulation of TfR REs underneath the cell surface that failed to fuse with the plasma membrane but was rescued by re-expression of MTM1. This suggests a critical role for PI(3)P in controlling the maturation of endosomal pools and for signaling and begs the question whether other aspects of the endosomal pathway are regulated by PIPs.

### 1.7.5. Phosphatidylinositol-3,4,5-trisphosphate

$PI(3,4,5)P_3$ is involved in pathways that control many aspects of cell physiology including cell proliferation, survival and metabolism. Proteins that contain PH domains can bind to $PI(3,4,5)P_3$ (Klippel et al., 1997). $PI(3,4,5)P_3$ is localized to the plasma membrane and is mainly produced from $PI(4,5)P_2$ by class I PI3Ks (Martini et al., 2014). PTEN reverses this reaction and is often mutated or otherwise rendered partly or completely non-functional in many types of cancers (Díaz et al., 2012; Downes et al., 2007). In addition to PTEN, $PI(3,4,5)P_3$ is negatively regulated by multiple 5-phosphatases, which convert $PI(3,4,5)P_3$ to $PI(3,4)P_2$, including SHIP2, synaptojanin-1 and OCRL (Nakatsu et al., 2010).

In resting cells, levels of $PI(3,4,5)P_3$ are nearly undetectable, however upon activation of PI3Ks by receptor tyrosine kinases and G protein-coupled receptors, levels of $PI(3,4,5)P_3$ increase (Asano et al., 2007; Toker and Cantley, 1997; Zhao and Vogt, 2008). One example of receptor tyrosine kinase signaling is insulin binding to the insulin receptor, which activates PI3K and also causes the translocation of the glucose transporter, GLUT4 to the plasma membrane (Asano et al., 2007). This pathway is necessary for glucose uptake into the cell.

### 1.7.6. $PI(3,4,5)P_3$ regulates PI3K/Akt signaling pathway

EGFR, also known as ErbB-1, is a receptor tyrosine kinase that can trigger signaling cascades that activate PI3K/Akt, MAPK and STAT pathways (Díaz et al., 2012; Garay et al., 2015) (Figure 1.8). The PI3K/Akt pathway controls cell survival, proliferation, migration and metabolism and is implicated in a number of different cancers. EGF ligand binding activates the kinase domain of EGFR resulting in the autophosphorylation of multiple tyrosine residues on its intracellular domain (Díaz et al., 2012; Garay et al., 2015; Wu et al., 2006). This recruits the adapter protein,

growth factor receptor-bound protein 2 (Grb2), which binds to the receptor and mediates the binding of growth factor receptor protein 1 (Gab1). Phosphorylation of Gab1, once recruited to the EGFR complex, creates a docking site for class I PI3K (Díaz et al., 2012). The tyrosine phosphatase SHP2 is also recruited to a distinct phospho-tyrosine motif on Gab1, and has been shown to dephosphorylate the PI3K-interacting motif on Gab1, resulting in termination of PI3K recruitment thereby impacting further signaling (Zhang et al., 2002). However, the regulation of PI3K by SHP2 is complex, as SHP2 may also directly recruit PI3K to receptor complexes.

PI3K contains two subunits, the catalytic subunit, p110 and the regulatory subunit, p85, p50 or p55 (Díaz et al., 2012; Downes et al., 2007; Fruman et al., 1998). The conversion of $PI(4,5)P_2$ to $PI(3,4,5)P_3$ by PI3K recruits Akt via its PH domain, which binds $PI(3,4,5)P_3$. This causes a conformational change in Akt, exposing two phosphorylation sites, Thr308 and S473 (Song et al., 2005). Phosphoinositide-dependent kinase-1 (PDK1) binds Akt directly and also binds $PI(3,4,5)P_3$ with its PH domain and phosphorylates Thr308 on Akt. Full activation of Akt also requires phosphorylation of S473 by mammalian target of rapamycin complex 2 (mTORC2) (Bago et al., 2014; Díaz et al., 2012; Downes et al., 2007).

Akt, or protein kinase B (PKB), is a serine/threonine protein kinase that exists in three different isoforms, Akt1, Akt2 and Akt3 in mammals. All three isoforms contain an N-terminal PH domain, a central kinase domain and a C-terminal regulatory domain (Song et al., 2005). Studies in mice have indicated that Akt1 plays a dominant role in fetal growth, embryonic development and fetal survival (Dummler et al., 2006), Akt2 functions in glucose homeostasis (Cho et al., 2001) and Akt3 functions in postnatal brain development (Yang et al., 2004). Using isoform specific antibodies, studies on the cellular localization of each isoform discovered that in basal

(unstimulated cells); Akt1 primarily localizes to the cytoplasm and plasma membrane, Akt2 localizes to the mitochondria and Akt3 localizes to the nucleus (Santi and Lee, 2010). Upon insulin-stimulated activation of Akt in adipocytes, using TIRF-M and Flag-tagged constructs, both Akt1 and Akt2 localized to the plasma membrane, though the levels of Akt2 recruiter were significantly greater (Gonzalez and McGraw, 2009) (Gonzalez and McGraw, 2009). However, rat adipocytes and skeletal muscle cells stimulated with insulin found Akt2 localizes to APPL1 endosomes as assessed by co-immunoprecipitation (Saito et al., 2007). Although the various Akt isoforms exhibit localization difference, no clear picture of this exists to date.

Activation of Akt modulates the activity of over 100 different substrates (Manning and Toker, 2017). Akt-mediated phosphorylation of its substrates has physiological consequences such as survival, proliferation or metabolism. The first Akt substrate identified was glycogen synthase kinase-3 (GSK3β) (Cross et al., 1995), which is a serine and threonine kinase that exists in two isoforms, GSK3α and GSK3β. In resting cells, GSK3 is active, however upon growth factor stimulation GSK3 becomes phosphorylated and inactivated. Akt phosphorylates GSK3α on Ser21 and GSK3β on Ser9 and regulates many different GSK3 substrates, which play a role in metabolism, proliferation or cell survival (Manning and Toker, 2017). For example, inactivation of GSK3β via its phosphorylation blocks its binding to c-Myc, a transcription factor, thereby stabilizing c-Myc and promoting cell growth and proliferation (Sears et al., 2000).

Another substrate of Akt is mTORC1, a serine/threonine kinase that activates downstream protein kinases that are required for ribosomal biosynthesis and translation of mRNA of proteins involved in cell growth (Díaz et al., 2012). Akt activates mTORC1 by phosphorylating tuberous sclerosis complex 2 (TSC2), which inhibits its binding to mTORC1

(Huang and Manning, 2009). mTORC1 promotes protein synthesis through the direct phosphorylation of p70S6 kinase (S6K) and eIF4E binding protein (4EBP). S6K can activate several substrates that are involved in mRNA translation initiation and enhances transcription efficiency (Saxton and Sabatini, 2017). Dysregulation of the PI3K/Akt signaling pathway results in tumor growth by promoting cell proliferation and survival.

It is well accepted that PI headgroup phosphorylation controls PIP function, localization and effector binding in distinct pathways and cellular processes. However, PI contains up to 70% of the unique acyl profile consisting of 1-stearoyl-2-arachidonoyl species (Baker and Thompson, 1972; D'Souza and Epand, 2015; Hicks et al., 2006). The role this unique acyl chain profile plays in regulating PI and PIP function is not well understood. Two acyltransferases have been identified to be involved in PI acyl enrichment. LYCAT has been postulated to be involved in the incorporation of stearic acid at the *sn1* position of PI and LPIAT1 has been shown to be responsible for the incorporation of arachidonic acid at the *sn2* position of PI. While the majority of research has focused on the function of LPIAT1 in PI arachidonoyl acyl enrichment (Anderson et al., 2013; Gijón et al., 2008; Lee et al., 2012), only a fraction of research has focused on understanding the function of LYCAT. Thus, to better understand PI and PIP regulation, it is important to understand the function of LYCAT.

### 1.8. LYCAT is an acyltransferase that is postulated to control the stearic acid enrichment in PI

Lysocardiolipin acyltransferase (LYCAT, also known as AGPAT8, ALCAT1 or LCLAT1) was first characterized as an acyl-CoA:lysocardiolipin acyltransferase involved in cardiolipin remodelling through *in vitro* enzyme assays (Cao et al., 2004). Since then, LYCAT has also been observed to

exhibit acyltransferase activity toward lysoPI and lysophosphatidylglycerol (Agarwal et al., 2006; Cao et al., 2009; Zhao et al., 2009). Phosphatidylglycerol is synthesised in the ER and mitochondria and is a direct precursor for the synthesis of cardiolipin. Phosphatidylglycerol, cardiolipin and PI are synthesized from CDP-DAG, a synthesis pathway that differs from that of other phospholipids, which can be synthesized directly from DAG without a CDP-DAG intermediate (Vance and Vance, 2008).

LYCAT contains a substrate binding pocket that binds to anionic lysophospholipids (Zhao et al., 2009). Murine LYCAT is a 376 amino acid protein of 44.4 kDa that is characterized by transmembrane domain containing motifs that are conserved among members of the GPAT family (Agarwal et al., 2006; Cao et al., 2004). The human primary sequence of LYCAT is 89% identical to murine. LYCAT is expressed in multiple tissues but appears highest in brain and liver in mice, but is highly expressed in heart and kidney in human tissues (Agarwal et al., 2006; Cao et al., 2004; Zhao et al., 2009).

Imae *el al* identified genes encoding acyltransferases, *acl-8, acl-9* and *acl-10* that work to incorporate stearic acid into the *sn1* position of PI in *C. elegans* (Imae et al., 2010). Furthermore, genetic manipulation of the *C. elegans* $PLA_1$ gene, *ipla-1*, reduced stearic acid levels at the *sn1* position of PI, a similar phenotype seen in *acl-8, acl-9* and *acl-10* triple mutants (Imae et al., 2010). This study proposed a PI-specific Lands cycle where $IPLA_1$ and ACL-8, -9 and -10 function together in fatty acid remodeling at the *sn1* position of PI.

ACL-8, -9 and -10 are members of the AGPAT family exhibiting lysophospholipid acyltransferase activity (Imae et al., 2011, 2010). Mammals contain 16 different AGPAT members and the closest homologue to ACL-8, -9 and -10 is LYCAT (Imae et al., 2011). Since the discovery

of LYCAT, *in vitro* and *in vivo* assays have shown that LYCAT is specific to PI and has no impact on the acyl species present in other phospholipids including phosphatidylcholine, phosphatidylethanolamine and phosphatidylserine (Cao et al., 2004; Imae et al., 2011). Analysis of LYCAT$^{-/-}$ tissues of mice showed major reductions in stearate incorporation into PI as well as significant reductions in overall 18:0/20:4 acyl species in PIPs, where $PIP_2$ species showed the greatest impact of 50% reduction (Imae et al., 2011). There were significant changes to the acyl profile of PI, however, no impact was seen on total PI levels in LYCAT$^{-/-}$ mice.

The yeast homologue, Psi1p, when knocked out, also caused significant reductions in stearic acid in PI and an increase in palmitoleic acid (16:1) content at the *sn1* position of PI, but showed no changes to the acyl species of cardiolipin (Le Guédard et al., 2009). This group of researchers went on to examine the molecular species of PIPs and found major reduction in stearic acid in both PIP and $PIP_2$ species, but had no effect on total PI levels (Doignon et al., 2015). Furthermore, they examined the impact of the yeast *psi1*Δ strain on cell polarity by assessing actin cytoskeletal organization and intracellular traffic and found the mutant strain had large disturbances to cell polarity including changes in localization of PI(4)P and PI(4,5)$P_2$ (Doignon et al., 2015).

Although the synthesis of PI, phosphatidylglycerol and cardiolipin are subject to a common synthesis pathway, produced from the intermediate, CDP-DAG, there are acyltransferases that selectively control the remodeling of each particular phospholipid. Several reports have shown that the acyl profile of PA and CDP-DAG are not enriched in 1-stearoyl-2-arachidonoyl acyl species (Nakagawa et al., 1989; Shulga et al., 2010), thus implying that PI acyl chain enrichment does not occur during the *de novo* synthesis pathway, but instead during the

Lands cycle where acyl chains are remodelled. Therefore, an important question remains; where does this acyl remodelling take place in the cell?

### 1.8.1. LYCAT localization

Since the discovery of LYCAT there have been multiple conflicting reports on the cellular localization. In 2004, researchers identified an ER retention signal on the C-terminus of LYCAT (Cao et al., 2004). Two studies that used immunohistological analysis showed FLAG-tagged LYCAT was localized to the ER in COS-7 and HEK293 cells (Cao et al., 2004; Zhao et al., 2009), while another study showed through subcellular fractionation that LYCAT-FLAG was localized to the mitochondria in COS-7 cells (Li et al., 2010). Imae *et al* however, were able to examine endogenous levels of LYCAT in MEFs and found LYCAT to be localized to the ER (Imae et al., 2011). Though, examination of the micrographs do show some localization to the ER, it is clear that not all LYCAT and perhaps not the majority localizes to the ER. The localization of LYCAT was further refined in 2010, when subcellular fractionation revealed that LYCAT-FLAG was localized to the contact sites between the ER and mitochondria, called the mitochondrial associated membrane. This was further confirmed by analyzing the acyltransferase activities in each fraction (Li et al., 2010). Despite these findings, the ER is a diverse network that contains many compartments, thus a systematic, quantitative analysis of the localization of LYCAT is needed to reveal the specific compartments to which it localizes.

### 1.8.2. LYCAT links oxidative stress and mitochondrial dysfunction to metabolic disease

In 2009, is was suggested that LYCAT played a role in regulating mitochondrial activity and reactive oxygen species (ROS) through cardiolipin remodeling (Cao et al., 2009; Li et al., 2010). Cardiolipin remodeling is important in repairing damage from tissues undergoing high levels of mitochondrial activity such as heart and liver, and is sensitive to ROS. Cao *et al* identified that defective cardiolipin remodeling can produce metabolic disease including hyperthyroidism (Cao et al., 2009). Further examination of a murine model mimicking hyperthyroidism showed LYCAT expression was decreased (Cao et al., 2009).

Diabetes and obesity are additional metabolic disorders associated with oxidative stress and production of ROS in the mitochondria. A murine LYCAT$^{-/-}$ model fed a normal diet showed no major disruptions to litter size and were found to be healthy overall (organ histology, plasma triglyceride and cholesterol levels) and no disruptions to cardiolipin fatty acid composition were identified (Imae et al., 2011). In a different study, which used high fat diet, LYCAT$^{-/-}$ mice had significant changes to the fatty acid composition of cardiolipin (Li et al., 2010). The LYCAT$^{-/-}$ mice showed improved glucose tolerance and had significantly lower weight gain compared to wild-type mice (Li et al., 2010). This study, however, did not examine the fatty acid composition of PI in LYCAT$^{-/-}$ mice. This phenotype of LYCAT$^{-/-}$ mice were only observed when mice where fed a high fat diet. Overexpression of LYCAT in C2C12 cells, a mouse skeletal muscle cell line typically used in metabolic research, caused a decrease in total cardiolipin levels, altered cardiolipin acyl chain composition, and oxidative stress (Li et al., 2010). Additionally, LYCAT expression increased in response to diet-induced obesity and at the onset of type-II diabetes in mice (Li et al., 2010), leading to production of ROS, but had no impact on the acyl chain composition of PI and phosphatidylglycerol (Li et al., 2010). This study suggested that targeted inactivation of LYCAT

prevents the onset of diet-induced obesity and its related metabolic conditions. LYCAT was thus implicated as a major regulator of abnormal cardiolipin remodeling in diet induced obesity.

In addition, overexpression of LYCAT in H9c2 cardiac cells caused oxidative stress and mitochondrial dysfunction, whereas knockout of LYCAT prevented the onset of cardiomyopathy (Liu et al., 2012). These studies show that LYCAT plays a role in responding to oxidative stress in diabetes, obesity and cardiomyopathy, three conditions that lead to ROS production, mitochondrial dysfunction and insulin resistance (Li et al., 2010; Liu et al., 2012). Furthermore, the overexpression of LYCAT was responsible for mitochondrial fusion defect or mitochondrial DNA instability in a mouse myoblast cell line used, C2C12 (Li et al., 2012).

LYCAT thus appears to have multiple functions in control of metabolism and ROS, linked to cardiolipin remodeling. The regulation of metabolism and ROS by LYCAT may only occur during systemic stress, such as in diet-induced obesity. While LYCAT controls PI acyl profile in otherwise healthy, unstressed animals (Imae et al., 2011), it will be important for future research to examine how the role of lipid enzymes and indeed lipid acyl profiles change under different metabolic conditions. Here, I focus on resolving the role of LYCAT in controlling PI acyl profile and function in unstressed cells and conditions.

Multiple studies have shown that LYCAT gene disruption alters the acyl chain composition of PI and PIPs (Agarwal et al., 2006; Cao et al., 2009; Zhao et al., 2009). Studies on yeast found that targeted disruption to Psi1p (LYCAT homologue) showed disruption to stearic acid incorporation into PI that impacted cell polarity and intracellular traffic (Doignon et al., 2015). Multiple studies have shown that LYCAT plays a significant role in regulating mitochondrial dysfunction that can ultimately lead to metabolic disease including hyperthyroidism and diet

induced obesity and heart disease. The impact of LYCAT on PI and PIP function and signaling capabilities at the molecular level has not yet been investigated or established.

## 1.9. Project Goals and Rationale

PIPs play crucial roles in regulating cellular process responsible for controlling nutrient uptake, intracellular traffic, cell motility and cell growth and development, all of which are important for cell homeostasis.

The role of LYCAT in controlling PI and PIP acyl chain species and the functional consequences of this unique acyl chain composition, remains elusive. Thus, for my Ph.D. thesis, I set out to explore the functional role of LYCAT in PI and PIP acyl chain remodeling and the impact on cellular processes. The following list encompasses my goals:

1) Characterize the function of LYCAT in the regulation of phospholipid acylation
2) Determine the significance of LYCAT in regulating endomembrane traffic
3) Determine the role of LYCAT in regulating hormone receptor signaling

Chapter 1 Figures

Figure 1.1. Maintenance and dynamics of membrane trafficking are fundamental in maintaining cellular homeostasis and cell survival. The exchange of membrane is key to the dynamic regulation of cell surface proteins. Endomembrane trafficking mediates nutrient uptake, product release and sensing of the external environment.

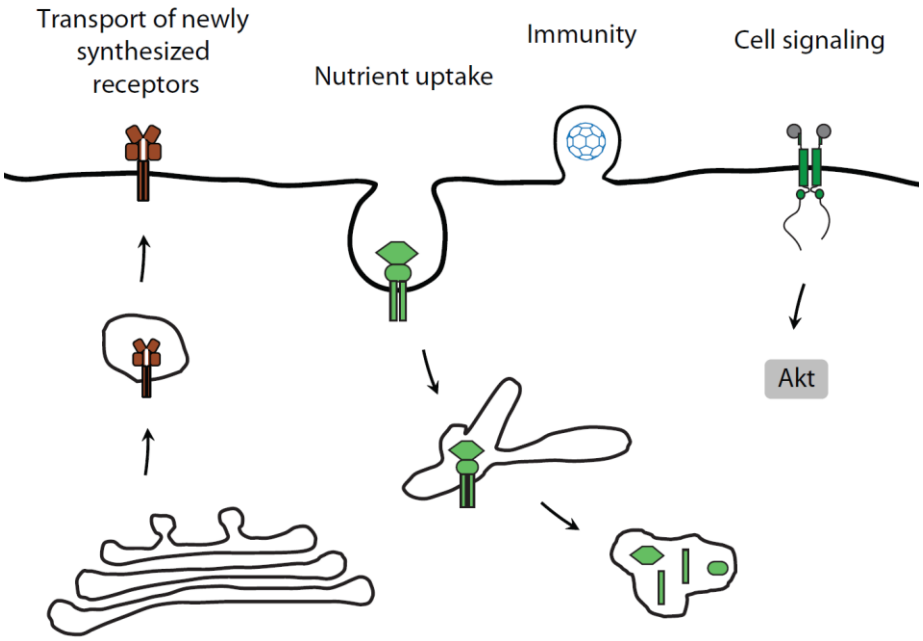

Figure 1.2. Synthesis of distinct phosphoinositide species. The parent, phosphatidylinositol is composed of a diacylglycerol (DAG) backbone containing two acyl chains in the *sn1* and *sn2* positions and an inositol headgroup connected to the glycerol backbone through a phosphodiester bond at the *sn3* position. The inositol headgroup can be phosphorylated on the 3, 4 or 5 positions generating seven molecularly distinct phosphoinositide (PIP) species. The generation and interconversion of the PIP species is tightly regulated through the action of inositol kinases (green) and phosphatases (blue). Purple circles represent positions of phosphate groups.

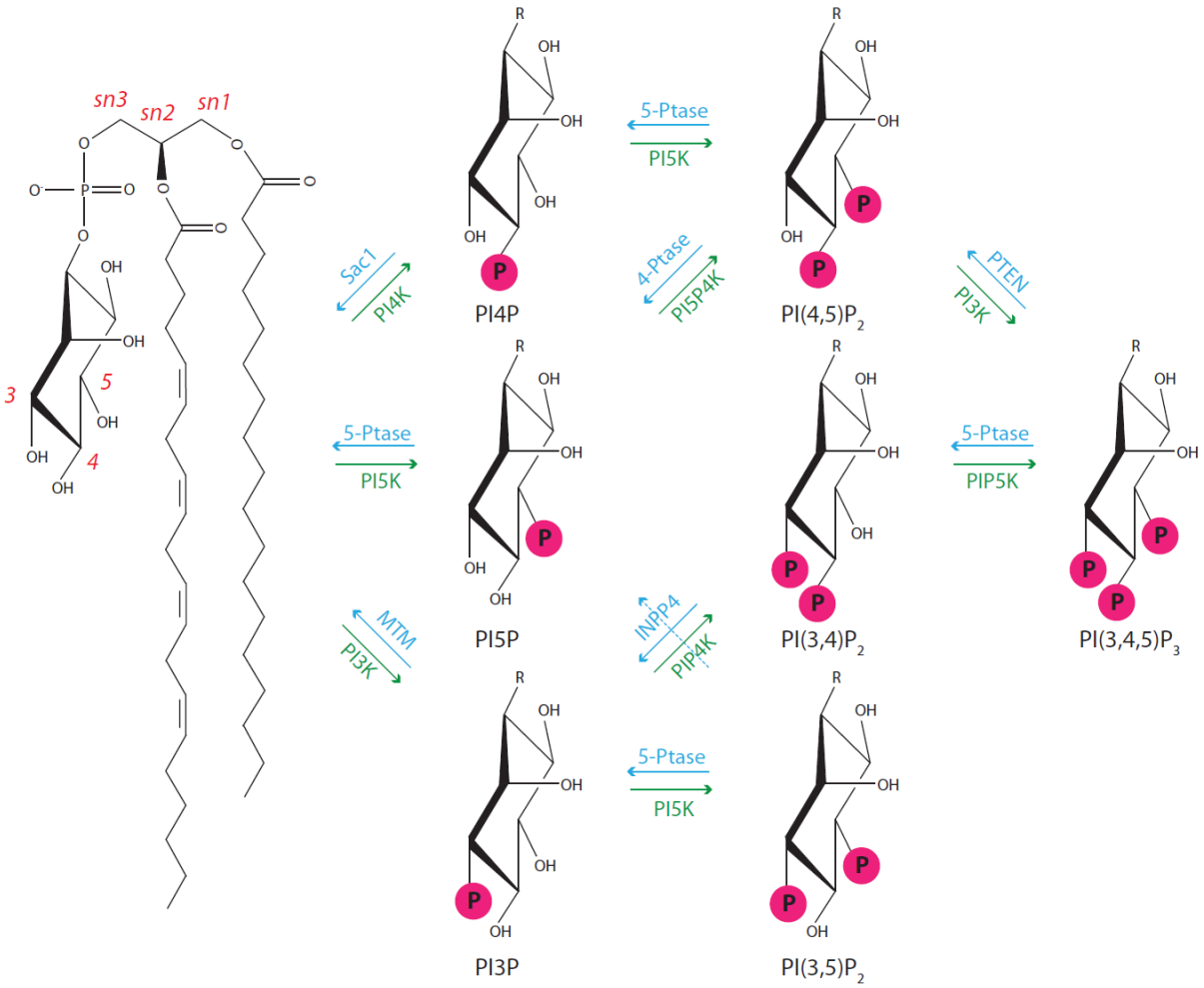

Figure 1.3. The cellular distribution of phosphoinositides. Phosphoinositides (PIPs) are localized to distinct membranes in the cell, where some membranes will have higher concentrations of certain species over others. The appearance of one species on a particular membrane can be very dynamic depending on cellular needs and, often times can localize to several membranes. The resulting PIP clusters on various membranes can give that membrane a unique identify and particular functions.

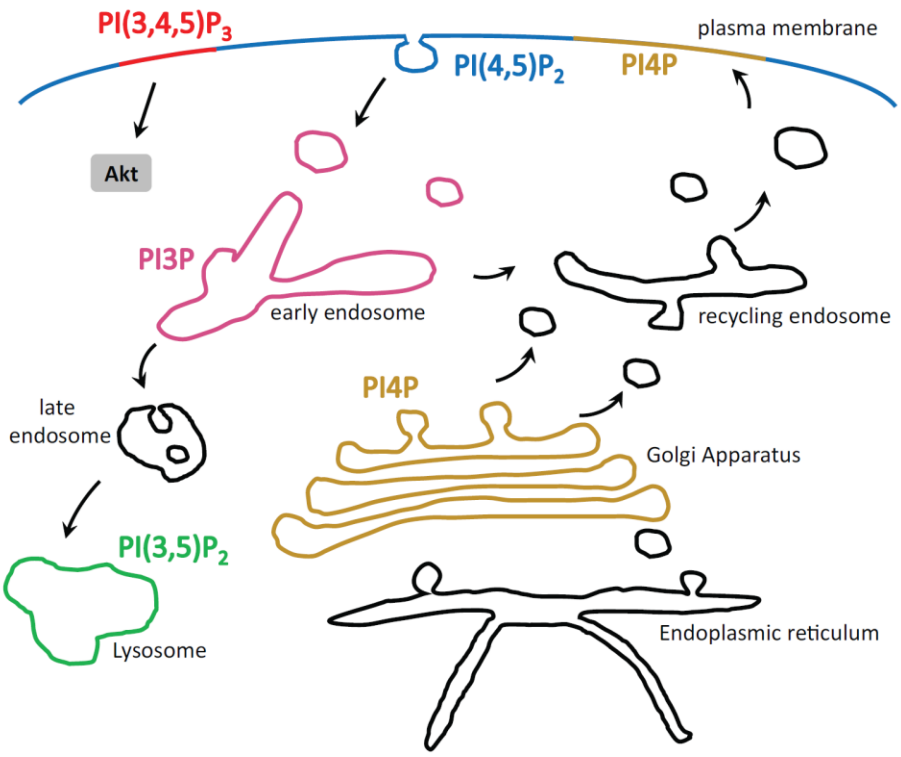

Figure 1.4. Phospholipid synthesis and acyl chain remodelling. The Kennedy pathway is responsible for the *de novo* synthesis of phospholipids, which occurs in the endoplasmic reticulum. The pathway begins with glycerol-3-phosphate (G3P), which is converted to phosphatidic acid (PA) through the action of acyltransferases, G3P acyltransferase (GPAT) and lysoPA acyltransferase (LPAAT). Cytidine-diphosphate synthase enzymes (CDS1/2) convert PA to cytidine diphosphate diacylglycerol (CDP-DAG) and phosphatidylinositol (PI) is formed by phosphatidylinositol synthase. Following *de novo* synthesis is the Lands cycle where phospholipids undergo acyl chain remodeling through the action of phospholipase A (PLA) enzymes and acyltransferases. Shown is the Lands cycle specific to PI synthesis.

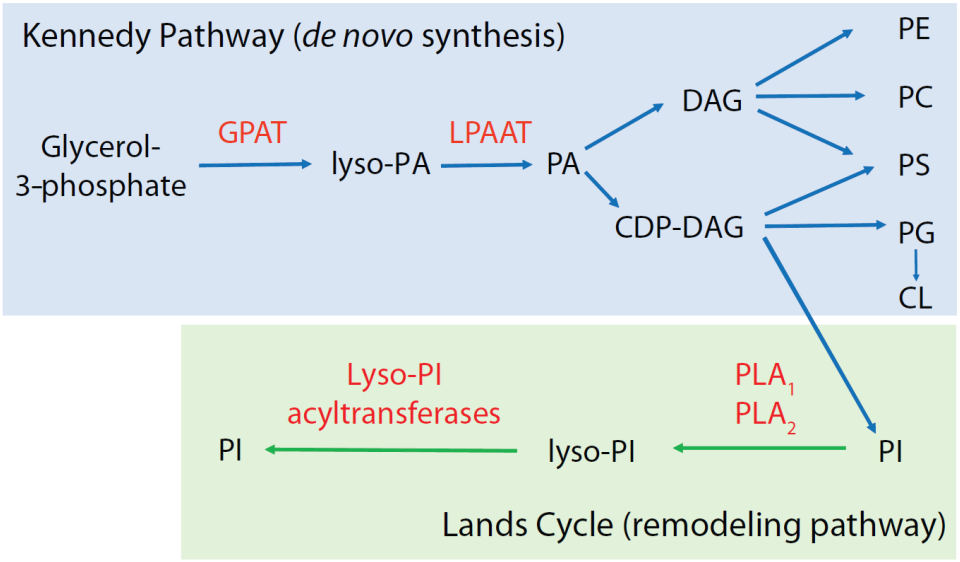

Figure 1.5. Phosphatidylinositol cycle in the cell. In addition to the *de novo* pathway, the phosphatidylinositol (PI) cycle also contributes to PI synthesis. Phosphatidic acid (PA) is produced from the phosphorylation of diacylglycerol (DAG) by diacylglycerol kinases (DGKs), which is formed by the cleavage of $PI(4,5)P_2$ by phospholipase C (PLC). $PI(4,5)P_2$ is resynthesized at the plasma membrane from PI via lipid kinases. The PI cycles requires both the endoplasmic reticulum (ER) and plasma membrane (PM).

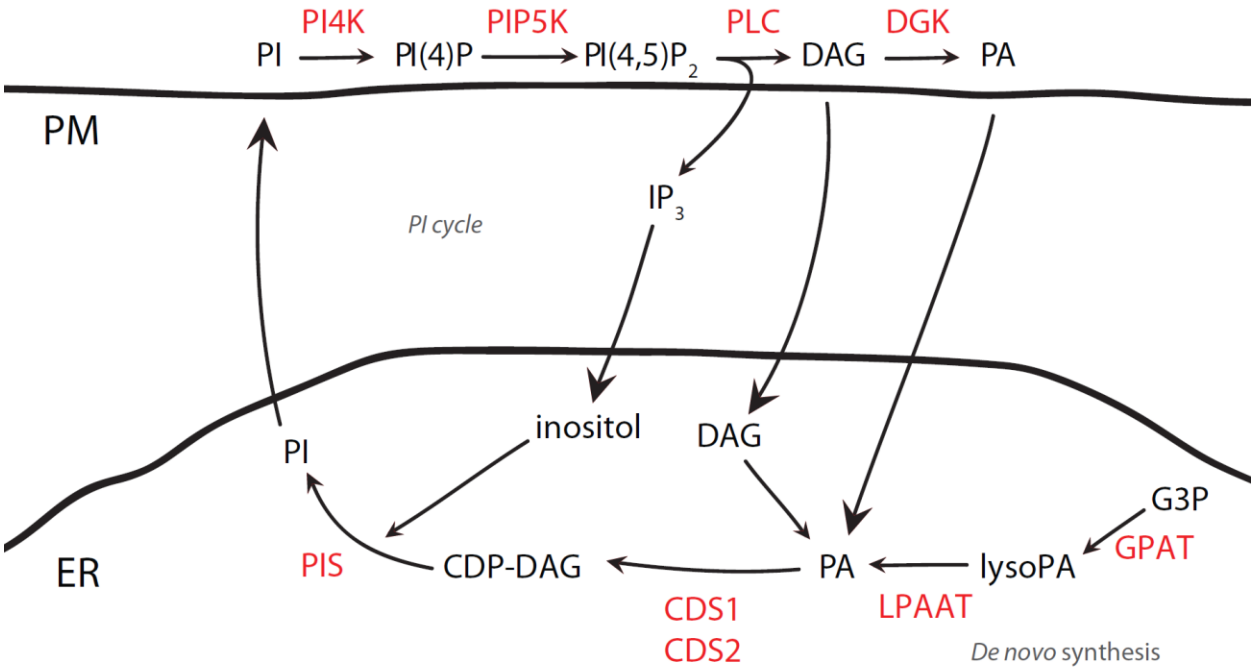

Figure 1.6. Regulation of phosphoinositides at PM-ER membrane contact sites. Membrane contact sites (MCSs) are the site of lipid transport where tethering proteins and lipid transfer proteins work together to deliver lipids to the appropriate membrane. VAP proteins in the endoplasmic reticulum (ER) are key tethering proteins that bind to many different lipid transfer proteins. Shown is a contact site between the ER and plasma membrane (PM). (i) ORP5 and ORP8 tether the ER and plasma membrane by binding VAP and PI(4)P, respectively, and are responsible for transporting phosphatidylserine (PS) to the plasma membrane and PI(4)P to the ER for conversion into phosphatidylinositol (PI) by the 4-phosphatase, Sac1. (ii) Upon phospholipase C activation, Nir2 localizes and tethers contact sites between the ER and plasma membrane by binding to VAP and PI(4)P, respectively. Nir2 transports phosphatidic acid (PA) to the ER and PI to the plasma membrane. E-Syt1 works alongside Nir2 to mediate these ER-plasma membrane contacts.

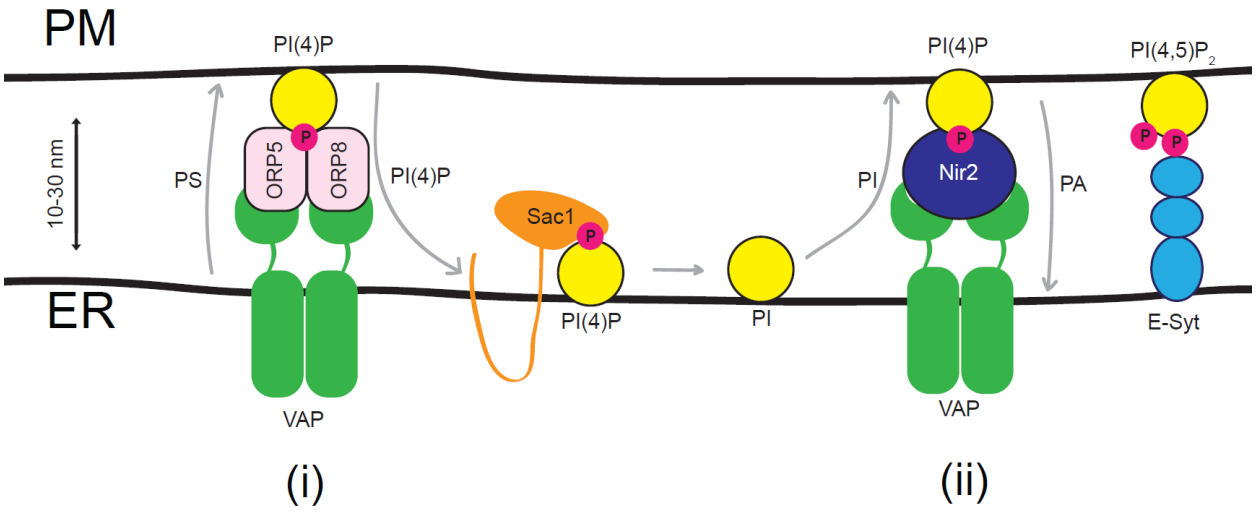

Figure 1.7. Transferrin receptor endomembrane traffic. Iron-bound transferrin (Tfn) binds to transferrin receptor (TfR) at the cell surface which is internalized by clathrin-mediated endocytosis. In the slightly acidic environment of early endosomes (EE), iron disassociates from Tfn and is retained intracellularly. The TfR/Tfn complex is then recycled back to the plasma membrane through the fast recycling pathway and the slow recycling pathway, which transits the TfR/Tfn complex through recycling endosomes (REs).

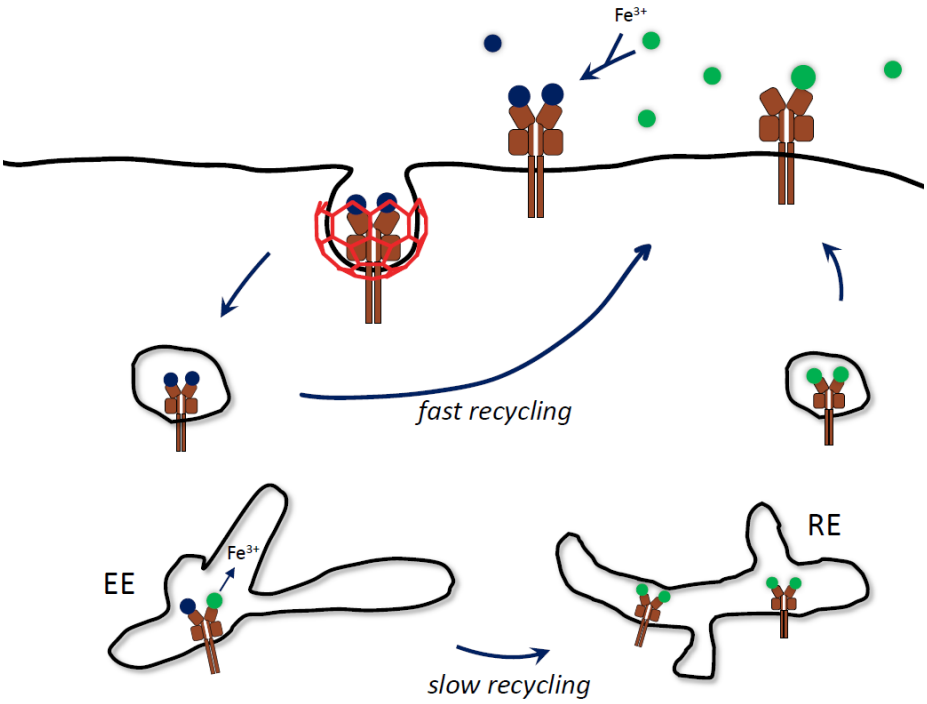

Figure 1.8. PI3K/Akt signaling pathway. A simplified schematic showing the activation of Akt by epidermal growth factor (EGF) binding to epidermal growth factor receptor (EGFR) at the plasma membrane. Ligand binding recruits phosphatidylinositol-3 kinase (PI3K) to the cell surface, which is responsible for converting $PI(4,5)P_2$ into $PI(3,4,5)P_3$. Akt becomes activated by its phosphorylation and can then act on over 100 different substrates resulting in cell survival, metabolism, proliferation and migration.

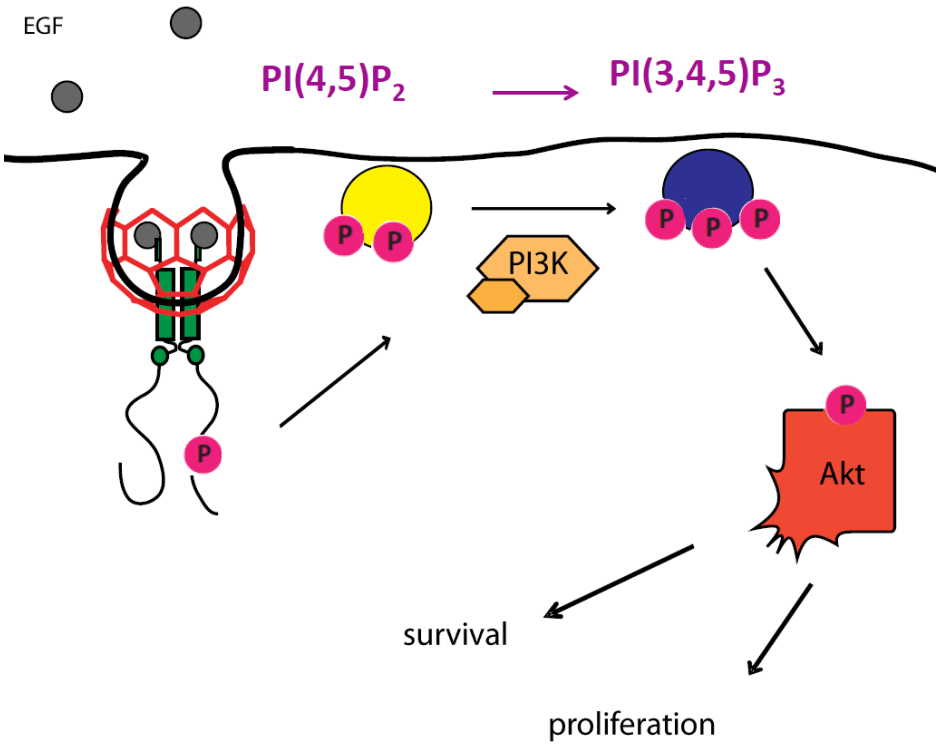

# Chapter 2
# Experimental Procedures

## 2.1. Materials

Antibodies and fluorescent ligands used were as follows: anti-EEA1 and actin from Cell Signaling; anti-TfR from Santa Cruz Biotechnology; Tfn-antibodies (used in Tfn uptake assay) were from Bethyl Laboratories and Alexa 647-conjugated Tfn (A647-Tfn) from Life Technologies. Fluorophore-conjugated or horseradish peroxidase (HRP) secondary antibodies were from Jackson ImmunoResearch (West Grove, PA).

Antibodies used were as follows: anti-phospho-EGFR (pY1068), anti-EGFR, anti-Akt (pan), anti-phospho-Akt1 (S473), anti-phospho-Akt2 (S474), anti-phospho-GSK-3β (S9), anti-GSK-3β, anti-phospho-p70 S6 kinase (T389), anti-p70 S6 kinase, phospho-p42/44 MAPK (T202/Y204), p42/44 MAPK and phospho-Akt substrate RXXS*/T* were from Cell Signaling Technology; anti-phospho-Akt (pS473) antibody was from Life Technologies; anti-actin and anti-clathrin heavy chain (TD.1) were from Santa Cruz Biotechnology. Fluorophore-conjugated or horseradish peroxidase (HRP) secondary antibodies were from Jackson ImmunoResearch (West Grove, PA).

## 2.2. Cell culture

Wild-type ARPE-19 (RPE) human retinal pigment epithelial cells (RPE-WT) and a derivative line stably expressing clathrin light chain fused to eGFP (RPE eGFP-CLCa) were previously described (Aguet et al., 2013; Garay et al., 2015). RPE cells were cultured in DMEM/F12 media and MDA-MB-231 cells were cultured in DMEM media. Both media were supplemented with 10% fetal bovine serum, 100 U/mL penicillin and 100 µg/mL streptomycin at 37°C and 5% $CO_2$. DMEM/F12 media, DMEM media, fetal bovine serum and penicillin/streptomycin solution were obtained from Life Technologies.

## 2.3. Gene silencing by siRNA

To silence LYCAT expression in both RPE and MDA-MB-231 cells, I used two independent siRNA oligonucleotides LYCAT$^1$ with the sequence 5'-GGAAAUGGAAGGAUGACAAUU and LYCAT$^2$ with the sequence 5'-CCUCAAAGCGAGUCUCAAAUU. As controls for silencing, I also transfected cells with non-targeting control siRNA oligonucleotides with the sequence 5'-CGUACUGCUUGCGAUACGGUU. All were obtained from Dharmacon. Oligonucleotides were

transfected using Lipofectamine RNAiMAX (Life Technologies), as per manufacturer's instructions. Briefly, once cells reached 50-60% confluency (0 h), 110 pmol of each siRNA oligonucleotide (5.5 µL of 20 µM siRNA stock) was pre-complexed with 6.25 µL transfection reagent and 200 µL Opti-MEM medium (Life Technologies) for 15-20 min at room temperature. Afterwards, the 200 µL siRNA pre-complex solution was added dropwise to cells in 1.8 mL Opti-MEM medium and incubated for 4 h, after which cells were washed three times in phosphate buffered saline (PBS) (Life Technologies) and replaced in regular growth media. siRNA transfections were performed twice (0 h and 24 h) prior to each experiment. Experiments took place at 72 h.

### 2.4. Transfection and plasmids

A plasmid encoding LYCAT-myc-FLAG (henceforth, LYCAT-FLAG) was from Origene (plasmid MR226119). Plasmids expressing VSVG-GFP protein were previously characterized (Fairn et al., 2011; Lippincott-Schwartz et al., 1997). Plasmids encoding eGFP-PIS and eGFP-P4M were kindly provided by T. Balla (National Institutes of Health, Bethesda, MD) (Hammond et al., 2014; Kim et al., 2011). A plasmid encoding eGFP-E-Syt2 (Addgene # 66831) was kindly provided by P. de Camilli (Yale School of Medicine, CT) (Giordano et al., 2013b). Plasmids encoding eGFP-KDEL, eGFP-PH-PLC-δ1, eGFP-2-FYVE, eGFP-P4M and eGFP-PH-Akt were from the Botelho and Antonescu labs.

For plasmid transfection of RPE cells and MDA-MB-231 cells, I used Lipofectamine 2000 (Life Technologies) as per manufacturer's instructions. Briefly, for each well of a 6-well plate, 2 µg of cDNA was pre-complexed with 6 µL of transfection reagent in 100 µL Opti-MEM medium at room temperature for 15-20 min. DNA-reagent complexes were added dropwise to each well containing 1.8 mL Opti-MEM medium and were subsequently incubated for 4 h, followed by washing with PBS three times and incubation of cells in regular growth media for 24 h prior to the start of the experiment. If transfection of cDNA was occurring after siRNA, transfection took place at 48 h.

### 2.5. Cell treatment with inhibitors

Validation assay for detection of radiolabelled PI(3)P: Cells were treated with LY294002 (Cell Signaling) (10 µM) for 30 min. Validation assay for detection of radiolabelled PI(4,5)$P_2$: Cells were serum deprived for 1 h in DMEM media, during that 1 h cells were treated with 10 µM ionomycin (Sigma-Aldrich) for 20 min supplemented with 15 mM HEPES. Project completed in collaboration for Delos Santos *et al*, 2017. Accepted to *Molecular Biology of the Cell*).

Detection of phospho-proteins: Cells were serum deprived for 1 h in DMEM media before experimental assays and stimulated with 5ng/ml EGF (human; Life Technologies) for 5 min.

Detection of pAkt substrates: Cells were serum deprived for 1 h in DMEM media, during which some conditions were treated with 5 µM Akti-1/2 (Toronto Research Chemicals) for 1 h. Cells were then stimulated with 5 ng/ml EGF (human; Life Technologies) for 5 min.

PH-Akt probe localization*:* Cells were serum deprived for 1 h and then stimulated with 5 ng/ml EGF for 5 min. During the 1 h serum deprivation, cells were treated with LY294002 (10 µM) for 30 min.

Detection of cell surface EGFR levels: Cells were serum deprived for 1 h in DMEM media while simultaneously stimulated with EGF (100 ng/ml) for 1 h.

## 2.6. SDS-PAGE and western blotting

Whole cell lysates were prepared in Laemmli sample buffer (LSB; 0.5 M Tris, pH 6.8, glycerol, 10% SDS, 10% β-mercaptoethanol, and 5% bromophenol blue; all from BioShop) supplemented with a protease and phosphatase cocktail (1 mM sodium orthovanadate, 10 nM okadaic acid, and 20 nM Protease Inhibitor Cocktail [BioShop]). Lysates were then heated at 65°C for 15 min, passed through a 27.5-gauge syringe and then centrifuged for 5 min at 101 *x g*. Proteins were resolved by Glycine-Tris SDS–PAGE, a 9% polyacrylamide gel for 1 h at 120V at room temperature, followed by transfer onto a PVDF membrane for 2 h at 100V at room temperature or for 12 h at 20 V at 4°C. The PVDF membranes were washed in 5% milk blocking solution or 3% bovine serum albumin (BSA) blocking solution, both made in tris-buffered saline, 0.05% tween 20 (TBST) plus 0.05% NP-40 alternative and then washed three times in TBST. Membranes were incubated with 1:1000 primary antibody (made in TBST) overnight at 4°C, washed four times for 10 min each and then incubated with 1:000 secondary antibody (made in TBST) for 1 h at room temperature, as

previously described (Garay et al., 2015). Membranes were exposed to Clarity ECL reagent (1:5 in water) (BioRad) for 20 sec to 1 min and then exposed to a cooled CDC detector (BioRad).

Images were analysed with ImageJ software. Western blot ECL signals to detect the intensity corresponding to total protein was obtained by signal integration in an area corresponding to the appropriate lane and band for each condition. This measurement is then normalized to the loading control signal. Western blot signals to detect the intensity corresponding to phosphorylated proteins (e.g., pAkt) were obtained as previously described (Antonescu et al., 2005) by signal integration in an area corresponding to the appropriate lane and band for each condition. This measurement is then normalized to the loading control (e.g., actin) signal, and subsequently normalized to the total Akt signal, obtained either following blot stripping or reblotting. In each experiment, the resulting normalized pAkt / total Akt signal in each condition was expressed as a fraction of the normalized pAkt / total Akt measurement in the control condition stimulated with EGF for 5 min.

Antibodies used were as follows: anti-LYCAT (cat. 106759) from Genetex; anti-TfR (cat. 32272) from Santa Cruz Biotechnology; anti-phospho-EGFR (pY1068, cat. 3777), anti-EGFR (cat. 03), anti-Akt (pan, cat. 2920), anti-phospho-Akt1 (S473, cat. 9018), anti-phospho-Akt2 (S474, cat. 8599), anti-phospho-GSK-3β (S9, cat. 9323), anti-GSK-3β (cat. 9832), anti-phospho-p70 S6 kinase (T389, cat. 9205), anti-p70 S6 kinase (cat. 2708), anti-phospho-p42/44 MAPK (T202/Y204, cat. 9101), anti-p42/44 MAPK (cat. 9102) and anti-phospho-Akt substrate RXXS*/T* (cat. 9614) were from Cell Signaling Technology; anti-phospho-Akt (pS473, cat. 44621) antibody was from Life Technologies; anti-actin (cat. 1616) and anti-clathrin heavy chain (TD.1, cat. 12734) were from Santa Cruz Biotechnology.

All primary and secondary antibodies were used at 1:1000 with the exception of anti-phospho-GSK-3β which was used at 1:700. IgG horseradish peroxidase (HRP)-linked secondary antibodies were from Jackson ImmunoResearch (West Grove, PA).

### 2.7. [$^3$H]*myo*-inositol labelling of PIPs

RPE cells were incubated for 24 h in inositol-free DMEM (MP Biomedicals) supplemented with 10 µCi/ml *myo*-[2-3 H(N)] inositol (PerkinElmer Life Sciences), 10% fetal bovine serum (Gibco), 4 mM

L-glutamine (Sigma-Aldrich), 1x insulin-transferrin-selenium-ethanolamine (Gibco), 20 mM HEPES (Gibco), and 1x penicillin/streptomycin. Cells were treated with 600 µL of 4.5% perchloric acid (v/v) on ice for 15 min, scraped, and pelleted at 12,000g for 10 min. Pellets were washed with 1 mL ice cold 0.1 M EDTA and resuspended in 50 µL of water. Phospholipids were deacylated with 500 µL of a solution of methanol/40% methylamine/1-butanol (45.7% methanol:10.7% methylamine:11.4% 1-butanol (v/v)) for 50 min at 53°C. Samples were vacuum-dried and washed twice with water. The dried samples were then resuspended in water, extracted with a solution of 1-butanol/ethyl ether/ethyl formate (20:4:1), vortexed for 5 min, and centrifuged at 12,000 × *g* for 2 min. The bottom aqueous layer was collected and extracted twice more. The aqueous layer was vacuum-dried and resuspended in 50 µL of water. Detailed protocol can be found (Ho et al., 2016).

### 2.8. Detection of radiolabelled PIPs

Equal counts of $^{3}H$ were separated by HPLC (Agilent Technologies) through an anion exchange 4.6 x 250 mm column (Phenomenex) with a flow rate of 1 mL/min and subjected to a gradient of water (buffer A) and 1 M $(NH_4)_2HPO_4$, pH 3.8 (adjusted with phosphoric acid) (buffer B) as follows: 0% B for 5 min, 0 to 2% B for 15 min, 2% B for 80 min, 2 to 10% B for 20 min, 10% B for 30 min, 10 to 80% B for 10 min, 80% B for 5 min, and 80 to 0% B for 5 min. The radiolabeled eluant was detected by β-RAM 4 (LabLogic) with a 1:2.5 ratio of eluate to scintillant (LabLogic) and analyzed using Laura 4 software. Each of the phosphoinositides was normalized against the parent phosphatidylinositol peak.

### 2.9. Acyl chain lipid detection

After siRNA transfection, cells were placed on ice and washed with ice cold PBS three times. Cells were scraped, flash frozen in liquid $N_2$ and then stored at -80°C until delivery to our collaborators in Japan where samples were transported on dry ice.

#### 2.9.1. Phospholipid acyl chain detection (LC-ESI-MS/MS)

Completed by the Arai lab in Tokyo, Japan as outlined below. Lipids were extracted by the method of Bligh and Dyer (Bligh and Dyer, 1959). Phospholipids in lipid extracts were quantitated by using the inorganic phosphorus assay. Internal standards (13:0/15:0 phosphatidylcholine, phosphatidylethanolamine, PI, and phosphatidylserine) were added to the samples prior to LC-ESI-MS/MS analysis. The LC-ESI-MS/MS analysis was performed on a Shimadzu Nexera ultra high performance liquid chromatography system (Shimadzu, Kyoto, Japan) coupled with a QTRAP 4500 hybrid triple quadrupole linear ion trap mass spectrometer (AB SCIEX, Framingham, MA, USA). Chromatographic separation was performed on an Acquity UPLC HSS T3 column (100 mm × 2.1 mm, 1.8 µm; Waters) maintained at 40°C using mobile phase A (water/methanol (50/50, v/v) containing 10 mM ammonium acetate and 0.2% acetic acid) and mobile phase B (isopropanol/acetone (50/50, v/v)) in a gradient program (0–3 min: 30% B→50% B; 3–24 min: 50% B→90% B; 24–28 min: 30% B) with a flow rate of 0.3 mL/min. Neutral loss scans of 74 and 87 Da in the negative ion mode were used to detect phosphatidylcholine and phosphatidylserine, respectively. Neutral loss scan of 141 Da in the positive ion mode was used to detect phosphatidylethanolamine. Precursor ion scan of m/z 241 in the negative ion mode was used to detect PI. The instrument parameters for negative ion mode were as follows: curtain gas, 10 psi; collision gas, 7 arb. unit; ionspray voltage, -4500 V; temperature, 700ºC; ion source gas 1, 30 psi; ion source gas 2, 70 psi; declustering potential, -96 V; entrance potential, -10 V; collision energy, -36 V; collision cell exit potential, -15.4 V. The instrument parameters for positive ion mode were as follows: curtain gas, 10 psi; collision gas, 7 arb. unit; ionspray voltage, 4500 V; temperature, 700ºC; ion source gas 1, 30 psi; ion source gas 2, 50 psi; declustering potential, 116 V; entrance potential, 10 V; collision energy, 31 V; collision cell exit potential, 12 V. Quantification was performed by integration of the peak area of the extracted ion chromatograms for each phospholipid species.

### 2.9.2. Phosphatidylinositol acyl chain measurement (LC-ESI-MS/MS)

Cells (~$10^6$ cells) were washed with cold PBS, scraped in 1 M HCl, and centrifuged at 15,000 × *g* for 5 min. The pellets were resuspended in 170 µl of water and 750 µl of $CHCl_3$/MeOH/1 M HCl (2:1:0.1 [vol/vol]) and incubated for 5 min at room temperature. To each sample, 725 µl of $CHCl_3$

and 170 µl of 2 M HCl were added, followed by vortexing. After centrifugation at 1500 × *g* for 5 min, the lower phase was collected and washed with 780 µl of pre-derivatization wash solution (the upper phase of $CHCl_3$/MeOH/0.01 M HCl (2:1:0.75 [vol/vol]). The lipid extracts were derivatized by adding 50 µl of 2 M TMS-diazomethane in hexane. The derivatization was carried out at room temperature for 10 min and stopped by adding 6 µl of glacial acetic acid. The derivatized samples were washed twice with 700 µl of post-derivatization wash solution (the upper phase of $CHCl_3$/MeOH/water (2:1:0.75 [vol/vol]). After addition of 100 µl of MeOH/H2O (9:1 [vol/vol]), the samples were dried under a stream of $N_2$, dissolved in 80 µl of MeOH, and sonicated briefly. After addition of 20 µl of water, the samples were subjected to LC-ESI-MS/MS analysis. The LC-ESI-MS/MS analysis was performed on a Shimadzu Nexera ultrahigh-performance liquid chromatography system coupled with a QTRAP 4500 hybrid triple quadrupole linear ion trap mass spectrometer. Chromatographic separation was performed on an Acquity UPLC C4 BEH column (100 mm × 2.1 mm, 1.8 µm; Waters) maintained at 40°C using mobile phase A (water containing 0.1% formate) and mobile phase B (acetonitrile containing 0.1% formate) in a gradient program (0–5 min: 45% B; 5–10 min: 45% B → 100% B; 10–15 min: 100% B; 15–16 min: 100% B → 45% B; 16–20 min: 45% B) with a flow rate of 0.1 ml/min. The instrument parameters for positive-ion mode were as follows: curtain gas, 10 psi; collision gas, 7 arbitrary units; ionspray voltage, 4500 V; temperature, 600°C; ion source gas 1, 30 psi; ion source gas 2, 50 psi; declustering potential, 121 V; entrance potential, 10 V; collision energy, 39 V; and collision cell exit potential, 10 V. Phosphoinositides were identified and quantified by multiple reaction monitoring (MRM) (Bone et al., 2017).

For these measurements, an internal standard of 10 ng of 32:0 $PIP_2$ was added to each sample. However, normalization of lipid counts to this internal standard was impractical due to the increase in 32:0 and 34:0 $PIP_2$ in lipid samples from LYCAT-silenced cells. That the raw counts of PI and PIP between control and LYCAT-silenced cells are very similar indicates that the differences in abundance of specific acyl species of $PIP_2$ between these silencing conditions is not due to differences in whole-sample preparation and instead reflects changes in the levels of $PIP_2$ acyl species relative to the cellular levels of PI and PIP. Indeed, normalization of each $PIP_2$ acyl

species to the amount of 38:4 PI in each control or LYCAT-silenced sample illustrates the alterations of $PIP_2$ acyl species levels relative to PI upon LYCAT silencing.

## 2.10. Immunofluorescence staining and fluorescent probes

### 2.10.1. Permeabilized cells

Immunofluorescence staining for detecting proteins in permeabilized cells was performed as previously described (Antonescu et al., 2008a). Samples were fixed in 4% paraformaldehyde for 15 min, permeabilized in 0.1% Triton X-100 for 10 min, blocked in 3% milk solution (BioShop) and then probed with primary anti-FLAG antibodies (1:400), anti-TfR antibodies (1:400) or anti-EGFR (mAb 108) antibodies (1:400) for 1 h at room temperature. After washing, appropriate fluorophore-conjugated secondary antibodies (1:200, Jackson ImmunoResearch) were used for 1 h at room temperature, stained with 1 µg/mL Dapi for 5 min and then mounted in fluorescence mounting medium (Dako) or retained within aqueous medium for imaging by TIRF-M.

### 2.10.2. Cell surface TfR or EGFR

Cell surface proteins were detected as previously described (Antonescu et al., 2008a). Samples were immediately placed on ice and washed three times in ice-cold $PBS^{2+}$ (PBS supplemented with 1 mM $CaCl_2$ and 1 mM $MgCl_2$) and blocked in 3% milk solution (on ice; BioShop). Cells were then incubated with 1:400 anti-TfR antibodies (also on ice; Santa Cruz Biotechnology) or 1:400 anti-EGFR antibodies (also on ice; mAb108, collected in-house from a hybridoma cell line from the America Type Culture Collection). After washing to remove unbound antibodies, cells were fixed in 4% paraformaldehyde, permeabilized in 0.1% Triton X-100, stained with appropriate secondary antibodies (1:200) for 1 h at room temperature, stained with 1 µg/mL Dapi (Life Technologies) and then mounted in fluorescence mounting medium (Dako). For EGFR cell surface levels, prior to placing cells on ice, cells were serum deprived for 1 h in DMEM while simultaneously stimulated with EGF (100 ng/ml) for 1 h.

### 2.10.3. Tfn colocalization with EEA1 or TfR

Colocalization of two proteins was determined as previously described (Bradley et al., 2015). RPE cells were incubated with 20 µg/ml of A647-Tfn for indicated times at 37°C and then immediately placed on ice and washed three times in ice-cold $PBS^{2+}$ to remove unbound ligand, fixed in 4% paraformaldehyde, permeabilized in 0.1% Triton X-100, stained with either anti-EEA1 (Cell Signaling Technology) or anti-TfR (Santa Cruz Biotechnology) and appropriate secondary antibodies, and then mounted in fluorescence mounting medium (Dako).

### 2.10.4. VSVG Biosynthetic membrane traffic assay

VSVG traffic assay was performed as previously described (Fairn et al., 2011). RPE cells were transfected with VSVG-GFP and incubated overnight at 40°C. To allow VSVG-GFP to exit the ER and accumulate in the Golgi, the cells were switched to HEPES-buffered DMEM/F12 and incubated at 20°C for 2 h. To visualize secretory vesicles in transit to the plasma membrane, after the 20°C block, the cells were transferred to medium pre-warmed to 37°C and incubated for 0, 15, 30, 60 or 90 min. After incubation at 37°C for the indicated time points, cells were washed and fixed with 4% paraformaldehyde for 15 min, and washed with PBS. Results were subjected to two-way ANOVA followed by Bonferonni's multiple comparison posttest.

### 2.10.5. Tfn internalization assay

Tfn internalization assay was performed as previously described (Antonescu et al., 2010). Cells were then incubated with 10 µg/ml biotinylated transferrin (Invitrogen) for the indicated times at 37°C, after which they were immediately placed on ice and washed 3 times in ice-cold $PBS^{2+}$ to remove excess (unbound) ligand and arrest membrane traffic. Uninternalized (surface-exposed) biotin-Tfn was quenched by sequential incubation with free avidin (3.1 µg/ml) and biocytin (5 µg/ml). Cells were then solubilized in blocking buffer (0.05% Triton X-100 and 0.05% SDS in Superblock solution; ThermoFisher), and cell lysates were plated onto ELISA plates coated with anti-Tfn antibodies and assayed for detectable (internalized) biotin-Tfn using HRP-conjugated streptavidin. Measurements of internalized Tfn were normalized to the total levels of surface ligand binding measured at 4°C, measured in parallel for each condition. The results were subjected to two-way ANOVA followed by Bonferonni's multiple comparison post-test.

Biotin-xx-Tfn was obtained from Life Technologies. Avidin and o-Phenylenediamine hydrochloride reagent were obtained from Biobasic and biocytin was obtained from Santa Cruz Biotechnology. Superblock blocking buffer was obtained from Thermo Fisher.

#### 2.10.6. TfR recycling assay

TfR recycling was measured as previously described for the measurement of recycling of glucose transporters; these assays allow orthogonal measurement of internalization and recycling kinetics (Antonescu et al., 2008b; Ishikura et al., 2010). TfR recycling was performed by incubating cells with 1:400 anti-TfR antibodies (Santa Cruz Biotechnology) in serum free DMEM, which recognize an exofacial epitope on the receptor. Antibodies were added to cells for 0, 1, 2, or 3 h at 37°C. This process results in labeling of TfR molecules upon their exposure to the extracellular milieu, as occurs during recycling to the cell surface. Subsequently cells were washed three times in ice-cold $PBS^{2+}$ to remove unbound TfR antibodies, fixed in 4% paraformaldehyde, permeabilized in 0.1% Triton X-100, and then probed with 1:200 secondary antibodies to detect all anti-TfR antibodies bound during this assay (whether internalized or not). Samples were then mounted in fluorescence mounting medium (Dako). The amount of antibody bound during a given time interval, corresponding to TfR recycling, was normalized to total cell TfR, measured in parallel. All TfR staining intensity measurements were performed with ImageJ. These measurements were subjected to two-way ANOVA followed by Bonferonni's multiple comparison posttest.

### 2.11. Fluorescence microscopy

#### 2.11.1. Wide-field epifluorescence microscopy

Wide-field epifluorescence microscopy experiments were obtained using a 63× (numerical aperture [NA] 1.2) oil objective on a Zeiss Axiovert 200 M epifluorescence microscope using an ORCA-Flash 4.0 camera (Hamamatsu).

#### 2.11.2. Laser scanning confocal microscopy

VSVG biosynthetic assay used a laser scanning confocal microscopy experiments and were obtained using a Zeiss LSM700 with a 63× (NA 1.4) oil objective. Excitation light was provided by 488-nm laser illumination.

### 2.11.3. Spinning disc confocal microscopy

Spinning disc confocal microscopy experiments were obtained using a Leica DMIRE2 equipped with a Yokogawa CSU X1 scan head and a 60× (NA 1.35) oil objective using a Hamamatsu C9100-13 electron-multiplying charge-coupled device (EM-CCD) camera. Excitation light was provided by 491-nm (50 mV) and 561-nm (50 mW) laser illumination, and emitted light was collected after passage through 515/40 and 594/40-nm emission filters, as appropriate.

### 2.11.4. Total internal reflection fluorescence microscopy

TIRF-M experiments were processed as described in *Immunofluorescence staining*. TIRF-M was performed using a 150× (NA 1.45) objective on an Olympus IX81 instrument equipped with CellTIRF modules (Olympus Canada) using 491-nm (50 mW) and 561-nm (50 mW) laser illumination and 520/35-nm and 624/40-nm emission filters. Images were acquired using a C9100-13 EM-CCD camera.

For TIRF-M, live-cell imaging was performed on cells incubated in DMEM/F12 lacking phenol red supplemented with 5% fetal bovine serum and oxyrase (1/100; Oxyrase). Cells were placed at 37°C with 5% $CO_2$. Time-lapse image sequences were acquired at 1 s frame rate. TIRF-M was performed using a 150× (NA 1.45) objective on an Olympus IX81 instrument equipped with CellTIRF modules (Olympus Canada) using 491-nm (50 mW) laser illumination and 520/35-nm emission filter. Images were acquired using a C9100-13 EM-CCD camera.

Three channel TIRF-M experiments were processed as described in *Immunofluorescence staining.* TIRF-M was performed using a 100x (NA1.46) objective on an Axio Observer Z1 instrument equipped with Zeiss Zen 2012 software using 488-nm (200 mW), 561-nm (200 mW) and 640-nm (150 mW) laser illumination.

TIRF microscopy experiments of eGFP-PH-Akt localization were performed on a Quorum Diskovery TIRF-M, comprised of a Leica DMi8 microscope equipped with a 63x (NA 1.49) TIRF

objective with a 1.8x camera relay (total 108x magnification). Imaging was done using 488 nm and 561 nm laser illumination using 527/30 and 630/75 emission filters. Images were acquired using a Zyla 4.2Plus sCMOS camera (Hamamatsu Corporation).

## 2.12. Fluorescence microscopy image analysis

### 2.12.1. Localization correlation score

Analysis of LYCAT localization was performed by CN Antonescu. Dual-channel fluorescence micrographs were subjected to automated and unbiased detection of LYCAT structures and subsequent analysis using custom software in Matlab. Determination of the LCS was done by quantifying the correlation of fluorescence intensities of LYCAT and a second compartment marker signal (eGFP-KDEL, eGFP-PIS, or eGFP-E-Syt2) within LYCAT structures. In dual-channel images, LYCAT objects were detected by a Gaussian model–based approach (Aguet et al., 2013; Garay et al., 2015), using only the LYCAT fluorescence channel for initial object detection. Within LYCAT objects, the fluorescence intensity corresponding to the amount of LYCAT or other protein within each object was determined by the amplitude of the Gaussian model in each structure in each channel.

Given the variability of LYCAT and compartment marker expression levels in each cell and image, fluorescence intensity values ($f$) were rescaled by converting raw fluorescence values to a fluorescence standard score ($z$) as follows: $z = (f - \mu)/\sigma$, where $\mu$ and $\sigma$ are the mean and SD of fluorescence values of that channel in that particular image, respectively. For each object, the LCS between two channels, $z1$ and $z2$, was determined as $LCS = 1 - | z1 - z2 |$.

To validate this method, we examined the LCS measurements in sample images, see Bone *et al,* 2017 for images (Bone et al., 2017). We performed LCS analysis on a pair of identical images (“model overlap”) and the same pair of identical images in which one of the images had undergone spatial randomization (180° rotation; “scrambled channel position”). Before LCS analysis, the correlation of raw pixel intensities of each channel in each detected LYCAT object shows the expected result: virtually total complete correlation between “model overlap” intensities and no correlation between the “scrambled channel position” intensities. Note that

the correlation in the “model overlap” images is not perfect despite the images in each channel being identical, as the detection of LYCAT structures by Gaussian model was done assuming two distinct wavelengths for each channel (as per analysis of experimental images), which was not the case in the sample data. Nonetheless, despite the slight offset of the Gaussian model in the secondary channel in the model images, this validation demonstrates the usefulness of this analysis.

A histogram of the calculated LCS values in these image sets shows that the “model overlap” images have LCS values in the 0.85–1.0 range (close correlation), whereas, as expected, the “scrambled channel position” images have LYCAT puncta with LCS values that span the entire possible range (0–1.0). LCS values were calculated for many “model overlap” and “scrambled channel position” images, showing strong median correlation scores for “model overlap” images (∼0.9) and poor correlation (∼0.2) for “scrambled channel position” images.

A sample analysis of LYCAT and eGFP-PIS images shows a strong correlation of raw fluorescence intensities of LYCAT and eGFP-PIS within detected LYCAT objects, as well as an LCS distribution heavily skewed toward high LCS values.

#### 2.12.2. Quantification of cell surface TfR and EGFR, internal TfR distribution and total fluorescence.

Cell surface TfR or EGFR was quantified by measurement of the mean fluorescence intensity over the area of the whole cell. The relative concentration of TfR staining within the perinuclear region was measured by kurtosis of a Gaussian model of the TfR staining intensity over the area of the whole cell. Total TfR, clathrin and EGFR levels were quantified by measurement of the mean fluorescence over the area of the whole cell. Analyses were performed with ImageJ (National Institutes of Health), and data were normalized to control. Measurements were subjected to *t* test.

#### 2.12.3. Automated detection, tracking, and analysis of CCPs.

Timelapse image series obtained by TIRF-M of cells expressing eGFP-CLCa were subjected to automated detection, tracking, and analysis using custom software in Matlab (MathWorks)

(Aguet et al., 2013). Briefly, CCPs were detected using a Gaussian-model based approach to approximate the point spread function, followed by tracking of CCPs through each image series (Jaqaman et al., 2008). Because CCPs are diffraction-limited objects, the amplitude of the Gaussian model of the fluorescence intensity of eGFP-CLCa informs about CCP size. Given the heterogeneity of CCP lifetimes, for eGFP-CLCa fluorescence intensity measurements of CCP size, objects were separated into lifetime cohorts.

#### 2.12.4. Quantification of colocalization of Tfn with EEA1 or TfR.

Colocalization of A647-Tfn with either EEA1 or TfR was performed in ImageJ using Pearson's *r,* measured using the Just Another Colocalization Plugin (JACoP) (Bolte and Cordelières, 2006). The results were subjected to two-way analysis of variance (ANOVA) followed by Bonferonni's multiple comparison posttest.

#### 2.12.5. Quantification of PI(3,4,5)$P_3$ localization.

To obtain the relative cell surface localization index for the PH-Akt probe, the ratio of TIRF/epifluorescence fluorescence was determined for each cell. Measurements were subjected to *t* test.

### 2.13. Statistical analysis

Experiments comparing siControl and siLYCAT were analyzed for statistical significance using an independent *t* test. For experiments with two or more independent variables (such as silencing conditions, EGF stimulation, pulse of Tfn or time of uptake) were analyzed by two way ANOVA with post hoc Bonferroni pairwise comparisons. Significant pairwise comparisons were marked on the graphs. Data are displayed as mean ± the standard error of the mean (SEM).

# Chapter 3
# Results: Characterizing the function of LYCAT in the regulation of phospholipid acylation

## 3.1. Rationale

LYCAT has been postulated to regulates the levels of stearic acid on the *sn1* position of PI in murine tissues as well as in some cells lines (Agarwal et al., 2006; Cao et al., 2009; Imae et al., 2011; Zhao et al., 2009). In these reports, the effects of altered LYCAT expression on acyl chain profile of cardiolipin, phosphatidylglycerol and/or PI was assessed. Additionally, LYCAT localization and effects on mitochondrial function were also evaluated. Though there were conflicting reports, it was suggested LYCAT is localized, at least in part, to the ER and mitochondria (Imae et al., 2011; Li et al., 2010), although the latter was observed in cells from metabolically stressed animals. These studies also found that altered LYCAT expression caused a selective decrease in stearic acid enrichment in certain phospholipids examined (Cao et al., 2004; Imae et al., 2011). More specifically, altered LYCAT expression caused significant reductions in PI containing stearic acid and in some cases, where examined, reductions in 1-stearoyl-2-arachidonoyl acyl species in PIP and $PIP_2$ species were also observed (Imae et al., 2011).

I was particularly interested in assessing the impact of specific acyl chain composition on PI and PIP function. Up to 70% of PI contains 1-stearoyl-2-arachidonoyl acyl species (18:0/20:4) (Baker and Thompson, 1972; D'Souza and Epand, 2015; Hicks et al., 2006). This particular enrichment of PI can occur during *de novo* synthesis, the PI cycle or the Lands cycle. PI is synthesized via two mechanisms in the cell. The first is through the *de novo* pathway in the ER where PI is produced from the sequential reactions from G3P to form CDP-DAG, which is also used in the production of phosphatidylglycerol and cardiolipin. One of the key enzymes of this pathway is PIS, which is responsible for incorporating inositol and CDP-DAG to form PI. PIS has been shown to localize to the ER and to ER-derived motile vesicles called PIPEROsomes (Kim et al., 2011). Following *de novo* synthesis, PI can undergo fatty acid remodeling in the Lands cycle by the action of phospholipases and acyltransferases. PI is also produced through the PI cycle following $PI(4,5)P_2$ breakdown at the plasma membrane, which can also be coupled to a Lands cycle for acyl profile remodeling.

There are a handful of enzymes involved in the synthesis of PI and PIPs that exhibit substrate acyl chain preference including DGKε (Bunting et al., 1996; Lung et al., 2009; Shulga et al., 2011c; Topham and Epand, 2009; Walsh et al., 1994), CDS2 (D'Souza et al., 2014), PIP5K

(Shulga et al., 2012, 2011b), OCRL and synaptojanin-1 (Schmid et al., 2004) and LPIAT1 (Gijón et al., 2008). Therefore there are many different ways a cell can enrich PI with 1-stearoyl-2-arachidonoyl acyl species. Since many of the enzymes are localized in part to the ER or to ER-derived vesicles, it is possible that lipid acyl chain remodelling may involve MCSs to mediate access to lipid substrates in target membranes.

It is well established that proper PIP function is required for regulation of traffic, signaling and cell growth pathways and that dysregulation can lead to disease and cancer. The function of LYCAT and acyl chain enrichment in PI and PIPs has not been elucidated in RPE cells, which is a necessary precursor to study of the role of LYCAT-dependent acyl profile enrichment of PI and PIPs in membrane traffic and signaling. Thus, in order to determine the role and significance of LYCAT on PI and PIP function, I set out to first characterize the function of LYCAT in the regulation of phospholipid acylation using biochemical, microscopic and functional assays.

## 3.2. Results

### 3.2.1. Perturbation of LYCAT using silencing RNA

To characterize the function of LYCAT in RPE cells, I used silencing RNA (siRNA) to knockdown LYCAT mRNA and thus, protein levels. To ensure there were no off target effects, I designed two different oligonucleotides that targeted different sequences of LYCAT mRNA. When examined by western blot, LYCAT had a molecular mass of 44kDa (Figure 3.1A), a value consistent with previous reports (Agarwal et al., 2006; Imae et al., 2011; Li et al., 2012). I detected a strong knockdown of 76% and 86% for oligo1 and oligo2, respectively (Figure 3.1B).

### 3.2.2. LYCAT controls the acyl chain profile of select PIPs

To confirm the function of LYCAT in phospholipid acyl enrichment, I assessed the acyl chain profile of various phospholipids in control and LYCAT-silenced cells. The fatty acid composition of phospholipids was detected using mass spectrometry coupled with liquid chromatography electrospray ionization (LC-ESI). LC-ESI-MS/MS has been proven to be one of the most powerful methods in detecting the molecular species of phospholipids (Yamashita et al., 2014). The acyl chain composition of each lipid is presented as a combination of the *sn1* and *sn2* acyl groups (e.g.,

the 1-stearoyl-2-arachidonyl species corresponds to 38:4). Comparing the acyl profile in control RPE cells, PI shows a unique and striking enrichment for the 38:4 acyl composition that is not seen in other phospholipids (Figure 3.2A) and is consistent with other reports (D'Souza and Epand, 2014; Hicks et al., 2006; Holub and Kuksis, 1978; Imae et al., 2011). Just under 48% of PI contains 38:4 acyl species while the other phospholipids examined including phosphatidylcholine, phosphatidylethanolamine and phosphatidylserine did not show such a unique acyl chain enrichment compared to PI. This establishes that RPE cells are a good model to study the 38:4 acyl profile enrichment of PI and PIPs.

Furthermore, I examined the effect of LYCAT silencing on the acyl chain profile of PI, phosphatidylcholine, phosphatidylethanolamine and phosphatidylserine. I found no major disruptions to the acyl chain composition in phosphatidylcholine, phosphatidylethanolamine and phosphatidylserine in LYCAT-silenced cells (Figure 3.2B-D). Surprisingly, I also found that LYCAT silencing did not affect the acyl chain profile of total PI (Figure 3.2E).

Since there was no disruption to the acyl profile of PI in LYCAT-silenced cells, I hypothesized that LYCAT may be preferentially affecting the acyl chain profiles of specific PIP species. To address this, I analyzed the acyl composition of PIP species using phosphate methylation and LC-ESI-MS/MS to resolve PI, monophosphorylated PIPs ($PIP_1$) and bisphosphorylated PIPs ($PIP_2$; Clark *et al.*, 2011). Interestingly, I found the acyl chain profile of PI and $PIP_1$, which predominantly contains PI(4)P (Stephens et al., 1993), were unaltered in LYCAT-silenced cells (Figure 3.3 A and B). In contrast, however, $PIP_2$, which is predominantly PI(4,5)$P_2$, exhibited reduced levels of many acyl combinations in LYCAT-silenced cells, including 38:4 (Figure 3.3C).

Of importance, I observed a shift in the acyl chain profile in $PIP_2$ upon LYCAT silencing, which was determined by the ratio of 38:*x* to 36:*x* acyl species (where *x* refers to any level of unsaturation). The 38:*x* to 36:*x* ratios of PI and $PIP_1$ were unaffected by LYCAT silencing (Figure 3.4C). In line with the altered acyl chain profile of $PIP_2$, I observed a shift in the acyl profile of $PIP_2$ species. These findings are consistent with the report by Imae *et al* (2011) and suggest that LYCAT preferentially affects the acyl chain profile of a subset of PIPs, including PI(4,5)$P_2$.

### 3.2.3. LYCAT controls total levels of PI(4,5)$P_2$ and PI(3)P

I discovered that LYCAT silencing shifts the acyl chain profile of select PIP species. To determine whether this had an impact on the levels and localization of specific PIPs, I first used [$^3$H]*myo*-inositol radiolabelling technique coupled with high performance liquid chromatography (HPLC) and detection by scintillation to determine total levels of PIPs. This particular setup had not been used on mammalian cells, so it required extensive validation before it was used to experimentally test the impact of LYCAT silencing in RPE cells.

The majority of experimental set up of the flow scintillation system and radiolabelling of PIPs was carried out by two PhD students, Shannon Ho and Christopher Choy in yeast cells (Ho et al., 2016). After radiolabelling incorporation, lipid deacylation and extraction, samples were run through HPLC. To establish and optimize a protocol that would allow study of PIPs in mammalian cells, and thus to investigate LYCAT silencing in RPE cells, two different protocols were initially examined. The two protocols differed in the time that samples spent in the column thus interacting with the column for different times. One protocol ran the samples through the column for 60 min while the other ran the samples through the column for 165 min. It was determined that PI(3)P, PI(4)P and PI(4,5)$P_2$ were detected in similar abundance in each of the protocols therefore I opted to use the shorter of the two protocols, 60 min (Figure 3.5A). The abundance of each PIP species was determined by the counts that were integrated under the area of the peak and subsequently normalized to its parent PI to account for differences in sample loading.

Both protocols however were unable to detect PI(3,4,5)$P_3$, likely due to the extraction protocol. The protocol uses 1-butanol/ethyl ether/ethyl formate to extract lipids. Due to the highly acidic nature of PI(3,4,5)$P_3$, a stronger extraction reagent may be required for efficient extraction. A slightly altered protocol has been established, which uses chloroform/methanol to extract lipids but is awaiting to be validated. In any case, this novel extraction method that would allow measurement of PI(3,4,5)$P_3$ levels was not available and thus, I focused on the study of PI(3)P, PI(4)P and PI(4,5)$P_2$ levels.

To confirm that I correctly identified the peaks corresponding to PI(3)P and PI(4,5)$P_2$ by HPLC, I treated cells with various inhibitors. Addition of the PI3K inhibitor LY294002 for 30 min

caused a 60% reduction in the putative PI(3)P peak present, suggesting the peak indeed represents PI(3)P (data not shown). To confirm proper identification of PI(4,5)$P_2$, cells were treated with ionomycin for 20 min, as ionomycin is an ionophore, which increases intracellular levels of $Ca^{2+}$ that leads to the hydrolysis of PI(4,5)$P_2$. Treatment with ionomycin caused a significant reduction in the size of the putative PI(4,5)$P_2$ peak at 27 min elution (Figure 3.5B) thus identifying it as PI(4,5)$P_2$. Treatment with ionomycin resulted in a 97% reduction in PI(4,5)$P_2$ levels (Figure 3.5C).

Following validation of PIP detection by radiolabelling and HPLC, I set out to determine the effect of LYCAT silencing on PIP levels. I found that LYCAT silencing resulted in significant reductions in PI(3)P and PI(4,5)$P_2$ levels, which were reduced by 25% ± 0.05% and 21% ± 0.06%, respectively (Figure 3.6). Interestingly, I did not see any effect on PI(4)P levels, suggesting that LYCAT silencing affects the levels of a subset of PIPs. It is possible that the changes in the acyl profile of $PIP_2$ (Figure 3.3C) are due to the reduction in PI(4,5)$P_2$ levels in these cells. The acylation data and detection of total PIP levels suggest that LYCAT selectively controls certain PIPs by selectively controlling the acyl chain profile of $PIP_2$ species and total levels of PI(3)P and PI(4,5)$P_2$.

### 3.2.4. LYCAT silencing alters localization of select PIPs

In order to functionally characterize the impact of altered acyl chain content of PIPs, in addition to the results from biochemical isolation and quantification of PIP levels by HPLC and flow scintillation, I transfected cell with PIP specific probes to determine if LYCAT silencing impacted PIP localization. Fluorescently labelled protein binding domains, 2FYVE, PH-PLCδ and P4M are highly specific to binding PI(3)P, PI(4,5)$P_2$ and PI(4)P, respectively (Gillooly et al., 2000; Hammond et al., 2014; Stauffer et al., 1998; Stenmark et al., 2002). The localization of 2FYVE-GFP was punctate in structure, indicative of endosomes (Liu et al., 2016). LYCAT silencing caused a 29% reduction in the number of 2FYVE-GFP positive structures, which is consistent with abated levels of PI(3)P (Figure 3.7 A and B).

Furthermore, LYCAT silencing significantly altered the localization of the PI(4,5)$P_2$ probe, PH-PLCδ (Figure 3.7A). Control cells show PH-PLCδ-GFP predominantly and uniformly decorated on the plasma membrane (Várnai and Balla, 1998), however LYCAT silencing causes a

redistribution of the probe to tubular and punctate-like structures throughout the cell, which suggests a redistribution of PI(4,5)$P_2$ from its enrichment in the plasma membrane to intracellular membrane structures.

In contrast to the changes in PI(3)P and PI(4,5)$P_2$ localization, P4M-GFP probe localization was indistinguishable between control and LYCAT-silenced cells, a distribution consistent with the plasma membrane and the *trans*-Golgi network (Figure 3.7A) (Hammond et al., 2014). Collectively these data are consistent with the biochemical measurements of PI(4,5)$P_2$ levels and indicates that LYCAT selectively affects the localization of PI(3)P and PI(4,5)$P_2$ but not PI(4)P.

### 3.2.5. LYCAT is localized to ER-derived PIS vesicles

In addition to determining the function of LYCAT in regulating PIP acyl chain profile, levels and localization, I focused on LYCAT localization in the cell, in order to understand whether specific cellular localization(s) could explain the selective control of certain PIPs by LYCAT. The selective control of certain PIPs would suggest that it is unlikely that LYCAT would function in the ER during *de novo* PI synthesis, as this would result in broad control of all PIPs and PI. Given our results that show selective control of PI(4,5)$P_2$ and PI(3)P by LYCAT, I might expect LYCAT to localize to compartments other than the ER, thus allowing specific control of certain PIPs.

Previous studies suggested that LYCAT exhibits some localization to the ER (Cao et al., 2004; Imae et al., 2011; Zhao et al., 2009). However, these studies did not perform a broader analysis of LYCAT localization with other relevant markers, an important consideration, since the ER has several sub-compartments (A. R. English and Voeltz, 2013). To monitor LYCAT localization, I transfected RPE cells with LYCAT-FLAG and viewed localization by spinning disc and TIRF-M. I found modest localization with eGFP-KDEL, a generic ER marker (Figure 3.8A), suggesting that LYCAT may predominantly localize to other sub-compartments.

PIS, which plays a key role in PI synthesis and is localized to ER-derived vesicles that rapidly move between the ER and various organelle membranes, as observed in cells expressing eGFP-PIS (Kim et al., 2011). I hypothesized that LYCAT may localize to PIS vesicles. I found striking and extensive colocalization between LYCAT and eGFP-PIS (Figure 3.8A). PIS vesicles make dynamic and transient contacts with a number of compartments. To focus on their interaction with the

plasma membrane, I examined these transient contact sites by focusing on extended synaptotagmin 2 (E-Syt2) (Giordano et al., 2013a; Min et al., 2007). LYCAT exhibited partial colocalization with E-Syt2 (Figure 3.8A) suggesting that LYCAT localized to PIS-containing vesicles does colocalize to ER-plasma membrane contact sites.

To allow better understanding of the relative localization of LYCAT with eGFP-KDEL, eGFP-PIS, and eGFP-E-Syt2, I analyzed this by automated detection of LYCAT puncta followed by measurement of the localization correlation score (LCS) of the fluorescence intensities of LYCAT and that of secondary channel proteins within each object (Bone et al., 2017). LCS is a quantitative, unbiased, and systematic analysis and revealed a very strong intensity correlation of LYCAT-FLAG with eGFP-PIS within LYCAT structures (Figure 3.8B). In contrast, eGFP-KDEL and LYCAT exhibited very low intensity correlation in LYCAT structures, whereas eGFP-E-Syt2 and LYCAT had intermediate intensity correlation. Thus LYCAT is extensively localized to ER-derived PIS-containing vesicles, known to transiently interact with ER-plasma membrane contact sites, but not the ER domains marked by eGFP-KDEL (Kim et al., 2011).

Furthermore, as PIS-vesicles were proposed to form transient contacts with the plasma membrane (Kim et al., 2011), I used TIRF-M to visualize structures restricted to roughly 200 nm from the cell surface, allowing us to specifically examine LYCAT localization to PIS vesicles, contact sites and general ER within close proximity to the plasma membrane. Similar colocalization patterns were seen with TIRF-M as were seen with confocal spinning disc microscopy. LYCAT exhibited extensive overlap with PIS vesicles, little overlap with KDEL and moderate overlap with E-Syt2 (Figure 3.9).

LYCAT tends to localize significantly to PIS vesicles and moderately with E-Syt2. I investigated whether these represent separate pools of vesicles in the cell or whether all three localize to similar pools of vesicles. Using TIRF-M I examined cells transfected with LYCAT-FLAG, eGFP-PIS and eGFP-E-Syt2. I observed some punctate structures that contained LYCAT, PIS and E-Syt2 (Figure 3.10A). There were vesicles that were positive for PIS and LYCAT that did not exhibit overlap with E-SYt2. Furthermore, I examined the overlap between LYCAT, PIS and KDEL. Consistent with confocal spinning disc and TIRF-M imaging, there was poor overlap between LYCAT/PIS vesicles with KDEL (Figure 3.10B). These data highlight that LYCAT is largely localized

to PIS vesicles, but not general ER, where a portion of these vesicles also localize to E-Syt2 ER-plasma membrane contact sites.

Hence, this work revealed the function of LYCAT in the selective regulation of acylation of specific PIPs, as I found that LYCAT selectively impacts the acyl profile of $PIP_2$ species but not other PIPs or phospholipids. Furthermore, I found that LYCAT impacts total levels of PI(3)P and PI(4,5)$P_2$ and their localization in the cell but was without effect on PI(4)P levels and localization. I also performed a more thorough investigation into the localization of LYCAT and found LYCAT localizes to PIS vesicles that are known to make transient contacts with the plasma membrane and partially localized to ER-plasma membrane contact sites mediated by E-Sty2. I next assessed the significance of LYCAT in regulating TfR endomembrane traffic by assessing the various stages of traffic including endocytosis, intracellular sorting and recycling.

Chapter 3 Figures

Figure 3.1. LYCAT silencing is efficient in RPE cells. RPE cells or a derivative RPE line stably expressing eGFP fused to clathrin light chain (eGFP-CLCa) were transfected with one of two distinct siRNA sequences targeting LYCAT (siLYCAT$^{1}$ or siLYCAT$^{2}$) or non-targeting siRNA (siControl). (***A, B***) Following siRNA transfection, whole cell lysates were subjected to western blotting to detect total LYCAT levels. Shown in (*A*) are representative immunoblots loaded with a rage of sample dilutions (depicted as %), showing detection of LYCAT or actin (loading control). Shown in (*B*) are the quantified LYCAT protein levels following normalization to actin loading control in RPE cells treated with siLYCAT$^{1}$ (n = 7) and siLYCAT$^{2}$ (n = 4), mean ± SEM, independent *t* test, * $p < 0.05$.

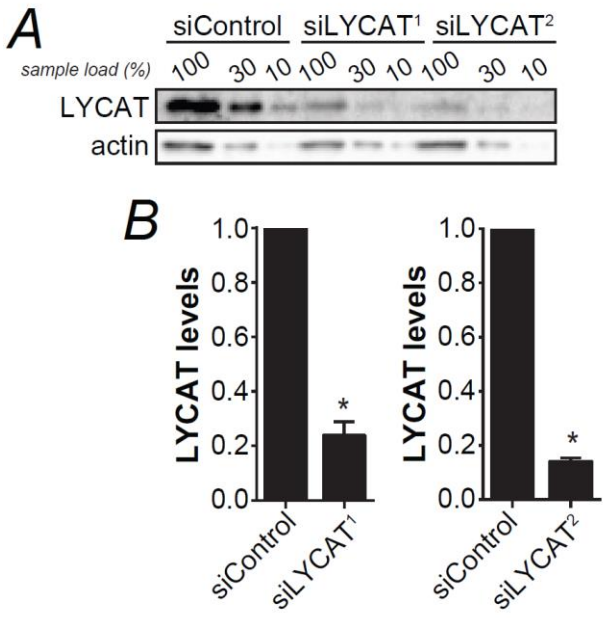

Figure 3.2. LYCAT silencing does not broadly impact the acyl chain composition of various phospholipids. RPE cells were transfected with siRNA targeting LYCAT (siLYCAT) or nontargeting siRNA (siControl). Cell extracts were subjected to quantitative measurement of acyl group composition of various phospholipid species by LC-ESI-MS/MS. Note that the molecular species indicate the mass and saturation combination of acyl chains on the *sn*-1 and *sn*-2 positions. (***A***) Shown are the mean ± SEM (n = 5) of the percent of total of each phospholipid species harbouring the indicated acyl compositions in control RPE samples (not treated with siRNA). Also shown are the acyl chain composition of phosphatidylcholine (PC) (***B***), phosphatidylethanolamine (PE) (***C***), phosphatidylserine (PS) (***D***) and phosphatidylinositol (***E***), (siContol; black bars and siLYCAT; grey bars) showing that LYCAT silencing is largely without effect on acyl composition of these phospholipids. Note that phosphorylated PIPs are a minor species relative to total PI (Balla, 2013) (n = 4), independent *t* test,* $p < 0.05$.

Figure 3.2.

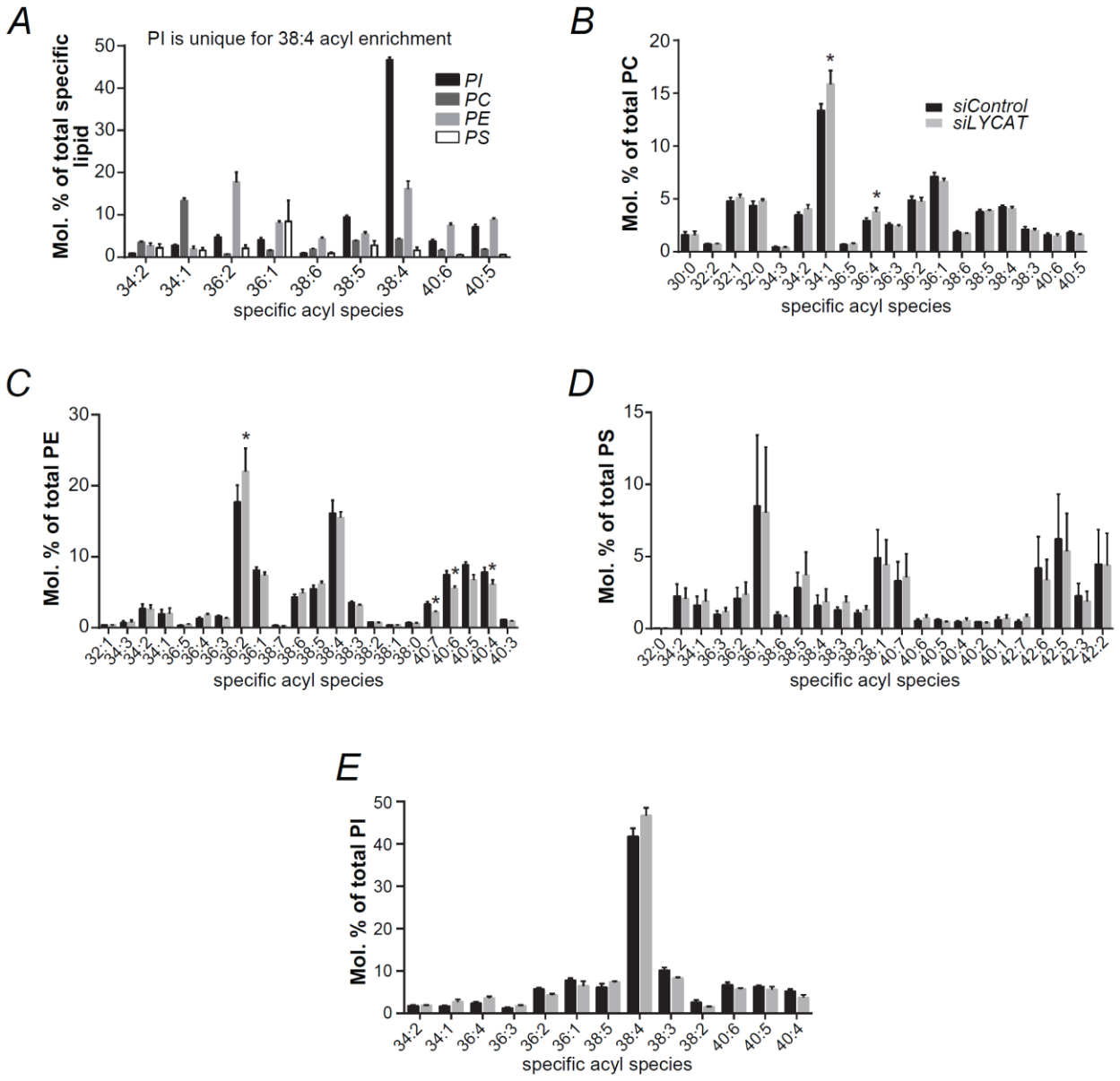
A
PI is unique for 38:4 acyl enrichment
PI
PC
PE
PS
Mol. % of total specific lipid
specific acyl species
B
siControl
siLYCAT
Mol. % of total PC
specific acyl species
C
Mol. % of total PE
specific acyl species
D
Mol. % of total PS
specific acyl species
E
Mol. % of total PI
specific acyl species

Figure 3.3. LYCAT knockdown alters acyl chain profile of $PIP_2$ but not that of PI or $PIP_1$. RPE cells were transfected with siRNA targeting LYCAT (siLYCAT; gray bars) or nontargeting siRNA (siControl; black bars). Cell extracts were subjected to quantitative measurement of acyl group composition of various PIP species by phosphate group methylation, followed by LC-ESI-MS/MS. Mean ± SEM of the measurements of molecular compositions of PI (***A***), $PIP_1$ (***B***), and $PIP_2$ (***C***). Note that the molecular species indicate the mass and saturation combination of acyl chains on the *sn*-1 and *sn*-2 positions ($n = 4$), independent *t* test, $*p < 0.05$.

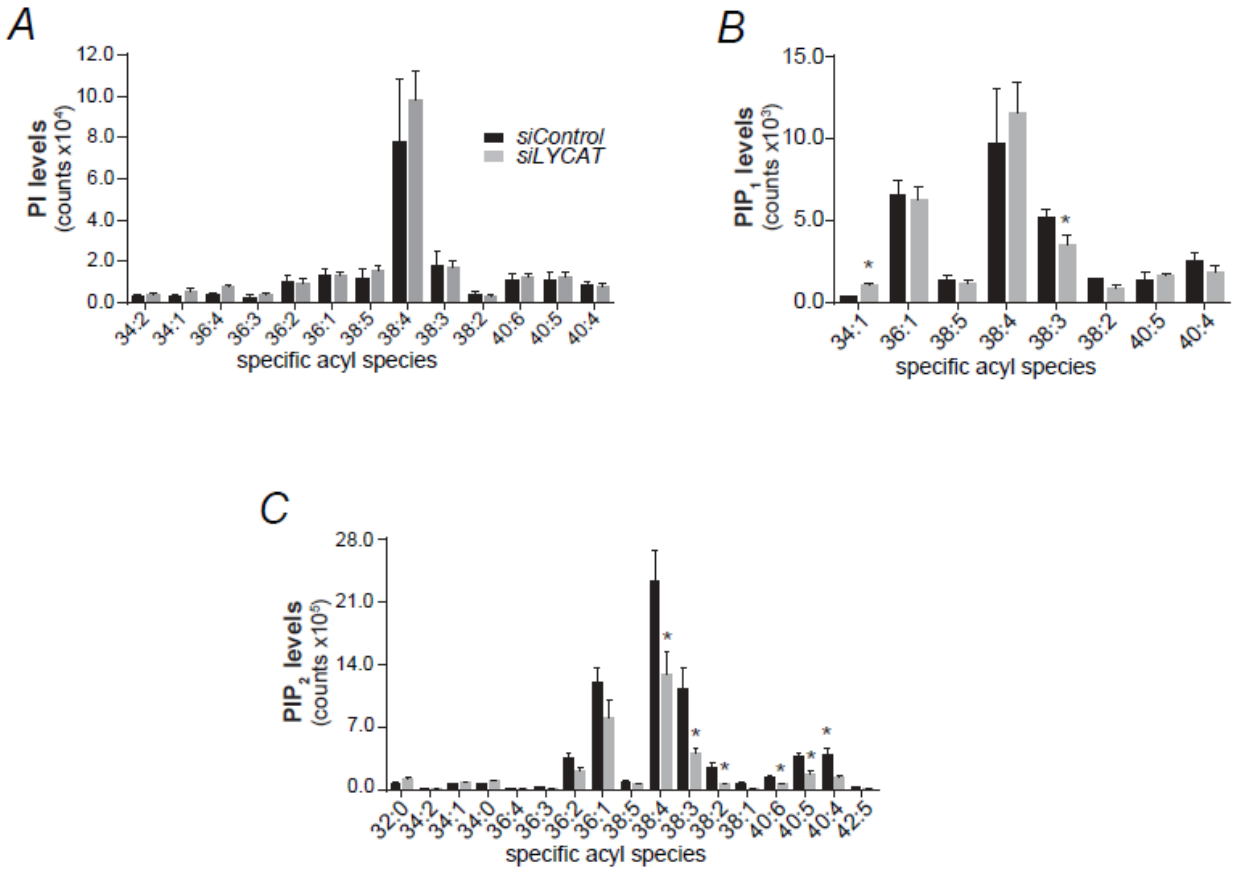

Figure 3.4. LYCAT knockdown shifts the acyl chain profile of $PIP_2$ and alters the levels of stearate. RPE cells were transfected with siRNA targeting LYCAT (siLYCAT; gray bars) or nontargeting siRNA (siControl; black bars). Cell extracts were subjected to quantitative measurement of acyl group composition of various PIP species by phosphate group methylation, followed by LC-ESI-MS/MS. $PIP_1$ (***A***) and $PIP_2$ (***B***) raw intensities of acyl chains were normalized to that of 38:4 PI for each silencing condition in each experiment. Shown are the mean ratios of each lipid to 38:4 PI. (***C***) Ratios of the mean 38:*x* to 36:*x* levels in PI, $PIP_1$ and $PIP_2$ (*n* = 4), independent *t* test, * $p < 0.05$.

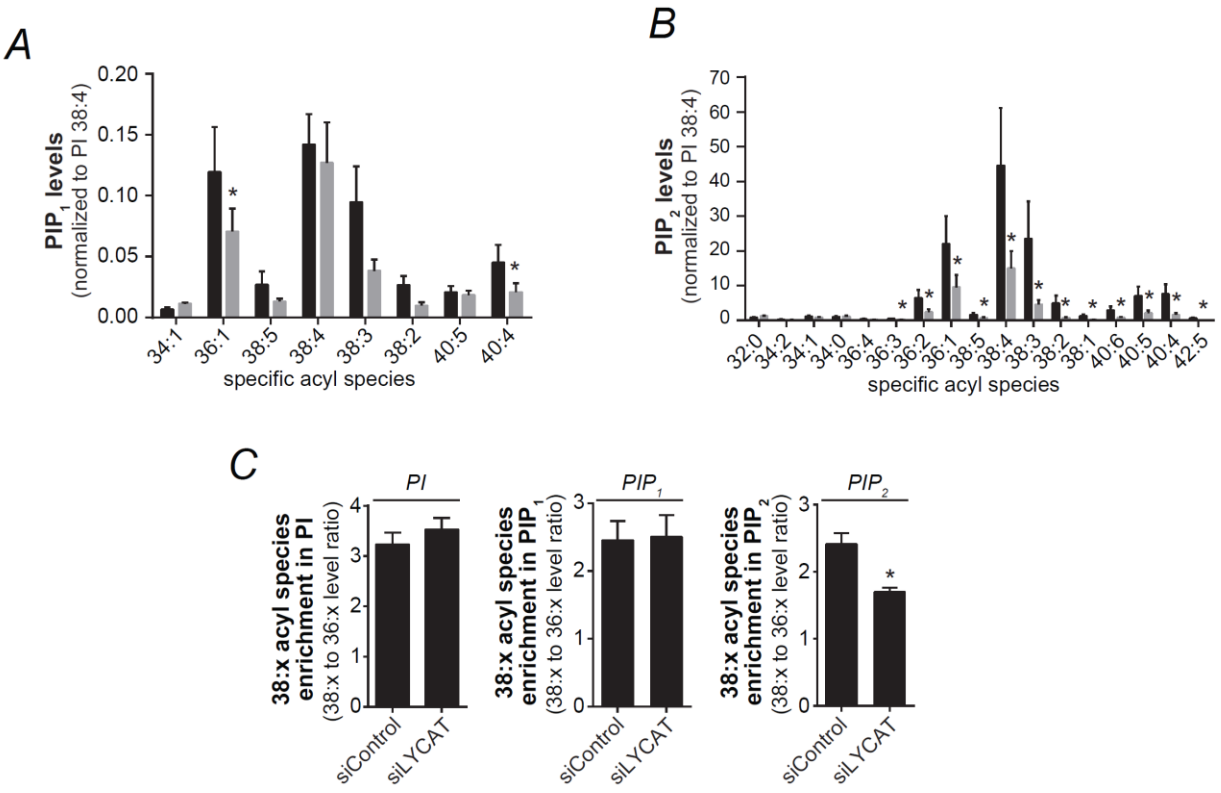

Figure 3.5. Validation of PIP species detected by radiolabelling and HPLC. After 24 hr of [$^3$H]*myo*-inositol labelling, samples were run through HPLC and then detected by two different protocols to determine optimal conditions for PIP detection. (***A, B***) Representative chromatography spectra of HPLC flow scintillation detection. Each PIP species is indicated by a different colour on each chromatogram. (*A*) Control cells showing the profile of PI, PI(3)P, PI(4)P and PI(4,5)$P_2$. (*B*) To validate detection of PI(4,5)$P_2$, cells were treated with ionomycin (10 μM) for 20 min to induce PI(4,5)$P_2$ hydrolysis. Shown in (***C***) is the mean ± SEM of PI(4,5)$P_2$ loss in cells treated with ionomycin. PI(4,5)$P_2$ levels were normalized to total PI, $n = 3$, independent *t* test, * $p < 0.05$.

Figure 3.5.

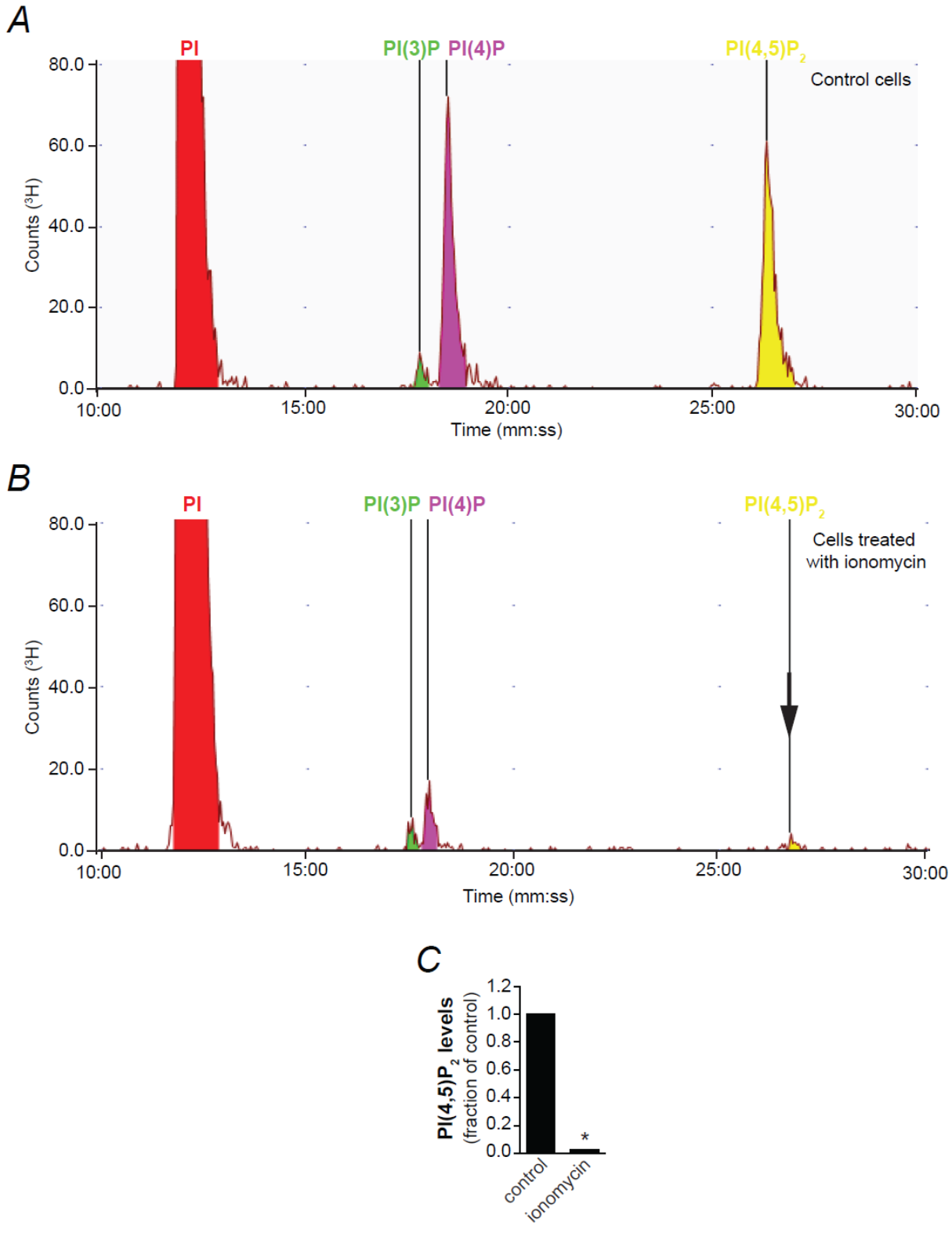
A
PI
PI(3)P
PI(4)P
PI(4,5)P2
Control cells
Counts (3H)
80.0
60.0
40.0
20.0
0.0
10:00
15:00
20:00
25:00
30:00
Time (mm:ss)
B
PI
PI(3)P
PI(4)P
PI(4,5)P2
Cells treated with ionomycin
Counts (3H)
Time (mm:ss)
C
PI(4,5)P2 levels (fraction of control)
1.2
1.0
0.8
0.6
0.4
0.2
0.0
*
control
ionomycin

Figure 3.6. LYCAT silencing reduces total levels of PI(3)P and PI(4,5)$P_2$ but not PI(4)P. RPE cells were transfected with siRNA targeting LYCAT (siLYCAT) or nontargeting siRNA (siControl). The levels of PI(3)P, PI(4,5)$P_2$, and PI(4)P were measured after [$^3$H]*myo*-inositol labeling, HPLC, and detection by flow scintillation. Mean ± SEM, $n$ = 4, independent $t$ test, * $p < 0.05$.

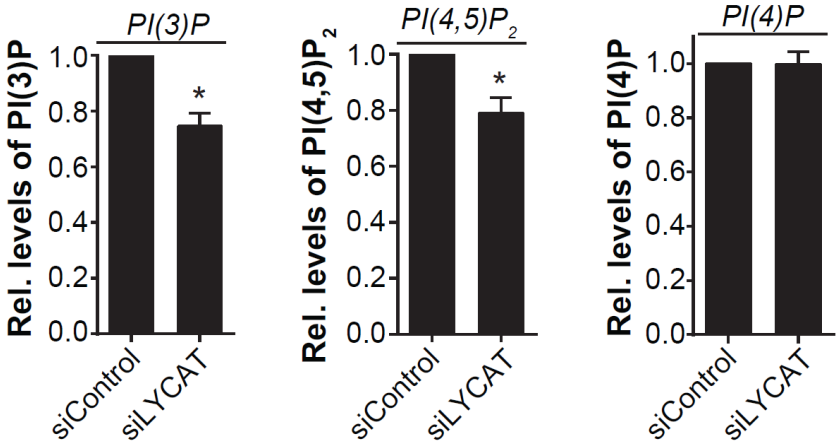

Figure 3.7. LYCAT silencing alters localization of PI(3)P and PI(4,5)$P_2$. RPE cells were transfected with siRNA targeting LYCAT (siLYCAT) or nontargeting siRNA (siControl). Cells were transfected with cDNAs encoding 2FYVE-GFP, PH-PLCδ-GFP or P4M-GFP to probe for PI(3)P, PI(4,5)$P_2$, and PI(4)P respectively. (***A***) Representative spinning disc confocal micrographs (scale 20 µm). (***B***) Median, 25th and 75th percentiles (boxes), and Tukey range (whiskers) of the number of 2FYVE-GFP–positive structures per cell (*n* = 3). *Work completed by Ms. RM Dayam.*

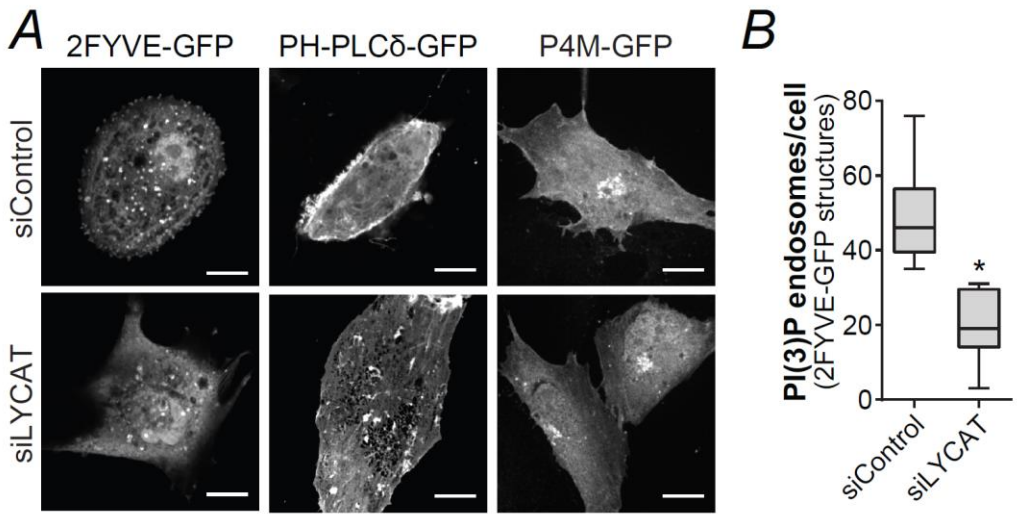

Figure 3.8. LYCAT is localized to ER-derived PIS vesicles. RPE cells were transfected with cDNAs encoding LYCAT-FLAG along with either eGFP-PIS, eGFP-KDEL or eGFP-E-Syt2 and were subjected to immunofluorescence staining to detect LYCAT-FLAG. (***A***) Representative spinning disc confocal micrographs (scale 10 µm). (***B***) LYCAT-positive structures were subjected to automated detection, followed by measurement of the LCS between LYCAT and eGFP-PIS, eGFP-KDEL, or eGFP-E-Syt2 in these structures. Median, 25th and 75th percentiles (boxes), and Tukey range (whiskers) of LCS values. The numbers of LYCAT structures and cells for each condition are, for eGFP-PIS, 24,907 and 29, for eGFP-KDEL, 14,359 and 24, and for eGFP-ESyt2, 23,567 and 23, respectively. * $p < 0.05$.

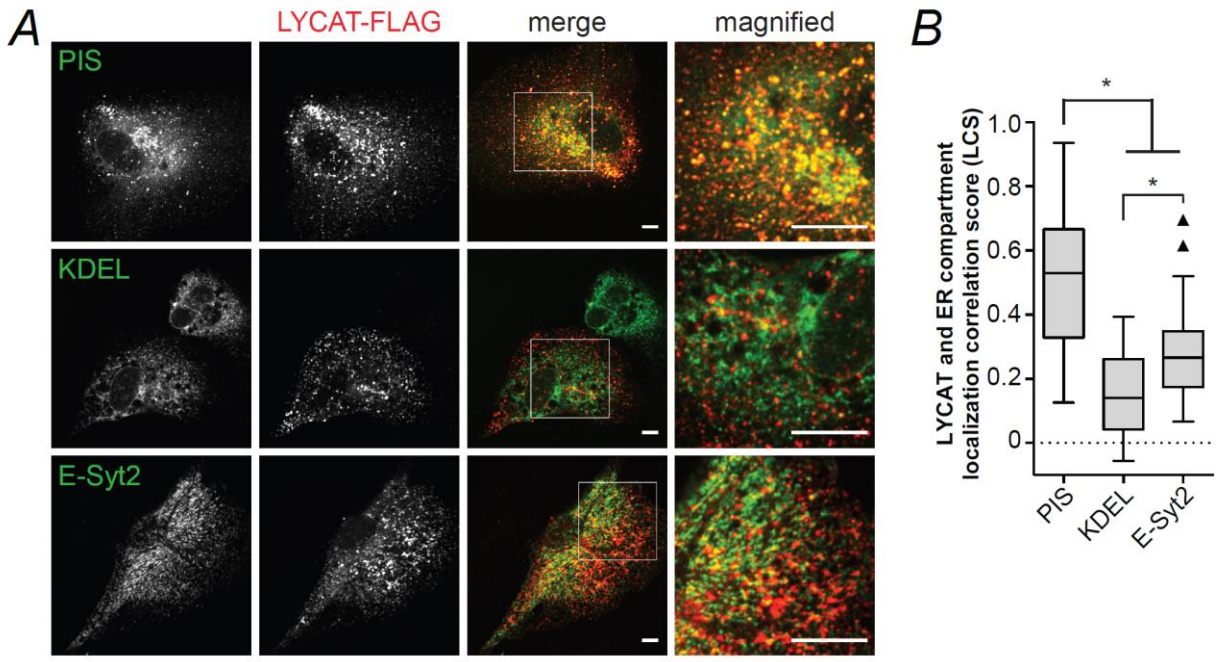

Figure 3.9. LYCAT is localized to peripheral PIS vesicles detected by TIRF-M. RPE cells were transfected with cDNAs encoding LYCAT-FLAG along with either eGFP-PIS, eGFP-KDEL, eGFP-E-Syt2 or eGFP-E-Syt3, subjected to immunofluorescence staining to detect LYCAT-FLAG and imaged using TIRF-M to selectively examine the structures proximal to the cell surface. Shown are representative micrographs (scale 5 µm).

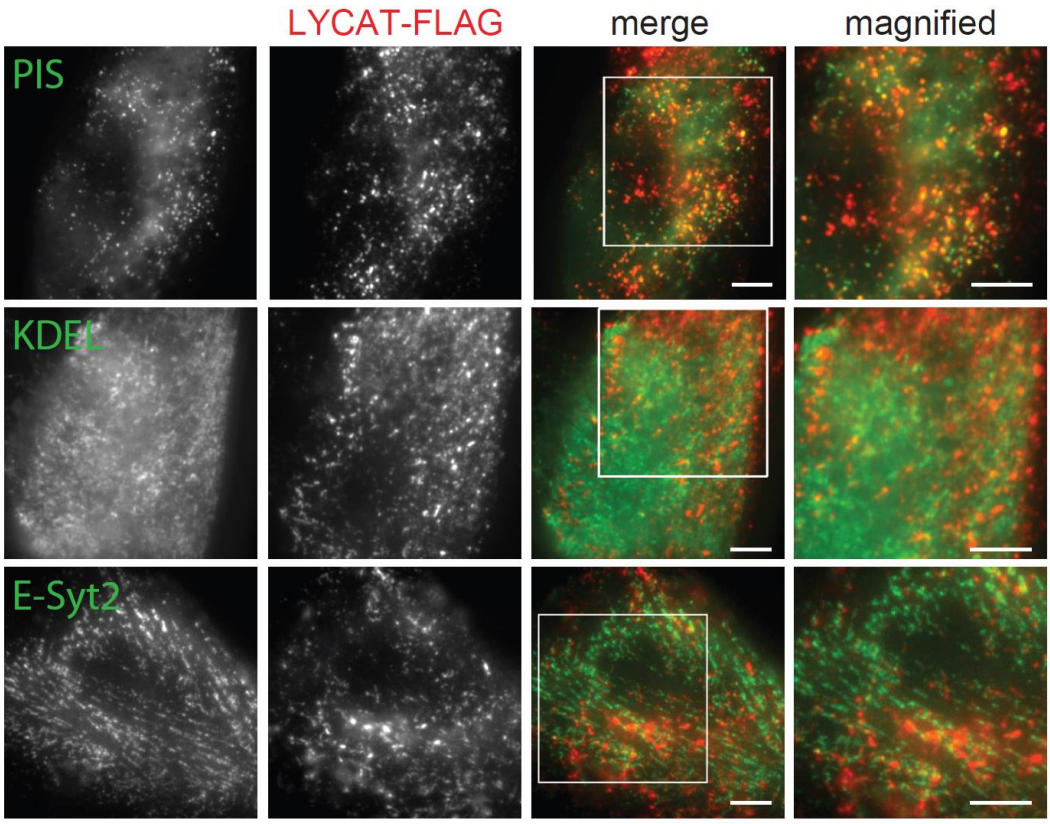

Figure 3.10. LYCAT-positive PIS vesicles localize to E-Syt2 membrane contact sites. RPE cells were transfected with cDNAs encoding LYCAT-FLAG, eGFP-PIS and eGFP-E-Syt2 (***A***) or LYCAT FLAG, eGFP-PIS and eGFP-KDEL (***B***) and then subjected to immunofluorescence staining to detect LYCAT-FLAG. Cells were imaged using TIRF-M to examine the overlap of three probes to examine LYCAT localization. Shown are representative micrographs (scale 5 µm).

Figure 3.10.

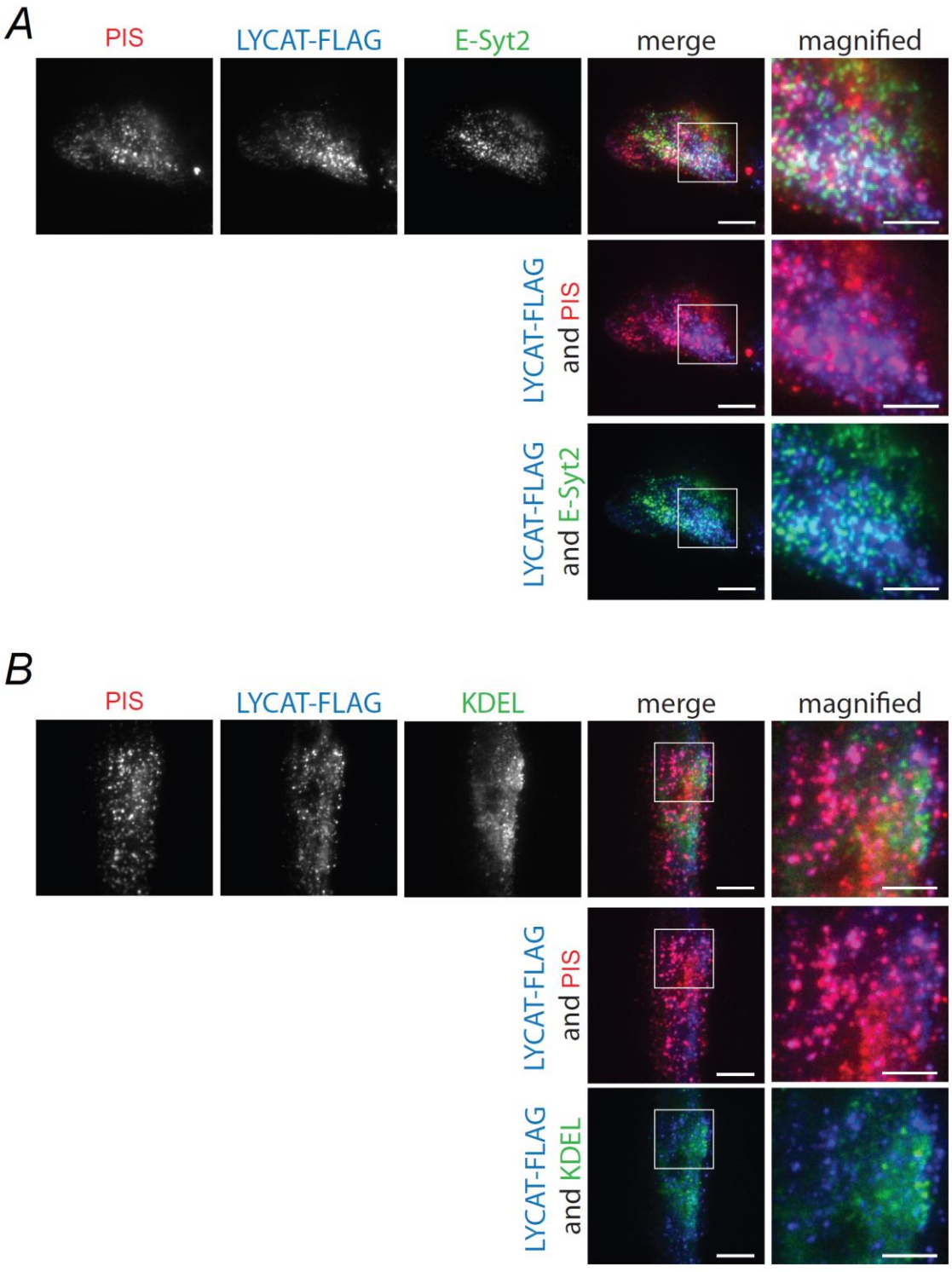
A
PIS
LYCAT-FLAG
E-Syt2
merge
magnified
LYCAT-FLAG and PIS
LYCAT-FLAG and E-Syt2
B
PIS
LYCAT-FLAG
KDEL
merge
magnified
LYCAT-FLAG and PIS
LYCAT-FLAG and KDEL

# Chapter 4
# Results: Significance of LYCAT in regulating endomembrane traffic

## 4.1. Rationale

Using biochemical, microscopic and functional assays I characterized the function of LYCAT in the regulation of PIP acylation in RPE cells. Using silencing RNA, I determined that knockdown of LYCAT shifts the acyl profile from longer acyl chains (38:*x*) to shorter ones (36:*x*) in $PIP_2$ species but has no effect on PI or PIP species. I also determined that total levels of PI(4,5)$P_2$ and PI(3)P decreased upon LYCAT silencing but had no impact on PI(4)P total levels. Using PIP probes, I determined that the localization of PI(4,5)$P_2$ and PI(3)P were altered causing PI(4,5)$P_2$ to localize to internal tubular structures and the number of PI(3)P endosomes to decrease, but had no effect on the localization of PI(4)P. Furthermore, I found LYCAT localized to PIS-containing ER-derived vesicles, but not to the general ER. Thus, given these alterations in PI(4,5)$P_2$ and PI(3)P upon LYCAT silencing, LYCAT may specifically control membrane traffic processes dependent on these two lipids.

To functionally assess the alterations in PI(4,5)$P_2$ acyl profile and decrease in PI(4,5)$P_2$ and PI(3)P levels, I used TfR endomembrane traffic as our model. TfR traffic has been extensively studied and is commonly used for studying CME, intracellular sorting and recycling (Maxfield and McGraw, 2004; Navaroli et al., 2012; Sheff et al., 2002). In addition, TfR traffic is dependent on multiple PIPs including PI(4,5)$P_2$ (Varnai et al., 2006) and PI(3)P (van Dam et al., 2002). TfR is internalized through CME which requires PI(4,5)$P_2$ for recruitment of AP2 and clathrin to sites at the plasma membrane for initiation of CME. Once inside the cell the receptor is sorted at the EE and directed toward the fast or slow recycling pathways (van Dam et al., 2002). Both of these processes require PI(3)P for the recruitment of proteins involved in tethering and fusion at the EE, such as EEA1. I used immunofluorescence techniques, alongside tracking of fluorescent ligand and automated analysis of live cell imaging to assess the impact of altered acyl chain content on TfR traffic.

## 4.2. Results

### 4.2.1. LYCAT silencing alters TfR endomembrane traffic

I first investigated whether LYCAT-dependent alterations in PIP acyl chain content affects TfR endomembrane traffic. To do this I first examined cell surface levels of TfR, a measurement that

acts as a general reporter of the overall efficiency of endomembrane traffic. LYCAT silencing by each of two different siRNA sequences caused a 36% ± 0.03% and 41% ± 0.04% decrease in the amount of TfR at the cell surface, respectively (Figure 4.1 A and B). In order to confirm the decrease in cell surface TfR was specifically due to a deficiency of LYCAT, following knockdown of LYCAT, I transfected an siRNA resistant exogenous LYCAT-FLAG into cells and measured the cell surface levels of TfR. This expression of exogenous LYCAT-FLAG rescued cell surface TfR levels in LYCAT-silenced cells (Figure 4.1C) demonstrating that the altered surface levels of TfR were due to specific perturbation of LYCAT.

TfR exhibits a pronounced perinuclear morphology as it traffics through intracellular compartments, including recycling endosomes (Dugani et al., 2008). We stained for TfR in permeabilized cells to determine whether LYCAT silencing impacts the intracellular distribution of TfR. I observed perinuclear clustering in control cells (Figure 4.1D, top panel), however LYCAT silencing caused a dispersal of the perinuclear accumulation (Figure 4.1D, bottom panel). To quantitatively measure and assess the change in TfR distribution in LYCAT-silenced cells this, I used kurtosis, which is a measure of the spread of fluorescent signal. The more densely packed fluorescent signal would result in a high kurtosis while a more dispersed signal would result in a decrease in kurtosis. LYCAT deficiency caused a 34% ± 0.04% and 46% ± 0.12% reduction in kurtosis for LYCAT sequence 1 and 2, respectively, indicating a dispersal of signal (Figure 4.1E). Together with the observation of reduced cell surface TfR levels in LYCAT-silenced cells, these results indicate that LYCAT silencing perturbs the endomembrane traffic of TfR.

To confirm the decrease in cell surface TfR was not due to a decrease in total TfR, I examined total TfR by fluorescence microscopy and by western blot. By quantifying total fluorescent signal (Figure 4.1F) and assessing total protein content by western blot (Figure 4.1G), LYCAT silencing did not reduce total levels of TfR. This result supports my interpretation that LYCAT silencing disrupts the endomembrane traffic of TfR, and not total TfR expression levels. The decrease in cell surface levels and the change in TfR distribution could be due to a number of different factors including a defect in endocytosis, a defect in intracellular sorting or a defect in recycling of the receptor back to the cell surface.

### 4.2.2. LYCAT silencing alters clathrin-mediated endocytosis

To assess the defect in TfR endosomal traffic, I first evaluated CME since this process is responsible for TfR internalization and is controlled by $PI(4,5)P_2$. Additionally, LYCAT silencing caused a reduction in $PI(4,5)P_2$ levels and caused the PH-PLCδ1 probe to relocalize from the cell surface to intracellular tubular and punctate structures. First, I evaluated CCP dynamics by performing time-lapse TIRF-M in RPE cells stably expressing eGFP-CLCa (Figure 4.2A) followed by automated detection, tracking and analysis of CCPs (Aguet et al., 2013). This is an established and validated method that allows analysis of CCP number, lifetimes and fluorescence intensity that measure the rate of CCP initiation, the efficiency of formation of internalized vesicles and CCP size, respectively. Consistent with a reduction in $PI(4,5)P_2$ levels and perturbation of $PI(4,5)P_2$ localization, LYCAT silencing reduced CCP initiation density (Figure 4.2B) and caused a reduction in overall CCP size (Figure 4.2C). CCP size were measured by the fluorescence intensity of eGFP-CLCa of CCPs, as the latter are diffraction-limited structures. LYCAT-silencing also slightly altered CCP lifetimes, reducing the number of short-lived CCPs (Figure 4.2D). To confirm the alterations in CCP dynamics were not due to a reduction in total clathrin, I examined total clathrin levels by immunofluorescence and found LYCAT silencing had no effect on total clathrin levels (Figure 4.2E).

Furthermore, I investigated the effect of LYCAT silencing on Tfn internalization by employing an established assay that uses a biotin-conjugated Tfn (biotin-Tfn) and avidin-based quenching of uninternalized ligand followed by ELISA-based detection of internalized biotin-Tfn to monitor the levels of internalized Tfn (Antonescu et al., 2010). Consistent with defects in CCP dynamics, I observed that LYCAT silencing led to a significant reduction in the rate of Tfn internalization (Figure 4.2F). Together these data indicate that LYCAT regulates CME, likely by affecting $PI(4,5)P_2$ levels and localization.

### 4.2.3. LYCAT silencing alters intracellular traffic of TfR to EEA1 compartments

A reduction of TfR endocytosis is not sufficient to explain how LYCAT silencing results in a reduction in cell surface levels of TfR. Instead, these results suggest that LYCAT silencing may also impact some stage of TfR intracellular membrane traffic. Thus, the next step I examined to

investigate the effects of LYCAT silencing on TfR endomembrane traffic was the intracellular traffic of TfR. LYCAT silencing caused a reduction in total PI(3)P levels and a decrease in the number of 2FYVE structures. Thus, I predicted that PI(3)P-dependent processes would be disturbed. Intracellular sorting and recycling are PI(3)P-dependent so we first examined traffic at the EE. Immediately after endocytosis, CCVs mature into vesicles that acquire PI(3)P and Rab5, and eventually fuse with other membranes to deliver TfR into EEA1-positive early endosomes. To test this pathway, we monitored the arrival of fluorescently labelled Tfn pulsed for various time points into EEA1-positive endosomes (Figure 4.3A). Using Pearson's coefficient, I quantitatively assessed the localization of fluorescent Tfn and EEA1. LYCAT silencing significantly delayed the arrival of Tfn to EEA1 compartments compared to control cells (Figure 4.3B). This is consistent with the effect of reduced PI(3)P levels by other manipulations (van Dam et al., 2002). After approximately 30 min, the levels of Tfn at EEA1 positive vesicles in LYCAT-silenced cells reach levels seen in control cells, indicating that LYCAT silencing causes a delay, but not a block, in TfR membrane traffic.

To confirm the delay in arrival of Tfn to EEA1 vesicles was not due to alteration of the number of EEA1-positive early endosomes upon LYCAT silencing, I assessed the effect of LYCAT silencing on the number and intensity of EEA1-positive puncta and found there was no appreciable change (Figure 4.3C). This result suggests that LYCAT silencing does not impact the formation of early endosomes.

Furthermore, I measured the ability of recently internalized Tfn to access the total cellular pool of TfR-labeled endosomes (Figure 4.3D). Using fluorescently labelled Tfn pulsed into cells for 15 min, I assessed its localization to total TfR by immunofluorescence. I found a significant decrease in the localization of Tfn to the total cellular pool of TfR as assessed by Pearson's coefficient (Figure 4.3E). This result suggests that LYCAT silencing does impact the traffic of Tfn to total TfR. Overall, these results suggest that the altered levels and function of PI(3)P impair the delivery of vesicles harbouring internalized cargo to the EE.

### 4.2.4. LYCAT silencing alters TfR recycling

The final stage of TfR intracellular traffic that I investigated was TfR recycling. To measure the rate of TfR recycling, I treated cells in serum for various lengths of times with an antibody that recognized an exofacial epitope of TfR. Any receptor that was present at the cell surface or recycled to the cell surface would become labelled with antibody. I measured the rate of TfR arrival to the plasma membrane, thus measuring TfR recycling (Antonescu et al., 2008b). Over time, LYCAT silencing reduced the total levels of TfR that were labelled with TfR antibody (Figure 4.4), indicating that TfR recycling is slower in LYCAT deficient cells. Collectively these studies reveal that PI(3)P-dependent intracellular sorting and recycling of TfR is dependent on LYCAT.

### 4.2.5. LYCAT silencing has no impact on biosynthetic traffic

My results provide evidence that LYCAT controls endomembrane traffic of TfR. To contrast this, we examined the biosynthetic membrane traffic pathway, which is controlled by PI(4)P (Szentpetery et al., 2010). Previously, I found that LYCAT silencing had no impact on PI(4)P levels and localization in the cell. To assess the biosynthetic pathway, we used a temperature sensitive form of vesicular stomatitis virus G (VSVG) that becomes trapped in and then released from the ER by temperature shift (Presley et al., 1997; Szentpetery et al., 2010). LYCAT silencing did not alter VSVG traffic or distribution (Figure 4.5 A and B). The above results highlight that LYCAT silencing alters TfR traffic, which relies on PI(4,5)$P_2$ and PI(3)P, but has no apparent effect on the PI(4)P-dependent biosynthetic pathway.

In summary of the work presented in this Chapter, I found that LYCAT silencing altered CCP dynamics by reducing the size, lifetime and initiation density of CCPs and decreases rates of endocytosis, all processes dependent on PI(4,5)$P_2$. Additionally, LYCAT silencing affects intracellular sorting at the EE and decreases rates of recycling, processes that are dependent on PI(3)P. Furthermore, LYCAT silencing had no impact on the biosynthetic pathway, which is dependent on PI(4)P. Collectively these results suggest that LYCAT controls the endomembrane traffic of TfR. As I used TfR as a model receptor that undergoes constitutive endocytosis and recycling, these results suggest that LYCAT may broadly control the endomembrane traffic of other receptors as well.

The final model I used to determine the significance of the role of LYCAT in PIP function was the PI3K/Akt signaling pathway. Using similar methods of LYCAT perturbation, I assessed the effect of LYCAT silencing on EGF-dependent activation of Akt by evaluating the impact on EGFR activation, Akt activation and alterations in regulating Akt substrates.

Chapter 4 Figures

Figure 4.1. LYCAT silencing perturbs TfR endomembrane traffic. RPE cells were transfected with one of two distinct siRNA sequences targeting LYCAT (siLYCAT$^{1}$ or siLYCAT$^{2}$) or nontargeting siRNA (siControl). (***A, B***) Detection of cell surface TfR levels by immunofluorescence staining of intact (nonpermeabilized) cells. (*A*) Representative epifluorescence micrographs (scale 20 µm). (*B*) Mean cell surface TfR ± SEM from at least four independent experiments. Independent *t* test, **p* < 0.05. (***C***) After silencing, cells were transfected with a cDNA encoding LYCAT-FLAG, followed by detection of cell surface TfR levels by immunofluorescence staining of intact cells; mean cell surface TfR ± SEM (*n* = 4), two-way ANOVA with post hoc Bonferroni pairwise comparisons, **p* < 0.05. (***D-F***) Detection of total cellular TfR levels (permeabilized cells). (*D*) Representative epifluorescence micrographs (scale 20 µm). (*E*) Quantitative measurements (mean ± SEM) of the relative concentration of TfR staining within the perinuclear region (*n* = 4), independent *t* test, **p* < 0.05 and (*F*) mean total TfR fluorescence signal per cell, per experiment ± SEM, of at least 5 independent experiments. Shown in (***G***) are representative immunoblots showing detection of TfR or actin (loading control).

Figure 4.1.

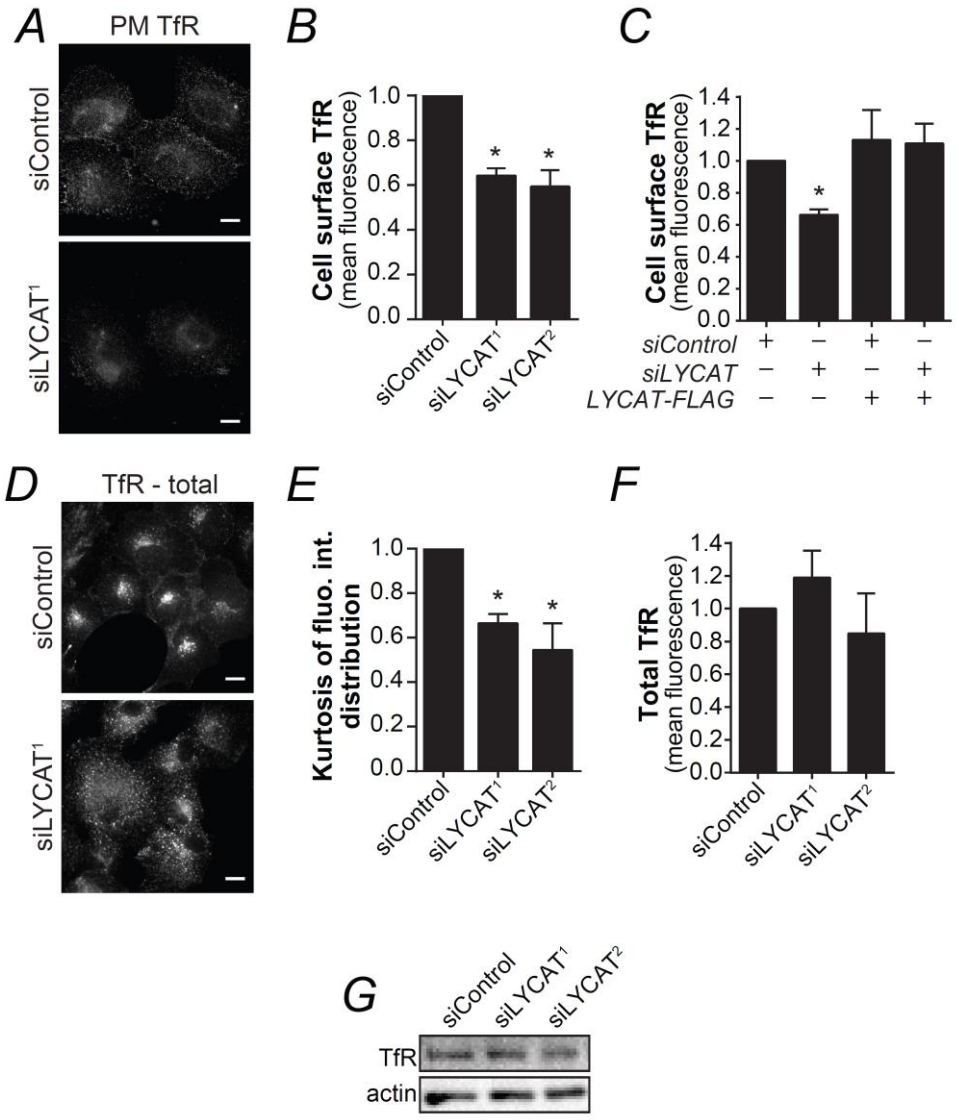
A
PM TfR
siControl
siLYCAT1
B
Cell surface TfR
(mean fluorescence)
1.0
0.8
0.6
0.4
0.2
0.0
*
*
siControl
siLYCAT1
siLYCAT2
C
Cell surface TfR
(mean fluorescence)
1.4
1.2
1.0
0.8
0.6
0.4
0.2
0.0
*
siControl + − + −
siLYCAT − + − +
LYCAT-FLAG − − + +
D
TfR - total
siControl
siLYCAT1
E
Kurtosis of fluo. int. distribution
1.0
0.8
0.6
0.4
0.2
0.0
*
*
siControl
siLYCAT1
siLYCAT2
F
Total TfR
(mean fluorescence)
1.4
1.2
1.0
0.8
0.6
0.4
0.2
0.0
siControl
siLYCAT1
siLYCAT2
G
siControl
siLYCAT1
siLYCAT2
TfR
actin

Figure 4.2. LYCAT silencing alters clathrin-mediated endocytosis. RPE cells stably expressing eGFP-CLCa were transfected with siRNA targeting LYCAT (siLYCAT) or nontargeting siRNA (siControl). (***A–D***) Cells were imaged using time-lapse TIRF-M. (*A*) Single-frame representative fluorescence micrographs (scale 5 μm). Time-lapse TIRF-M image series were subjected to automated detection, tracking, and analysis of CCPs, which was conducted by CN Antonescu (*B*) Median, 25th and 75th percentiles (boxes), and Tukey range (whiskers) for CCP initiation densities. (*C*) Mean eGFP-CLCa fluorescence intensity grouped into CCP lifetime cohorts; error bars reflect cell-to-cell variation. The numbers of CCP trajectories and cells for each condition are, for siControl, 7181 and 16, and for siLYCAT, 2354 and 16, respectively. (*D*) Shown is CCP lifetime distribution. (***E***) Mean total clathrin fluorescence signal ± SEM from at least six independent experiments. (***F***) Measurement of Tfn internalization; means ± SEM ($n = 4$), two-way ANOVA with post hoc Bonferroni pairwise comparisons, $^*p < 0.05$.

Figure 4.2.

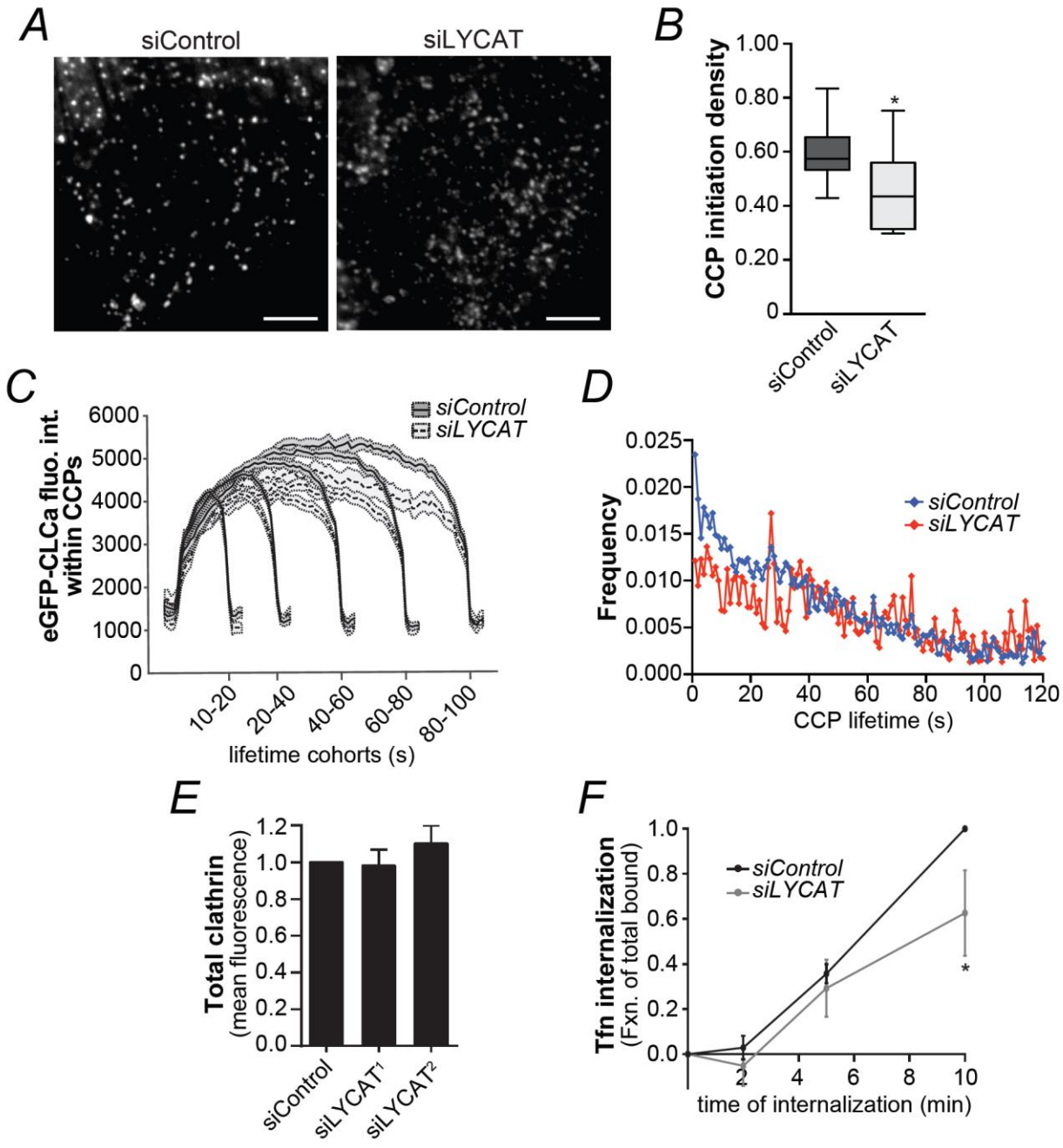
A
siControl
siLYCAT
B
CCP initiation density
1.00
0.80
0.60
0.40
0.20
0
*
siControl
siLYCAT
C
eGFP-CLCa fluo. int. within CCPs
6000
5000
4000
3000
2000
1000
0
siControl
siLYCAT
10-20
20-40
40-60
60-80
80-100
lifetime cohorts (s)
D
Frequency
0.025
0.020
0.015
0.010
0.005
0.000
siControl
siLYCAT
0
20
40
60
80
100
120
CCP lifetime (s)
E
Total clathrin
(mean fluorescence)
1.2
1.0
0.8
0.6
0.4
0.2
0.0
siControl
siLYCAT1
siLYCAT2
F
Tfn internalization
(Fxn. of total bound)
1.0
0.8
0.6
0.4
0.2
0.0
siControl
siLYCAT
*
2
4
6
8
10
time of internalization (min)

Figure 4.3. LYCAT silencing alters PI(3)P-dependent traffic of TfR through early endosomes. RPE cells were transfected with one of two distinct siRNA sequences targeting LYCAT (siLYCAT$^1$ or siLYCAT$^2$) or nontargeting siRNA (siControl). (***A, B***) Cells were incubated with Tfn-647 for various times and then immediately fixed and stained with EEA1 antibodies. (*A*) Representative epifluorescence micrographs of the 20 min pulse of Tfn (scale 20 µm). (*B*) Mean colocalization scores of Tfn and EEA1, normalized to the 20-min control condition, ± SEM (*n* = 3), two-way ANOVA with post hoc Bonferroni pairwise comparisons, **p* < 0.05. (***C***) Shown are epifluorescence micrographs of EEA1 staining representative of 3 independent experiments (scale 20 µm). (***D, E***) Following siRNA transfection, cells were incubated with Tfn-647 for 20 min and were then immediately fixed and stained with anti-TfR antibodies to label all cellular TfR membrane compartments. Shown in (*D*) are representative epifluorescence micrographs (scale 20 µm). (*E*) Images were subjected to quantification of the colocalization of Tfn-A647 and TfR by Pearson's Coefficient; shown are mean colocalization scores ± SEM (n = 3), independent *t* test, * p < 0.05. LYCAT silencing delays the arrival of recently internalized Tfn into the total intracellular pool of TfR.

Figure 4.3.

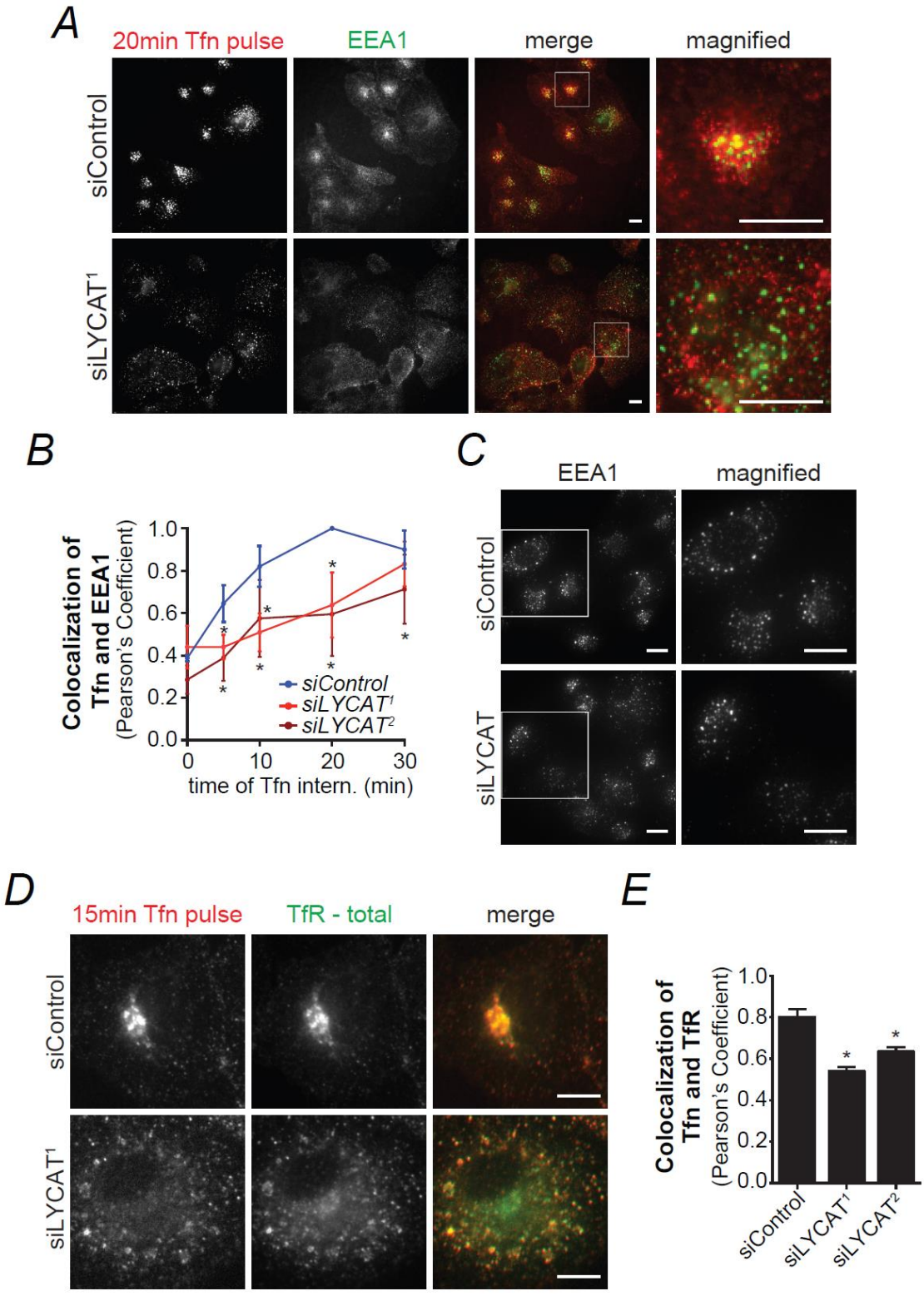
A
20min Tfn pulse
EEA1
merge
magnified
siControl
siLYCAT1
B
Colocalization of Tfn and EEA1 (Pearson's Coefficient)
1.0
0.8
0.6
0.4
0.2
0.0
0
10
20
30
time of Tfn intern. (min)
siControl
siLYCAT1
siLYCAT2
C
EEA1
magnified
siControl
siLYCAT
D
15min Tfn pulse
TfR - total
merge
siControl
siLYCAT1
E
Colocalization of Tfn and TfR (Pearson's Coefficient)
1.0
0.8
0.6
0.4
0.2
0.0
siControl
siLYCAT1
siLYCAT2

Figure 4.4. LYCAT silencing alters PI(3)P-dependent traffic of TfR through recycling endosomes. RPE cells were transfected with one of two distinct siRNA sequences targeting LYCAT (siLYCAT$^1$ or siLYCAT$^2$) or nontargeting siRNA (siControl). Measurement of the rate of TfR recycling; mean TfR recycling ± SEM ($n$ = 3), two-way ANOVA with post hoc Bonferroni pairwise comparisons, *$p$ < 0.05.

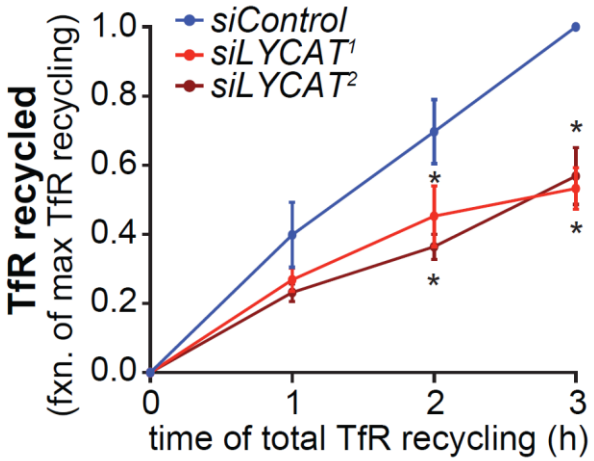

Figure 4.5. LYCAT silencing has no effect on biosynthetic traffic. RPE cells were transfected with siRNA targeting LYCAT (siLYCAT) or non-targeting siRNA (siControl). (***A, B***) Measurement of biosynthetic traffic from the Golgi to plasma membrane. GFP-VSVG was released from Golgi arrest for indicated times. (*A*) Representative laser scanning confocal micrographs (scale 5 µm). (*B*) Mean ± SEM (*n* = 3) of the amount of VSVG-GFP remaining in the Golgi at various times. *Work completed by Mr. M. Lee.*

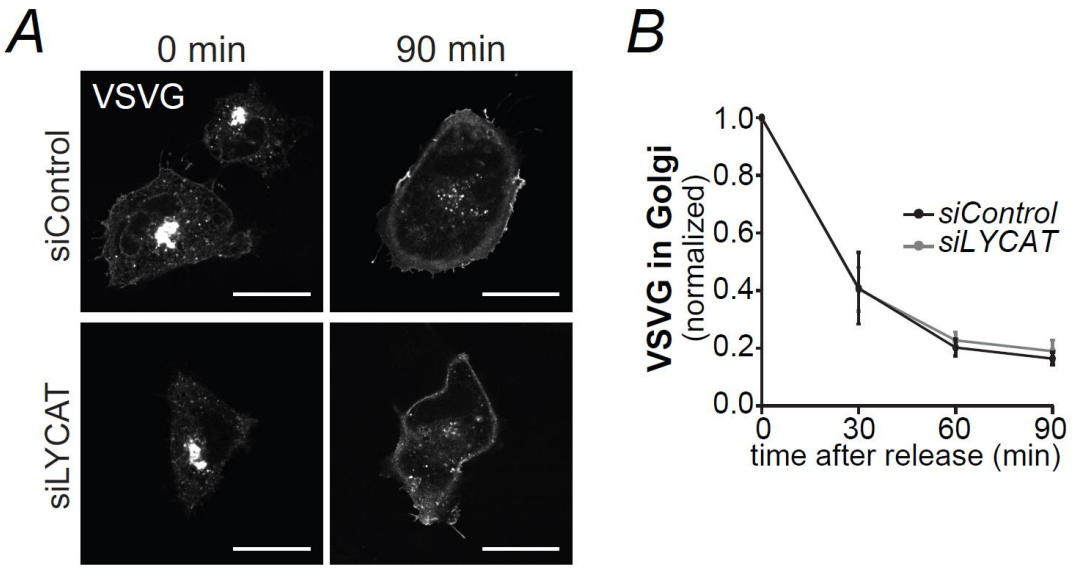

# Chapter 5
# Results: Role of LYCAT in modulating hormone receptor signaling

## 5.1. Rationale

I found that LYCAT silencing significantly impacted TfR endomembrane traffic by altering clathrin-mediated endocytosis, intracellular sorting and recycling. I next investigated the effect of LYCAT silencing on hormone receptor signaling. Here, I focus on EGF-dependent activation of PI3K/Akt. I found that LYCAT silencing altered CCP dynamics and altered Tfn internalization. As EGFR signalling is dependent on clathrin, I investigated whether EGFR signaling was impacted in LYCAT silenced cells. Additionally, EGFR-dependent activation of Akt is PI3K dependent, and thus PI3K may be sensitive to the regulation of the PI/$PIP_2$ acylation profile. The PI3K/Akt pathway plays a very important role in regulating fundamental cellular processes including cell survival, transcription, proliferation and growth. Disruption of normal PI3K/Akt signaling is implicated in a variety of cancers. This is an important pathway to study the effects of altered acyl chain content on PIP function because this pathway is dependent on the conversion of $PI(4,5)P_2$ to $PI(3,4,5)P_3$.

Briefly, EGF binding to EGFR results in activation of the receptor tyrosine kinase domain leading to autophosphorylation on multiple intracellular domain residues including Tyr1068 (Downward et al., 1984) and Tyr1045 (Levkowitz et al., 1999). Important adaptor proteins such as Grb2 and Gab1 are involved in the recruitment and activation of class 1 PI3K, which converts $PI(4,5)P_2$ into $PI(3,4,5)P_3$. The production of $PI(3,4,5)P_3$ then recruits a number of effector proteins including Akt and PDK1 to the plasma membrane by binding to $PI(3,4,5)P_3$ via intrinsic PH domains. Akt becomes activated upon phosphorylation of Thr308 by PDK1 and Ser473 by mTORC2 (Díaz et al., 2012). Akt has a number of different direct substrates including GSK3β and TSC2, the latter of which leads to activation of mTORC1 and S6K upon Akt phosphorylation.

Since I saw defects in $PI(4,5)P_2$-dependet processes upon LYCAT silencing, I hypothesized that $PI(3,4,5)P_3$-dependent Akt activation would be altered upon LYCAT silencing.

## 5.2. Results

### 5.2.1. LYCAT silencing reduces $PI(3,4,5)P_3$ levels

I first set out to monitor the levels of $PI(3,4,5)P_3$ in response to EGF stimulation as $PI(3,4,5)P_3$. In basal (unstimulated) cells, $PI(3,4,5)P_3$ is present in extremely low levels as it is not constitutively produced. I used the PH domain of Akt fused to GFP as a reporter of relative $PI(3,4,5)P_3$ levels

(Gray et al., 1999). To obtain a relative quantitative measurement of PI(3,4,5)$P_3$ levels, I examined the ratio of TIRF-M fluorescence to total fluorescence as an indicator of PI(3,4,5)$P_3$ levels, since PI(3,4,5)$P_3$ is produced at or near the plasma membrane, which results in localization of the PI(3,4,5)$P_3$ probe in the TIRF-M illumination field in a manner proportional to the cellular levels of PI(3,4,5)$P_3$ (Figure 5.1A). Examination of the membrane localization of the PH-Akt probe in EGF-stimulated control cells indicated a significant reduction when treated with the PI3K inhibitor, LY294002, thus suggesting that PI(3,4,5)$P_3$ was reduced, and that EGF-stimulated activation of PI3K is responsible for PI(3,4,5)$P_3$ production (Figure 5.1B). Conversely, in LYCAT-silenced cells, the levels of apparent PI(3,4,5)$P_3$ at the cell surface following EGF stimulation were very low. These levels were comparable to the levels seen in cells following EGF and PI3K inhibitor treatment. LYCAT silencing showed a reduction in the readout of the PH-Akt probe binding 32% ± 0.09%. Although, this apparent reduction in PI(3,4,5)$P_3$ levels in LYCAT-silenced cells could be due to the PH-Akt probe showing sensitivity to acyl chain content of PI(3,4,5)$P_3$. Future work should use the PH domain from Bruton tyrosine kinase, another probe for PI(3,4,5)$P_3$ detection. Additionally, levels of PI(3,4,5)$P_3$ should be measured biochemically following [$^3$H]*myo*-inositol incorporation, extraction and running through HPLC. LYCAT silencing seems to not only impact the levels of PI(3)P and PI(4,5)$P_2$ (Chapter 3, Figure 3.6), my data also suggest that LYCAT may also impact EGF-stimulated production of PI(3,4,5)$P_3$, though future work is required to confirm this.

### 5.2.2. LYCAT perturbs activation of Akt

The apparent reduced levels of EGF-stimulated PI(3,4,5)$P_3$ prompted us to investigate the downstream effects of LYCAT silencing on Akt activation. First, I examined total levels of Akt using a pan antibody that recognizes all three isoforms of Akt. LYCAT silencing caused a 25% ± 0.07% decrease in total Akt levels (Figure 5.2 A and B). The absolute levels of Akt phosphorylation in LYCAT-silenced cells were significantly reduced in both the basal and EGF-stimulated conditions (Figure 5.2C). Additionally, relative to the overall decrease in total Akt levels, I found that LYCAT silencing significantly reduced Akt phosphorylation (Figure 5.2D) and the EGF-stimulated gain in phospho-Akt decreased by 43% ± 0.12% (Figure 5.2E, phospho-Akt is normalized to total Akt).

Even though LYCAT-silenced cells have slightly reduced levels of total Akt, of this total available pool of Akt, less Akt is becoming activated in LYCAT-silenced cells. This suggests that PI3K signaling leading to Akt activation is less efficient in LYCAT-silenced cells.

Akt isoforms exhibit different temporal activation profiles following receptor activation and also are recruited to different subcellular localizations. Upon insulin stimulation, Akt1 localizes to the plasma membrane while Akt2 localizes to APPL1 endosomes and the plasma membrane (Gonzalez and McGraw, 2009; Saito et al., 2007). Therefore, I probed the effects of LYCAT silencing on the activation of the different Akt isoforms, focusing on Akt1 and Akt2. Absolute levels of phospho-Akt1 and phospho-Akt2 were significantly reduced in EGF-stimulated cells (Figure 5.2 F and I). Furthermore, relative to total Akt levels, the levels of phospho-Akt1 relative to total Akt were also significantly reduced (Figure 5.2G) and the EGF-stimulated increase in Akt1 activation was reduced by 42% ± 0.12% (Figure 5.2H). In contrast to the alterations in EGF-stimulated phosphorylation of Akt1, LYCAT silencing did not significantly impact the EGF-stimulated levels of phospho-Akt2 relative to total Akt levels (Figure 5.2 J and K). Our examination of phospho-Akt1 and phospho-Akt2 were relative to pan Akt levels so it is important that in the future these are compared to total Akt1 and Akt2 for a better understanding of the effect of LYCAT silencing on isoform specific Akt. Additionally, while these experiments were performed in RPE cells, it will be important to assess Akt signaling in other cell lines, including cancer cell lines. Preliminary data show that LYCAT silencing similarly impacts EGF-stimulated Akt signaling in MDA-MB-231 cells, a breast cancer cell line. Please see *Chapter 7 Future Directions* for a discussion of how to extend these observations of the role of LYCAT in EGF-stimulated Akt signaling in RPE cells to other cells lines to probe the generality of this novel function of LYCAT. Nonetheless, I uncovered that LYCAT silencing abrogates EGF-stimulated Akt activation in RPE cells, more specifically it reduces activation of Akt1, suggesting that LYCAT modulates specific aspects of PI3K/Akt signaling.

### 5.2.3. LYCAT silencing does not alter EGFR cell surface levels or activation

LYCAT silencing significantly altered the apparent production of $PI(3,4,5)P_3$ and the activation of Akt. Given that LYCAT silencing reduced cell surface levels of TfR and altered TfR membrane

traffic, it is possible that LYCAT may impair EGF-stimulated PI3K/Akt signaling by altering cell surface EGFR levels. Alternatively, LYCAT silencing may more directly impact PI3K/Akt signaling, perhaps by altering the preferred acyl profile for PI3K substrates. To determine if LYCAT silencing may directly alter EGFR cell surface levels of receptor activation or alter PI3K/Akt signaling downstream of otherwise normal receptor activation, I first sought to examine cell surface levels and activation of EGFR.

Cell surface levels of EGFR were assessed by staining non-permeabilized cells with an EGFR antibody that recognizes an exofacial epitope of EGFR. I tested EGFR cell surface levels in resting cells and in cell stimulated with high dose EGF for 1 h. The stimulation with high dose (100 ng/ml) EGF results in internalization and partial degradation of EGFR within 1 h, thus allowing control for the specificity of the anti-EGFR antibodies used in this assay. LYCAT silencing did not alter levels of cell surface EGFR compared to control in both the resting and stimulated conditions (Figure 5.3A). These results suggest that LYCAT does not seem to be broadly impacting EGFR endomembrane traffic, as 1) resting cell surface EGFR is not impacted and 2) EGFR is able to internalize following EGF stimulation similarly to control cells.

While the cell surface abundance of EGFR is unaltered by LYCAT silencing, the decrease in EGF-stimulated Akt activation could still be due to altered receptor binding of ligand or reduced tyrosine kinase activity, thus broadly dampening receptor signaling. In contrast, LYCAT silencing could result in more selective disruption of PI3K and Akt. To resolve between these two possibilities, I first examined total EGFR levels by western blotting in RPE cells (Figure 5.3B). There was a 34% ± 0.07% reduction in total EGFR levels (Figure 5.3C). I then investigated the activation of EGFR by probing for Tyr1068, a site that is autophosphorylated upon receptor ligand binding and that is upstream of PI3K and Akt activation (Downward et al., 1984). I found that LYCAT silencing did not decrease the activation of the receptor (Figure 5.3D), thus indicating that the levels of cell surface EGFR and activation of the receptor were not the cause of reduced Akt activation in LYCAT-silenced RPE cells. These data also suggest that cells may have compensatory mechanisms that ensure that cell surface levels of EGFR and activation occurs despite an abatement in total EGFR levels. Collectively, these results suggest that the defect in Akt activation upon LYCAT silencing could be due to altered $PI(4,5)P_2$ and $PI(3,4,5)P_3$ levels, localization and/or

conversion. These results show that LYCAT silencing selectively altered PI3K-Akt signaling. Since LYCAT silencing abrogated the activation of Akt1 more than Akt2, the effect of LYCAT silencing on phosphorylation of Akt substrates may also be selective. Thus, next I sought to determine the effects of altered Akt activation on Akt substrates.

### 5.2.4. LYCAT silencing impacts a number of Akt substrates

First I examined the general phosphorylation of a wide range of Akt substrates by western blotting in RPE cells using an antibody that recognizes a phosphorylated Akt substrate consensus sequence: RXXS*/T*, which recognizes phospho-serine/threonine preceded by arginine at the -3 position, thereby identifying Akt substrates. The antibody was able to recognize many different protein bands ranging from approximately 37-250 kDa that became more prominent upon EGF stimulation (data not shown), consistent with many Akt substrates undergoing EGF-stimulated Akt phosphorylation (Figure 5.4A). By plotting the profiles of each condition, I was able to have a quantitative, graphic representation of the effects of LYCAT silencing on the EGF-stimulated phosphorylation of Akt substrates (Figure 5.4B). Comparing the intensity of protein phosphorylation (grey value) plotted against the Rf value, it is evident that LYCAT silencing results in significantly impaired phosphorylation of diverse Akt substrates. When I focused on proteins in the molecular weight range of 50-100 kDa (Figure 5.4 C and D), I saw that the effects of LYCAT silencing are, indeed, quite pronounced. Akt has over 100 different substrates (Manning and Toker, 2017) and although this experiment did not identify which substrates are affected by LYCAT silencing, I did see a broad overall disruption to phosphorylation of Akt substrates. Importantly, these results show that while LYCAT silencing only partially reduced EGF-stimulated Akt phosphorylation, and had selective effects on Akt1 more so than Akt2, LYCAT silencing had broad and substantial impact on the phosphorylation of Akt substrates upon EGF stimulation. I selected a couple of known Akt substrates to further investigate the effects of LYCAT silencing.

### 5.2.5. LYCAT silencing does not alter GSK3β function

I choose to investigate the effects of altered Akt activation on the EGF-stimulated phosphorylation of GSK3β in RPE cells. Phosphorylation of GSK3β by Akt causes an alteration in

GSK3β substrate specificity and controls metabolism, survival and proliferation (Manning and Toker, 2017). LYCAT silencing did not reduce total levels of GSK3β (Figure 5.5 A and D) and also had no significant effect on the phosphorylation of GSK3β absolute levels and relative to total levels (Figure 5.5 B and C). I have presented data from one Akt substrate that did not show any effect upon LYCAT silencing. However, multiple proteins were tested, but are not presented here, either due to problems in probing for particular proteins, or data being inconclusive. In the future it will be important to investigate several other Akt substrates to understand the role of LYCAT in Akt signaling.

### 5.2.6. The parallel pathway, Ras/Erk is not affected by LYCAT silencing

Many different signal transduction pathways are activated by EGFR including the Ras/Raf/Mek/Erk pathway, which results in cell survival, cell proliferation and cell motility (McCubrey et al., 2006). Both the PI3K/Akt pathway and Ras-Erk (extracellular-regulated-signal kinase) signaling pathway are activated by EGF. The Ras/Erk pathway is an appropriate signaling pathway to determine if the effects of LYCAT silencing seen with the PI3K/Akt pathway were specific or had broad effects. I evaluated the effects on Erk signaling upon EGF stimulation and found that, consistent with the elevated phosphorylation of EGFR seen upon LYCAT silencing (Figure 5.3D, $p = 0.34$), there was also elevated basal phospho-Erk (Figure 5.6 A and B). This shows that EGFR signaling is intact and that certain signals are even upregulated upon LYCAT silencing. The EGF-stimulated response of certain signals is normal as I saw with the phosphorylation of GSK3β (Figure 5.5 B and C), thus confirming that the effects of LYCAT are selective for attenuation of PI3K-Akt signaling.

My data suggest that LYCAT modulates EGF-dependent activation of the PI3K/Akt signaling pathway. I found that LYCAT silencing decreased Akt activation, more specifically Akt1 activation in RPE cells, which impacted a number of different Akt substrates. GSK3β was investigated here and showed no altering in phosphorylation in LYCAT-silenced cells. Further investigation into other Akt substrates is an important consideration for the future. These data highlight the importance of understanding the acyl profile of PIPs to further our understanding

of cell physiology. These data show that alterations in acyl chain profile seem to regulate PI3K/Akt signaling. This pathway is often disrupted in cancer, and therefore it is an important pathway to study to gain insights into future treatments for cancer.

Chapter 5 Figures

Figure 5.1. LYCAT silencing alters apparent levels of PI(3,4,5)$P_3$. RPE cells were transfected with siRNA targeting LYCAT (siLYCAT) or nontargeting siRNA (siControl). Subsequently, cells were transfected with cDNA encoding the PI(3,4,5)$P_3$-specific probe comprised of the PH domain of Akt fused to GFP (PH-Akt-GFP). Cells were treated with 5 ng/ml EGF for 5 min and, in some conditions treated with LY294002, fixed, and then subjected to sequential imaging by TIRF microscopy (to selectively image cell-surface proximal fluorescence) and epifluorescence microscopy (to measure whole cell fluorescence). The TIRF/epifluorescence intensity measurement ratio in each cell is indicative of the relative binding of GFP-PH to the cell surface, and thus of apparent PI(3,4,5)$P_3$ levels. Mean ± SEM, two-way ANOVA with post hoc Bonferroni pairwise comparisons, *$p < 0.05$.

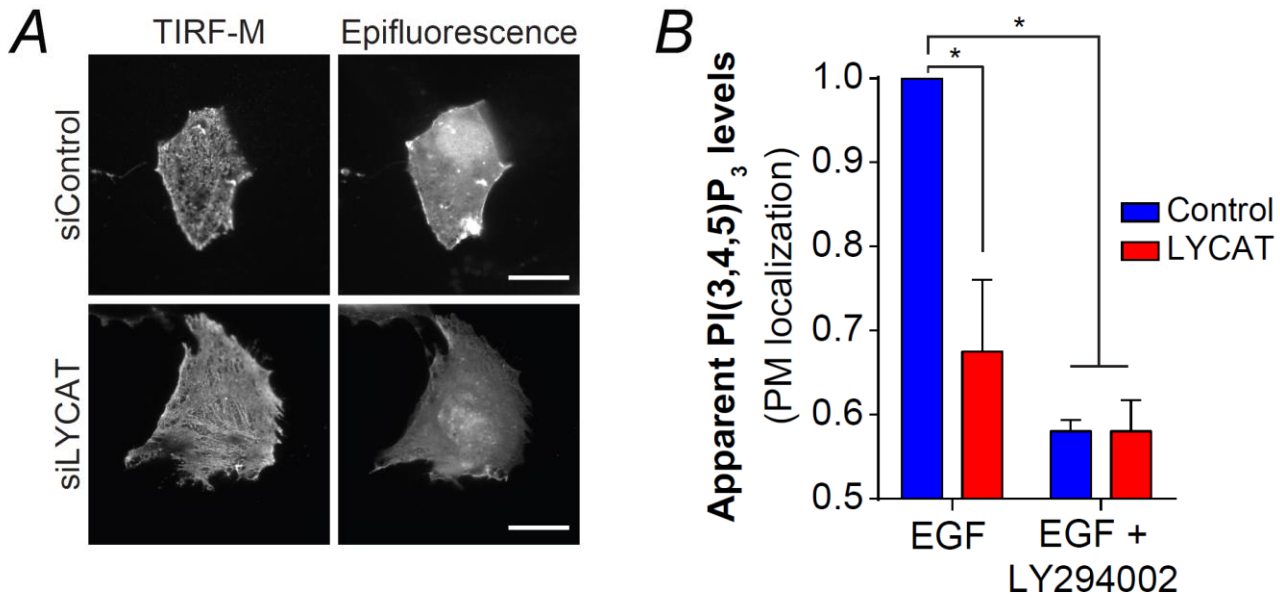

Figure 5.2. LYCAT silencing impairs Akt activation. RPE cells were transfected with siRNA targeting LYCAT (siLYCAT) or nontargeting siRNA (siControl). Following siRNA transfection cells were serum starved for 1 h and treated with EGF (5 ng/ml) for 5 min and then whole cell lysates were subjected to western blotting. (***A***) Representative immunoblots showing detection of pS473-Akt, pS473-Akt1, pS474-Akt2, total Akt or loading control (clathrin or actin). Shown in (***B***) is the quantified pan Akt protein levels (n = 12). (***C-E***) Quantitative measurements (mean ± SEM) of absolute levels of pS473-Akt values, relative to total Akt or EGF-stimulated gain in pS473-Akt values, (*n* = 6). Similar quantitative measurements are shown in (***F-H***) for pS473-Akt1 (n = 4) and (***I-K***) for pS474-Akt2 (n = 4). Mean ± SEM, two-way ANOVA with post hoc Bonferroni pairwise comparisons was conducted for all figures except figures B, E, H and K which underwent an independent *t* test, $*p < 0.05$.

Figure 5.2.

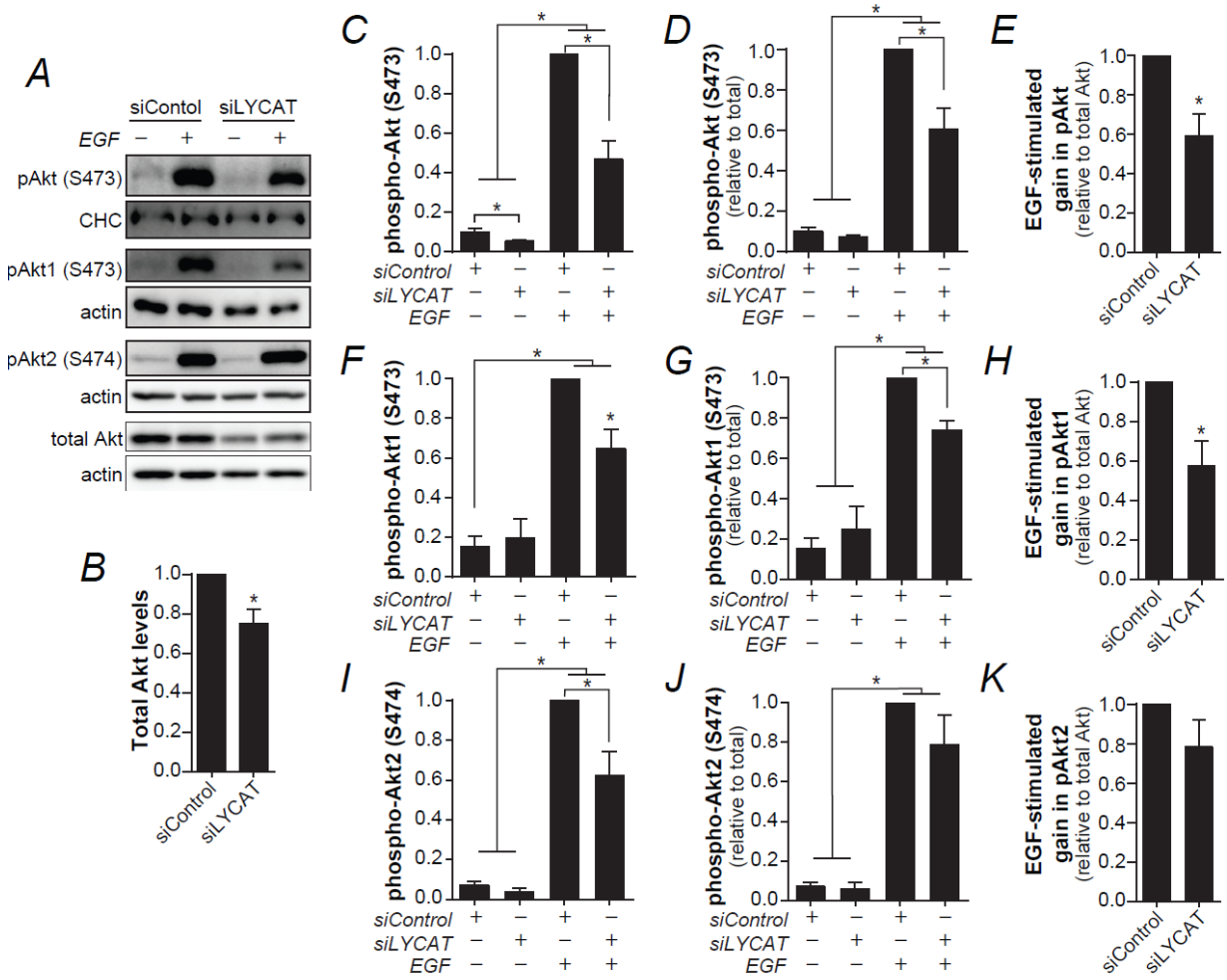
A
siContol
siLYCAT
EGF
pAkt (S473)
CHC
pAkt1 (S473)
actin
pAkt2 (S474)
actin
total Akt
actin
B
Total Akt levels
siControl
siLYCAT
C
phospho-Akt (S473)
siControl
siLYCAT
EGF
D
phospho-Akt (S473) (relative to total)
E
EGF-stimulated gain in pAkt (relative to total Akt)
F
phospho-Akt1 (S473)
G
phospho-Akt1 (S473) (relative to total)
H
EGF-stimulated gain in pAkt1 (relative to total Akt)
I
phospho-Akt2 (S474)
J
phospho-Akt2 (S474) (relative to total)
K
EGF-stimulated gain in pAkt2 (relative to total Akt)

Figure 5.3. LYCAT silencing does not affect plasma membrane levels or activation of EGFR. RPE cells were transfected with siRNA sequence targeting LYCAT (siLYCAT) or nontargeting siRNA (siControl). (***A***) Detection of RPE cell surface EGFR levels by immunofluorescence staining of intact (nonpermeabilized) cells. Following transfection cells were serum starved for 1 h and treated with EGF for 1 h (100 ng/ml), (n = 2-3), two-way ANOVA with post hoc Bonferroni pairwise comparisons. (***B-D***) Following siRNA transfection, RPE cells were serum starved for 1 h and treated with EGF (5 ng/ml) for 5 min, then whole cell lysates were subjected to western blotting. Shown in (*B*) are representative immunoblots showing detection of pY1068-EGFR, EGFR or clathrin (loading control). Quantitative measurements (*C*) total EGFR levels (n = 5), independent *t* test and (*D*) pY1068-EGFR relative to total EGFR values (n = 4), two-way ANOVA with post hoc Bonferroni pairwise comparisons. Mean ± SEM, $*p < 0.05$.

Figure 5.3.

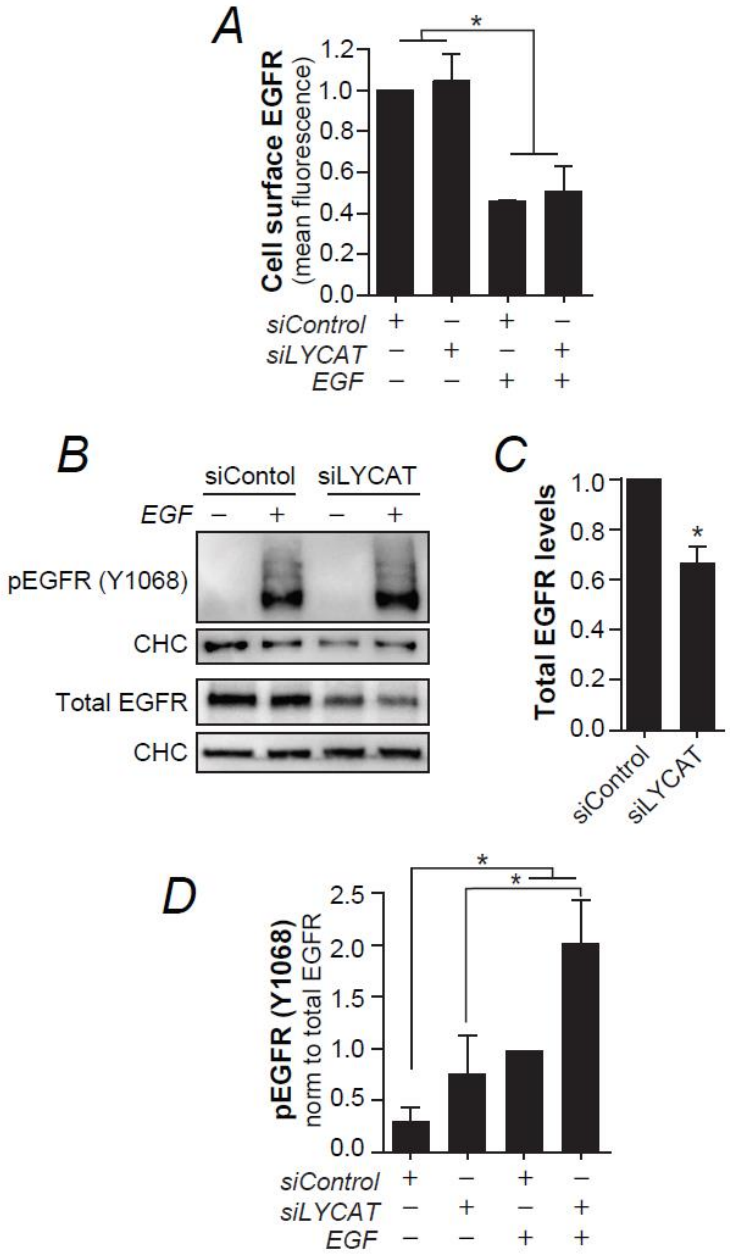
A
Cell surface EGFR
(mean fluorescence)
1.2
1.0
0.8
0.6
0.4
0.2
0.0
*
siControl + − + −
siLYCAT − + − +
EGF − − + +
B
siContol
siLYCAT
EGF − + − +
pEGFR (Y1068)
CHC
Total EGFR
CHC
C
Total EGFR levels
1.0
0.8
0.6
0.4
0.2
0.0
*
siControl
siLYCAT
D
pEGFR (Y1068)
norm to total EGFR
2.5
2.0
1.5
1.0
0.5
0.0
*
*
siControl + − + −
siLYCAT − + − +
EGF − − + +

Figure 5.4. LYCAT silencing impacts phosphorylation of Akt substrates. RPE cells were transfected with siRNA sequence targeting LYCAT (siLYCAT) or nontargeting siRNA (siControl). Western blot analysis of cell lysates that were serum starved for 1 h and treated with EGF (5 ng/ml) for 5 min, using a phospho-Akt substrate (RXXS*/T*) antibody that detects phosphorylated Akt target sites. Shown in (***A***) are representative immunoblots showing detection of phospho-Akt substrates. (***B***) Profile plots of each immunoblot showing the intensity of bands and retention factor. (***C, D***) Immunoblots showing proteins ranging from 50-100 kDa (*C*) and the profile of these proteins in control and LYCAT-silenced cells (*D*). Both siControl and siLYCAT profiles were normalized to protein content in each condition.

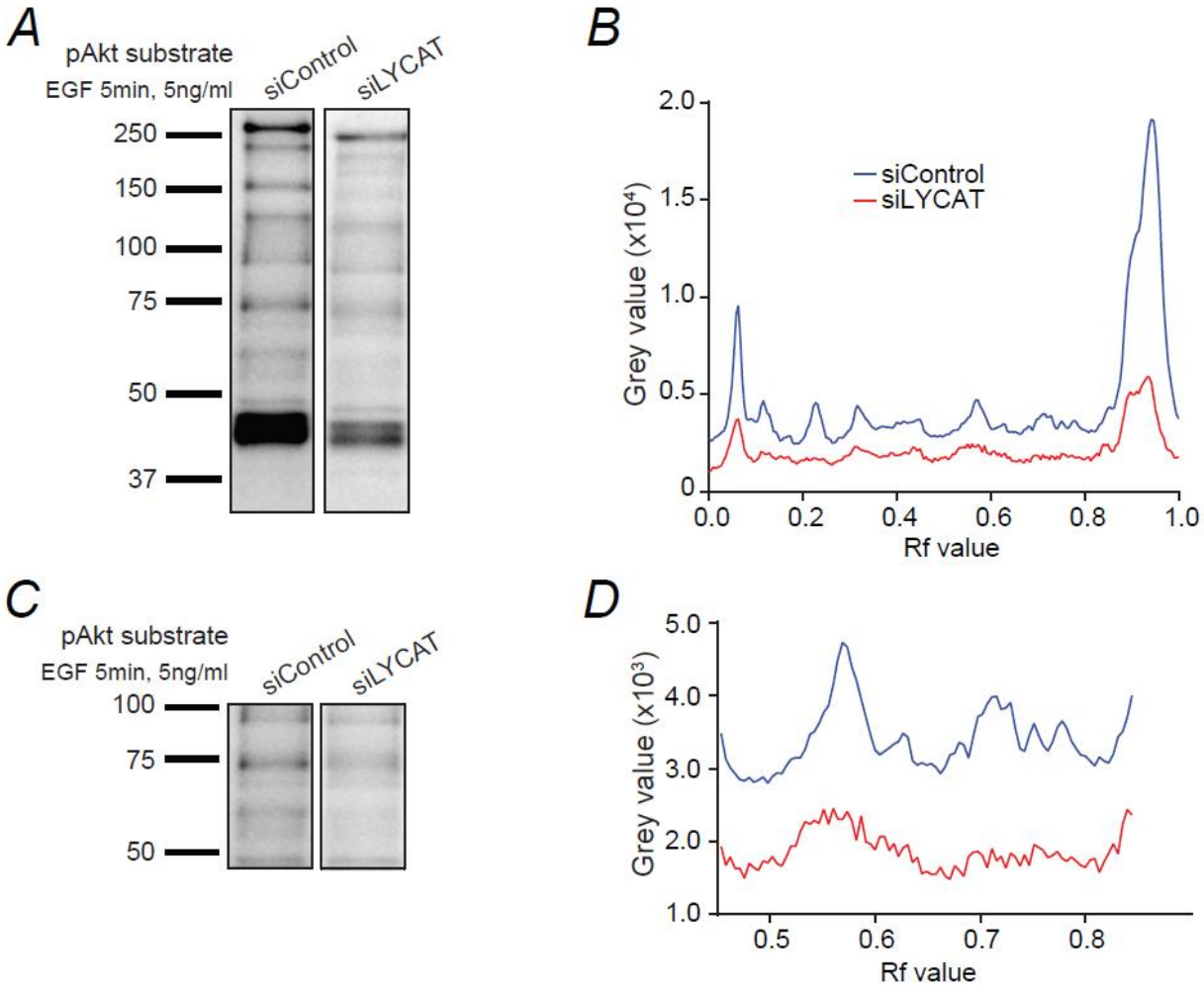

Figure 5.5. LYCAT silencing does not alter GSK3β signaling. RPE cells were transfected with siRNA sequence targeting LYCAT (siLYCAT) or nontargeting siRNA (siControl). Western blot analysis of cell lysates that were serum starved for 1 h and treated with EGF (5 ng/ml) for 5 min. Shown in (***A***) are representative immunoblots showing detection of pS9-GSK3β, total GSK3β, or clathrin (loading control). (***B-D***) Quantitative measurements of absolute levels of pS9-GSK3β values (n = 5), relative to total GSK3β and total GSK3β (n = 4), all normalized to loading control. Two way ANOVA with post hoc Bonferroni pairwise comparisons (B and C) and independent *t* test, mean ± SEM, * $p < 0.05$.

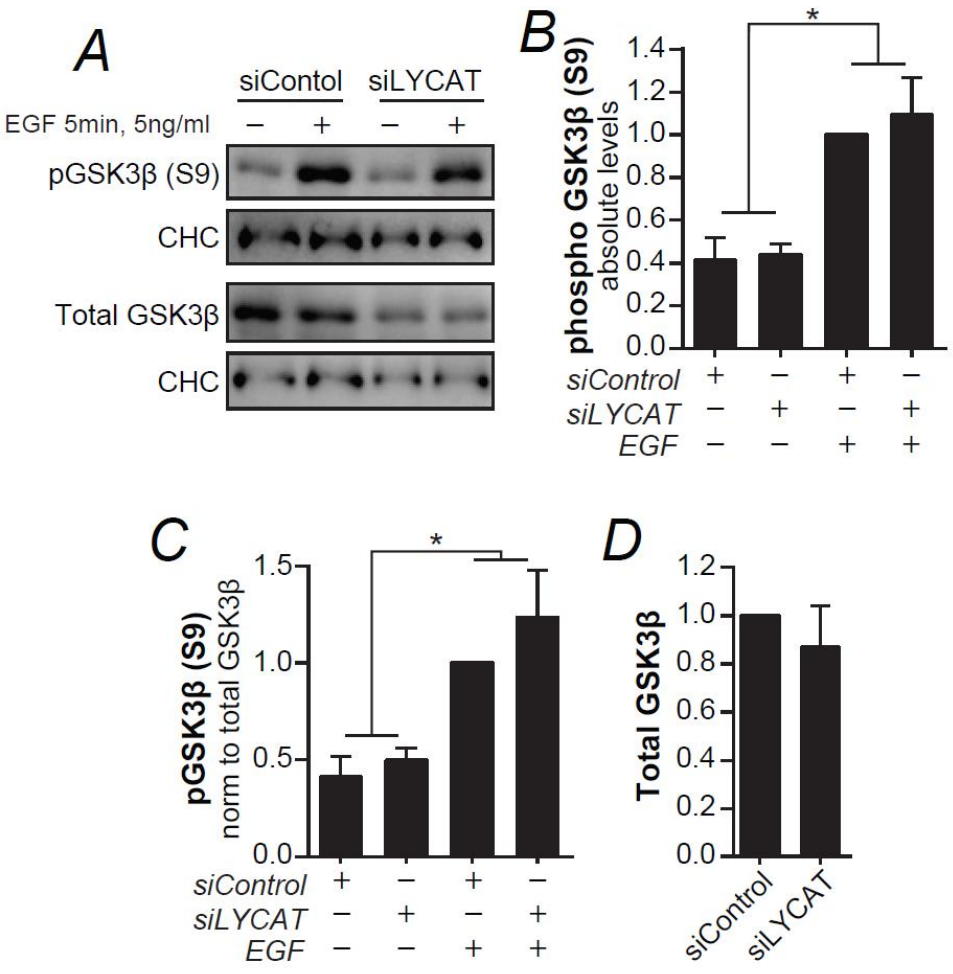

Figure 5.6. The Ras/Erk signaling pathway is not impacted by LYCAT silencing. RPE cells were transfected with siRNA sequence targeting LYCAT (siLYCAT) or nontargeting siRNA (siControl). Cells were serum starved for 1 h followed by 5 min of EGF stimulation (5 ng/ml) and then whole cell lysates were subjected to western blotting. Shown in (***A***) are representative immunoblots for RPE cells probed for pT202/Y204-Erk, total Erk or clathrin (loading control). Shown in (***B, C***) is the quantitative measurements for RPE cells of (*B*) pT202/Y204-Erk relative to total Erk values (n = 3), two-way ANOVA with post hoc Bonferroni pairwise comparisons and (*C*) total Erk (n = 4), independent *t* test, all normalized to loading control. Mean ± SEM, * $p < 0.05$.

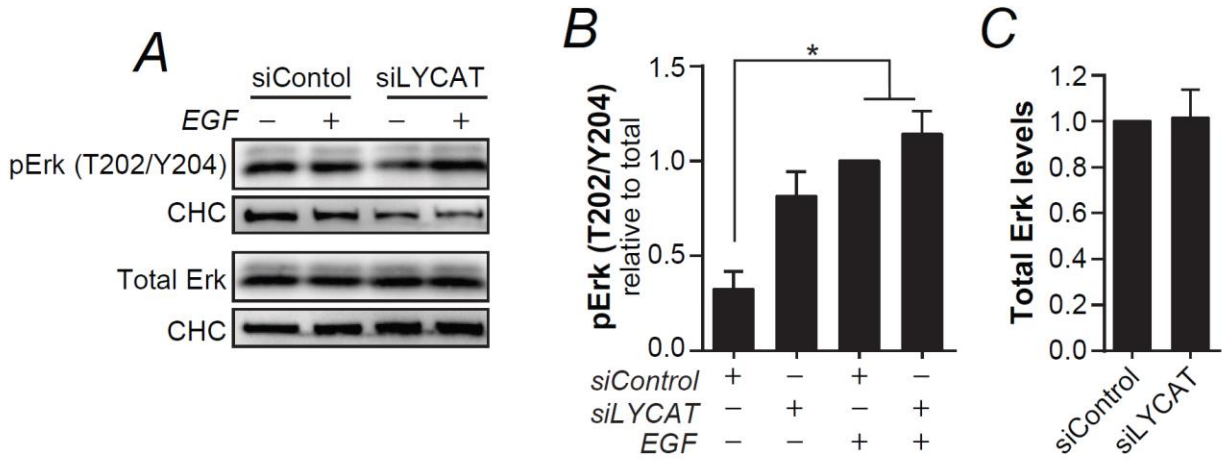

# Chapter 6
# Discussion

The most common acyl chain profile of PI is 1-stearoyl-2-arachidonoyl (Baker and Thompson, 1972; D'Souza and Epand, 2015; Hicks et al., 2006; Holub and Kuksis, 1978; Imae et al., 2011). *In vitro* and *in vivo* assays have shown that LYCAT specifically recognizes PI as a substrate (over other phospholipids) and LYCAT plays a role in stearic acid enrichment onto the *sn1* position of PI *in vivo* (Cao et al., 2004; Imae et al., 2011). Upon knockout of LYCAT in mice, there were significant reductions in the levels of stearic acid incorporated into PI (Imae et al., 2011). Further analysis of the livers of LYCAT$^{-/-}$ mice showed a 27%, 42% and 50% decrease in the levels of 18:0/20:4 PI, $PIP_1$ and $PIP_2$ species, respectively (Imae et al., 2011). Consistent with these previous studies, my research found that targeted silencing of LYCAT in RPE cells caused significant alterations in the acyl profile of $PIP_2$ species. However, in contract to studies in LYCAT$^{-/-}$ mice, LYCAT knockdown in RPE cells had no effect on the acyl profile of PI or $PIP_1$ species (or that of other phospholipids). Specifically, I observed a shift towards shorter acyl chains in $PIP_2$ species in the absence of LYCAT expression relative to control cells.

### 6.1. The PI acyltransferase LYCAT preferentially affects the acyl profile of $PIP_2$ species

PI and PI(4,5)$P_2$ synthesis appears highly dependent on ER-plasma membrane contact sites and substrate channeling (Kim et al., 2011). Non-vesicular transport of PA, DAG and PI between the ER and plasma membrane is also implicated in this process (Chang and Liou, 2015; Kim et al., 2015; Saheki et al., 2016). Furthermore, PIS-silenced cells showed reduced total levels of PI, PI(4)P and PI(4,5)$P_2$, suggesting PIS plays a significant role in production of PI and various PIP species. (Kim et al., 2011). I propose that PIS generates two pools of PI. In the general ER, PIS produces bulk PI and in ER-derived vesicles such as PIPEROsomes, it regulates a special pool of PI that is channeled for the synthesis of PI(4,5)$P_2$. In support of this model are several studies that have found reduction of plasma membrane PI(4)P by treatment with PI4-kinase inhibitors or recruitment of the 4-phosphatase to the plasma membrane, had little effect on plasma membrane PI(4,5)$P_2$ levels (Bojjireddy et al., 2014; Hammond et al., 2009, 2014). Thus suggesting a different pool of PI(4)P is used to generate PI(4,5)$P_2$ than bulk PI(4)P in the plasma membrane. Notably, that PI(4,5)$P_2$ levels are not affected by PI(4)P depletion also argues that the conversion

of this distinct pool of PI(4)P to PI(4,5)$P_2$ is very efficient, which is highly suggestive of substrate channeling.

How might LYCAT be impacting PI(4,5)$P_2$? I hypothesize that the preferential effect of LYCAT silencing on the acyl chain profile of PI(4,5)$P_2$ but not to PI/$PIP_1$ may be in part due to its restricted localization to specific cellular sub-compartments. To date, there have been conflicting reports about the localization of LYCAT. However, using a systematic, quantitative analysis I was able to conclude that LYCAT largely localizes to PIS vesicles (Chapter 3, Figure 3.8). These vesicles are proposed to make transient contacts with the plasma membrane (Kim et al., 2011). Thus, I hypothesize that PI(4,5)$P_2$ acyl remodelling by LYCAT may be coupled to PIS activity in PIPEROsomes.

I hypothesize that LYCAT may act alongside other acyltransferases, in a redundant way, in general PI acyl remodeling in addition to also specifically acting on a distinct pool of PI that is part of a substrate channeling system. In LYCAT-silenced cells, I did not see an effect on the acyl profile of PI (Chapter 3, Figure 3.2). Thus, in the absence of LYCAT, it is possible that the other redundant acyltransferases are able to enrich PI with the proper acyl profile. Furthermore, I hypothesize that LYCAT also acts on a distinct pool of PI which is converted to PI(4)P and then PI(4,5)$P_2$ at the plasma membrane. LYCAT silencing caused a shift in the acyl profile of $PIP_2$ species (Chapter 3, Figure 3.4). Thus, in the absence of LYCAT, I suggest that other acyltransferases that don't have the same acyl chain specificity, act in place of LYCAT resulting in misacylated pool of lipids channeled toward PI(4,5)$P_2$ synthesis. The mechanism of LYCAT acting on plasma membrane PI(4,5)$P_2$ could be due to i) PIPEROsome localization to ER-plasma membrane junctions where PI-transfer proteins transfer PI(4,5)$P_2$ from the plasma membrane to LYCAT localized in PIS vesicles (Chang and Liou, 2015; Cockcroft, 2001) or ii) the plasma membrane and ER are able to localize within close proximity giving LYCAT access to PI(4,5)$P_2$ and act in *trans*.

PI-transfer proteins have been shown to play key roles in PI transport. The ability to transport these lipids is dependent on how the lipid sits within the PI-transfer protein binding cavity. Elucidation of the PI-transfer protein crystal structure has shown that the lipid headgroup gets buried deep in the lipid binding cavity while the acyl chains face outwards toward the solvent face of the binding cavity (Yoder et al., 2001). The crystal structure of PI-transfer protein α

revealed two channels within the binding cavity that accommodate the *sn1* and *sn2* acyl chains (Tilley et al., 2004) and has been shown to prefer PI containing shorter acyl chains (Hunt et al., 2004). Therefore, it is possible that alterations in PI and PIP acyl chain content could impact the transport of lipids in the cell, thus impacting the flow of molecules involved in PI synthesis.

### 6.2. The PI acyltransferase LYCAT preferentially controls the levels of PI(4,5)$P_2$

LYCAT silencing caused a reduction in total levels of PI(4,5)$P_2$ (Chapter 3, Figure 3.6). I speculate that two mechanisms are responsible for this reduction. Firstly, in the absence of LYCAT, a small pool of misacylated PI is produced (which is perhaps part of PI to PI(4)P to PI(4,5)$P_2$ substrate channeling described above), which is then converted into PI(4)P by PI4-kinases (Dickson et al., 2014; Graham and Burd, 2011). However, PIP5K, responsible for the conversion of PI(4)P to PI(4,5)$P_2$ prefers substrates with 18:0/20:4 (Schmid et al., 2004). Thus, PIP5K may have a difficult time recognizing the 18:0/20:4 PI(4)P in the presence of a small pool of misacylated PI(4)P, resulting in decreased efficiency of PIP5K-dependent production of PI(4,5)$P_2$ from PI(4)P. Secondly, in the absence of LYCAT, the smaller pool of PI(4,5)$P_2$ that is produced, results in an accumulation of misacylated PI(4,5)$P_2$. I propose that as a part of a quality control mechanism of the cell, this misacylated PI(4,5)$P_2$ undergoes preferential hydrolysis of the 5-inositol position by an acyl chain sensitive phosphatase. The 5-phosphatase, INPP5B shows greater preference for PI(4,5)$P_2$ containing shorter acyl chains over the endogenous PI(4,5)$P_2$ *in vitro* (Schmid et al., 2004). Thus, INPP5B may be the quality control enzyme. Together, I propose that enzyme efficiency and a quality control mechanism are responsible for reduced levels of PI(4,5)$P_2$ in LYCAT-silenced cells.

### 6.3. PI cycle may be coupled with a PI-specific Lands cycle to produce PI and PIPs with 38:4 acyl species

I propose a model that couples PI synthesis (i.e. the PI cycle) with PI/PIP acyl remodelling (i.e. a PI-specific Lands cycle). In this model, I propose that there is fundamental and/or physical overlap between the PI cycle and a PI-specific Lands cycle, combining the actions of PIS and PI-specific acyltransferases. More specifically, I propose that both LYCAT and LPIAT1 work within this model.

LPIAT1 has been shown to incorporate arachidonic acid on the *sn2* position of PI (Anderson et al., 2013; Gijón et al., 2008; Lee et al., 2012). Examination of liver and brain of LPIAT1$^{-/-}$ mice showed reduced levels of 38:4 $PIP_1$ and $PIP_2$ and showed reduced total levels of $PIP_1$ and $PIP_2$ (Anderson et al., 2013). LYCAT$^{-/-}$ mice and siRNA silencing of LYCAT in HeLa cells showed not only an impact on the levels of stearic acid in PI, there were also reductions in arachidonic acid in PI (Imae et al., 2011). However, this was not due to reduced LPIAT1 acyltransferase activity nor was it due to altered LPIAT1 expression (Imae et al., 2011). It is possible that the acyltransferase activity of LPIAT1 incorporation of 20:4 on the *sn2* position of PI prefers substrates containing 18:0 on the *sn1* position. Thus, replacement of other fatty acids (such as 16:0 or 18:1) may lead to reduced incorporation of 20:4 into PI, though this has not been tested. Therefore, I hypothesize that LYCAT and LPIAT1 may work together to enrich PI with 18:0/20:4. In this model, I propose that the PI cycle is coupled with a PI-specific Lands cycle involving the acyltransferases, LYCAT and LPIAT1 that act to enrich PI and $PI(4,5)P_2$ with 1-stearoyl-2-arachidonoyl acyl species.

### 6.4. LYCAT controls PIP function possibly by altering membrane characteristics and effector binding

My data indicate that LYCAT regulates PIP levels and localization. LYCAT silencing reduced the number of PI(3)P endosomes and caused major disruptions to $PI(4,5)P_2$ localization causing the $PI(4,5)P_2$ probe to relocalize from the plasma membrane to intracellular tubular structures. Additionally, LYCAT silencing decreased total levels of $PI(4,5)P_2$ and PI(3)P. LYCAT perturbation also resulted in the incorporation of shorter acyl chain species in PI and PIPs, which could alter PIP function. Here I will discuss the general effect of altered acyl chains in PI and PIPs and then below I will discuss how this may impact $PI(4,5)P_2$, PI(3)P and $PI(3,4,5)P_3$-dependent functions.

My results found that LYCAT perturbation resulted in shorter acyl chains in $PIP_2$ species. Shorter acyl chains could potentially impact the position of the lipid in the membrane thereby affecting effector protein binding. Changes in chain length could affect the orientation of the lipid relative to the membrane (Wakelam, 2014) and/or cause the lipid to sit deeper in the membrane (van Meer et al., 2008). Alterations in acyl chain content could also affect 1) lipid dynamics, in particular lateral diffusion, 2) lipid packing within lipid ordered domains, 3) enrichment of the

lipid within curved vs flat lipid bilayers and 4) the interaction of the lipid with proteins that have certain membrane inserting domains. For example Drp1, a GTPase involved in mitochondrial division, recognizes the headgroup of PA and two fatty acyl chains of other phospholipids within the membrane (Adachi et al., 2016). The positioning of a lipid in the membrane plays an important role in coincidence detection as many effector lipid binding domains bind directly to particular lipids and make contact with other lipids or proteins at the membrane in a non-specific manner. For example, the C2 domain of protein kinase Cα specifically binds to phosphatidylserine and non-specifically to $PI(4,5)P_2$ at the plasma membrane when cytosolic $Ca^{2+}$ increases, resulting in higher affinity and selectivity of protein kinase Cα to the plasma membrane (Guerrero-Valero et al., 2009). Thus, $PI(4,5)P_2$ contained altered acyl chains, coincidence detection involved in protein kinase Cα signaling could be impacted. Additionally, proteins that function in homodimers, such as the hepatocyte receptor tyrosine kinase substrate protein that interacts through the FYVE domain, would likely exhibit altered binding due to changes in lipid orientation or axial position (Mao et al., 2000).

### 6.5. LYCAT controls clathrin-mediated endocytosis

In elucidation of the function of LYCAT in RPE cells, my data demonstrated that LYCAT perturbation causes alterations in CCP dynamics consistent with disruption of initiation and assembly of CCPs, and decreased rates of CME. It has been shown that perturbations in $PI(4,5)P_2$ impact CCP size, lifetime and frequency (Antonescu et al., 2011). Our findings that LYCAT silencing results in a reduction in $PI(4,5)P_2$ and a reduction in CCP initiation rate, size and frequency, are consistent with this previous work. $PI(4,5)P_2$ functions as a membrane ligand for many CCP proteins, including AP2, sorting nexin 9 and dynamin (Di Paolo and De Camilli, 2006; Gaidarov and Keen, 1999; Itoh et al., 2001; Jackson et al., 2010; Krauss and Haucke, 2007). Defects in CCP dynamics may be partially due to reduced $PI(4,5)P_2$ levels, but could also be due to altered CCP effector binding.

Endocytosis requires the turnover of $PI(4,5)P_2$ for proper CCP assembly and CCV formation and is highly dependent on 5-phosphatases, OCRL and synaptojanin-1 (Antonescu et al., 2011; Chang-Ileto et al., 2011). LYCAT silencing resulted in a redistribution of the $PI(4,5)P_2$ probe to

intracellular tubules. This resembles another study, which found that a disruption to OCRL resulted in accumulation of PI(4,5)$P_2$ on tubular structures (Nández et al., 2014). OCRL and, to a lesser extent, synaptojanin-1, preferentially selects for 18:0/20:4 PI(4,5)$P_2$ (Schmid et al., 2004). Synaptojanin-1 aides in the scission of CCPs from the plasma membrane (Chang-Ileto et al., 2011). If synaptojanin-1 is less efficient at acting on misacylated PI(4,5)$P_2$, I would expect less vesicle scission and production of tubules with PI(4,5)$P_2$ accumulation instead of vesicles. In LYCAT-silenced cells, the misacylated PI(4,5)$P_2$ may act as a poor substrate and cause accumulation of PI(4,5)$P_2$.

Regulation of CME by LYCAT seems to be specific and selective based on the receptor being internalized. My data found that LYCAT regulates TfR endocytosis but did not impact cell surface EGFR levels. Though, I did not investigate the rates of EGFR internalization, measurement of cell surface EGFR was used as an indicator of the efficiency of endomembrane traffic. Although endocytosis of TfR and EGFR rely on the same core machinery including clathrin, AP2 and dynamin, TfR and EGFR are generally localized to different CCPs, where only about 15% exhibit localization to the same CCPs (Delos Santos et al., 2017; Stang et al., 2004) and use different endocytic accessory proteins such as Grb2, which is required for EGFR internalization but not TfR internalization (Huang et al., 2004). It is also possible, that endocytic accessory proteins involved in TfR internalization may be sensitive to specific acyl species within PI(4,5)$P_2$.

### 6.6. LYCAT controls PI(3)P and early endosomal traffic

LYCAT silencing resulted in reduced levels of PI(3)P as assessed by the 2FYVE probe localization and biochemical measurement of PI(3)P levels. PI(3)P levels can be controlled by multiple mechanisms. Firstly, PI(3)P synthesis could rely on a specific precursor pool of PI that has been remodelled by LYCAT, as PIS vesicles have been shown to make transient contact with not only the plasma membrane but also with a number of different membranes including endosomes (Kim et al., 2011). However, I was unable to investigate the acyl chain profile of PI(3)P due to PI(4)P being the predominant $PIP_1$ species, which does not allow assessment of PI(3)P acyl profile by this technique. Secondly, PI(3)P synthesis may be dependent on PI(4,5)$P_2$ turnover. LYCAT silencing resulted in a reduction in PI(4,5)$P_2$ levels, and decreased PI(4,5)$P_2$ levels have separately

been shown to cause a decrease in PI(3)P levels (Shin et al., 2005). Thirdly, the defects in PI(3)P levels may be due to reduced CME and membrane flux. To determine if the decrease in PI(3)P was due to reduced PI(4,5)$P_2$ turnover, future studies could examine the number of 2FYVE structures in LYCAT-silenced cells transfected with mCherry-OCRL. I expect that if turnover of PI(4,5)$P_2$ limits production of PI(3)P, then overexpression of the 5-phosphatase OCRL will accelerate the rate of PI(4,5)$P_2$ turnover despite PI(4,5)$P_2$ being misacylated, thus allowing an enhancement of PI(3)P production and rescue of intracellular membrane traffic events.

Similar to the molecular switch of PI(4,5)$P_2$ hydrolysis by 5-phosphatases required for CME, the molecular switch of PI conversion into PI(3)P is implicated in the maturation of newly formed vesicles to early endosomes (Zoncu et al., 2009). Additionally, depletion of PI(3)P by either inhibition of PI3K or recruitment of a 3-phosphatase to early endosomes, caused these early endosomes to revert to immature vesicles (Zoncu et al., 2009). PI(3)P, together with Rab5, are important in the recruitment of tethering factors, such as EEA1 (via a FYVE domain) and other endosomal effectors involved in endosomal sorting (Christoforidis et al., 1999; Lawe et al., 2000). Reduced PI(3)P levels in LYCAT-silenced cells and reduced numbers of 2FYVE-positive endosomes is consistent with these known functions of PI(3)P. Reduction in PI(3)P levels by LYCAT silencing could impact recruitment of these effectors and cause issues with endosomal sorting. I found no major disruptions to EEA1 upon LYCAT silencing, but this is consistent with previous reports that show a portion of EEA1 is still recruited to early endosomes despite reduced PI(3)P levels (Fili et al., 2006; Johnson et al., 2006). Though there are many other PI(3)P effectors, such as Rabenosyn-5, it is an important consideration to investigate other PI(3)P effectors to determine if recruitment is altered due to LYCAT silencing.

### 6.7. LYCAT controls PI(3,4,5)$P_3$ and Akt signaling

I observed that LYCAT silencing caused an apparent reduction in PI(3,4,5)$P_3$ levels. Since PI(4,5)$P_2$ is a precursor for PI(3,4,5)$P_3$ synthesis one explanation for the reduction in PI(3,4,5)$P_3$ could be due to the effect of LYCAT silencing reducing PI(4,5)$P_2$ levels. However, the reduction of total PI(4,5)$P_2$ levels is modest, and the apparent reduction in PI(3,4,5)$P_3$ levels by LYCAT silencing appears to be more substantial, suggesting that a reduction in PI(4,5)$P_2$ substrate is not enough

to explain the reduction in PI(3,4,5)$P_3$ levels in LYCAT-silenced cells. Secondly, the apparent reduction in PI(3,4,5)$P_3$ upon LYCAT silencing could be due to sensitivity of PI3K to the acyl chain profile of its substrate. One study, which investigated the specific binding of PI3K to PI(3,4,5)$P_3$, found that the C-terminal SH2 domain of p85α subunit was sensitive to PI(3,4,5)$P_3$ acyl chain length, where a reduction in acyl chain length caused a decrease in binding affinity to p85α (Ching et al., 2001). Thirdly, EGF-stimulated Akt phosphorylation requires clathrin (likely as a result of requiring formation of CCPs (Garay et al., 2015), and the defect in activation of Akt in LYCAT-silenced cells could reflect a defect in formation and assembly of CCPs.

Analysis of PI and PIP acyl chain profile was conducted in unstimulated cells, thus I was unable to assess the various acyl chain species of PI(3,4,5)$P_3$. An interesting follow-up would be to investigate the effect of EGF-stimulation on the acyl profile of PI(3,4,5)$P_3$ in LYCAT-silenced cells. Nonetheless, there have been a number of research groups that have investigated the acyl profile of PI(3,4,5)$P_3$ in stimulated cells (Clark et al., 2011; Milne et al., 2005; Ogiso and Taguchi, 2008). Examination of these studies suggests that the acyl chain content of PI(3,4,5)$P_3$ following cell stimulation may be ligand specific. In an analysis of RAW 264.7 macrophage cells, the diversity of PI(3,4,5)$P_3$ acyl species varied from 32:0 to 40:6 PI(3,4,5)$P_3$ when stimulated with various ligands including lysoPA and zymosan which activate G protein-coupled receptors and NF-κB, respectively (Milne et al., 2005). This suggests that the different PI3K isoforms activated by different receptors use different PI(4,5)$P_2$ species as their substrate. However, there has been some variation in the molecular species of PI(3,4,5)$P_3$ detected, which could be due to differences in cell lines or detection methods (Wakelam, 2014). For example, analysis of A431 cells stimulated with EGF, researchers were only able to detect 36:4 PI(3,4,5)$P_3$ species (Ogiso and Taguchi, 2008). In another study, human breast epithelial cells contained 5 different PI(3,4,5)$P_3$ species after stimulation with EGF and found the species with the greatest magnitude of increase following stimulation was 18:0/20:4 PI(3,4,5)$P_3$ (Clark et al., 2011). Therefore, it seems that activation of EGFR and recruitment of PI3K may preferentially select PI(4,5)$P_2$ containing 18:0/20:4. Thus, upon LYCAT silencing the decrease in PI(4,5)$P_2$ levels and the alteration in $PIP_2$ acyl chain content, could explain the decrease in PI(3,4,5)$P_3$ levels. However, it is possible the PH-Akt probe is

sensitive to acyl chain content, therefore it is important to test PH-Btk, a different PI(3,4,5)$P_3$ probe.

## 6.8. Additional Contributions

During the course of my graduate studies, I have primarily focused on the projects investigating the function of LYCAT in regulating the acyl chain profile of PIPs and the impact this has on endomembrane traffic and hormone receptor signaling, as this thesis describes. Chapters 3 and 4 have resulted in one first-author publication.

**Leslie N. Bone**, Roya M. Dayam, Minhyoung Lee, Nozomu Kono, Gregory D. Fairn, Hiroyuki Arai, Roberto J. Botelho and Costin N. Antonescu 2017. The acyltransferase LYCAT controls specific phosphoinositides and related membrane traffic. *Molecular Biology of the Cell.* 1(28):161-172.

The introduction of my thesis will be used towards a review publication on PI and PIP synthesizing enzymes and substrate acyl chain specificity. Additionally, the results from Chapter 5 are almost a complete project and will be published after a few more experiments are conducted in the next few months.

Unique opportunities for collaboration with peers have presented themselves over the years and I was happy to lend my expertise to my collaborators toward the completion of several other projects. The following works are additional projects I have contributed to. I briefly describe the extent of each of my contributions.

The following article was published in *Traffic:*

Mathieu J. F. Crupi, Piriya Yoganathan, **Leslie N. Bone**, Eric Lian, Andrew Fetz, Costin N. Antonescu and Lois M. Mulligan 2015. Distinct Temporal Regulation of RET Isoform Internalization: Role of Clathrin and AP2. *Traffic.* 16(11):1155-1173.

This project elucidated the specific mechanisms of the membrane traffic of the receptor tyrosine kinase RET within the cell. The relative involvement of clathrin-dependent and –independent processes in internalization of both RET isoforms, RET9 and RET51, had not been investigated. My contribution to this work was TIRF-M imaging of RPE cells transfected with RET9 or RET51, stained for AP2 and stimulated with glial cell line-derived neurotrophic factor for various times. My work determined that RET51 was recruited more rapidly to AP2 structures following activation compared to RET9. The images are included here:

"The AP2 complex is involved in internalization of activated RET isoforms" (Figure 7A)

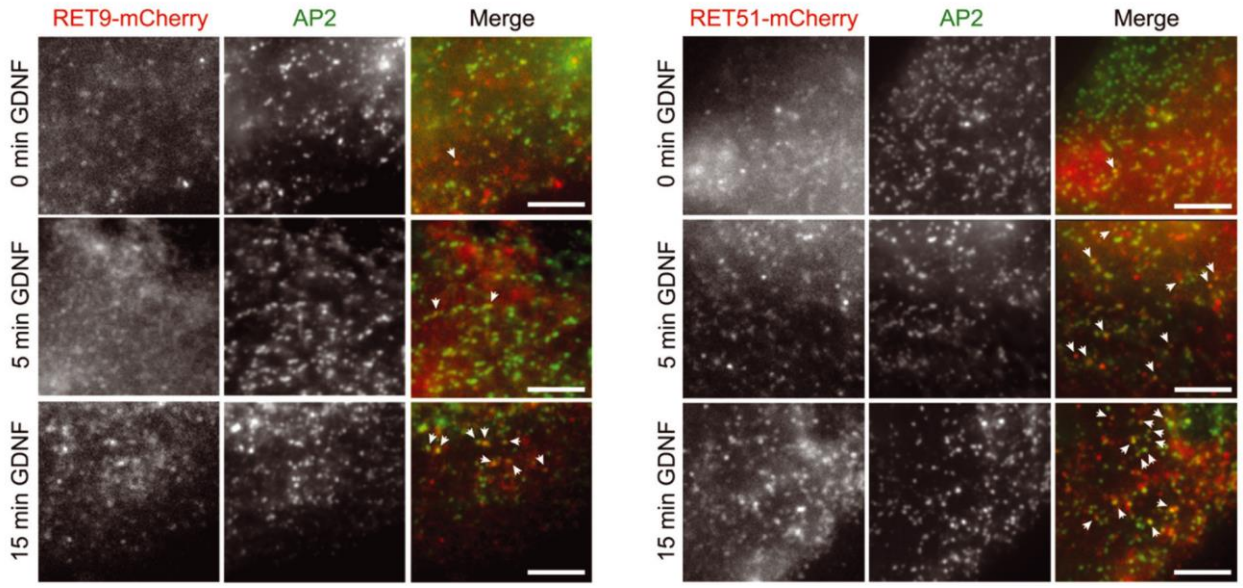


The following article will be published in *Molecular Biology of the Cell:*

Ralph Christian Delos Santos, Stephen Bautista, Stefanie Lucarelli, **Leslie N. Bone**, Roya M. Dayam, John Abousawan, Roberto J. Botelho and Costin N. Antonescu 2017. Selective regulation of clathrin-mediated EGFR signaling and endocytosis by phospholipase C and calcium. Accepted in Mole*cular Biology of the Cell*.

This project was on elucidation of the role of PLCγ1 in EGFR CME and EGFR signaling. We found that signals triggered by PLCγ1 (including cytosolic $Ca^{2+}$ and protein kinase C) regulate CME and allows for the selective control of a subset of CCPs harboring EGFR but not CCPs harbouring TfR. My contribution to this work was biochemical $PI(4,5)P_2$ analysis by [$^3$H]*myo*-inositol labelling in cells treated with EGF or ionomycin. I also contributed to TIRF-M imaging following transfection of synaptojanin-1 in RPE cells stably expressing GFP-CLC and treated with various inhibitors (BAPTA-AM and BIM, $Ca^{2+}$ chelator and protein kinase C inhibitor, respectively) and stimulated with EGF. My work showed that PLCγ1 control of EGFR is not due to robust, broad $PI(4,5)P_2$ depletion but likely due to generation of secondary signaling intermediates (calcium). Thus, I conducted the appropriate experiments and quantified data. The figure is included here:

"EGF stimulation elicits a PLCγ1-dependent increase in cytosolic $Ca^{2+}$" (Figure 2A)

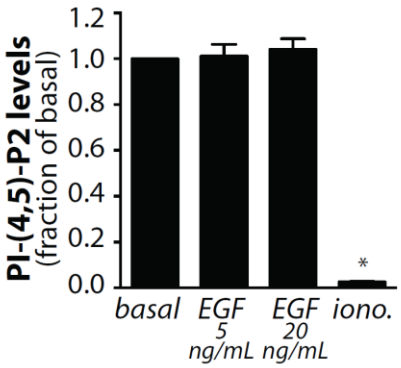


The following article will be published in the *Journal of Cell Science:*

Brandy D. Hyndman, Mathieu J.F. Crupi, Susan Peng, **Leslie N. Bone**, Simona M Wagner, Aisha N. Rekab, Costin N. Antonescu, and Lois M. Mulligan 2017. Differential recruitment of E3-ubiquitin ligase complexes regulates RET isoform internalization. Accepted in *Journal of Cell Science.*

This project examined the differences in the mechanics of RET9 and RET51 ubiquitination and internalization given that RET isoforms are internalized with distinct kinetics. My contribution to

this work was assistance in TIRF-M imaging of RET9 and AP2 in NEDD4 knockdown cells and imaging of RET51 and AP2 in CBL knockout or GRB2 knockdown cells, all in SH-SY5Y neuroblastoma cell line. This work suggested that RET9 ubiquitination by NEDD4 promotes its recruitment to CCPs and subsequent internalization. Furthermore, this work suggested that CBL-mediated ubiquitination is not essential for the early stages of RET51 recruitment or internalization into CCPs. Images are included here:

“RET isoform ubiquitin linkages and GDNF-stimulated recruitment to CCPs” (Figure 6 C-E)

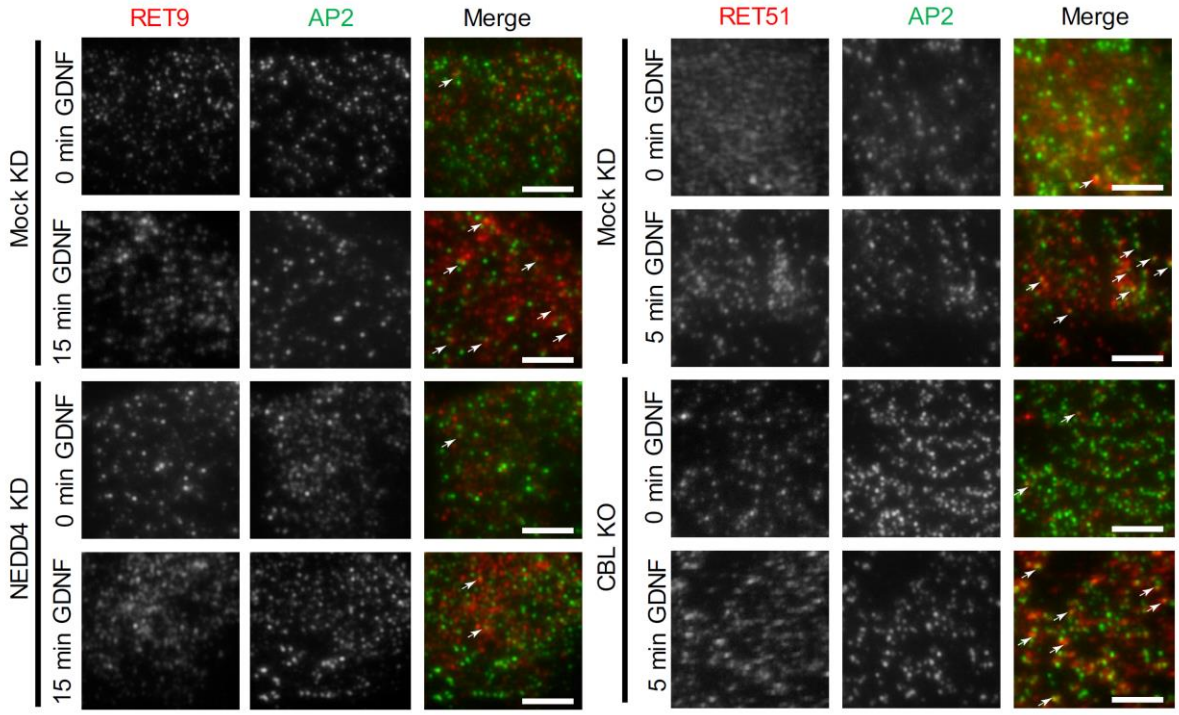


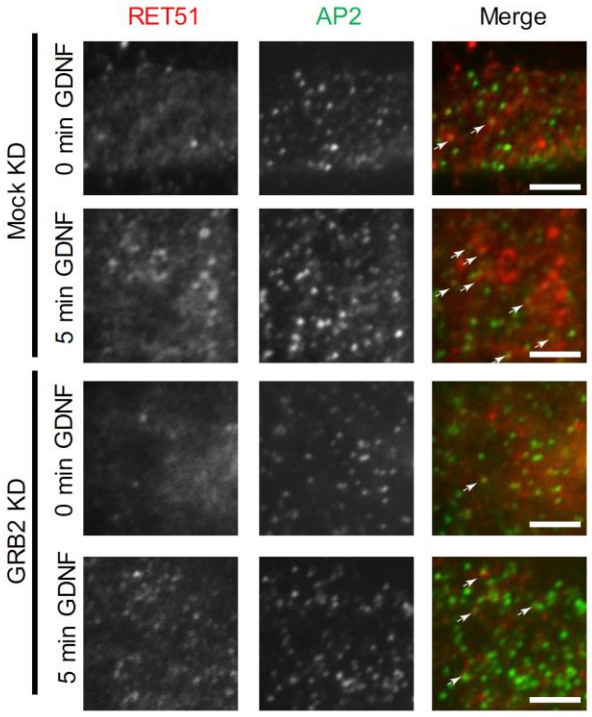

# Chapter 7
# Future Directions

My work showed that loss of LYCAT plays a role in acyl chain depletion in PI(4,5)$P_2$. I have also identified the functional role of LYCAT in controlling localization and total levels of PI(4,5)$P_2$, PI(3)P and PI(3,4,5)$P_3$, and the role of LYCAT in regulating PI(4,5)$P_2$, PI(3)P and PI(3,4,5)$P_3$-dependent processes in RPE cells. My work found that LYCAT perturbation impacted TfR endomembrane traffic and impaired PI3K/Akt signaling.

One of the key outstanding questions of this work is what is the mechanism of enrichment of 1-stearoyl-2-arachidonoyl acyl species into PI and PIPs? My work supports a model where the acyl enrichment of PI and PIPs occurs by coupling the PI cycle to a PI-specific Lands cycle. This model combines the action of PIS for PI synthesis and the actions of PI-specific acyltransferases, LYCAT and LPIAT1, which are spatially coupled to enrich PI and PI(4,5)$P_2$ with 38:4 acyl species. Future work should be directed to test this model. Given the alterations in PI and, in particular PI(3,4,5)$P_3$ dynamics in certain cancers, such as those resulting from PTEN or p53 mutations or deletions, I propose to probe the role of LYCAT in PI(3,4,5)$P_3$-dependent cancer cell survival/proliferation pathways, that are driven by receptor tyrosine kinases or G protein-coupled receptors. Using cBioPortal for cancer genomics, investigation into the tendency for p53 and LYCAT towards co-occurrence of alteration in breast cancer was significant with a p-value of $< 0.01$ (Cerami et al., 2012; Gao et al., 2013). In order to investigate these questions, I have outlined some projects below.

### 7.1. Mechanism of PI cycle/PI-specific Lands cycle for enrichment of PI and PIPs with 38:4 acyl species

I propose a model in which PI-specific acyltransferases, such as LYCAT and LPIAT1 work together to enrich PI with 1-stearoyl-2-arachidonoyl acyl species. I envision this to occur alongside PI synthesis in ER-derived vesicles containing PIS enzyme (Kim et al., 2011). In this way, it is possible that newly synthesized PI is then subjected to acyl chain remodelling by the acyltransferases. Future work should focus on the relationship between LYCAT and PIS localization. Does LYCAT play a role in PIS localization to these peripheral vesicles or vice-versa? Also, does silencing of LPIAT1 alter localization of PIS or LYCAT? I was able to conduct one experiment were I transfected cells with PIS-GFP following LYCAT silencing. Preliminary images showed no major disruption to

PIS localization following LYCAT silencing, suggesting that LYCAT may not play a role in PIS stability in these peripheral vesicles (Figure A2). However, further replicates and quantitative analysis is needed for a better understanding of the relationship between PIS and LYCAT localization.

To better understand if LYCAT and LPIAT1 are involved in this PI-specific Lands cycle, investigation into the localization of LPIAT1 and LYCAT is required to determine if they localize to similar cellular sub-compartments. Co-expressing LYCAT-GFP and epitope-tagged LPIAT1, one could use immunofluorescence and microscopy to identify the relative localization of the two acyltransferases. Spinning disc confocal and TIRF-M would be excellent tools for visualizing broad localization in the cell and of regions close to the cell surface such at ER-plasma membrane contact sites, respectively. My data indicate that LYCAT localized to peripheral PIS vesicles that partially overlap with ER-plasma membrane contact sites marked with E-Syt2. TIRF-M would be highly beneficially, in addition to spinning disc confocal, to determine if LYCAT and LPIAT1 localize to these peripheral PIS-vesicles. Currently, a graduate student, Ms. Y. Awadeh, and an undergraduate student, Mr. G. Shantz, have begun examining the localization of LPIAT1 in RPE cells. Indeed, their preliminary imaging data suggest that a portion of LPIAT1 localizes to punctate structures, which may represent the pool of LYCAT/PIS peripheral vesicles and similar to LYCAT localization, shows minimal overlap with KDEL. Co-transfection of LPIAT1 and LYCAT or LPIAT1 and PIS is required to further elucidate the localization of LPIAT1 with respect to PIS and LYCAT in RPE cells.

The activity of LYCAT and LPIAT1 are likely coupled alongside the action of $PLA_1$ and $PLA_2$ enzymes to remodel PI and PIP acyl profiles. Thus, I hypothesize that $PLA_1$ and/or PI-$PLA_2$ enzymes either localize to or are functionally linked to enzymes within PIS/LYCAT-positive vesicles. ER exit sites are specialized subdomains of the ER where newly synthesized proteins are transported via COPII-coated vesicles to the Golgi. COPII proteins are responsible for selection of cargo and ER-membrane deformation (Barlowe, 2002; Miller et al., 2003). The cycling of the GTPase, Sar1, is required for full COPII recruitment to the ER, membrane budding and COPII uncoating (Barlowe et al., 1994; Yoshihisa et al., 1993). More recently, p125 was identified to be localized to COPII ER exit sites (Shimoi et al., 2005). p125 is one of three known $PLA_1$ enzymes in mammals (Richmond and Smith, 2011) and exhibits sequence homology to PA-$PLA_1$ (DDHD1)

and an N-terminal region that binds to a subunit of COPII (Mizoguchi et al., 2000). Interestingly, the localization of PIS to peripheral vesicles is also dependent on Sar1 cycling (Kim et al., 2011). In my proposed model, a $PLA_1$ would be required to liberate the fatty acid at the *sn1* position to allow LYCAT to enrich PI/PIPs with stearic acid, as proposed by many groups (Cao et al., 2004; Imae et al., 2011). Thus, future work should focus on localization of p125 with respect to LYCAT and PIS to determine if p125 localizes to these peripheral vesicles. Additionally, future work should focus on whether p125 is required for proper acylation of PI and PIPs by investigating biological/chemical phenotypes that are produced upon p125 silencing. Firstly, future work should silence p125 and examine cell surface levels of TfR. I would expect that if p125 works in concert with LYCAT to remodel newly synthesized PI, then p125 silencing should have similar effects as LYCAT silencing and cause a decrease in cell surface TfR. Secondly, simultaneous knockdown of p125 and LYCAT should be performed to examine if these enzyme work in the same pathway. If they do work in the same pathway, then the silencing will not be additive. And, lastly, in p125 silenced cells, I suggest repeating some experiments to examine TfR traffic and EGF-activated Akt pathway, including CCP dynamics, endosomal sorting and Akt activation, to probe if LYCAT and p125 function in the same biochemical pathway. Similar methods should be used to study $PLA_2$ enzymes.

Another important aspect of this proposed model is whether this PI-specific Lands cycle is a dynamic system. Do various stimuli or stresses cause LYCAT to change localization in order for the enzymes to be delivered to subcellular locales at which PI synthesis is occurring? Live-cell imaging of PIS and LYCAT would provide further insight into the relationship between PI synthesis and acyl remodelling. I have proposed that LYCAT may control $PI(4,5)P_2$ levels and acyl profile, however it is not known whether LYCAT controls the synthesis of $PI(4,5)P_2$ by PIP5K. It is possible that LYCAT may use PI(4)P as a preferred substrate or that LYCAT localization is driven only to plasma membrane microdomains that are enriched in PI(4)P that is then shuttled to $PI(4,5)P_2$ synthesis. Furthermore, whether LYCAT is part of a pathway that replenishes $PI(4,5)P_2$ levels following stimuli is not known. One project currently underway by a graduate student, Ms. Y. Awadeh, is examining the role of LYCAT in $PI(4,5)P_2$ resynthesis following PLC activation. Treatment with ionomycin causes an increase in cytosolic $Ca^{2+}$, which activates PLC and causes a

rapid decrease in $PI(4,5)P_2$ levels. Ms. Y. Awadeh will be using the PH-PLCδ1 probe to determine a ratio of TIRF-M/epifluorescence signal as a quantitative measurement of plasma membrane $PI(4,5)P_2$ levels. Thus far, the protocol has been optimized and it has been determined that 10 min (10 μM) ionomycin treatment, followed by 30 min of recovery is an optimal time for replenishment of $PI(4,5)P_2$. The next steps of this project will examine recovery of $PI(4,5)P_2$ levels following PLC activation in LYCAT-silenced cells. This project will also investigate dynamics of PIS and LYCAT at ER-plasma membrane junctions following treatment with ionomycin. Using live cell imaging and object detection and tracking (Aguet et al., 2013; Jaqaman et al., 2008) of PIS vesicles to quantitatively measure the visits and overlap made by PIS vesicles to plasma membrane regions marked by E-Syt contact sites (Bone et al., 2017).

Another project would be to investigate the effects of metabolic stress, such as high fat diet on LYCAT and LPIAT1 localization. LYCAT appears to have multiple functions in control of metabolism and ROS (Li et al., 2012, 2010; Liu et al., 2012). However, the role of LYCAT in regulating metabolism and ROS may only occur during systemic stress. Does the localization of LYCAT and LPIAT1 change upon high fat diet? Do they translocate to the mitochondria? These are some of the questions that could be assessed by fluorescent probe localization and fatty acid supplementation, for example.

Determining the protein-protein associations of LYCAT is also an important approach to understanding LYCAT function, subcellular proteasome and biological mechanism. One approach to studying this uses proximity-dependent cellular biotinylation by a bacterial biotin ligase from *E. coli*, called BirA (Choi-Rhee et al., 2004). A mutant BirA, R118G, referred to as BirA*, gains promiscuous biotinylation ability and is able to biotinylate proteins in close proximity (Choi-Rhee et al., 2004; Roux et al., 2012). BirA* can be fused to a protein of interest, in this case, LYCAT and then transfected into cells. In media supplemented with biotin, the BirA* fusion protein will biotinylate proximal proteins, which can then be selectively isolated by biotin capture methods and identified by mass spectrometry (Kim et al., 2014; Roux et al., 2012). We have already established a collaboration to perform this experiment and construction of the appropriate vector is underway. Applying this strategy to identify proteins that are proximate to and/or

interact with LYCAT will contribute to our understanding of the mechanism of LYCAT function in the PI-specific Lands cycle.

### 7.2. Elucidation of the role of LYCAT in modulating PI3K/Akt signaling in a cancer cell line

My work found that LYCAT silencing had significant impact on the activation of Akt1 in RPE cells, which impacted a number of different Akt substrates. These observations should be investigated further in another cell line to probe for the generality of this novel function of LYCAT in EGF-stimulated Akt signalling. MDA-MB-468 cells are PTEN-null cells and contain high levels of EGFR, thus would be an appropriate cell line to study both the effect of LYCAT in the context of EGFR signaling and in the context of cell survival driven by EGFR. MDA-MB-231, a breast cancer cell line are p53 mutated cells (Hui et al., 2006) and are another appropriate cell line to study given the link between p53 and alterations in phospholipid acylation status (Naguib et al., 2015). Preliminary data has been collected from MDA-MB-231 cells and is presented here.

I discovered an apparent decrease in PI(3,4,5)$P_3$ levels in LYCAT silenced cells determined by fluorescent PH-Akt. However, it is possible that this probe was sensitive to acyl chain content and thus my observations of decreased PI(3,4,5)$P_3$ levels in LYCAT-silenced cells could be due to altered binding of the probe to the lipid headgroup. Therefore, I suggest that future studies examine localization of PI(3,4,5)$P_3$ using a different probe, such as PH-Btk, which is from Bruton tyrosine phosphatase, which has been used as a PI(3,4,5)$P_3$ probe (Manna et al., 2007). Thus, if both the PH-Akt and PH-Btk probes show reductions in PI(3,4,5)$P_3$ it is likely there is a reduction in PI(3,4,5)$P_3$ instead of the probe being sensitive to acyl chain content. However, to further confirm this, biochemical analysis of PI(3,4,5)$P_3$ levels should be investigated. Thus, future work should perform the optimized protocol for [$^3$H]*myo*-inositol labelling of PIPs and detection by HPLC.

Examination of total levels of pan Akt in MDA-MD-231 cells showed no change following LYCAT silencing (Figure A3 A and B). Additionally, levels of Akt1 and Akt2 activation in LYCAT-silenced cells showed reductions in EGF-stimulated pAkt1 (n = 2) and pAkt2 (n = 1) levels compared to control (Figure A3 C-F). However, further replicates are required as well as an investigation into the total levels of Akt1 and Akt2 in order to understand the impact of LYCAT

silencing on the individual Akt isoforms in MDA-MB-231 cells. Furthermore, RPE cells exhibited significantly lower levels of total Akt upon LYCAT silencing. Akt is known to undergo regulated proteolytic degradation, which is regulated by several different cues including ubiquitination (Chan et al., 2014). Thus, future studies should investigate Akt ubiquitin modification by Akt immunoprecipitation followed by anti-ubiquitin immunoblotting (Choo and Zhang, 2009).

Alterations in activation of Akt could be due to a number of factors including impairment of receptor activation upon ligand binding, alterations in adaptor protein recruitment or binding following receptor activation or issues with conversion of $PI(4,5)P_2$ into $PI(3,4,5)P_3$ by PI3K. Preliminary data tried to elucidate the cause of decreased phospho-Akt1 and phospho-Akt2 levels by examining altered receptor binding of ligand or reduced receptor tyrosine kinase activity. There were no significant reductions to total EGFR levels examined by western blot in MDA-MB-231 cells silenced for LYCAT (Figure A4 A and B). Furthermore, I probed activation of EGFR by examining phosphorylation of Tyr1068, a site that becomes autophosphorylated upon receptor ligand binding and is upstream of PI3K and Akt activation (Downward et al., 1984). I found that LYCAT silencing had no impact on the phosphorylation of EGFR (Figure A4C). These data suggest that the decrease in phospho-Akt1 and phospho-Akt2 were not due to a decrease in EGFR activation upon LYCAT silencing.

My data from both RPE and MDA-MB-231 cells suggest that the decrease in phospho-Akt is not due to a loss of EGFR phosphorylation upon LYCAT silencing. However, there may be alterations in the recruitment of adapter proteins, phosphorylation of adaptor proteins or impact on PI3K. Following EGFR activation, the adapter protein Grb2 is recruited to the cytosolic tails of EGFR and mediates binding of Gab1, which once phosphorylated, creates a docking site for PI3K (Díaz et al., 2012). Future studies should examine the effects of LYCAT silencing on Gab1 and Grb2 recruitment to the plasma membrane following EGFR activation by immunofluorescence and imaging by microscopy and assessing phosphorylation of Gab1 by western blot.

An important consideration for future studies is whether LYCAT controls or regulates Akt activation via PI3K. Akt1 phosphorylation is more sensitive to LYCAT perturbation than that of Akt2 (Chapter 5, Figure 5.2). This could be due to Akt2 undergoing phosphorylation that is less dependent on PI3K and $PI(3,4,5)P_3$. Wortmannin and LY294002 are typically used to inhibit PI3Ks,

but both of these inhibitors target class I and class III PI3Ks. Class I PI3Ks preferentially catalyze $PI(4,5)P_2$ to generate $PI(3,4,5)P_3$ (Martini et al., 2014). Future studies should use class I PI3K inhibitors to see the sensitivity of Akt1 and Akt2 to this inhibitor. Cells could be treated with class I PI3K inhibitors, such as Idelalisib, which specifically targets PI3Kδ or GDC-0941, which is a pan class 1 PI3K inhibitor (Zhao et al., 2017). If Akt2 is less sensitive, then it might suggest a preferential role for LYCAT in phosphorylation of Akt1 is due to a more substantial requirement for PI3K or possibly different PI3K isoforms that in turn have different acyl preferences.

My data also demonstrated that LYCAT silencing had major impacts on Akt-activated phosphorylation of Akt substrates in RPE cells. Using the same antibody, which recognizes a phosphorylated Akt substrate consensus sequence, I determined that Akt-dependent phosphorylation of substrates is also impacted in MDA-MB-231 cells (Figure A5). Though these are preliminary data, these, along with the decrease in pAkt1 and pAkt2 levels suggest that LYCAT silencing may also be regulating Akt activation and activity in MDA-MB-231 cells. Future studies should elucidate the effects of LYCAT silencing on specific Akt substrates, such as TSC2. TSC2 is an important protein which connects mitogenic signals to cell metabolism via mTOR (Huang and Manning, 2009).

Similar to results in RPE cells, I found that LYCAT silencing did not significantly alter Erk phosphorylation following EGF-stimulated Akt activation (Figure A6 A and B). Furthermore, there were no changes to total Erk levels upon LYCAT silencing (Figure A6C). Thus, the Ras/Erk pathway does not seem to be impacted by LYCAT silencing providing further evidence that the effects of LYCAT silencing on PI3K/Akt are specific. Future experiments should further examine the impact of LYCAT perturbation on both $PI(3,4,5)P_3$-dependent and -independent mechanisms to establish the specific functions impacted by LYCAT.

Finally, future studies should focus on evaluating the effects of LYCAT silencing on cell viability and proliferation in RPE and MDA-MB-231 cells. One of the issues with chemotherapy is increased chemotherapy resistance (Tao et al., 2016). Recently there have been numerous molecular-targeted agents designed to overcome this chemotherapy resistance. PI3K/Akt activation is closely involved in cell survival, proliferation and cell motility and is often dysregulated in cancer. My research has shown that LYCAT decreases Akt activation. Of clinical

relevance for treatment of various cancers, I hypothesize that LYCAT silencing may increase the efficiency of chemotherapeutic drugs, such as cisplatin. Cisplatin is a chemotherapeutic drug that has been shown to exhibit anticancer activity and has been clinically proven in the treatment of different types of cancers including sarcomas and cancers of the bones, soft tissue and muscle (Dasari and Tchounwou, 2014). A recent study found that treatment of cells with the Akt inhibitor, MK-2206, alongside cisplatin, resulted in an increase in apoptosis in gastric cancer cell line, AGS (Tao et al., 2016). The combined therapy resulted in a synergistic effect of proliferation inhibition, thus suggesting a new therapeutic strategy for treatment of cancer.

Currently a PhD student, Mr. S.J. Bautista, alongside an undergraduate student, Ms. S. Khuffash, are investigating proliferative effects following LYCAT silencing and treatment with cisplatin. They are using propidium iodide to assess number of living cells. Living cells are unable to take up propidium iodide whereas dead cells do and the number of red stained cells can be counted and used as determinant of cell viability. Preliminary results suggest that LYCAT silencing, in addition to cisplatin treatment, increases cell death.

Though, oftentimes propidium iodide is considered a viability test, it really only assess integrity of cell membrane, which is why additional assays are required to test intracellular activity. Therefore, to assess viability I suggest the MTT assay and a clonogenic assay. MTT assay is a tetrazolium reduction assay where viable cells convert MTT into a purple coloured formazan product that is measured at a particular wavelength (Riss et al., 2004). Clonogenic assays measure cells reproductive integrity and ability to proliferate following treatment with an agent (Munshi et al., 2005). Following simultaneous LYCAT silencing and treatment with cisplatin, a cell survival curve can be generated that describes the relationship between dose of cisplatin and the number of cells that survive. Together, these assays could provide details about the combined effects of LYCAT silencing and cisplatin treatment on cell viability and proliferation in various cell types.

# Conclusion

In conclusion, my work presents evidence that the acyltransferase LYCAT plays a significant role in regulating endomembrane traffic and modulating hormone receptor signaling. Moreover, this work is the first to elucidate the function of LYCAT in PI and PIP acyl chain content and function in RPE cells. My data suggest that LYCAT plays a role in proper PIP function by ensuring correct acyl enrichment. Altering acyl enrichment by LYCAT silencing impacted TfR traffic and PI3K/Akt signaling, which I hypothesize is partially due to alterations in acyl profile, which affects the dynamics, packing, and other properties of lipids in the membrane, effector binding or recognition by kinases and phosphatases for PIP turnover. Moreover, the model I propose, which couples PI synthesis with a PI-specific Lands cycle, is likely another reason why LYCAT silencing impacts TfR endomembrane traffic and PI3K/signaling as LYCAT is no longer able to remodel PI(4,5)$P_2$ at the plasma membrane.

Currently, many different thorough lipidomic approaches are being used to investigate and characterize tumors and provide new insights into the molecular mechanism of cancer. More recently, studies have shown cancer cells to contain altered phospholipid acyl profiles, which potentially could be used as possible diagnostic tools for cancers with p53 mutations, or cancer of the prostate, breast or lungs (Goto et al., 2014; Marien et al., 2015; Naguib et al., 2015). Examination of multiple cell lines of both human and mouse origin found that cancer cells contain PI with shorter, less saturated acyl chains and low levels of polyunsaturated acyl chains compared to normal cells (Naguib et al., 2015). Additionally, p53 mutations changes the acyl chain content of PI, which results in more 36:*x* species compared to normal cells, which contain more 38:*x* species (Naguib et al., 2015). Another study found a two-fold increase in 18:0/20:4 PI along the outer edge of colorectal cancer tissue compared to the medial regions (Hiraide et al., 2016), indicating that 18:0/20:4 PI species may play an important role in cancer progression and invasion. Therefore, increasing our knowledge of PIP acyl profile provides insight into detection of cancer and potential cancer treatments.

Additionally, the regulation of PI acyl profile by LYCAT and other acyltransferase may be sensitive to dietary lipids, which could be studied in detail once the molecular and cellular systems that control PI acyl chain profile, as proposed in *Future Directions*, are better understood.

My work adds to our extensive knowledge of how phosphorylation of inositol headgroup controls PIP function by revealing that the acyltransferase LYCAT also regulates dynamics, localization and function of specific PIPs. These results suggest that control of PIP acyl chain composition by dynamic remodeling by specific phospholipases and acyltransferases represents another dimension in the control of PI function and suggest that this process may control membrane traffic, hormone receptor signaling and cell physiology.

Appendix

Figure A1. PI(4)P is the predominant $PIP_1$. RPE cells transfected with nontargeting siRNA. The relative levels of PI(3)P and PI(4)P were measured after [$^3$H]*myo*-inositol labeling, HPLC and detection by flow scintillation. Mean ± SEM, *n* = 4.

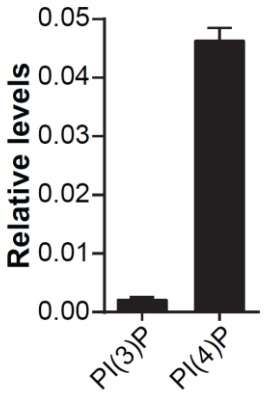

Figure A2. LYCAT silencing does not appear to alter PIS localization. RPE cells were transfected with siRNA sequence targeting LYCAT (siLYCAT) or nontargeting siRNA (siControl) and cDNA encoding eGFP-PIS. Shown are representative spinning disc confocal micrographs (scale 10 µm). *Shown is preliminary data.*

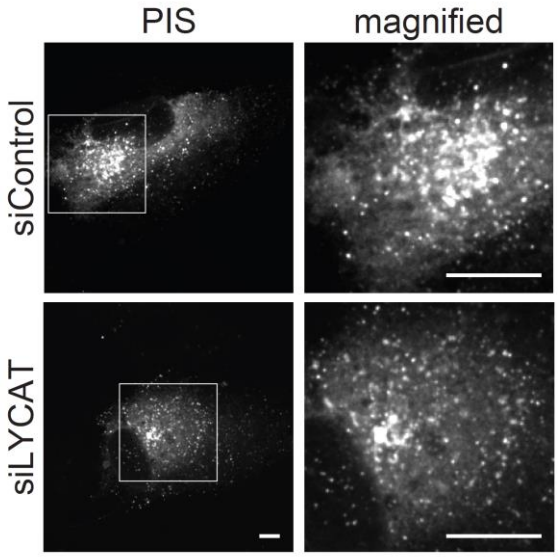

Figure A3. LYCAT silencing may have an impact on activation of Akt1 and Akt2 in MDA-MB-231 cells. MDA-MB-231 cells were transfected with siRNA targeting LYCAT (siLYCAT) or nontargeting siRNA (siControl). Following siRNA transfection cells were serum starved for 1 h and treated with EGF (5 ng/ml) for 5 min and then whole cell lysates were subjected to western blotting. (***A***) Representative immunoblots showing detection of pS473-Akt1, pS474-Akt2, total Akt or loading control (clathrin or actin). Shown in (***B***) is the quantified pan Akt protein levels (n = 7). (***C, D***) Preliminary quantitative measurements of absolute levels of pS473-Akt1 values and EGF-stimulated gain in pS473-Akt1 values, (*n* = 2). Similar preliminary quantitative measurements are shown in (***E, F***) for pS474-Akt2 (n = 1). Mean ± SEM.

Figure A3.

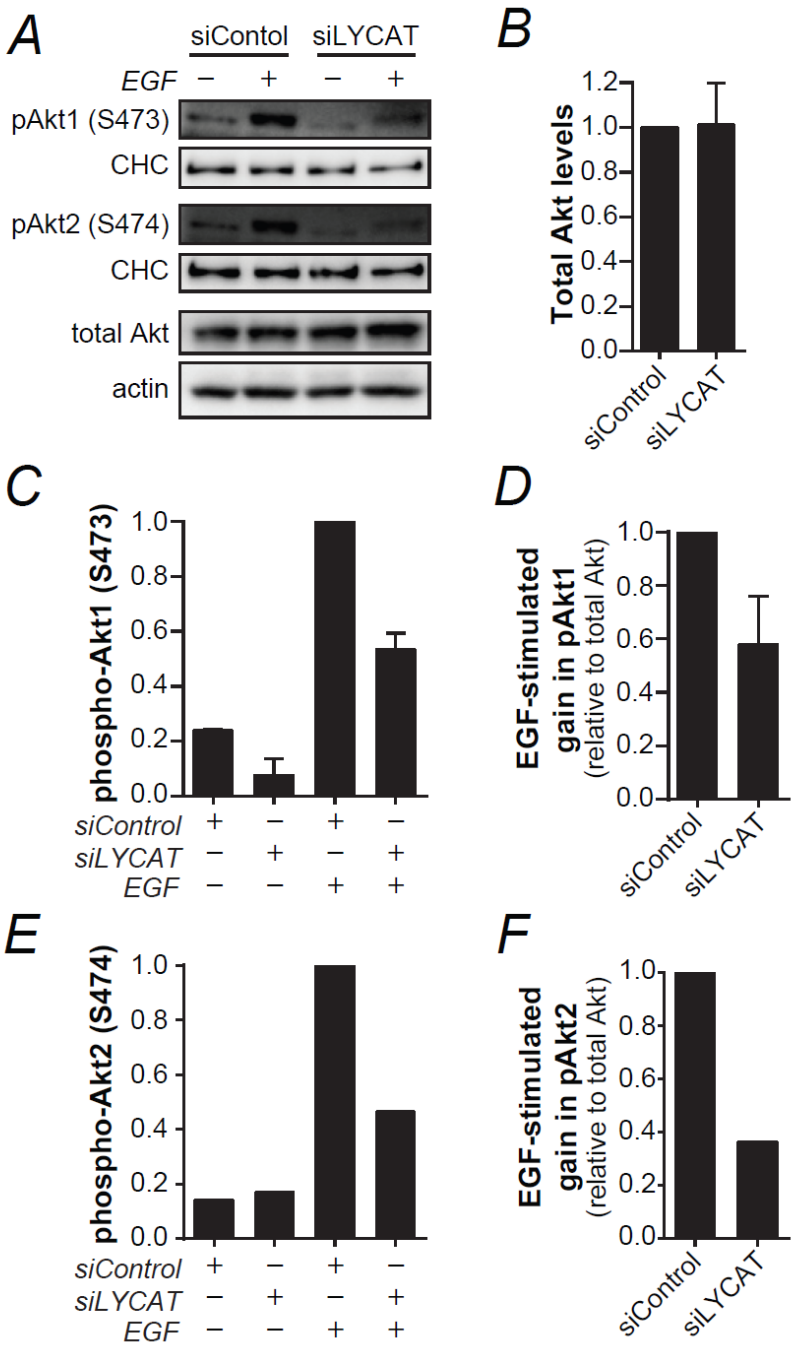
A
siContol
siLYCAT
EGF – + – +
pAkt1 (S473)
CHC
pAkt2 (S474)
CHC
total Akt
actin
B
Total Akt levels
1.2
1.0
0.8
0.6
0.4
0.2
0.0
siControl
siLYCAT
C
phospho-Akt1 (S473)
1.0
0.8
0.6
0.4
0.2
0.0
siControl + – + –
siLYCAT – + – +
EGF – – + +
D
EGF-stimulated gain in pAkt1 (relative to total Akt)
1.0
0.8
0.6
0.4
0.2
0.0
siControl
siLYCAT
E
phospho-Akt2 (S474)
1.0
0.8
0.6
0.4
0.2
0.0
siControl + – + –
siLYCAT – + – +
EGF – – + +
F
EGF-stimulated gain in pAkt2 (relative to total Akt)
1.0
0.8
0.6
0.4
0.2
0.0
siControl
siLYCAT

Figure A4. LYCAT silencing has no impact on activation of EGFR following ligand stimulation. Following siRNA transfection, MDA-MB-231 cells were serum starved for 1 h and treated with EGF (5 ng/ml) for 5 min, then whole cell lysates were subjected to western blotting. Shown in (***A***) are representative immunoblots showing detection of pY1068-EGFR, EGFR or loading control (clathrin or actin). Quantitative measurements of (***B***) total EGFR levels (n = 5), independent *t* test and (***C***) pY1068-EGFR values relative to total EGFR (n = 3), two-way ANOVA with post hoc Bonferroni pairwise comparisons. Mean ± SEM, **p* < 0.05.

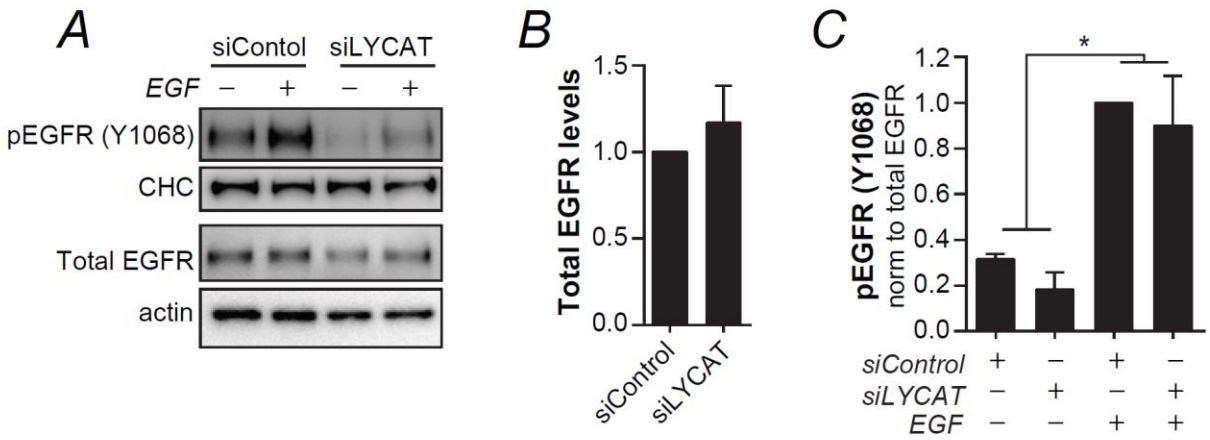

Figure A5. LYCAT silencing may impact phosphorylation of Akt substrates in MDA-MB-231 cells. MDA-MB-231 cells were transfected with siRNA sequence targeting LYCAT (siLYCAT) or nontargeting siRNA (siControl). Western blot analysis of cell lysates that were serum starved for 1 h and treated with EGF (5 ng/ml) for 5 min, using a phospho-Akt substrate (RXXS*/T*) antibody that detects phosphorylated Akt target sites. Shown in (***A***) are representative immunoblots showing detection of phospho-Akt substrates. (***B***) Profile plots of each immunoblot showing the intensity of bands and retention factor. Shown in (***D***) are immunoblots containing proteins ranging 50-100 kDa and (***C***) the profile of these proteins in control and LYCAT-silenced cells. Both siControl and siLYCAT profiles were normalized to protein content in each condition. *Shown is preliminary data.*

Figure A5.

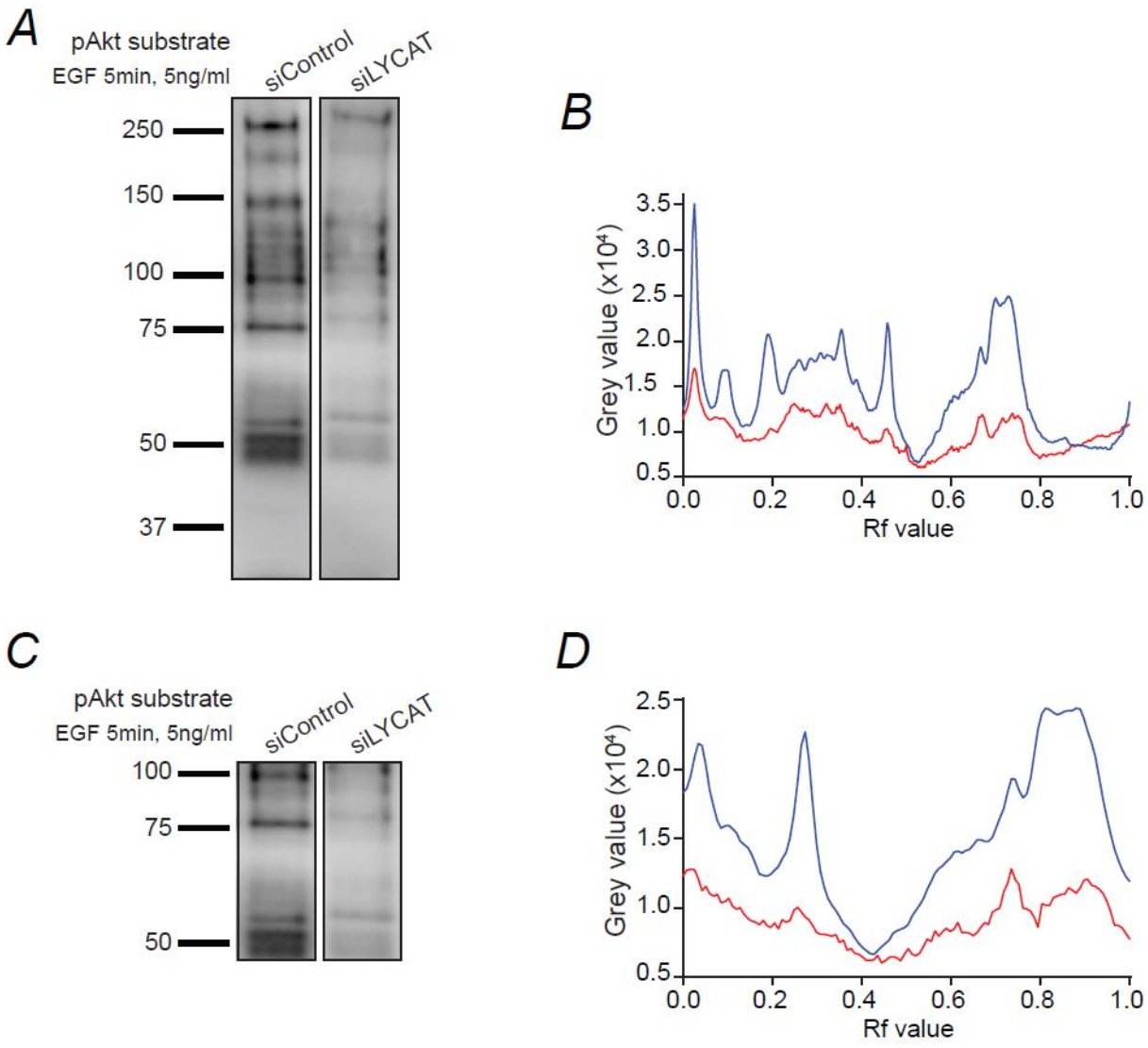
A
pAkt substrate
EGF 5min, 5ng/ml
siControl
siLYCAT
250
150
100
75
50
37
B
Grey value (x10⁴)
3.5
3.0
2.5
2.0
1.5
1.0
0.5
0.0
0.2
0.4
0.6
0.8
1.0
Rf value
C
pAkt substrate
EGF 5min, 5ng/ml
siControl
siLYCAT
100
75
50
D
Grey value (x10⁴)
2.5
2.0
1.5
1.0
0.5
0.0
0.2
0.4
0.6
0.8
1.0
Rf value

Figure A6. The Ras/Erk signaling pathway is not impacted by LYCAT silencing in MDA-MB-231 cells. MDA-MB-231 cells were transfected with siRNA sequence targeting LYCAT (siLYCAT) or nontargeting siRNA (siControl). Cells were serum starved for 1 h followed by 5 min of EGF stimulation (5 ng/ml) and then whole cell lysates were subjected to western blotting. Shown in (***A***) are representative immunoblots showing detection of pT202/Y204-Erk and total Erk. Quantitative measurements of (***B***) pT202/Y204-Erk relative to total Erk values (n = 2) and (***C***) total Erk (n = 6), independent *t* test. Mean ± SEM. *Work completed by Ms. R. Leung.*

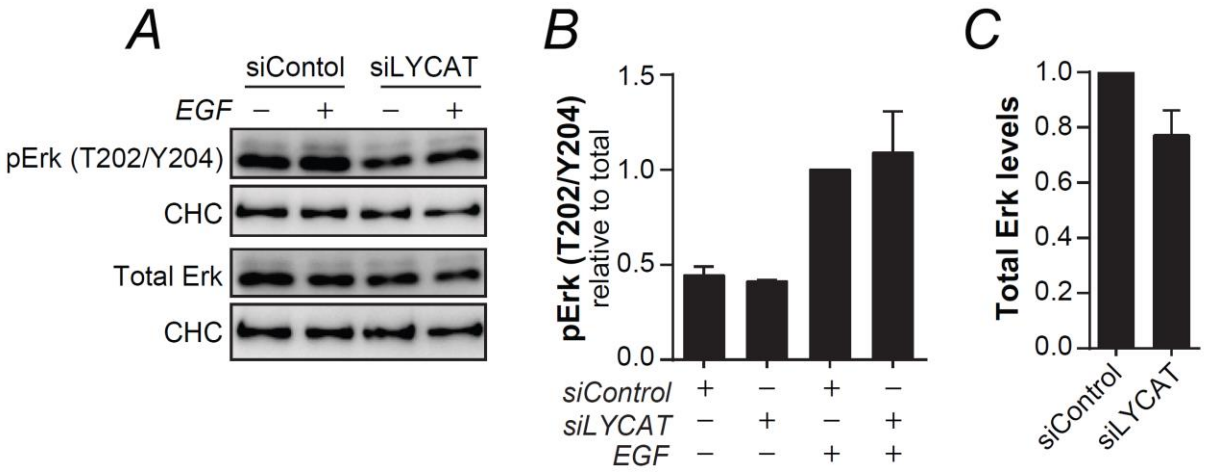

References

Adachi, Y., Itoh, K., Yamada, T., Cerveny, K.L., Suzuki, T.L., Macdonald, P., Frohman, M.A., Ramachandran, R., Iijima, M., Sesaki, H., 2016. Coincident Phosphatidic Acid Interaction Restrains Drp1 in Mitochondrial Division. Mol. Cell 63, 1034–1043.

Agarwal, A.K., Barnes, R.I., Garg, A., 2006. Functional characterization of human 1-acylglycerol-3-phosphate acyltransferase isoform 8: cloning, tissue distribution, gene structure, and enzymatic activity. Arch. Biochem. Biophys. 449, 64–76.

Aguet, F., Antonescu, C.N., Mettlen, M., Schmid, S.L., Danuser, G., 2013. Advances in analysis of low signal-to-noise images link dynamin and AP2 to the functions of an endocytic checkpoint. Dev. Cell 26, 279–91.

Anderson, K.E., Kielkowska, A., Durrant, T.N., Juvin, V., Clark, J., Stephens, L.R., Hawkins, P.T., 2013. Lysophosphatidylinositol-acyltransferase-1 (LPIAT1) is required to maintain physiological levels of PtdIns and PtdInsP(2) in the mouse. PLoS One 8, e58425.

Antonescu, C.N., Aguet, F., Danuser, G., Schmid, S.L., 2011. Phosphatidylinositol-(4,5)-bisphosphate regulates clathrin-coated pit initiation, stabilization, and size. Mol. Biol. Cell 22, 2588–600.

Antonescu, C.N., Danuser, G., Schmid, S.L., 2010. Phosphatidic Acid Plays a Regulatory Role in Clathrin-mediated Endocytosis 21, 2944–2952.

Antonescu, C.N., Díaz, M., Femia, G., Planas, J. V., Klip, A., 2008a. Clathrin-Dependent and Independent Endocytosis of Glucose Transporter 4 (GLUT4) in Myoblasts: Regulation by Mitochondrial Uncoupling. Traffic 9, 1173–1190.

Antonescu, C.N., Huang, C., Niu, W., Liu, Z., Eyers, P.A., Heidenreich, K.A., Bilan, P.J., Klip, A., 2005. Reduction of Insulin-Stimulated Glucose Uptake in L6 Myotubes by the Protein Kinase Inhibitor SB203580 Is Independent of p38MAPK Activity. Endocrinology 146, 3773–3781.

Antonescu, C.N., McGraw, T.E., Klip, A., 2014. Reciprocal regulation of endocytosis and metabolism. Cold Spring Harb. Perspect. Biol. 6, a016964.

Antonescu, C.N., Randhawa, V., Klip, A., 2008b. Dissecting GLUT4 traffic components in L6 myocytes by fluorescence-based, single cell assays. Methods Mol. Biol. Membr. Traffick. 457, 367–378.

Aoun, M., Feillet-Coudray, C., Fouret, G., Chabi, B., Crouzier, D., Ferreri, C., Chatgilialoglu, C., Wrutniak-Cabello, C., Cristol, J.P., Carbonneau, M.-A., et al., 2012. Rat liver mitochondrial membrane characteristics and mitochondrial functions are more profoundly altered by dietary lipid quantity than by dietary lipid quality: effect of different nutritional lipid patterns. Br. J. Nutr. 107, 647–659.

Asano, T., Fujishiro, M., Kushiyama, A., Nakatsu, Y., Yoneda, M., Kamata, H., Sakoda, H., 2007. Role of phosphatidylinositol 3-kinase activation on insulin action and its alteration in diabetic conditions. Biol. Pharm. Bull. 30, 1610–1616.

Astudillo, A.M., Pérez-Chacón, G., Balgoma, D., Gil-de-Gómez, L., Ruipérez, V., Guijas, C., Balboa, M.A., Balsinde, J., 2011. Influence of cellular arachidonic acid levels on phospholipid remodeling and CoA-independent transacylase activity in human monocytes and U937 cells. Biochim. Biophys. Acta - Mol. Cell Biol. Lipids 1811, 97–103.

Backer, J.M., 2008. The regulation and function of Class III PI3Ks: novel roles for Vps34. Biochem. J. 410, 1–17.

Bago, R., Malik, N., Munson, M.J., Prescott, A.R., Davies, P., Sommer, E., Shpiro, N., Ward, R., Cross, D., Ganley, I.G., et al., 2014. Characterization of VPS34-IN1, a selective inhibitor of Vps34, reveals that the phosphatidylinositol 3-phosphate-binding SGK3 protein kinase is a downstream target of class III phosphoinositide 3-kinase. Biochem. J. 463, 413–27.

Baker, R.R., Thompson, W., 1972. Positional distribution and turnover of fatty acids in phosphatidic acid, phosphoinositides, phosphatidylcholine and phosphatidylethanolamine in rat brain in vivo. Biochim. Biophys. Acta (BBA)/Lipids Lipid Metab. 270, 489–503.

Balla, T., 2013. Phosphoinositides: tiny lipids with giant impact on cell regulation. Physiol. Rev. 93, 1019–1137.

Balsinde, J., Balboa, M.A., Dennis, E.A., 1997. Antisense inhibition of group VI Ca2+-independent phospholipase A2 blocks phospholipid fatty acid remodeling in murine P388D1 macrophages. J. Biol. Chem. 272, 29317–21.

Barlowe, C., 2002. COPII-dependent transport from the endoplasmic reticulum. Curr. Opin. Cell Biol. 14, 417–422.

Barlowe, C., Barlowe, C., Schekman, R., Ravazzola, M., Helms, J.B., Rothman, J.E., Wieland, F.T.,

Tanigawa, G., Rothman, J.E., Balch, W.E., 1994. COPII: A membrane coat formed by Sec proteins that drive vesicle budding from the endoplasmic reticulum. Cell 77, 895–907.

Beh, C.T., Rine, J., 2004. A role for yeast oxysterol-binding protein homologs in endocytosis and in the maintenance of intracellular sterol-lipid distribution. J. Cell Sci. 117, 2983–2996.

Berridge, M.J., Irvine, R.F., 1984. Inositol trisphosphate, a novel second messenger in cellular signal transduction. Nature 312, 315–21.

Bigay, J., Antonny, B., 2012. Curvature, Lipid Packing, and Electrostatics of Membrane Organelles: Defining Cellular Territories in Determining Specificity. Dev. Cell 23, 886–895.

Bligh, E.G., Dyer, W.J., 1959. A rapid method of total lipid extraction and purification. Can. J. Biochem. Physiol. 37, 911–7.

Blind, R.D., Sablin, E.P., Kuchenbecker, K.M., Chiu, H.-J., Deacon, A.M., Das, D., Fletterick, R.J., Ingraham, H.A., 2014. The signaling phospholipid PIP3 creates a new interaction surface on the nuclear receptor SF-1. Proc. Natl. Acad. Sci. 111, 15054–15059.

Bojjireddy, N., Botyanszki, J., Hammond, G., Creech, D., Peterson, R., Kemp, D.C., Snead, M., Brown, R., Morrison, A., Wilson, S., et al., 2014. Pharmacological and Genetic Targeting of the PI4KA Enzyme Reveals Its Important Role in Maintaining Plasma Membrane Phosphatidylinositol 4-Phosphate and Phosphatidylinositol 4,5-Bisphosphate Levels. J. Biol. Chem. 289, 6120–6132.

Bolte, S., Cordelières, F.P., 2006. A guided tour into subcellular colocalization analysis in light microscopy. J. Microsc. 224, 213–32.

Bone, L.N., Dayam, R.M., Lee, M., Kono, N., Fairn, G.D., Arai, H., Botelho, R.J., Antonescu, C.N., 2017. The acyltransferase LYCAT controls specific phosphoinositides and related membrane traffic. Mol. Biol. Cell 28, 161–172.

Bradley, H., Shaw, C.S., Bendtsen, C., Worthington, P.L., Wilson, O.J., Strauss, J.A., Wallis, G.A., Turner, A.M., Wagenmakers, A.J.M., 2015. Visualization and quantitation of GLUT4 translocation in human skeletal muscle following glucose ingestion and exercise. Physiol. Rep. 3, e12375.

Bradley, R.M., Stark, K.D., Duncan, R.E., 2016. Influence of tissue, diet, and enzymatic remodeling on cardiolipin fatty acyl profile. Mol. Nutr. Food Res. 60, 1804–1818.

Bridges, J.P., Ikegami, M., Brilli, L.L., Chen, X., Mason, R.J., Shannon, J.M., 2010. LPCAT1 regulates surfactant phospholipid synthesis and is required for transitioning to air breathing in mice. J. Clin. Invest. 120, 1736–1748.

Brown, W.J., DeWald, D.B., Emr, S.D., Plutner, H., Balch, W.E., 1995. Role for phosphatidylinositol 3-kinase in the sorting and transport of newly synthesized lysosomal enzymes in mammalian cells. J. Cell Biol. 130, 781–96.

Bunting, M., Tang, W., Zimmerman, G.A., McIntyre, T.M., Prescott, S.M., 1996. Molecular cloning and characterization of a novel human diacylglycerol kinase zeta. J. Biol. Chem. 271, 10230–6.

Cao, J., Liu, Y., Lockwood, J., Burn, P., Shi, Y., 2004. A novel cardiolipin-remodeling pathway revealed by a gene encoding an endoplasmic reticulum-associated acyl-CoA:lysocardiolipin acyltransferase (ALCAT1) in mouse. J. Biol. Chem. 279, 31727–34.

Cao, J., Shen, W., Chang, Z., Shi, Y., 2009. ALCAT1 is a polyglycerophospholipid acyltransferase potently regulated by adenine nucleotide and thyroid status. Am. J. Physiol. Endocrinol. Metab. 296, E647-53.

Carlton, J.G., Cullen, P.J., 2005. Coincidence detection in phosphoinositide signaling. Trends Cell Biol. 15, 540–7.

Cerami, E., Gao, J., Dogrusoz, U., Gross, B.E., Sumer, S.O., Aksoy, B.A., Jacobsen, A., Byrne, C.J., Heuer, M.L., Larsson, E., et al., 2012. The cBio Cancer Genomics Portal: An Open Platform for Exploring Multidimensional Cancer Genomics Data. Cancer Discov. 2, 201–204.

Chan, C.-H., Jo, U., Kohrman, A., Rezaeian, A., Chou, P.-C., Logothetis, C., Lin, H.-K., 2014. Posttranslational regulation of Akt in human cancer. Cell Biosci. 4, 59.

Chang-Ileto, B., Frere, S.G., Chan, R.B., Voronov, S. V, Roux, A., Di Paolo, G., 2011. Synaptojanin 1-mediated PI(4,5)$P_2$ hydrolysis is modulated by membrane curvature and facilitates membrane fission. Dev. Cell 20, 206–218.

Chang, C.L., Hsieh, T.S., Yang, T.T., Rothberg, K.G., Azizoglu, D.B., Volk, E., Liao, J.C., Liou, J., 2013. Feedback regulation of receptor-induced ca2+ signaling mediated by e-syt1 and nir2 at endoplasmic reticulum-plasma membrane junctions. Cell Rep. 5, 813–825.

Chang, C.L., Liou, J., 2015. Phosphatidylinositol 4, 5-bisphosphate homeostasis regulated by

Nir2 and Nir3 proteins at endoplasmic reticulum-plasma membrane junctions. J. Biol. Chem. 290, 14289–14301.

Chicco, A.J., Sparagna, G.C., 2006. Role of cardiolipin alterations in mitochondrial dysfunction and disease. AJP Cell Physiol. 292, C33–C44.

Ching, T.T., Lin, H.P., Yang, C.C., Oliveira, M., Lu, P.J., Chen, C.S., 2001. Specific binding of the C-terminal Src homology 2 domain of the p85α subunit of phosphoinositide 3-kinase to phosphatidylinositol 3,4,5-trisphosphate: Localization and engineering of the phosphoinositide-binding motif. J. Biol. Chem. 276, 43932–43938.

Cho, H., Mu, J., Kim, J.K., Thorvaldsen, J.L., Chu, Q., Crenshaw, E.B., Kaestner, K.H., Bartolomei, M.S., Shulman, G.I., Birnbaum, M.J., 2001. Insulin Resistance and a Diabetes Mellitus-Like Syndrome in Mice Lacking the Protein Kinase Akt2 (PKBβ). Science 292, 1728–1731.

Choi-Rhee, E., Schulman, H., Cronan, J.E., 2004. Promiscuous protein biotinylation by Escherichia coli biotin protein ligase. Protein Sci. 13, 3043–50.

Choo, Y.S., Zhang, Z., 2009. Detection of protein ubiquitination. J. Vis. Exp.

Christoforidis, S., McBride, H.M., Burgoyne, R.D., Zerial, M., 1999. The Rab5 effector EEA1 is a core component of endosome docking. Nature 397, 621–5.

Chung, J., Torta, F., Masai, K., Lucast, L., Czapla, H., Tanner, L.B., Narayanaswamy, P., Wenk, M.R., Nakatsu, F., De Camilli, P., 2015. PI4P/phosphatidylserine countertransport at ORP5- and ORP8-mediated ER-plasma membrane contacts. Science 349, 428–32.

Clark, J., Anderson, K.E., Juvin, V., Smith, T.S., 2011. Quantification of PtdInsP 3 molecular species in cells and tissues by mass spectrometry. Nat Methods 8, 267–272.

Cockcroft, S., 2001. Phosphatidylinositol transfer proteins couple lipid transport to phosphoinositide synthesis. Semin. Cell Dev. Biol. 12, 183–91.

Coleman, R.A., Lee, D.P., 2004. Enzymes of triacylglycerol synthesis and their regulation. Prog. Lipid Res. 43, 134–76.

Cremona, O., De Camilli, P., 2001. Phosphoinositides in membrane traffic at the synapse. J. Cell Sci. 114, 1041–1052.

Cross, D.A.E., Alessi, D.R., Cohen, P., Andjelkovich, M., Hemmings, B.A., 1995. Inhibition of glycogen synthase kinase-3 by insulin mediated by protein kinase B. Nature 378, 785–789.

Cullen, P.J., 2011. Phosphoinositides and the regulation of tubular-based endosomal sorting. Biochem. Soc. Trans. 39, 839–50.

D'Souza, K., Epand, R.M., 2015. The phosphatidylinositol synthase-catalyzed formation of phosphatidylinositol does not exhibit acyl chain specificity. Biochemistry 54, 1151–3.

D'Souza, K., Epand, R.M., 2014. Enrichment of phosphatidylinositols with specific acyl chains. Biochim. Biophys. Acta - Biomembr. 1838, 1501–1508.

D'Souza, K., Kim, Y.J., Balla, T., Epand, R.M., 2014. Distinct properties of the two isoforms of CDP-diacylglycerol synthase. Biochemistry 53, 7358–7367.

Daniels, T.R., Delgado, T., Rodriguez, J. a, Helguera, G., Penichet, M.L., 2006. The transferrin receptor part I: Biology and targeting with cytotoxic antibodies for the treatment of cancer. Clin. Immunol. 121, 144–58.

Daniëls, V.W., Smans, K., Royaux, I., Chypre, M., Swinnen, J. V., Zaidi, N., 2014. Cancer Cells Differentially Activate and Thrive on De Novo Lipid Synthesis Pathways in a Low-Lipid Environment. PLoS One 9, e106913.

Darnell, J.C., Osterman, D.G., Saltiel, A.R., 1991a. Fatty acid remodelling of phosphatidylinositol under conditions of de novo synthesis in rat liver microsomes. Biochim. Biophys. Acta 1084, 279–91.

Darnell, J.C., Osterman, D.G., Saltiel, A.R., 1991b. Synthesis of phosphatidylinositol in rat liver microsomes is accompanied by the rapid formation of lysophosphatidylinositol. Biochim. Biophys. Acta 1084, 269–78.

Dasari, S., Tchounwou, P.B., 2014. Cisplatin in cancer therapy: molecular mechanisms of action. Eur. J. Pharmacol. 740, 364–78.

de Vries, K.J., Westerman, J., Bastiaens, P.I.H., Jovin, T.M., Wirtz, K.W.A., Snoek, G.T., 1996. Fluorescently Labeled Phosphatidylinositol Transfer Protein Isoforms (α and β), Microinjected into Fetal Bovine Heart Endothelial Cells, Are Targeted to Distinct Intracellular Sites. Exp. Cell Res. 227, 33–39.

Delos Santos, C.R., Bautista, S., Lucarelli, S., Bone, L.N., Dayam, R.M., Abousawan, J., Botelho, R.J., Antonescu, C.N., 2017. Selective regulation of EGFR signaling and endocytosis by phospholipase C and calcium, Molecular Biology of the Cell.

Di Paolo, G., De Camilli, P., 2006. Phosphoinositides in cell regulation and membrane dynamics. Nature 443, 651–7.

Díaz, M.E., González, L., Miquet, J.G., Martínez, C.S., Sotelo, A.I., Bartke, A., Turyn, D., 2012. Growth hormone modulation of EGF-induced PI3K-Akt pathway in mice liver. Cell. Signal. 24, 514–23.

Dickson, E.J., Jensen, J.B., Hille, B., 2014. Golgi and plasma membrane pools of PI(4)P contribute to plasma membrane PI(4,5)P2 and maintenance of KCNQ2/3 ion channel current. Proc. Natl. Acad. Sci. U. S. A. 111, E2281-90.

Doignon, F., Laquel, P., Testet, E., Tuphile, K., Fouillen, L., Bessoule, J.-J., 2015. Requirement of phosphoinositides containing stearic acid to control cell polarity. Mol. Cell. Biol. 36, 765–780.

Dong, R., Saheki, Y., Swarup, S., Lucast, L., Harper, J.W., De Camilli, P., 2016. Endosome-ER Contacts Control Actin Nucleation and Retromer Function through VAP-Dependent Regulation of PI4P. Cell 166, 408–423.

Downes, C.P., Ross, S., Maccario, H., Perera, N., Davidson, L., Leslie, N.R., 2007. Stimulation of PI 3-kinase signaling via inhibition of the tumor suppressor phosphatase, PTEN. Adv. Enzyme Regul. 47, 184–194.

Downward, J., Parker, P., Waterfield, M.D., 1984. Autophosphorylation sites on the epidermal growth factor receptor. Nature 311, 483–485.

Dugani, C.B., Randhawa, V.K., Cheng, A.W.P., Patel, N., Klip, A., 2008. Selective regulation of the perinuclear distribution of glucose transporter 4 (GLUT4) by insulin signals in muscle cells. Eur. J. Cell Biol. 87, 337–351.

Dummler, B., Tschopp, O., Hynx, D., Yang, Z.-Z., Dirnhofer, S., Hemmings, B.A., 2006. Life with a single isoform of Akt: mice lacking Akt2 and Akt3 are viable but display impaired glucose homeostasis and growth deficiencies. Mol. Cell. Biol. 26, 8042–51.

Ebine, K., Fujimoto, M., Okatani, Y., Nishiyama, T., Goh, T., Ito, E., Dainobu, T., Nishitani, A., Uemura, T., Sato, M.H., et al., 2011. A membrane trafficking pathway regulated by the plant-specific RAB GTPase ARA6. Nat. Cell Biol. 13, 853–859.

Eden, E.R., White, I.J., Tsapara, A., Futter, C.E., 2010. Membrane contacts between endosomes

and ER provide sites for PTP1B-epidermal growth factor receptor interaction. Nat. Cell Biol. 12, 267–72.

English, A.R., Voeltz, G.K., 2013. Rab10 GTPase regulates ER dynamics and morphology. Nat. Cell Biol. 15, 169–178.

English, A.R., Voeltz, G.K., 2013. Endoplasmic Reticulum Structure and Interconnections with Other Organelles. Cold Spring Harb. Perspect. Biol. 5, a013227–a013227.

Erneux, C., Govaerts, C., Communi, D., Pesesse, X., 1998. The diversity and possible functions of the inositol polyphosphate 5-phosphatases. Biochim. Biophys. Acta - Mol. Cell Biol. Lipids 1436, 185–199.

Fadeel, B., Xue, Di., 2009. Membrane : Roles in Health and Disease. Crit Rev Biochem Mol Biol 44, 264–277.

Fagone, P., Jackowski, S., 2009. Membrane phospholipid synthesis and endoplasmic reticulum function. J. Lipid Res. 50 Suppl, S311-6.

Fairn, G.D., Schieber, N.L., Ariotti, N., Murphy, S., Kuerschner, L., Webb, R.I., Grinstein, S., Parton, R.G., 2011. High-resolution mapping reveals topologically distinct cellular pools of phosphatidylserine. J. Cell Biol. 194, 257–275.

Fernández-Busnadiego, R., Saheki, Y., Camilli, P. de, De Camilli, P., 2015. Three-dimensional architecture of extended synaptotagmin-mediated endoplasmic reticulum-plasma membrane contact sites. Proc. Natl. Acad. Sci. U. S. A. 201503191.

Feske, S., 2007. Calcium signalling in lymphocyte activation and disease. Nat. Rev. Immunol. 7, 690–702.

Fili, N., Calleja, V., Woscholski, R., Parker, P.J., Larijani, B., 2006. Compartmental signal modulation: Endosomal phosphatidylinositol 3-phosphate controls endosome morphology and selective cargo sorting. Proc. Natl. Acad. Sci. U. S. A. 103, 15473–8.

Fruman, D.A., Meyers, R.E., Cantley, L.C., 1998. Phosphoinositide Kinases. Annu. Rev. Biochem. 67, 481–507.

Futter, C.E., Collinson, L.M., Backer, J.M., Hopkins, C.R., 2001. Human VPS34 is required for internal vesicle formation within multivesicular endosomes. J. Cell Biol. 155, 1251–1264.

Gadella, T., Wirtz, K., 1994. Phospholipid binding and transfer by the nonspecific lipid transfer

protein (sterol carrier protein 2): A kinetic model. Eur. J. Biochem. 220, 1019–1028.

Gaidarov, I., Keen, J.H., 1999. Phosphoinositide-AP-2 interactions required for targeting to plasma membrane clathrin-coated pits. J. Cell Biol. 146, 755–764.

Gao, J., Aksoy, B.A., Dogrusoz, U., Dresdner, G., Gross, B., Sumer, S.O., Sun, Y., Jacobsen, A., Sinha, R., Larsson, E., et al., 2013. Integrative Analysis of Complex Cancer Genomics and Clinical Profiles Using the cBioPortal. Sci. Signal. 6, pl1.

Garay, C., Judge, G., Lucarelli, S., Bautista, S., Pandey, R., Singh, T., Antonescu, C.N., 2015. Epidermal growth factor-stimulated Akt phosphorylation requires clathrin or ErbB2 but not receptor endocytosis. Mol. Biol. Cell 26, 3504–19.

Garner, K., Hunt, A.N., Koster, G., Somerharju, P., Groves, E., Li, M., Raghu, P., Holic, R., Cockcroft, S., 2012. Phosphatidylinositol transfer protein, cytoplasmic 1 (PITPNC1) binds and transfers phosphatidic acid. J. Biol. Chem. 287, 32263–32276.

Gericke, A., Leslie, N.R., Lösche, M., Ross, A.H., 2013. PtdIns(4,5)P2-mediated cell signaling: emerging principles and PTEN as a paradigm for regulatory mechanism. Adv. Exp. Med. Biol. 991, 85–104.

Gijón, M. a, Riekhof, W.R., Zarini, S., Murphy, R.C., Voelker, D.R., 2008. Lysophospholipid acyltransferases and arachidonate recycling in human neutrophils. J. Biol. Chem. 283, 30235–45.

Gillooly, D.J., Morrow, I.C., Lindsay, M., Gould, R., Bryant, N.J., Gaullier, J.M., Parton, R.G., Stenmark, H., 2000. Localization of phosphatidylinositol 3-phosphate in yeast and mammalian cells. EMBO J. 19, 4577–88.

Giordano, F., Saheki, Y., Idevall-Hagren, O., Colombo, S.F., Pirruccello, M., Milosevic, I., Gracheva, E.O., Bagriantsev, S.N., Borgese, N., De Camilli, P., 2013a. PI(4,5)P2-Dependent and Ca2+-Regulated ER-PM Interactions Mediated by the Extended Synaptotagmins. Cell 153, 1494–1509.

Giordano, F., Saheki, Y., Idevall-Hagren, O., Colombo, S.F., Pirruccello, M., Milosevic, I., Gracheva, E.O., Bagriantsev, S.N., Borgese, N., De Camilli, P., 2013b. PI(4,5)P(2)-dependent and Ca(2+)-regulated ER-PM interactions mediated by the extended synaptotagmins. Cell 153, 1494–509.

Gonzalez, E., McGraw, T.E., 2009. Insulin-modulated Akt subcellular localization determines Akt isoform-specific signaling. Proc. Natl. Acad. Sci. 106, 7004–7009.

Goto, T., Terada, N., Inoue, T., Nakayama, K., Okada, Y., Yoshikawa, T., Miyazaki, Y., Uegaki, M., Sumiyoshi, S., Kobayashi, T., et al., 2014. The expression profile of phosphatidylinositol in high spatial resolution imaging mass spectrometry as a potential biomarker for prostate cancer. PLoS One 9, 1–9.

Graham, T.R., Burd, C.G., 2011. Coordination of Golgi functions by phosphatidylinositol 4-kinases. Trends Cell Biol. 21, 113–21.

Gray, A., Van Der Kaay, J., Downes, C.P., 1999. The pleckstrin homology domains of protein kinase B and GRP1 (general receptor for phosphoinositides-1) are sensitive and selective probes for the cellular detection of phosphatidylinositol 3,4-bisphosphate and/or phosphatidylinositol 3,4,5-trisphosphate in vivo. Biochem. J. 344 Pt 3, 929–36.

Guerrero-Valero, M., Ferrer-Orta, C., Querol-Audi, J., Marin-Vicente, C., Fita, I., Gomez-Fernandez, J.C., Verdaguer, N., Corbalan-Garcia, S., 2009. Structural and mechanistic insights into the association of PKCalpha-C2 domain to PtdIns(4,5)P2. Proc. Natl. Acad. Sci. 106, 6603–6607.

Hammond, G.R., Schiavo, G., Irvine, R.F., 2009. Immunocytochemical techniques reveal multiple, distinct cellular pools of PtdIns4 P and PtdIns(4,5) P 2. Biochem. J. 422, 23–35.

Hammond, G.R. V, Fischer, M.J., Anderson, K.E., Holdich, J., Koteci, A., Balla, T., Irvine, R.F., 2012. PI4P and PI(4,5)P2 are essential but independent lipid determinants of membrane identity. Science 337, 727–30.

Hammond, G.R. V, Machner, M.P., Balla, T., 2014. A novel probe for phosphatidylinositol 4-phosphate reveals multiple pools beyond the Golgi. J. Cell Biol. 205, 113–126.

Hankins, H.M., Baldridge, R.D., Xu, P., Graham, T.R., 2015. Role of Flippases, Scramblases and Transfer Proteins in Phosphatidylserine Subcellular Distribution. Traffic 16, 35–47.

Hardie, D.G., 2007. AMP-Activated Protein Kinase as a Drug Target. Annu. Rev. Pharmacol. Toxicol. 47, 185–210.

Hayashi, M., Raimondi, A., O'Toole, E., Paradise, S., Collesi, C., Cremona, O., Ferguson, S.M., De Camilli, P., 2008. Cell- and stimulus-dependent heterogeneity of synaptic vesicle endocytic

recycling mechanisms revealed by studies of dynamin 1-null neurons. Proc. Natl. Acad. Sci. U. S. A. 105, 2175–80.

Hermansson, M., Hokynar, K., Somerharju, P., 2011. Mechanisms of glycerophospholipid homeostasis in mammalian cells. Prog. Lipid Res. 50, 240–257.

Hicks, A.M., DeLong, C.J., Thomas, M.J., Samuel, M., Cui, Z., 2006. Unique molecular signatures of glycerophospholipid species in different rat tissues analyzed by tandem mass spectrometry. Biochim. Biophys. Acta - Mol. Cell Biol. Lipids 1761, 1022–1029.

Higgs, H.N., Glomset, J.A., 1996. Purification and properties of a phosphatidic acid-preferring phospholipase A1 from bovine testis. Examination of the molecular basis of its activation. J. Biol. Chem. 271, 10874–83.

Hiraide, T., Ikegami, K., Sakaguchi, T., Morita, Y., Hayasaka, T., Masaki, N., Waki, M., Sugiyama, E., Shinriki, S., Takeda, M., et al., 2016. Accumulation of arachidonic acid-containing phosphatidylinositol at the outer edge of colorectal cancer. Sci. Rep. 6, 29935.

Ho, C.Y., Alghamdi, T. a, Botelho, R.J., 2012. Phosphatidylinositol-3,5-bisphosphate: no longer the poor PIP2. Traffic 13, 1–8.

Ho, C.Y., Choy, C.H., Botelho, R.J., 2016. Radiolabeling and Quantification of Cellular Levels of Phosphoinositides by High Performance Liquid Chromatography-coupled Flow Scintillation. J. Vis. Exp.

Hokin, L.E., 1987. The road to the phosphoinositide-generated second messengers. Trends Pharmacol. Sci. 8, 53–56.

Hokin, L.E., 1985. Receptors and phosphoinositide-generated second messengers. Annu. Rev. Biochem. 54, 205–35.

Holub, B.J., Kuksis, A., 1978. Metabolism of molecular species of diacylglycerophospholipids. Adv. Lipid Res. 16, 1–125.

Howell, G.J., Holloway, Z.G., Cobbold, C., Monaco, A.P., Ponnambalam, S., 2006. Cell Biology of Membrane Trafficking in Human Disease. Int. Rev. Cytol. 252, 1–69.

Hsu, F., Mao, Y., 2015. The structure of phosphoinositide phosphatases: Insights into substrate specificity and catalysis. Biochim. Biophys. Acta - Mol. Cell Biol. Lipids 1851, 698–710.

Huang, F., Khvorova, A., Marshall, W., Sorkin, A., 2004. Analysis of Clathrin-mediated

Endocytosis of Epidermal Growth Factor Receptor by RNA Interference. J. Biol. Chem. 279, 16657–16661.

Huang, J., Manning, B.D., 2009. A complex interplay between Akt, TSC2 and the two mTOR complexes. Biochem. Soc. Trans. 37, 217–22.

Hui, L., Zheng, Y., Yan, Y., Bargonetti, J., Foster, D.A., 2006. Mutant p53 in MDA-MB-231 breast cancer cells is stabilized by elevated phospholipase D activity and contributes to survival signals generated by phospholipase D. Oncogene 25, 7305–7310.

Hunt, A.N., Skippen, A.J., Koster, G., Postle, A.D., Cockcroft, S., 2004. Acyl chain-based molecular selectivity for HL60 cellular phosphatidylinositol and of phosphatidylcholine by phosphatidylinositol transfer protein ? Biochim. Biophys. Acta - Mol. Cell Biol. Lipids 1686, 50–60.

Huotari, J., Helenius, A., 2011. Endosome maturation. EMBO J. 30, 3481–500.

Imae, R., Inoue, T., Kimura, M., Kanamori, T., Tomioka, N.H., Kage-nakadai, E., Mitani, S., Arai, H., 2010. Intracellular Phospholipase A 1 and Acyltransferase, Which Are Involved in Caenorhabditis elegans Stem Cell Divisions, Determine the sn-1 Fatty Acyl Chain of Phosphatidylinositol 21, 3114–3124.

Imae, R., Inoue, T., Nakasaki, Y., Uchida, Y., Ohba, Y.Y., Kono, N., Nakanishi, H., Sasaki, T., Mitani, S., Arai, H., 2011. LYCAT, a homologue of C. elegans acl-8, acl-9 and acl-10, determines the fatty acid composition of phosphatidylinositol in mice. J. Lipid Res. 53, 335–347.

Ishikura, S., Antonescu, C.N., Klip, A., 2010. Documenting GLUT4 Exocytosis and Endocytosis in Muscle Cell Monolayers, in: Current Protocols in Cell Biology. John Wiley & Sons, Inc., Hoboken, NJ, USA, p. Unit 15.15.

Itoh, T., Koshiba, S., Kigawa, T., Kikuchi, a, Yokoyama, S., Takenawa, T., 2001. Role of the ENTH domain in phosphatidylinositol-4,5-bisphosphate binding and endocytosis. Science 291, 1047–51.

Jackson, L.P., Kelly, B.T., McCoy, A.J., Gaffry, T., James, L.C., Collins, B.M., Höning, S., Evans, P.R., Owen, D.J., 2010. A large-scale conformational change couples membrane recruitment to cargo binding in the AP2 clathrin adaptor complex. Cell 141, 1220–1229.

Jaqaman, K., Loerke, D., Mettlen, M., Kuwata, H., Grinstein, S., Schmid, S.L., Danuser, G., 2008. Robust single-particle tracking in live-cell time-lapse sequences. Nat. Methods 5, 695–702.

Jarquin-Pardo, M., Fitzpatrick, A., Galiano, F.J., First, E.A., Davis, J.N., 2007. Phosphatidic acid regulates the affinity of the murine phosphatidylinositol 4-phosphate 5-kinase-1β for phosphatidylinositol-4-phosphate. J. Cell. Biochem. 100, 112–128.

Jenkins, G.H., Fisette, P.L., Anderson, R.A., 1994. Type I phosphatidylinositol 4-phosphate 5-kinase isoforms are specifically stimulated by phosphatidic acid. J. Biol. Chem. 269, 11547–54.

Johnson, E.E., Overmeyer, J.H., Gunning, W.T., Maltese, W.A., 2006. Gene silencing reveals a specific function of hVps34 phosphatidylinositol 3-kinase in late versus early endosomes. J. Cell Sci. 119, 1219–1232.

Jost, M., Simpson, F., Kavran, J.M., Lemmon, M.A., Schmid, S.L., 1998. Phosphatidylinositol-4,5-bisphosphate is required for endocytic coated vesicle formation. Curr Biol 8, 1399–1402.

Jovic, M., Sharma, M., Rahajeng, J., Caplan, S., 2010. The early endosome: A busy sorting station for proteins at the crossroads. Histol. Histopathol. 25, 99–112.

Kamp, H.H., Wirtz, W.A., Baer, P.R., Slotboom, A.J., Rosenthal, A.F., Paltauf, F., van Deenem, L.L., 1977. Specificity of the phosphatidylcholine exchange protein from bovine liver. Biochemistry 16, 1310–6.

Kanno, K., Wu, M.K., Scapa, E.F., Roderick, S.L., Cohen, D.E., 2007. Structure and function of phosphatidylcholine transfer protein (PC-TP)/StarD2. Biochim. Biophys. Acta - Mol. Cell Biol. Lipids 1771, 654–662.

Kasper, A.M., Helmkamp, G.M., 1981. Intermembrane phospholipid fluxes catalyzed by bovine brain phospholipid exchange protein. Biochim. Biophys. Acta (BBA)/Lipids Lipid Metab. 664, 22–32.

Kawano, M., Kumagai, K., Nishijima, M., Hanada, K., 2006. Efficient Trafficking of Ceramide from the Endoplasmic Reticulum to the Golgi Apparatus Requires a VAMP-associated Protein-interacting FFAT Motif of CERT. J. Biol. Chem. 281, 30279–30288.

Ketel, K., Krauss, M., Nicot, A.-S., Puchkov, D., Wieffer, M., Müller, R., Subramanian, D., Schultz, C., Laporte, J., Haucke, V., 2016. A phosphoinositide conversion mechanism for exit from

endosomes. Nature 529, 408–412.

Kim, D., KC, B., Zhu, W., Motamedchaboki, K., Doye, V., Roux, K.J., 2014. Probing nuclear pore complex architecture with proximity-dependent biotinylation. Proc. Natl. Acad. Sci. 111, E2453–E2461.

Kim, J., Kim, Y.C., Fang, C., Russell, R.C., Kim, J.H., Fan, W., Liu, R., Zhong, Q., Guan, K.-L., 2013. Differential regulation of distinct Vps34 complexes by AMPK in nutrient stress and autophagy. Cell 152, 290–303.

Kim, S., Kedan, A., Marom, M., Gavert, N., Keinan, O., Selitrennik, M., Laufman, O., Lev, S., 2013. The phosphatidylinositol-transfer protein Nir2 binds phosphatidic acid and positively regulates phosphoinositide signalling. EMBO Rep. 14, 891–9.

Kim, Y.J., Guzman-Hernandez, M.L., Balla, T., 2011. A highly dynamic ER-derived phosphatidylinositol-synthesizing organelle supplies phosphoinositides to cellular membranes. Dev. Cell 21, 813–824.

Kim, Y.J., Guzman-Hernandez, M.L., Wisniewski, E., Balla, T., 2015. Phosphatidylinositol-Phosphatidic Acid Exchange by Nir2 at ER-PM Contact Sites Maintains Phosphoinositide Signaling Competence. Dev. Cell 33, 549–561.

Kim, Y.J., Hernandez, M.-L.G., Balla, T., 2013. Inositol lipid regulation of lipid transfer in specialized membrane domains. Trends Cell Biol. 23, 270–278.

Klippel, A., Kavanaugh, W.M., Pot, D., Williams, L.T., Klippel, A., Kavanaugh, W.M., Pot, D., Williams, L.T., 1997. A specific product of phosphatidylinositol 3-kinase directly activates the protein kinase Akt through its pleckstrin homology domain . A Specific Product of Phosphatidylinositol 3-Kinase Directly Activates the Protein Kinase Akt through Its Pleckstrin Hom. Mol. Cell. Biol. 17, 338–344.

Koeberle, A., Shindou, H., Harayama, T., Shimizu, T., 2010. Role of lysophosphatidic acid acyltransferase 3 for the supply of highly polyunsaturated fatty acids in TM4 Sertoli cells. FASEB J. 24, 4929–38.

Krauss, M., Haucke, V., 2007. Phosphoinositide-metabolizing enzymes at the interface between membrane traffic and cell signalling. EMBO Rep. 8, 241–6.

Kubo, K., Kobayashi, M., Nozaki, S., Yagi, C., Hatsuzawa, K., Katoh, Y., Shin, H.-W., Takahashi, S.,

Nakayama, K., 2015. SNAP23/25 and VAMP2 mediate exocytic event of transferrin receptor-containing recycling vesicles. Biol. Open 4, 910–20.

Kwiatkowska, K., 2010. One lipid, multiple functions: How various pools of PI(4,5)P2 are created in the plasma membrane. Cell. Mol. Life Sci. 67, 3927–3946.

Lacalle, R.A., De Karam, J.C., Martínez-Muñoz, L., Artetxe, I., Peregil, R.M., Sot, J., Rojas, A.M., Goñi, F.M., Mellado, M., Mañes, S., 2015. Type I phosphatidylinositol 4-phosphate 5-kinase homoand heterodimerization determines its membrane localization and activity. FASEB J. 29, 2371–2385.

Lahiri, S., Chao, J.T., Tavassoli, S., Wong, A.K.O., Choudhary, V., Young, B.P., Loewen, C.J.R., Prinz, W.A., Prinz, W., Osman, C., et al., 2014. A Conserved Endoplasmic Reticulum Membrane Protein Complex (EMC) Facilitates Phospholipid Transfer from the ER to Mitochondria. PLoS Biol. 12, e1001969.

Lahiri, S., Toulmay, A., Prinz, W.A., 2015. Membrane contact sites, gateways for lipid homeostasis. Curr. Opin. Cell Biol. 33, 82–87.

Lalanne, F., Ponsin, G., 2000. Mechanism of the phospholipid transfer protein-mediated transfer of phospholipids from model lipid vesicles to high density lipoproteins. Biochim. Biophys. Acta 1487, 82–91.

Lands, W.E., 1958. Metabolism of glycerolipides; a comparison of lecithin and triglyceride synthesis. J. Biol. Chem. 231, 883–8.

Lawe, D.C., Patki, V., Heller-Harrison, R., Lambright, D., Corvera, S., 2000. The FYVE domain of early endosome antigen 1 is required for both phosphatidylinositol 3-phosphate and Rab5 binding. Critical role of this dual interaction for endosomal localization. J. Biol. Chem. 275, 3699–3705.

Le Guédard, M., Bessoule, J.-J., Boyer, V., Ayciriex, S., Velours, G., Kulik, W., Ejsing, C.S., Shevchenko, A., Coulon, D., Lessire, R., et al., 2009. PSI1 is responsible for the stearic acid enrichment that is characteristic of phosphatidylinositol in yeast. FEBS J. 276, 6412–24.

Lee, H., Inoue, T., Sasaki, J., Kubo, T., Matsuda, S., Nakasaki, Y., Hattori, M., Tanaka, F., Udagawa, O., Kono, N., et al., 2012. LPIAT1 regulates arachidonic acid content in phosphatidylinositol and is required for cortical lamination in mice. Mol. Biol. Cell 23,

4689–700.

Lee, S.D., Tontonoz, P., 2015. Liver X receptors at the intersection of lipid metabolism and atherogenesis. Atherosclerosis 242, 29–36.

Lemmon, M.A., 2008. Membrane recognition by phospholipid-binding domains. Nat. Rev. Mol. Cell Biol. 9, 99–111.

Lev, S., 2010. Non-vesicular lipid transport by lipid-transfer proteins and beyond. Nat. Rev. Mol. Cell Biol. 11, 739–750.

Levine, T.P., Munro, S., 1998. The pleckstrin homology domain of oxysterol-binding protein recognises a determinant specific to Golgi membranes. Curr. Biol. 8, 729–739.

Levkowitz, G., Waterman, H., Ettenberg, S.A., Katz, M., Tsygankov, A.Y., Alroy, I., Lavi, S., Iwai, K., Reiss, Y., Ciechanover, A., et al., 1999. Ubiquitin ligase activity and tyrosine phosphorylation underlie suppression of growth factor signaling by c-Cbl/Sli-1. Mol. Cell 4, 1029–40.

Li, J., Liu, X., Wang, H., Zhang, W., Chan, D.C., Shi, Y., 2012. Lysocardiolipin acyltransferase 1 (ALCAT1) controls mitochondrial DNA fidelity and biogenesis through modulation of MFN2 expression. Proc. Natl. Acad. Sci. U. S. A. 109, 6975–80.

Li, J., Romestaing, C., Han, X., Li, Y., Hao, X., Wu, Y., Sun, C., Liu, X., Jefferson, L.S., Xiong, J., et al., 2010. Cardiolipin remodeling by ALCAT1 links oxidative stress and mitochondrial dysfunction to obesity. Cell Metab. 12, 154–65.

Lippincott-Schwartz, J., Presley, J.F., Cole, N.B., Schroer, T.A., Hirschberg, K., Zaal, K.J.M., 1997. ER-to-Golgi transport visualized in living cells. Nature 389, 81–85.

Litvak, V., Dahan, N., Ramachandran, S., Sabanay, H., Lev, S., 2005. Maintenance of the diacylglycerol level in the Golgi apparatus by the Nir2 protein is critical for Golgi secretory function. Nat. Cell Biol. 7, 225–234.

Liu, K., Jian, Y., Sun, X., Yang, C., Gao, Z., Zhang, Z., Liu, X., Li, Y., Xu, J., Jing, Y., et al., 2016. Negative regulation of phosphatidylinositol 3-phosphate levels in early-to-late endosome conversion. J. Cell Biol. 212, 181–198.

Liu, X., Ye, B., Miller, S., Yuan, H., Zhang, H., Tian, L., Nie, J., Imae, R., Arai, H., Li, Y., et al., 2012. Ablation of ALCAT1 mitigates hypertrophic cardiomyopathy through effects on oxidative

stress and mitophagy. Mol. Cell. Biol. 32, 4493–504.

Loerke, D., Mettlen, M., Yarar, D., Jaqaman, K., Jaqaman, H., Danuser, G., Schmid, S.L., 2009. Cargo and Dynamin Regulate Clathrin-Coated Pit Maturation. PLoS Biol. 7.

Loewen, C.J.R., Roy, A., Levine, T.P., 2003. A conserved ER targeting motif in three families of lipid binding proteins and in Opi1p binds VAP. EMBO J. 22, 2025–2035.

Logan, M.R., Mandato, C. a, 2006. Regulation of the actin cytoskeleton by PIP2 in cytokinesis. Biol. Cell 98, 377–88.

Ludwig, H., Evstatiev, R., Kornek, G., Aapro, M., Bauernhofer, T., Buxhofer-Ausch, V., Fridrik, M., Geissler, D., Geissler, K., Gisslinger, H., et al., 2015. Iron metabolism and iron supplementation in cancer patients. Wien. Klin. Wochenschr. 127, 907–19.

Lung, M., Shulga, Y. V, Ivanova, P.T., Myers, D.S., Milne, S.B., Brown, H.A., Topham, M.K., Epand, R.M., 2009. Diacylglycerol kinase epsilon is selective for both acyl chains of phosphatidic acid or diacylglycerol. J. Biol. Chem. 284, 31062–73.

Luthra, M.G., Sheltawy, A., 1976. The Metabolic Turnover of Molecular Species of Phosphatidylinositol and its Precursor Phosphatidic Acid in Guinea-pig Cerebral Hemisperes. J. Neurochem. 27, 1503–1511.

MacDonald, G., Baker, R.R., Thompson, W., 1975. Selective synthesis of molecular classes of phosphatidic acid, diacylglycerol and phosphatidylinositol in rat brain. J. Neurochem. 24, 655–61.

Manna, D., Albanese, A., Park, W.S., Cho, W., 2007. Mechanistic Basis of Differential Cellular Responses of Phosphatidylinositol 3,4-Bisphosphate- and Phosphatidylinositol 3,4,5-Trisphosphate-binding Pleckstrin Homology Domains. J. Biol. Chem. 282, 32093–32105.

Manning, B.D., Toker, A., 2017. AKT/PKB Signaling: Navigating the Network. Cell 169, 381–405.

Mao, Y., Nickitenko, A., Duan, X., Lloyd, T.E., Wu, M.N., Bellen, H., Quiocho, F.A., 2000. Crystal Structure of the VHS and FYVE Tandem Domains of Hrs, a Protein Involved in Membrane Trafficking and Signal Transduction. Cell 100, 447–456.

Marien, E., Meister, M., Muley, T., Fieuws, S., Bordel, S., Derua, R., Spraggins, J., Van De Plas, R., Dehairs, J., Wouters, J., et al., 2015. Non-small cell lung cancer is characterized by dramatic changes in phospholipid profiles. Int. J. Cancer 137, 1539–1548.

Martini, M., De Santis, M.C., Braccini, L., Gulluni, F., Hirsch, E., 2014. PI3K/AKT signaling pathway and cancer: an updated review. Ann. Med. 34, 1–12.

Maxfield, F.R., McGraw, T.E., 2004. Endocytic recycling. Nat. Rev. Mol. Cell Biol. 5, 121–32.

Mayle, K.M., Le, A.M., Kamei, D.T., 2012. The intracellular trafficking pathway of transferrin. Biochim. Biophys. Acta - Gen. Subj. 1820, 264–281.

McCartney, A.J., Zhang, Y., Weisman, L.S., 2014. Phosphatidylinositol 3,5-bisphosphate: Low abundance, high significance. BioEssays 36, 52–64.

McCrea, H.J., De Camilli, P., 2009. Mutations in phosphoinositide metabolizing enzymes and human disease. Physiology (Bethesda). 24, 8–16.

McCubrey, J. a, Steelman, L.S., Abrams, S.L., Lee, J.T., Chang, F., Bertrand, F.E., Navolanic, P.M., Terrian, D.M., Franklin, R. a, D'Assoro, A.B., et al., 2006. Roles of the RAF/MEK/ERK and PI3K/PTEN/AKT pathways in malignant transformation and drug resistance. Adv. Enzyme Regul. 46, 249–79.

McLaughlin, S., Smith, S.O., Hayman, M.J., Murray, D., 2005. An electrostatic engine model for autoinhibition and activation of the epidermal growth factor receptor (EGFR/ErbB) family. J. Gen. Physiol. 126, 41–53.

Mellman, I., 1996. Endocytosis and Molecular Sorting. Annu. Rev. Cell Dev. Biol. 12, 575–625.

Mesmin, B., Bigay, J., Moser Von Filseck, J., Lacas-Gervais, S., Drin, G., Antonny, B., 2013. A four-step cycle driven by PI(4)P hydrolysis directs sterol/PI(4)P exchange by the ER-Golgi Tether OSBP. Cell 155.

Michell, R.H., 2008. Inositol derivatives: evolution and functions. Nat. Rev. Mol. Cell Biol. 9, 151–161.

Miller, E.A., Beilharz, T.H., Malkus, P.N., Lee, M.C.S., Hamamoto, S., Orci, L., Schekman, R., Kato, R., Earnest, T., Nakayama, K., et al., 2003. Multiple cargo binding sites on the COPII subunit Sec24p ensure capture of diverse membrane proteins into transport vesicles. Cell 114, 497–509.

Milne, S.B., Ivanova, P.T., Armstrong, M.D., Myers, D.S., Lubarda, J., Shulga, Y. V., Topham, M.K., Brown, H.A., Epand, R.M., 2008. Dramatic Differences in the Roles in Lipid Metabolism of Two Isoforms of Diacylglycerol Kinase. Biochemistry 47, 9372–9379.

Milne, S.B., Ivanova, P.T., DeCamp, D., Hsueh, R.C., Brown, H.A., 2005. A targeted mass spectrometric analysis of phosphatidylinositol phosphate species. J. Lipid Res. 46, 1796–802.

Min, S.W., Chang, W.P., Sudhof, T.C., 2007. E-Syts, a family of membranous Ca2+-sensor proteins with multiple C2 domains. Proc Natl Acad Sci U S A 104, 3823–3828.

Mizoguchi, T., Nakajima, K., Hatsuzawa, K., Nagahama, M., Hauri, H.-P., Tagaya, M., Tani, K., 2000. Determination of Functional Regions of p125, a Novel Mammalian Sec23p-Interacting Protein. Biochem. Biophys. Res. Commun. 279, 144–149.

Mochly-Rosen, D., Das, K., Grimes, K. V, 2012. Protein kinase C, an elusive therapeutic target? Nat. Rev. Drug Discov. 11, 937–57.

Morikawa, R., Tsujimoto, M., Arai, H., Aoki, J., 2007. Phospholipase A1 Assays Using a Radiolabeled Substrate and Mass Spectrometry, in: Methods in Enzymology. pp. 1–13.

Moser von Filseck, J., opi , A., Delfosse, V., Vanni, S., Jackson, C.L., Bourguet, W., Drin, G., 2015. Phosphatidylserine transport by ORP/Osh proteins is driven by phosphatidylinositol 4-phosphate. Science 349, 432–436.

Munshi, A., Hobbs, M., Meyn, R.E., 2005. Clonogenic Cell Survival Assay. Methods Mol. Med. Chemosensitivity 110, 021–028.

Murray, D.H., Jahnel, M., Lauer, J., Avellaneda, M.J., Brouilly, N., Cezanne, A., Morales-Navarrete, H., Perini, E.D., Ferguson, C., Lupas, A.N., et al., 2016. An endosomal tether undergoes an entropic collapse to bring vesicles together. Nature 537, 107–111.

Naguib, A., Bencze, G., Engle, D.D., Chio, I.I.C., Herzka, T., Watrud, K., Bencze, S., Tuveson, D.A., Pappin, D.J., Trotman, L.C., 2015. P53 mutations change phosphatidylinositol acyl chain composition. Cell Rep. 10, 8–19.

Nakagawa, Y., Rüstow, B., Rabe, H., Kunze, D., Waku, K., 1989. The de novo synthesis of molecular species of phosphatidylinositol from endogenously labeled CDP diacylglycerol in alveolar macrophage microsomes. Arch. Biochem. Biophys. 268, 559–66.

Nakatsu, F., Perera, R.M., Lucast, L., Zoncu, R., Domin, J., Gertler, F.B., Toomre, D., De Camilli, P., 2010. The inositol 5-phosphatase SHIP2 regulates endocytic clathrin-coated pit dynamics. J. Cell Biol. 190, 307–15.

Nández, R., Balkin, D.M., Messa, M., Liang, L., Paradise, S., Czapla, H., Hein, M.Y., Duncan, J.S., Mann, M., De Camilli, P., 2014. A role of OCRL in clathrin-coated pit dynamics and uncoating revealed by studies of Lowe syndrome cells. Elife 3, e02975.

Navaroli, D.M., Bellvé, K.D., Standley, C., Lifshitz, L.M., Cardia, J., Lambright, D., Leonard, D., Fogarty, K.E., Corvera, S., 2012. Rabenosyn-5 defines the fate of the transferrin receptor following clathrin-mediated endocytosis. Proc. Natl. Acad. Sci. U. S. A. 109, E471-80.

Nemoto, Y., Kearns, B.G., Wenk, M.R., Chen, H., Mori, K., Alb, J.G., De Camilli, P., Bankaitis, V.A., 2000. Functional characterization of a mammalian Sac1 and mutants exhibiting substrate-specific defects in phosphoinositide phosphatase activity. J. Biol. Chem. 275, 34293–34305.

Ogiso, H., Nakamura, K., Yatomi, Y., Shimizu, T., Taguchi, R., 2010. Liquid chromatography/mass spectrometry analysis revealing preferential occurrence of non-arachidonate-containing phosphatidylinositol bisphosphate species in nuclei and changes in their levels during cell cycle. Rapid Commun. Mass Spectrom. 24, 436–442.

Ogiso, H., Taguchi, R., 2008. Reversed-Phase LC / MS Method for Polyphosphoinositide Analyses : Changes in Molecular Species Levels during Epidermal Growth Factor Activation in A431 Cells Reversed-Phase LC / MS Method for Polyphosphoinositide Analyses : Changes in Molecular Species Le. Anal. Chem. 80, 9226–9232.

Pasqualato, S., Senic-Matuglia, F., Renault, L., Goud, B., Salamero, J., Cherfils, J., 2004. The structural GDP/GTP cycle of Rab11 reveals a novel interface involved in the dynamics of recycling endosomes. J. Biol. Chem. 279, 11480–8.

Perera, R.M., Zoncu, R., Lucast, L., De Camilli, P., Toomre, D., 2006. Two synaptojanin 1 isoforms are recruited to clathrin-coated pits at different stages. Proc Natl Acad Sci U S A 103, 19332–19337.

Petiot, A., Ogier-Denis, E., Blommaart, E.F., Meijer, A.J., Codogno, P., 2000. Distinct classes of phosphatidylinositol 3'-kinases are involved in signaling pathways that control macroautophagy in HT-29 cells. J. Biol. Chem. 275, 992–8.

Phillips, M.J., Voeltz, G.K., 2016. Structure and function of ER membrane contact sites with other organelles. Nat. Rev. Mol. Cell Biol. 17, 69–82.

Phillips, S.E., Ile, K.E., Boukhelifa, M., Huijbregts, R.P.H., Bankaitis, V.A., 2006. Specific and

nonspecific membrane-binding determinants cooperate in targeting phosphatidylinositol transfer protein beta-isoform to the mammalian trans-Golgi network. Mol. Biol. Cell 17, 2498–512.

Pirola, L., Zvelebil, M.J., Bulgarelli-Leva, G., Van Obberghen, E., Waterfield, M.D., Wymann, M.P., 2001. Activation loop sequences confer substrate specificity to phosphoinositide 3-kinase alpha (PI3Kalpha). Functions of lipid kinase-deficient PI3Kalpha in signaling. J. Biol. Chem. 276, 21544–21554.

Platre, M.P., Jaillais, Y., 2017. Anionic lipids and the maintenance of membrane electrostatics in eukaryotes. Plant Signal. Behav. 12, e1282022.

Porat-Shliom, N., Weigert, R., Donaldson, J.G., 2013. Endosomes derived from clathrin-independent endocytosis serve as precursors for endothelial lumen formation. PLoS One 8, e81987.

Presley, J.F., Cole, N.B., Schroer, T. a, Hirschberg, K., Zaal, K.J., Lippincott-Schwartz, J., 1997. ER-to-Golgi transport visualized in living cells. Nature 389, 81–85.

Qi, Y., Kapterian, T.S., Du, X., Ma, Q., Fei, W., Zhang, Y., Huang, X., Dawes, I.W., Yang, H., 2016. CDP-diacylglycerol synthases regulate the growth of lipid droplets and adipocyte development. J. Lipid Res. 57, 767–780.

Raiborg, C., Wenzel, E.M., Pedersen, N.M., Olsvik, H., Schink, K.O., Schultz, S.W., Vietri, M., Nisi, V., Bucci, C., Brech, A., et al., 2015. Repeated ER–endosome contacts promote endosome translocation and neurite outgrowth. Nature 520, 234–238.

Raychaudhuri, S., Im, Y.J., Hurley, J.H., Prinz, W.A., 2006. Nonvesicular sterol movement from plasma membrane to ER requires oxysterol-binding protein-related proteins and phosphoinositides. J. Cell Biol. 173, 107–119.

Richmond, G.S., Smith, T.K., 2011. Phospholipases A 1. Int. J. Mol. Sci. 12, 588–612.

Riss, T.L., Moravec, R.A., Niles, A.L., Duellman, S., Benink, H.A., Worzella, T.J., Minor, L., 2004. Cell Viability Assays, Assay Guidance Manual. Eli Lilly & Company and the National Center for Advancing Translational Sciences.

Rocha, N., Kuijl, C., Van Der Kant, R., Janssen, L., Houben, D., Janssen, H., Zwart, W., Neefjes, J., 2009. Cholesterol sensor ORP1L contacts the ER protein VAP to control Rab7-RILP-

p150Glued and late endosome positioning. J. Cell Biol. 185, 1209–1225.

Roth, M.G., 2004. Phosphoinositides in constitutive membrane traffic. Physiol. Rev. 84, 699–730.

Roux, K.J., Kim, D.I., Raida, M., Burke, B., 2012. A promiscuous biotin ligase fusion protein identifies proximal and interacting proteins in mammalian cells. J. Cell Biol. 196, 801–810.

Saheki, Y., Bian, X., Schauder, C.M., Sawaki, Y., Surma, M.A., Klose, C., Pincet, F., Reinisch, K.M., De Camilli, P., 2016. Control of plasma membrane lipid homeostasis by the extended synaptotagmins. Nat. Cell Biol. 18, 504–515.

Saito, T., Jones, C.C., Huang, S., Czech, M.P., Pilch, P.F., 2007. The Interaction of Akt with APPL1 Is Required for Insulin-stimulated Glut4 Translocation. J. Biol. Chem. 282, 32280–32287.

Santagata, S., Boggon, T.J., Baird, C.L., Gomez, C.A., Zhao, J., Shan, W.S., Myszka, D.G., Shapiro, L., 2001. G-Protein Signaling Through Tubby Proteins. Science 292, 2041–2050.

Santi, S. a, Lee, H., 2010. The Akt isoforms are present at distinct subcellular locations. Am. J. Physiol. Cell Physiol. 298, C580–C591.

Sasaki, T., Takasuga, S., Sasaki, J., Kofuji, S., Eguchi, S., Yamazaki, M., Suzuki, A., 2009. Mammalian phosphoinositide kinases and phosphatases. Prog. Lipid Res. 48, 307–343.

Sathappa, M., Alder, N.N., 2016. The ionization properties of cardiolipin and its variants in model bilayers. Biochim. Biophys. Acta - Biomembr. 1858, 1362–1372.

Saxton, R.A., Sabatini, D.M., 2017. mTOR Signaling in Growth, Metabolism, and Disease. Cell 169, 361–371.

Schauder, C.M., Wu, X., Saheki, Y., Narayanaswamy, P., Torta, F., Wenk, M.R., De Camilli, P., Reinisch, K.M., 2014. Structure of a lipid-bound extended synaptotagmin indicates a role in lipid transfer. Nature 510, 552–5.

Schenck, A., Goto-Silva, L., Collinet, C., Rhinn, M., Giner, A., Habermann, B., Brand, M., Zerial, M., 2008. The Endosomal Protein Appl1 Mediates Akt Substrate Specificity and Cell Survival in Vertebrate Development. Cell 133, 486–497.

Schmid, A.C., Wise, H.M., Mitchell, C. a, Nussbaum, R., Woscholski, R., 2004. Type II phosphoinositide 5-phosphatases have unique sensitivities towards fatty acid composition and head group phosphorylation. FEBS Lett. 576, 9–13.

Sears, R., Nuckolls, F., Haura, E., Taya, Y., Tamai, K., Nevins, J.R., 2000. Multiple Ras-dependent phosphorylation pathways regulate Myc protein stability. Genes Dev. 14, 2501–14.

Sheff, D., Pelletier, L., O'Connell, C.B., Warren, G., Mellman, I., 2002. Transferrin receptor recycling in the absence of perinuclear recycling endosomes. J. Cell Biol. 156, 797–804.

Shimoi, W., Ezawa, I., Nakamoto, K., Uesaki, S., Gabreski, G., Aridor, M., Yamamoto, A., Nagahama, M., Tagaya, M., Tani, K., 2005. p125 is localized in endoplasmic reticulum exit sites and involved in their organization. J. Biol. Chem. 280, 10141–8.

Shin, H.-W., Hayashi, M., Christoforidis, S., Lacas-Gervais, S., Hoepfner, S., Wenk, M.R., Modregger, J., Uttenweiler-Joseph, S., Wilm, M., Nystuen, A., et al., 2005. An enzymatic cascade of Rab5 effectors regulates phosphoinositide turnover in the endocytic pathway. J. Cell Biol. 170, 607–618.

Shindou, H., Hishikawa, D., Harayama, T., Yuki, K., Shimizu, T., 2009. Recent progress on acyl CoA: lysophospholipid acyltransferase research. J. Lipid Res. 50 Suppl, S46-51.

Shindou, H., Shimizu, T., 2009. Acyl-CoA:lysophospholipid acyltransferases. J. Biol. Chem. 284, 1–5.

Shulga, Y. V., Anderson, R.A., Topham, M.K., Epand, R.M., 2012. Phosphatidylinositol-4-phosphate 5-kinase isoforms exhibit acyl chain selectivity for both substrate and lipid activator. J. Biol. Chem. 287, 35953–35963.

Shulga, Y. V, Myers, D.S., Ivanova, P.T., Milne, S.B., Brown, H.A., Topham, M.K., Epand, R.M., 2010. Molecular species of phosphatidylinositol-cycle intermediates in the endoplasmic reticulum and plasma membrane. Biochemistry 49, 312–7.

Shulga, Y. V, Topham, M.K., Epand, R.M., 2011a. Regulation and functions of diacylglycerol kinases. Chem. Rev. 111, 6186–208.

Shulga, Y. V, Topham, M.K., Epand, R.M., 2011b. Study of arachidonoyl specificity in two enzymes of the PI cycle. J. Mol. Biol. 409, 101–12.

Shulga, Y. V, Topham, M.K., Epand, R.M., 2011c. Substrate specificity of diacylglycerol kinase-epsilon and the phosphatidylinositol cycle. FEBS Lett. 585, 4025–8.

Song, G., Ouyang, G., Bao, S., 2005. The activation of Akt/PKB signaling pathway and cell survival. J. Cell. Mol. Med. 9, 59–71.

Sönnichsen, B., De Renzis, S., Nielsen, E., Rietdorf, J., Zerial, M., 2000. Distinct membrane domains on endosomes in the recycling pathway visualized by multicolor imaging of Rab4, Rab5, and Rab11. J. Cell Biol. 149, 901–913.

Stang, E., Blystad, F.D., Kazazic, M., Bertelsen, V., Brodahl, T., Raiborg, C., Stenmark, H., Madshus, I.H., 2004. Cbl-dependent ubiquitination is required for progression of EGF receptors into clathrin-coated pits. Mol. Biol. Cell 15, 3591–604.

Stauffer, T.P., Ahn, S., Meyer, T., 1998. Receptor-induced transient reduction in plasma membrane PtdIns(4,5)P2 concentration monitored in living cells. Curr. Biol. 8, 343–6.

Stefan, C.J., Manford, A.G., Baird, D., Yamada-Hanff, J., Mao, Y., Emr, S.D., 2011. Osh proteins regulate phosphoinositide metabolism at ER-plasma membrane contact sites. Cell 144, 389–401.

Steinman, R.M., Mellman, I.S., Muller, W.A., Cohn, Z.A., 1983. Endocytosis and the recycling of plasma membrane. J. Cell Biol. 96, 1–27.

Stenmark, H., Aasland, R., Driscoll, P.C., 2002. The phosphatidylinositol 3-phosphate-binding FYVE finger. FEBS Lett. 513, 77–84.

Stephens, L.R., Jackson, T.R., Hawkins, P.T., 1993. Agonist-stimulated synthesis of phosphatidylinositol(3,4,5)-trisphosphate: a new intracellular signalling system? Biochim. Biophys. Acta 1179, 27–75.

Szentpetery, Z., Várnai, P., Balla, T., 2010. Acute manipulation of Golgi phosphoinositides to assess their importance in cellular trafficking and signaling. Proc. Natl. Acad. Sci. U. S. A. 107, 8225–8230.

Szymańska, E., Sobota, A., Czuryło, E., Kwiatkowska, K., 2008. Expression of PI(4,5)P2-binding proteins lowers the PI(4,5)P2 level and inhibits FcγRIIA-mediated cell spreading and phagocytosis. Eur. J. Immunol. 38, 260–272.

Takeuchi, K., Reue, K., 2009. Biochemistry, physiology, and genetics of GPAT, AGPAT, and lipin enzymes in triglyceride synthesis. Am. J. Physiol. Endocrinol. Metab. 296, E1195-209.

Tao, K., Yin, Y., Shen, Q., Chen, Y., Li, R., Chang, W., Bai, J., Liu, W., Shi, L., Zhang, P., 2016. Akt inhibitor MK-2206 enhances the effect of cisplatin in gastric cancer cells. Biomed. reports 4, 365–368.

Tilley, S.J., Skippen, A., Murray-Rust, J., Swigart, P.M., Stewart, A., Morgan, C.P., Cockcroft, S., McDonald, N.Q., Martin, T.F., Luo, M., et al., 2004. Structure-function analysis of human [corrected] phosphatidylinositol transfer protein alpha bound to phosphatidylinositol. Structure 12, 317–26.

Toker, A., Cantley, L.C., 1997. Signalling through the lipid products of phosphoinositide-3-OH kinase. Nature 387, 673–676.

Tomas, A., Futter, C.E., Eden, E.R., 2014. EGF receptor trafficking: Consequences for signaling and cancer. Trends Cell Biol. 24, 26–34.

Topham, M.K., Epand, R.M., 2009. Mammalian diacylglycerol kinases: Molecular interactions and biological functions of selected isoforms. Biochim. Biophys. Acta - Gen. Subj. 1790, 416–424.

Toulmay, A., Prinz, W.A., 2011. Lipid transfer and signaling at organelle contact sites: the tip of the iceberg. Curr. Opin. Cell Biol. 23, 458–463.

Ullrich, O., Reinsch, S., Urbé, S., Zerial, M., Parton, R.G., 1996. Rab11 regulates recycling through the pericentriolar recycling endosome. J. Cell Biol. 135, 913–24.

Urbé, S., Tooze, S.A., Barr, F.A., 1997. Formation of secretory vesicles in the biosynthetic pathway. Biochim. Biophys. Acta - Mol. Cell Res. 1358, 6–22.

van Dam, E.M., Ten Broeke, T., Jansen, K., Spijkers, P., Stoorvogel, W., 2002. Endocytosed transferrin receptors recycle via distinct dynamin and phosphatidylinositol 3-kinase-dependent pathways. J. Biol. Chem. 277, 48876–83.

van Meer, G., Voelker, D.R., Feigenson, G.W., 2008. Membrane lipids: where they are and how they behave. Nat. Rev. Mol. Cell Biol. 9, 112–124.

Van Paridon, P.A., Gadella, T.W., Somerharju, P.J., Wirtz, K.W., 1987. On the relationship between the dual specificity of the bovine brain phosphatidylinositol transfer protein and membrane phosphatidylinositol levels. Biochim. Biophys. Acta 903, 68–77.

Vance, D.E., Vance, J.E., 2008. Phospholipid biosynthesis in eukaryotes. Biochem. Lipids, Lipoproteins Membr. 128, 213–244.

Vance, J., Steenbergen, R., 2005. Metabolism and functions of phosphatidylserine. Prog. Lipid Res. 44, 207–234.

Vance, J.E., Vance, D.E., 2004. Phospholipid biosynthesis in mammalian cells. Biochem. Cell Biol. 82, 113–128.

Várnai, P., Balla, T., 1998. Visualization of phosphoinositides that bind pleckstrin homology domains: calcium- and agonist-induced dynamic changes and relationship to myo-[3H]inositol-labeled phosphoinositide pools. J. Cell Biol. 143, 501–10.

Varnai, P., Thyagarajan, B., Rohacs, T., Balla, T., 2006. Rapidly inducible changes in phosphatidylinositol 4,5-bisphosphate levels influence multiple regulatory functions of the lipid in intact living cells. J Cell Biol 175, 377–382.

Vicinanza, M., D'Angelo, G., Di Campli, A., De Matteis, M.A., 2008. Function and dysfunction of the PI system in membrane trafficking. EMBO J. 27, 2457–70.

Wakelam, M.J.O., 2014. The uses and limitations of the analysis of cellular phosphoinositides by lipidomic and imaging methodologies. Biochim. Biophys. Acta - Mol. Cell Biol. Lipids 1841, 1102–1107.

Walsh, J.P., Suen, R., Lemaitre, R.N., Glomset, J.A., 1994. Arachidonoyl-diacylglycerol kinase from bovine testis. Purification and properties. J. Biol. Chem. 269, 21155–64.

Whatmore, J., Wiedemann, C., Somerharju, P., Swigart, P., Cockcroft, S., 1999. Resynthesis of phosphatidylinositol in permeabilized neutrophils following phospholipase Cbeta activation: transport of the intermediate, phosphatidic acid, from the plasma membrane to the endoplasmic reticulum for phosphatidylinositol resynthesis is not . Biochem. J. 341 ( Pt 2, 435–444.

Wirtz, K.W.A., 2006. Phospholipid transfer proteins in perspective. FEBS Lett. 580, 5436–5441.

Wu, S.-L., Kim, J., Bandle, R.W., Liotta, L., Petricoin, E., Karger, B.L., 2006. Dynamic Profiling of the Post-translational Modifications and Interaction Partners of Epidermal Growth Factor Receptor Signaling after Stimulation by Epidermal Growth Factor Using Extended Range Proteomic Analysis (ERPA). Mol Cell Proteomics 5, 1610–1627.

Yamashita, A., Hayashi, Y., Nemoto-Sasaki, Y., Ito, M., Oka, S., Tanikawa, T., Waku, K., Sugiura, T., 2014. Acyltransferases and transacylases that determine the fatty acid composition of glycerolipids and the metabolism of bioactive lipid mediators in mammalian cells and model organisms. Prog. Lipid Res. 53, 18–81.

Yamashita, A., Kumazawa, T., Koga, H., Suzuki, N., Oka, S., Sugiura, T., 2010. Generation of lysophosphatidylinositol by DDHD domain containing 1 (DDHD1): Possible involvement of phospholipase D/phosphatidic acid in the activation of DDHD1. Biochim. Biophys. Acta - Mol. Cell Biol. Lipids 1801, 711–720.

Yang, Z.-Z., Tschopp, O., Baudry, A., Hynx, D., Hemmings, B.A., 2004. Physiological functions of protein kinase B/Akt. Biochem. Soc. Trans. 32.

Yeung, T., Gilbert, G.E., Shi, J., Silvius, J., Kapus, A., Grinstein, S., 2008. Membrane phosphatidylserine regulates surface charge and protein localization. Science 319, 210–3.

Yeung, T., Terebiznik, M., Yu, L., Silvius, J., Abidi, W.M., Philips, M., Levine, T., Kapus, A., Grinstein, S., 2006. Receptor activation alters inner surface potential during phagocytosis. Science 313, 347–51.

Yoder, M.D., Thomas, L.M., Tremblay, J.M., Oliver, R.L., Yarbrough, L.R., Helmkamp, G.M., 2001. Structure of a multifunctional protein: Mammalian phosphatidylinositol transfer protein complexed with phosphatidylcholine. J. Biol. Chem. 276, 9246–9252.

Yoshihisa, T., Barlowe, C., Schekman, R., 1993. Requirement for a GTPase-activating protein in vesicle budding from the endoplasmic reticulum. Science 259, 1466–1468.

Yu, Y., Kovacevic, Z., Richardson, D.R., 2007. Tuning cell cycle regulation with an iron key. Cell Cycle 6, 1982–1994.

Zeigerer, A., Gilleron, J., Bogorad, R.L., Marsico, G., Nonaka, H., Seifert, S., Epstein-Barash, H., Kuchimanchi, S., Peng, C.G., Ruda, V.M., et al., 2012. Rab5 is necessary for the biogenesis of the endolysosomal system in vivo. Nature 485, 465–70.

Zhang, S.Q., Tsiaras, W.G., Araki, T., Wen, G., Minichiello, L., Klein, R., Neel, B.G., 2002. Receptor-specific regulation of phosphatidylinositol 3’-kinase activation by the protein tyrosine phosphatase Shp2. Mol. Cell. Biol. 22, 4062–72.

Zhao, L., Vogt, P.K., 2008. Class I PI3K in oncogenic cellular transformation. Oncogene 27, 5486–5496.

Zhao, W., Qiu, Y., Kong, D., 2017. Class I phosphatidylinositol 3-kinase inhibitors for cancer therapy. Acta Pharm. Sin. B 7, 27–37.

Zhao, Y., Chen, Y.-Q., Li, S., Konrad, R.J., Cao, G., 2009. The microsomal cardiolipin remodeling

enzyme acyl-CoA lysocardiolipin acyltransferase is an acyltransferase of multiple anionic lysophospholipids. J. Lipid Res. 50, 945–56.

Zoncu, R., Perera, R.M., Balkin, D.M., Pirruccello, M., Toomre, D., De Camilli, P., 2009. A Phosphoinositide Switch Controls the Maturation and Signaling Properties of APPL Endosomes. Cell 136, 1110–1121.